Tatjana Peroš-Golubičić
Om P. Sharma

# Clinical Atlas
## of Interstitial Lung Disease

Springer

# Clinical Atlas of Interstitial Lung Disease

Tatjana Peroš-Golubičić, MD, PhD, and
Om P. Sharma, MD, FRCP

# Clinical Atlas of Interstitial Lung Disease

Foreword by Talmadge E. King, Jr., MD

Springer

Tatjana Peroš-Golubičić, MD, PhD
University of Zagreb
Medical School
University Hospital for Lung Diseases "Jordanovac"
Zagreb
Croatia

Om P. Sharma, MD, FRCP
Keck School of Medicine at University of Southern California
Los Angeles, California
USA

British Library Cataloguing in Publication Data

Peroš-Golubičić, Tatjana
Clinical atlas of interstitial lung disease
1. Interstitial lung diseases—Atlases
I. Title II. Sharma, Om P.
616.2′4
ISBN-13: 9781846283208

ISBN-10: 1846283205

Library of Congress Control Number: 2005938495

ISBN-10: 1-84628-320-5 e-ISBN-10: 1-84628-326-4
ISBN-13: 978-1-84628-320-8 e-ISBN-13: 978-1-84628-326-0
Printed on acid-free paper



9 8 7 6 5 4 3 2 1

Springer Science+Business Media, LLC

# Foreword

The interstitial lung diseases, also called diffuse parenchymal lung diseases, are a diverse group of pulmonary disorders classified together because of similar clinical, roentgenographic, physiologic, or pathologic features. During the past 50 years, we have experienced remarkable advances in the classification, diagnosis, and management of these diseases. Technological advances, particularly high-resolution computed tomography, bronchoalveolar lavage, and video-assisted thoracic surgery, have provided access to information that has vastly improved our understanding of these entities. In addition, genetic medicine, the use of new technologies (e.g., microarrays, mass spectroscopic analysis of proteins, and laser capture microdissection) and the development of animal models have led to better understanding of the pathogenesis of these disorders.

Unfortunately, patients with diffuse parenchymal lung disease continue to present a difficult diagnostic and management challenge to clinicians. A major reason is that the topic of "interstitial lung disease" is vast and difficult to grasp. Some 25 years ago when I first became interested in interstitial lung diseases, there was no ready source of information relating specifically to these processes. Even today, there is a need for a comprehensive, yet easy to read, manual of the key information about the important interstitial lung diseases.

The purpose of this atlas is to provide the clinician, from medical student to lung specialist, with a ready reference helpful in their attempts to master this topic and to provide guidance in their daily practice. The subject of interstitial lung disease is inherently multidisciplinary; consequently, the authors have provided a consistent approach to each entity that includes the key clinical, physiologic, radiologic, and pathologic features.

The *Clinical Atlas of Interstitial Lung Disease* is composed of 37 chapters loosely divided into six sections. The first section provides a historical background to the interstitial lung diseases and an overview of the basis for recognizing the key features that allow a specific diagnosis to be achieved. The second section is dedicated to the interstitial lung diseases of unknown etiology, including sarcoidosis, the idiopathic interstitial pneumonias, and eosinophilic pneumonias. The third section describes interstitial lung diseases of known etiology (e.g., drug-induced, radiation, hypersensitivity pneumonitis, and pneumoconioses). The fourth section addresses interstitial lung diseases associated with the connective tissue diseases and pulmonary vasculitidies. The fifth section deals with a number of specific entities (e.g., alveolar proteinosis, lymphangioleiomyomatosis, and Langerhans cell histiocytosis). The final section devotes several chapters to the pulmonary manifestations of systemic diseases, such as paraproteinemias, liver and gastrointestinal disease, and malignancy.

We owe a debt of gratitude to all those who were involved in producing this *Clinical Atlas of Interstitial Lung Disease*. The authors have succeeded in creating a readable, concise atlas that is up to date and user friendly.

Talmadge E. King, Jr., M.D.
Department of Medicine
University of California San Francisco; and
San Francisco General Hospital
San Francisco, California

Om P. Sharma, MD, FRCP, and Tatjana Peroš-Golubičić, MD, PhD.

# Preface

The Oxford English Dictionary defines *atlas* as: "A similar volume containing illustrative plates, large engravings, etc., or the conspectus of any subject arranged in tabular forms; e.g. 'an atlas of anatomical plates,' 'an ethnographical atlas.'" In that vein, the *Clinical Atlas of Interstitial Lung Disease* is a visual representation of common and uncommon interstitial lung diseases.

Is there a need for such an atlas on interstitial lung disease? There has been an unprecedented revision and expansion of scientific and clinical knowledge of interstitial lung disease that now begs for such a volume. Dense, voluminous texts and review manuscripts on the topic grace the shelves of medical libraries and personal collections of many physicians; alas, perusal of these volumes requires considerable time and effort that is not easily available to a practicing clinician. Our aim in writing this atlas has been to produce a compendium that is easy to read, comprehensive, and light enough to be carried in a briefcase or to be enjoyed as a bedside reading. Designed to complement the existing scientific knowledge of interstitial lung disease, it enhances the bedside clinical education of the various disciplines of practitioners who treat patients with interstitial lung disease. It is a true pictorial supplement to the texts available on the topic.

Averill Liebow said, "A man's medical history, and the traces of his habits and his trades are often inscribed upon the lungs—for him who can read." As medical students, we are taught to obtain complete and relevant history and then perform a complete physical examination. This book leads a physician to create appropriate diagnostic patterns by combining the symptoms and signs with radiographic and laboratory findings. Once a clinical pattern or syndrome is successfully recognized and integrated in the memory, it can be conveniently recalled. A student of medical science will never regret mastering this art.

The book opens with a brief description of the relevant history, anatomy of the lung, and definitions of the common terms used. It is followed by a clinical classification of interstitial lung diseases due to known cause and those whose cause is not known.

Each brief chapter deals with the incidence, clinical features, and biochemical and molecular tests. Chest x-ray, HRCT imaging features, and bronchoscopic findings bring to life clinical pictures of the disease. The establishment of a correlation between histological findings and the associated radiographic appearances convey the strong message that the simple chest x-ray and especially the HRCT scan in many interstitial lung diseases have become an invaluable aid to clinical diagnosis. Appropriately placed tables broaden the scope of differential diagnosis. Sarcoidosis, idiopathic interstitial pneumonias, eosinophilic interstitial lung disease (ILD), a group of ILD of known cause, lung in diffuse connective diseases and vasculitis, rare pulmonary diseases, lung manifestations of liver and gastrointestinal diseases, and finally cancer and ILD are the titles of chapters that follow.

This atlas can be best categorized as a manual or handbook with the pictorial images enhancing a concise and practical description of the disease. Medical students, postgraduate trainees, and practitioners of all disciplines will benefit from the book. Because there is no atlas on interstitial lung disease, this will be the first such book on the topic.

Tatjana Peroš-Golubičić
Om. P. Sharma

# Acknowledgments

It is not possible to acknowledge individually all friends and colleagues who have directly or indirectly contributed to this atlas. We are particularly indebted to our contributors but also to numerous other colleagues. **Mirna Sentić**, MD, clinical immunologist, University Hospital Centre, Department of Internal Medicine, Zagreb, provided Figures 19.1(c), 19.2(a), 20.1, and 20.2(a, b, c); **Branko Malenica**, MD, PhD, Professor, University of Zagreb, Medical school, University Hospital Center, Immunology Lab, Zagreb, Figures 20.4, 21.2(a, b, c), 21.3, 22.4, 23.5, 24.7, 25.3, 26.2, and 27.1; **Igor Petriček**, MD, Ophthalmologist, University Hospital Centre, Department of Eye Diseases, Zagreb, Figures 4.2(a), 23.1(a, b, c), and 23.2(a, c); **Sanja Grle-Popović,** MD, PhD, Pulmonologist, University Hospital for Lung Diseases, Jordanovac, Zagreb, Figures 2.8(a, b), 8.1(d), and 16.2(e); **Vesna Matijević**, MD, Neurologist, University Hospital Centre, Department of Neurologic Diseases, Zagreb, Figure 20.3(b); **Tomislav Jukić**, MD, Ophthalmologist, University Hospital Centre, Department of Eye Diseases, Zagreb, Figures 4.2(c, d), 28.2, and 36.3; **Nenad Vukoja**, MD, Ophthalmologist, University Hospital Centre, Department of Eye Diseases, Zagreb, Figures 4.2(e), 19.2(b), and 28.2(c); **Ivo Sjekavica**, MD, Radiologist, University Hospital Centre, Zagreb, Figures 20.5 and 36.6; **Sonoko Nagai**, MD, Professor, Kyoto University, Japan, Figure 28.3; and **Ivan Dobrić**, MD, PhD, Professor of Dermatology, Department of Dermatology, University Hospital Center, Zagreb, Figures 21.1 and 22.1(c).

Finally, the atlas would never have been completed without the love, support, and patience of our families. Thank you **Maggie**, **Zdravko**, **and Maša**!

Tatjana Peroš-Golubičić
Om. P. Sharma

# Contents

# Contributors

Tatjana Peroš-Golubičić, MD, PhD
Associate Professor, Pulmonologist
University of Zagreb, Medical School
University Hospital for Lung Diseases
"Jordanovac"
Zagreb, Croatia

Om P. Sharma, MD, FRCP
Professor of Medicine
Keck School of Medicine at University
of Southern California
Los Angeles, California, USA

Jasna Tekavec-Trkanjec, MD, PhD
Pulmonologist and Bronchologist
Department of Pneumonology
University Hospital for Lung Disease
"Jordanovac"
Zagreb, Croatia

Silvana Smojver-Ježek, MD
Clinical Cytologist
Department of Cytology
University Hospital for Lung Disease
"Jordanovac"
Zagreb, Croatia

Šimun Križanac, MD, PhD
Professor of Pathology
Department of Pathology
University of Zagreb, Medical School
Zagreb, Croatia

Marijan Gorečan, MD
Radiologist
Department of Radiology
University Hospital for Lung Disease
"Jordanovac"
Zagreb, Croatia

# 1

# Interstitial Lung Diseases: A Historical Note

> Sophisticated people can hardly understand how vague experience is at bottom, and how truly that vagueness supports whatever clearness is afterwards attained.
>
> George Santayana
> *The Life of Reason*

*De morbis artificium diatriba*, one of the most influential documents on occupational medicine, written by Bernardino Ramazzini da Capri (1633–1714), (Figure 1.1), surfaced in Padua in 1700. In the chapter "Diseases of Sifters, Measurers, and Handlers of Grain," the author described the occurrence of dry cough, cachexia, asthma, and dropsy in these workers. In addition, he commented on the role of humidity, and suggested that "small worms" not visible to the eye present in the wheat dust might be responsible for the illness. This was the first clinical description of an interstitial lung disease caused by occupational exposure.

In 1868, Austin Flint described a vague, nondescript lung disease that he called *chronic pneumonitis*. It was characterized by florid inflammatory exudation without pus, and it caused solidification and fibrosis of the lungs. Flint alluded that Carl Freiherr von Rokitansky had described a similar condition in which exudation had occurred into the interlobular and intervesicular areolar tissue. Furthermore, he asserted that the illness was different from florid tuberculosis. A few years earlier, Dominic Corrigan, an Irish cardiologist, called the similar entity *cirrhosis of the lung* because it was analogous, not identical, to cirrhosis of the liver. Although Flint had thought that the condition was rare; two significant observations were made during the period. First, Corrigan described the occurrence of traction bronchiectasis in interstitial pneumonitis. Second, Flint observed that the fingertips of one patient with interstitial pneumonitis had assumed a bulbous appearance, and he therefore became the first to notice the association of clubbing and interstitial pneumonitis/fibrosis.

Two decades later, Wilson Fox, professor of pathological anatomy at the University College, London, recorded the microscopic changes of capillary edema; accumulation of pigmented epithelium in the alveoli; and thickening of the walls of the alveoli and veins in lungs with interstitial pneumonitis. Fox also credited Rokitansky for recognizing the fibrous thickening of the alveoli in this condition (Figure 1.2a, b, c).

In 1892, William Osler, while at Johns Hopkins Hospital, Baltimore, observed, "In one of Charcot's cases . . . death occurred about three months after the onset of the acute disease and the lung was two thirds of the normal size, grayish in color, hard as cartilage. In only case of the kind that has come under my observation, the patient died about a month from the onset of the chill. The lung was uniformly solid and grayish in color. Microscopically these areas showed advanced fibrotic changes and great thickening of the alveolar walls." Osler recommended that the term *cirrhosis* should be applied only to the cases in which a lung was densely fibrosed, whether fibrosis had originated in the parenchyma or the pleura. Additionally, like Flint, Osler advised that this new entity be distinguished from the fibrosis caused by tuberculosis (Figure 1.3).

In 1944, Louis Hamman and Arnold Rich (Figure 1.4), both at the Johns Hopkins University School of Medicine, described four young patients who died of progressive


**Figure 1.1.** Bernardino Ramazzini (1633–1714).

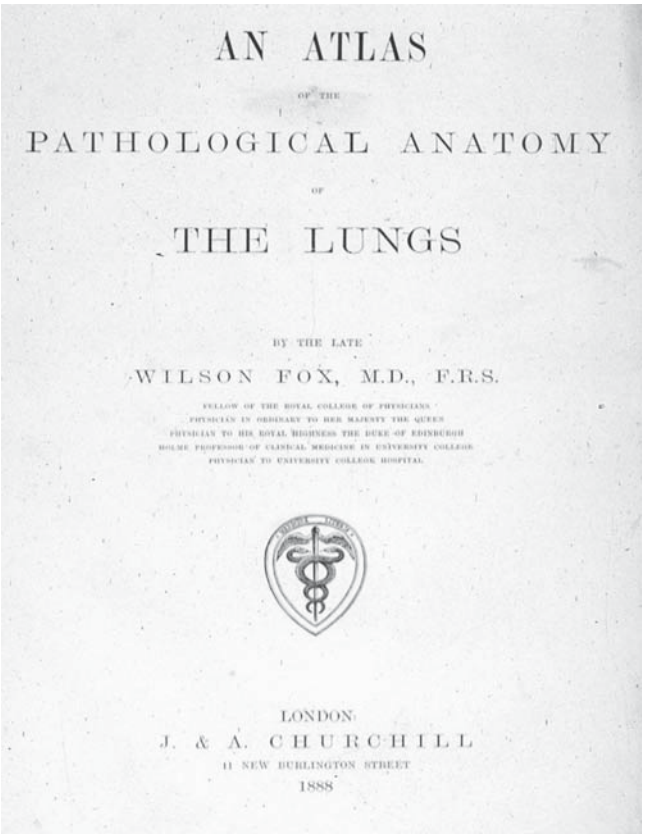


a

**Figure 1.2.** Title page: *An Atlas of the Pathological Anatomy* (a). Chronic pneumonitis caused by syphilis (b). Various stages in the development of fibrosis in chronic phthisis (c).
(continued below)

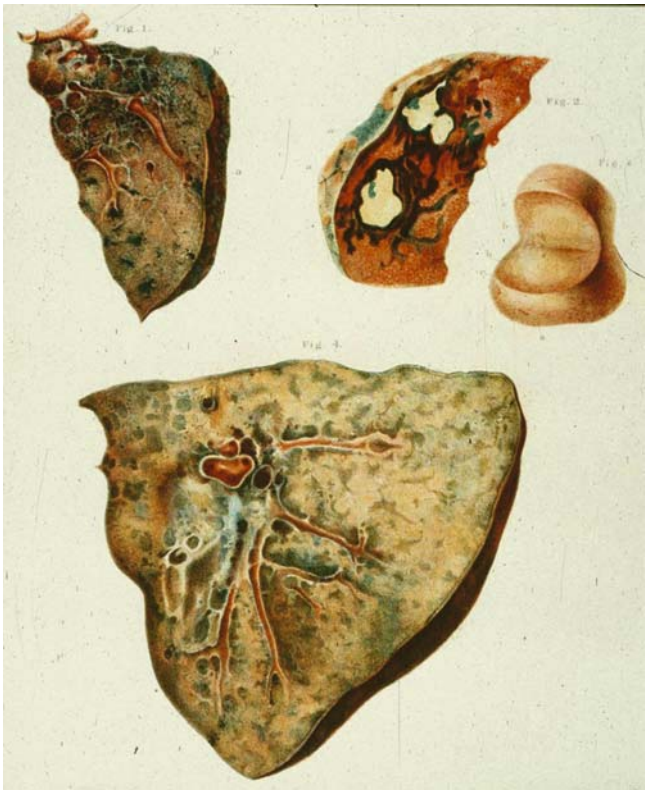

b

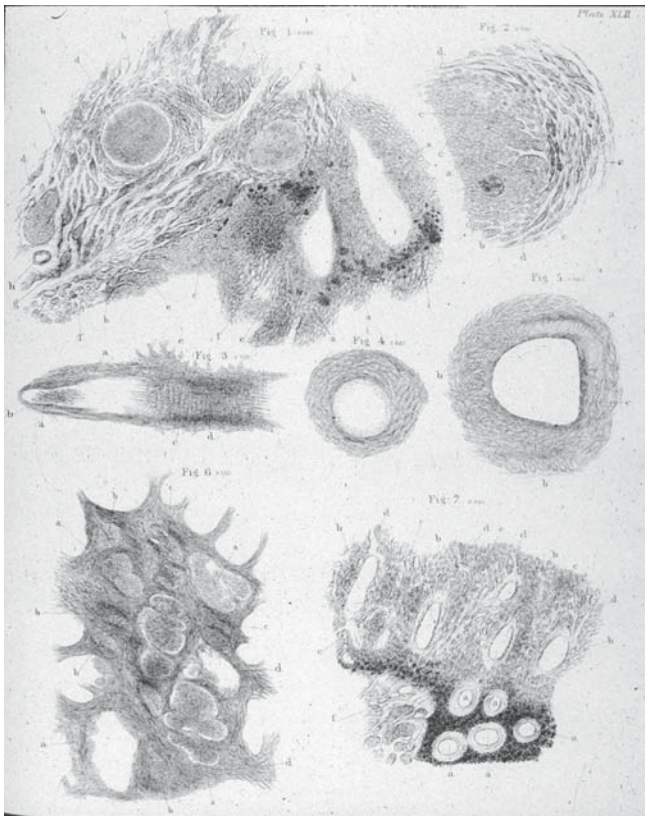

c

**Figure 1.2.** (continued)

**Figure 1.3.** Sir William Osler (1849–1919).

**Figure 1.4.** Louis Hamman and Arnold Rich at Johns Hopkins Medical Center, Baltimore, Maryland.

dyspnea within 6 months of onset. The clinical profile of the illness was similar to that described earlier by Flint, Corrigan, Fox, Charcot, and Osler. The term *Hamman-Rich syndrome* became a synonym for an interstitial pneumonia of unknown cause followed by fulminating pulmonary fibrosis. It was soon apparent that the course of this new disease was not always acute, progressive, or fatal. In 1957, Rubin and Lubliner reviewed 48 cases of the Hamman-Rich syndrome and added 15 cases of their own. From that point on, diffuse interstitial pneumonitis/fibrosis could no longer be considered a rare disease.

In 1960, interstitial pneumonias acquired two new terms: *idiopathic pulmonary fibrosis* and *cryptogenic fibrosing alveolitis*. Scadding and Hinson, working at Brompton Chest Hospital, London, preferred the latter term to define the inflammatory and fibrotic changes in the lung parenchyma. They advised that the word *idiopathic* be dropped in favor of the term *cryptogenic* in describing the illness of unknown cause. *Cryptogenic fibrosing alveolitis* is an accepted term in Europe; whereas, in North America, the usual *interstitial pneumonia* remains a popular description.

Averill Liebow (Figure 1.5), on the basis of his extensive clinical and pathologic sciences, classified interstitial pneumonitis into five different histologic types: usual interstitial pneumonitis (UIP), desquamative interstitial pneumonia (DIP), bronchiolitis obliterans interstitial pneumonia (BIP), lymphoid interstitial pneumonia (LIP), and giant cell interstitial pneumonia (GIP).

The classification of idiopathic or primary interstitial lung disease was further simplified by removing BIP, LIP, and GIP, and by adding nonspecific interstitial

**Figure 1.5.** Averill Liebow in San Diego, California.

pneumonia (NSIP). The new classification of idiopathic interstitial pneumonia includes UIP and DIP from Liebow's original classification and two new entities, acute interstitial pneumonia (AIP; or Hamman-Rich syndrome) and NSIP. Bronchiolitis obliterans organizing pneumonia (BOOP) was not initially included because it is primarily an intraluminal disease, but later the American Thoracic Society/European Respiratory Society (ATS/ERS) consensus included it again for its similar diagnostic algorithm and clinical behavior as other IIPs. Lymphoid interstitial pneumonias (LIP) were also added to the list. Clinical recognition of these disorders is easier today than it used to be in the early days.

## Bibliography


1. Ramazzini B. De morbis artificium diatriba. Modena, Italy 1700.
2. Flint A. A Treatise on the Principles and Practice of Medicine. Philadelphia: Henry C. Lea; 1868:193.
3. Fox W. An Atlas of the Pathological Anatomy of the Lungs. London: J & A; 1888:52.
4. Osler W. Practice of Medicine. New York: Appleton & Co.; 1892:533.
5. Hamman L, Rich A. Acute diffuse interstitial fibrosis of the lungs. Bull Johns Hopkins Hosp 1944;74:177–212.
6. Rubin E, Lubliner H. The Hamman-Rich syndrome: Review of the literature and analysis of 15 cases. Medicine (Baltimore) 1957;36:397–405.
7. Scadding G, Hinson K. Diffuse fibrosing alveolitis (diffuse interstitial fibrosis of the lungs): Correlation of histology at biopsy and prognosis. Thorax 1967;22:291–303.
8. Liebow A. Definition and classification of interstitial pneumonias in human pathology. Prog Respir Dis 1975;8:1–39.
9. Katzenstein A-L, Myers J. Idiopahtic pulmonary fibrosis: A clinical relevance of pathologic classification. Am J Respir Crit Care Med 1998;157:1301–1318.

10. Nagai S, Kitaichi M, Izumi T. Classification and recent advances in idiopathic interstitial pneumonia. Curr Opin Pulm Med 1998;4:256–260.
11. Myers J. NSIP, UIP and the ABC of idiopathic interstitial pneumonias. Eur Respir J 1998;12:1003–1014.
12. Ryu J, Colby T, Hartman T. Idiopathic pulmonary fibrosis: Current concepts. Mayo Clin Proc 1998;73:1085–1101.
13. ATS/ERS. International multidisciplinary consensus classification of the idiopathic interstitial pneumonias. Am J Respir Crit Care Med 2002;165:277–304.

# 2

# Definition, Classification, and Clinical Features

The term *interstitial lung disease* (ILD), or *diffuse parenchymal lung disease* (DPLD), comprises a number of clinical disorders that affect the alveolar structures, pulmonary interstitium, and small airways (Figures 2.1, 2.2, 2.3a, b, and 2.4a, b). These disorders include bacterial, fungal, viral, protozoal, and parasitic infections or infestations; diffuse connective tissue diseases (systemic lupus erythematosus, rheumatoid arthritis, systemic sclerosis, ankylosing spondylitis, mixed connective tissue); hypersensitivity pneumonitis or extrinsic allergic alveolitis; pneumoconiosis; drug-induced and iatrogenic syndromes; and disorders of unknown origin (e.g., sarcoidosis, idiopathic pulmonary fibrosis, Langerhans cell histiocytosis, lymphangioleiomyomatosis, and idiopathic interstitial pneumonias) (Figure 2.5). Many of these diseases are benign and self-limiting; others are chronic, progressive, irreversible, and fatal. The lung manifestation may be the one manifestation of a systemic process. Or it may be the only organ affected. All ILDs, however, have certain common clinical, radiologic, and physiologic features that should be recognized.

## 2.1. Diagnosis of ILD

### 2.1.1. History

A thorough occupational history of the patient is of paramount importance in evaluating ILD. Every occupation or job experience that the patient ever had should be recorded, including summer and part-time activities. Also, a list should be drawn of the spouse's or live-in partner's occupation because many disorders including asbestosis may be transmitted by dust brought home in clothing. History of recent or past exposure to inorganic or mineral particles or to organic dusts and animal antigens (pets) should be identified. Inquiry should be made for drugs and chemicals known to cause ILD, history of pulmonary infections (particularly HIV), immune disorders, and collagen vascular disorders. A smoking history may alter the diagnostic algorithm because many ILDs, including Langerhans cell histiocytosis, alveolar proteinosis, amiodarone toxicity, idiopathic pulmonary fibrosis, asbestosis, and Goodpasture syndrome are common in smokers, whereas nonsmokers are susceptible to sarcoidosis and hypersensitivity pneumonitis. The country of origin and recent travel history are often critical for establishing the diagnosis. A diffuse nodular interstitial roentgenographic pattern in an Indian patient is highly suggestive of tropical eosinophilia, whereas the similar picture in an Egyptian patient would point toward pulmonary schistosomiasis.

### 2.1.2. Symptoms

Dyspnea is the most frequent symptom of ILD. At first, dyspnea is evident on exercise; later it progresses to breathlessness at rest. The duration of progressive dyspnea usually

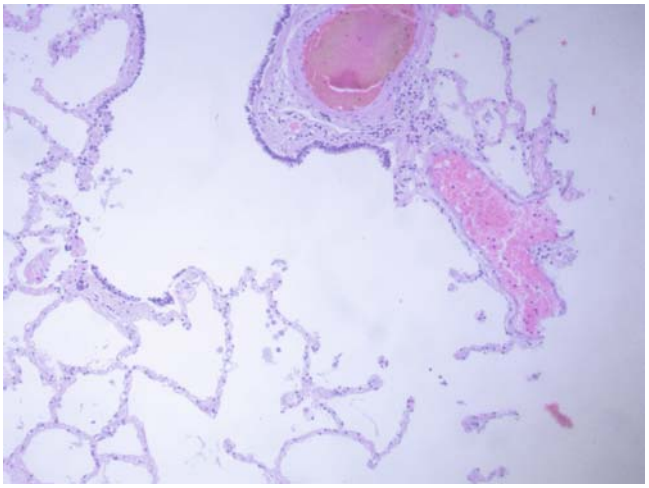

**Figure 2.1.** The structure of lung parenchyma. Lung parenchyma is composed of structures distal to the terminal bronchioles that include respiratory bronchioli, alveolar ducts, alveolar sacs, and alveolus. Normal lung histology showing terminal bronchiole and alveoli.

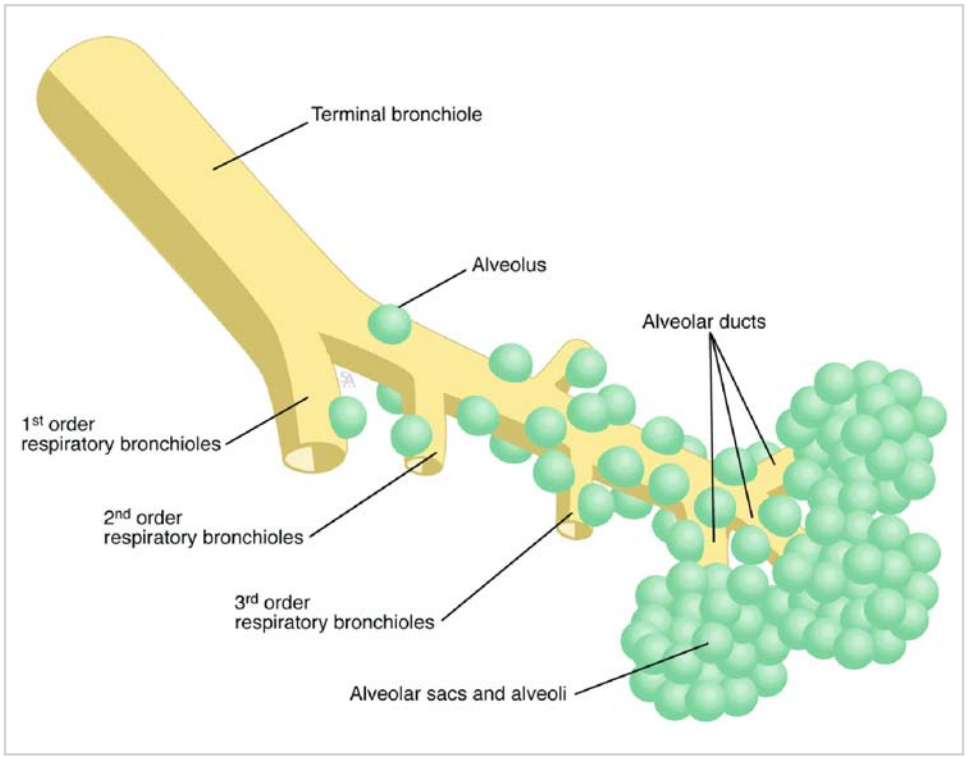


**Figure 2.2.** The structure of lung parenchyma. Acinus-terminal respiratory unit. The pulmonary acinus is composed of those structures that are distal to the terminal bronchiole.

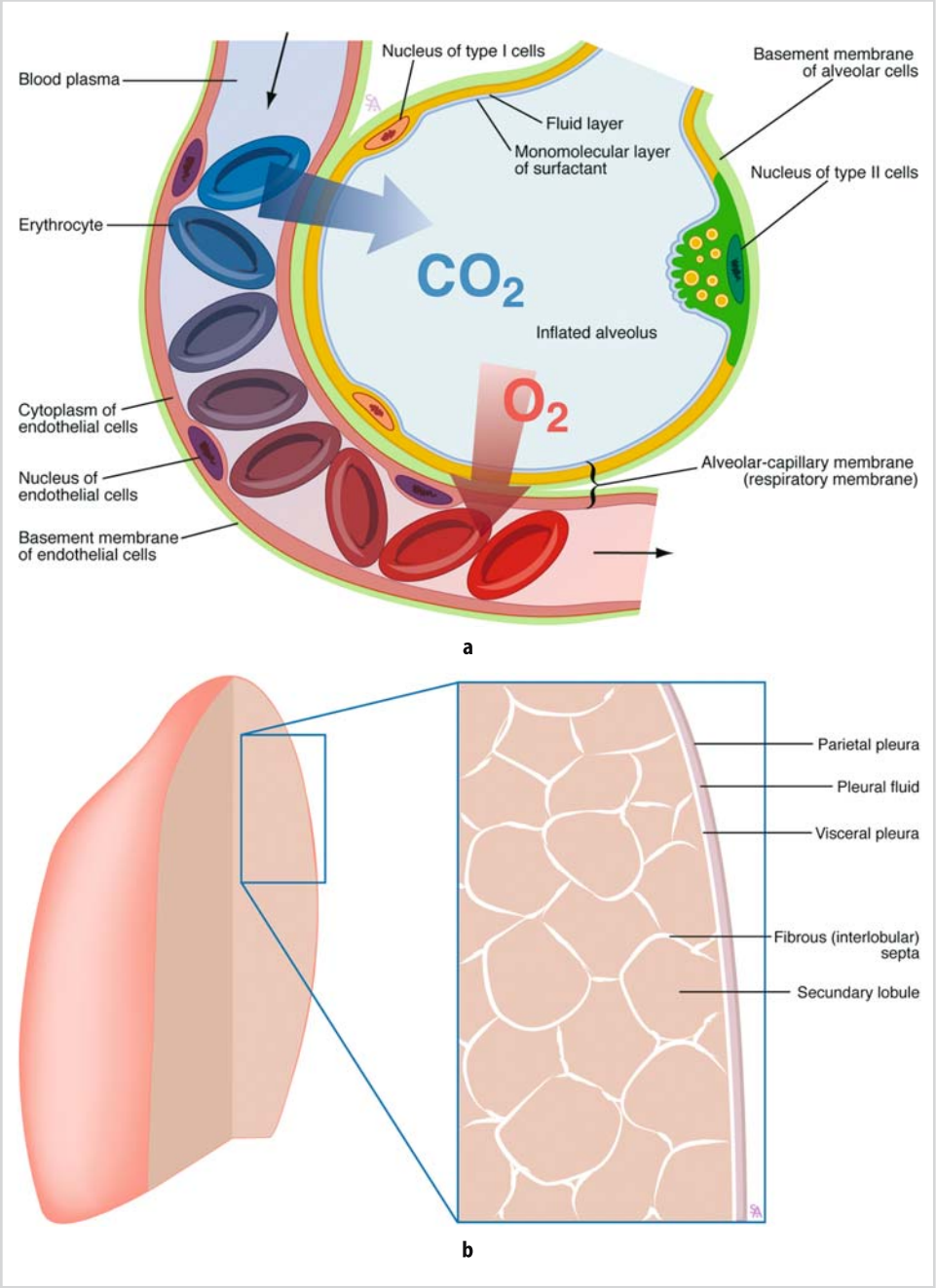


**Figure 2.3.** The structure of lung parenchyma. Alveolocapillary membrane is composed of capillary endothelium, alveolar epithelium (type I and II pneumocytes), surfactant, epithelial and endothelial basal membranes (a). The extremely thin barrier between air and capillaries allows oxygen to move from the alveoli into the blood and allows carbon dioxide to move from the blood in the capillaries into the alveoli. The pulmonary blood-gas barrier is an extraordinary bioengineering structure because of its vast area but extreme thinness. Interstitium is the integral part of the alveolocapillary membrane. It has been investigated extensively and described in detail by Weibel and associates. It is a continuous structure that runs from the visceral pleura to the hilum and follows the fiber skeleton of the lung (b). The thin alveolar walls comprise alveolar capillaries that are suspended by fiber strands and are covered by type I pneumocytes. Within the alveolar walls is a continuation of the interstitium that is in intimate contact with the alveolar basement membrane, alveolar capillaries, and epithelial cells. It contains matrix of connective tissue, elastic fibers and proteoglycans, but also other cells (fibroblasts and lymphoid cells) and represents a potential space.

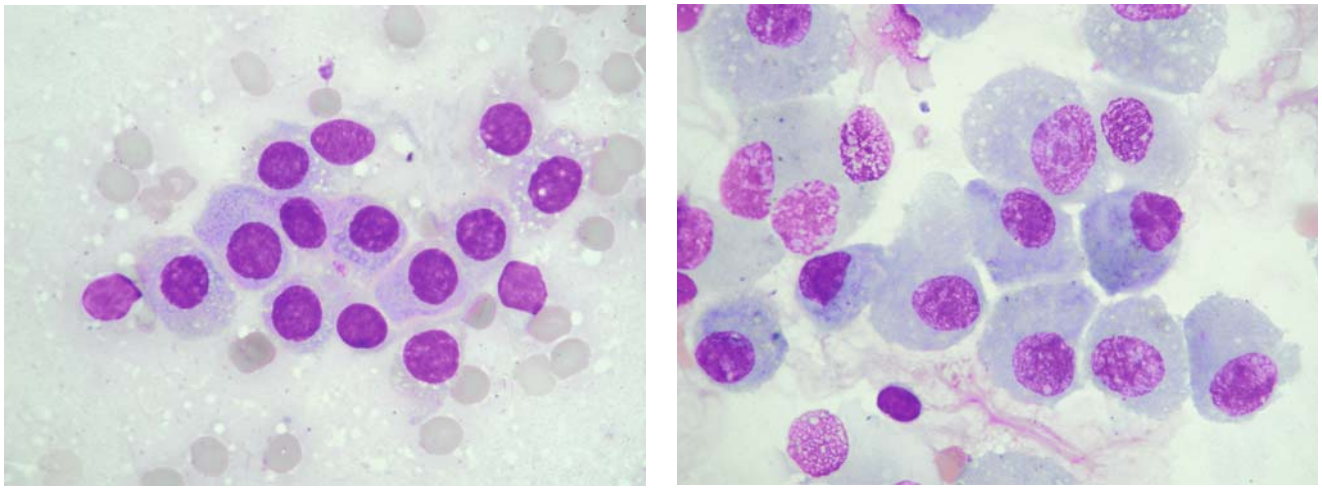

a b

**Figure 2.4.** The structure of lung parenchyma. The numerous types of cells plant the lung parenchyma. These are type I pneumocyte, type II pneumocyte, alveolar macrophage, and neuroendocrine cell. Type II pneumocyte manufactures surfactant. Pneumocyte type II, transbronchial lung biopsy imprint cytology, original magnification ×1000, MGG stain (May-Grünwald-Giemsa) (a). Alveolar macrophages represent the main cellular host defense mechanism in the alveolar space. Cluster of macrophages, BAL fluid cytology, original magnification ×1000, MGG stain (May-Grünwald-Giemsa) (b).

ranged from months to years. Dyspnea is commonly associated with dry cough, particularly on exertion, and fatigue is frequently present. Fever, chills, and weight loss are the main symptoms in interstitial pulmonary infections but may also occur in collagen vascular disorders. The combination of fever, cough, and dyspnea in an immunosuppressed host is often due to *Pneumocystis jiroveci* pneumonitis, cytomegalovirus infection, miliary tuberculosis, or fungal infection. On the other hand, the constellation of fever, cough, chest tightness, and dyspnea that occur 4 to 6 hours after exposure to an organic dust strongly suggests hypersensitivity pneumonitis. Severe dyspnea with weight loss but without fever occurs in lymphangitic carcinomatosis, diffuse connective tissue diseases, and, rarely disseminated tuberculosis.

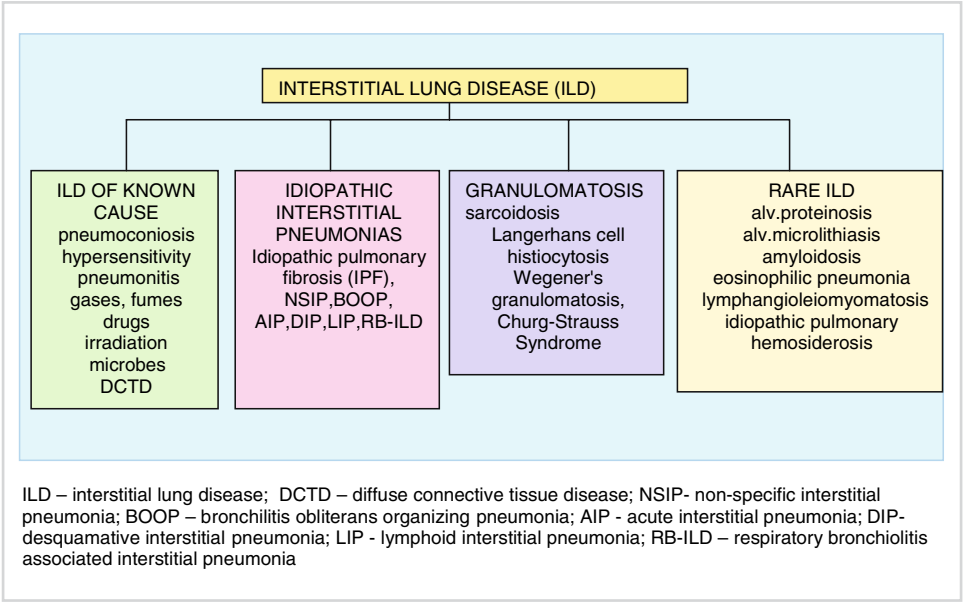


**Figure 2.5.** Classification of interstitial lung diseases. Reprinted from Classification of Interstitial Lung Disease, ATS/ERS international multidisciplinary consensus classification of the idiopathic interstitial pneumonias. Adapted from data published in ATS/ERS international multidisciplinary consensus classification of the idiopathic interstitial pneumonias. *Am J Respir Crit Care Med* 2002;165:277–304.

### 2.1.3. Signs

In 10% to 15% of the patients who have ILD, tachypnea is present. Auscultation of the lungs reveals diffuse, fine end-inspiratory crackles or rales in 60% to 90% of the patients who have idiopathic pulmonary fibrosis (IPF), asbestosis, and acute hypersensitivity. On the other hand, rales are infrequent in sarcoidosis and heard in less than 20% of the patients. Rhonchi or wheezing, present in 20% of the patients with hypersensitivity pneumonitis, are not a feature of IPF. The loud pulmonary second associated with right-sided third sound is often heard in pulmonary hypertension and right heart failure secondary to ILD. Digital clubbing is characteristically common in idiopathic pulmonary fibrosis (IPF) and asbestosis (Figure 2.6).

### 2.1.4. Extrapulmonary Features of ILD

The combination of erythema nodosum, uveitis, and parotid enlargement is an important feature of sarcoidosis. Multiorgan involvement is present in sarcoidosis, diffuse connective tissue diseases, vasculitis, Langerhans cell histiocytosis, amyloidosis, and neurofibromatosis.

### 2.1.5. Radiologic Studies

Chest roentgenogram is abnormal in more than 90% of the patients who have ILD. Often the first to be recognized, the radiographic abnormality is of paramount importance in elucidating the diagnosis. It is important to review the past chest x-ray films to assess the course and progression of the disease. Although radiographic features may not always provide the definite diagnosis, certain roentgenographic patterns are highly suggestive (Table 2.1).

In general, parenchymal shadows may be classified into four categories: normal in about 10% of the cases; ground-glass haziness; linear, nodular, reticular, or reticulonodular infiltrate; and honeycombing, representing the end-stage fibrosis (Figure 2.7a, b, c, d, e).

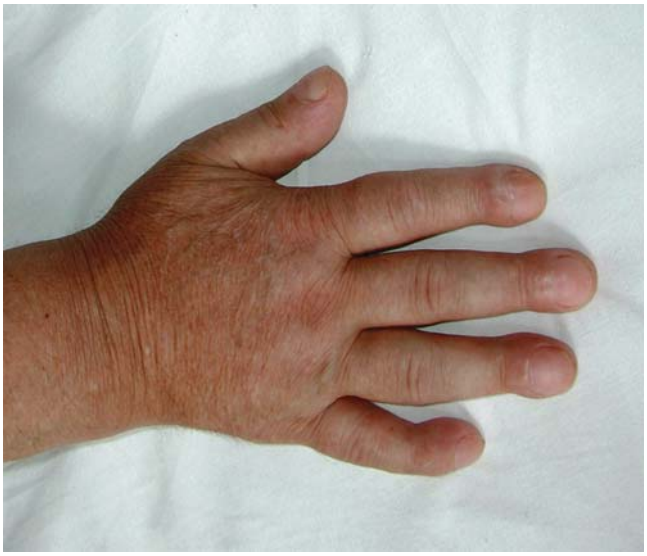

**Figure 2.6.** The figure depicts finger clubbing. Clubbing is common in IPF. Other pulmonary conditions that cause clubbing of the fingers are carcinoma, asbestosis, cystic fibrosis, and arterio-venous malformation.

**Table 2.1.** Chest roentgenographic features of interstitial lung disease.

| Hilar Adenopathy | Upper Lobe Involvement | Diffuse Involvement + Pneumothorax |
|---|---|---|
| Sarcoidosis | Tuberculosis | Langerhans cell histiocytosis |
| Lymphoma | Histoplasmosis | Lymphangioleiomyomatosis, neurofibromatosis |
| Pneumoconiosis | Coccidioidomycosis | Neurofibromatosis, sarcoidosis |
| Lung cancer | Allergic bronchopulmonary aspergillosis | Idiopathic pulmonary fibrosis |
| Tuberculosis | Sarcoidosis | Marfan syndrome |
| Coccidioidomycosis | Hypersensitivity pneumonitis | |
| Histoplasmosis | Langerhans cell histiocytosis | |
| Phenytoin-induced lung disease | Progressive massive fibrosis | |
| Talc granulomatosis | Ankylosing spondylitis | |
| Brucellosis | *Pneumocystis jerovici* pneumonitis | |
| Infectious mononucleosis | Radiation pneumonitis | |
| Amyloidosis | Marfan syndrome | |
| | Cystic fibrosis | |

## 2.1.6. High-Resolution Computed Tomography

Both high-resolution computed tomography (HRCT) and the traditional computed tomography are superior to conventional radiography in delineating the presence and extent of parenchymal involvement in ILD. HRCT is also useful in characterization of the pattern of the disease, narrowing the differential diagnosis, as a guide to the site of biopsy and as an aid in the follow-up of the patients. HRCT can help differentiate between reversible, mostly inflammatory, and irreversible presumably fibrotic changes. Reversible changes include nodules, irregularly marginated nodules, alveolar or pseudo-alveolar consolidation, and ground-glass haziness. Irreversible changes include septal or nonseptal lines, cysts, bronchiectasis, and honeycombing. HRCT is extremely useful in differentiating between two common ILDs, namely sarcoidosis and idiopathic pulmonary fibrosis (Table 2.2). HRCT due to the lack of diagnostic specificity in most cases has not replaced the need for histological confirmation of ILD.

## 2.1.7. Lung Function Tests

As a result of inflammation and fibrosis of the alveolar and the vicinal structures, the lung becomes stiff and has low lung compliance. Lung volume is reduced, diffusing capacity is impaired, and alveolar-to-arterial oxygen difference is widened either at rest or exercise or both (Figure 2.8a, b). The large airway function usually remains normal, but small airway dysfunction is often present. Airway obstruction is prominent in some interstitial lung disorders (Table 2.3). As a rule, lung function measurements correlate poorly with the degree of histopathological changes and radiographic appearance, but the tests provide a baseline value important in assessing the impact of the disease and monitoring its course. The role of exercise testing in everyday management of ILD needs to be further refined.

## 2.1.8. Laboratory and Immunologic Studies

Laboratory and immunologic tests are of limited value in establishing the cause of ILD. Only tests that are relevant to a clinical situation should be administered. Complete blood counts, sedimentation rate, C-reactive protein, total eosinophil count, screening for HIV, collagen vascular disease panel, serum calcium and angiotensin converting enzyme are some of the useful tests (Table 2.4).

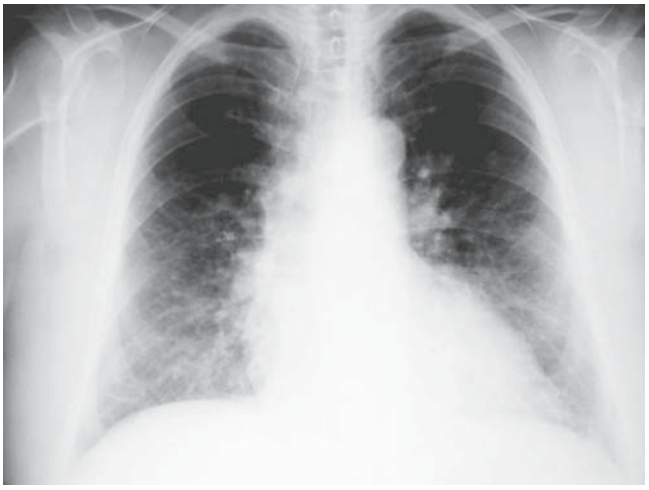

a

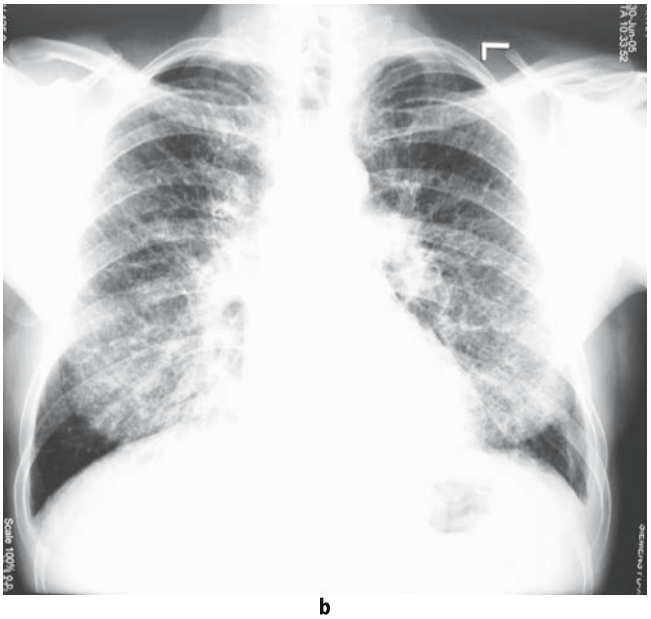

b

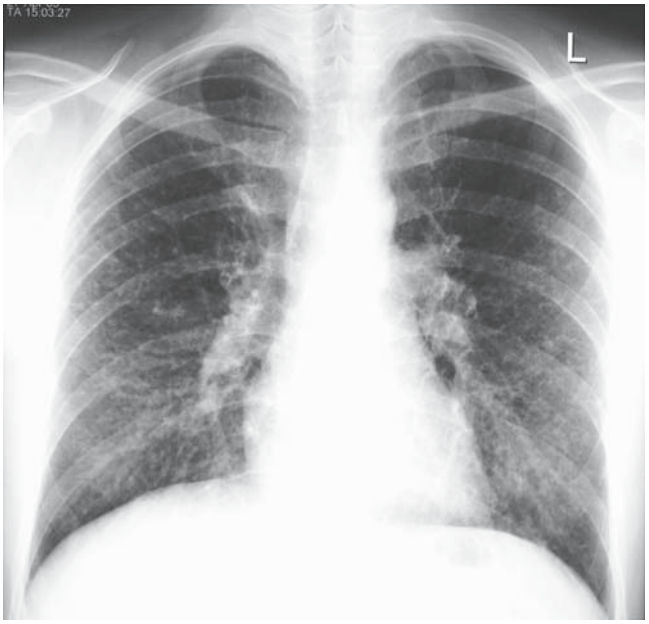

c

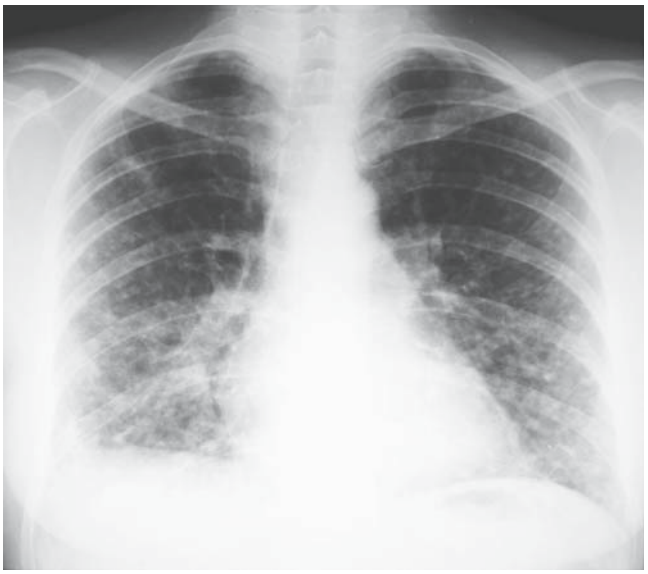

d

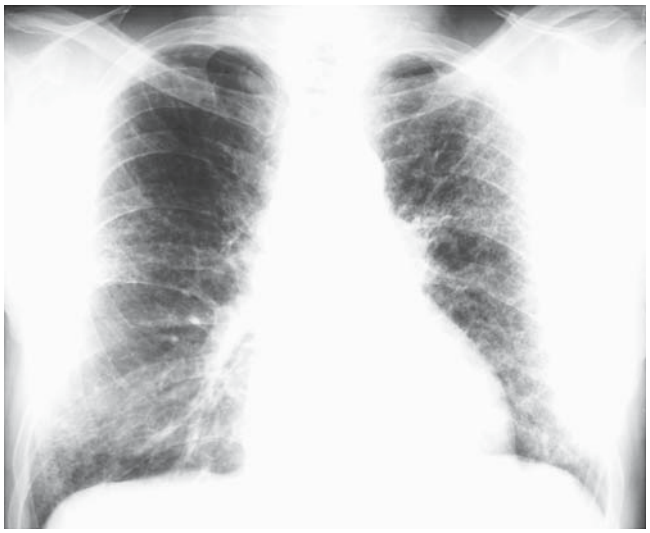

e

**Figure 2.7.** In general, parenchymal shadows by chest roentgenogram may be classified into four categories: normal in about 10% of the cases, ground-glass haziness (a), linear (b), nodular (c), reticular or reticulonodular infiltrate (d), and honeycombing (e), representing the end-stage fibrosis.

**Table 2.2.** High-resolution computed tomographic findings in sarcoidosis and idiopathic pulmonary fibrosis (IPF).

| | Sarcoidosis | IPF |
|---|---|---|
| Abnormalities | Nodular or beaded bronchovascular bundles, interlobular septa, and subpleural interstition | Irregular |
| Distribution | Central, perihilar, medullary | Peripheral, patchy, subpleural, cortical |
| Predominance | Upper lobes | Lower lobes |
| Nodules | Frequent | Rare |
| Adenopathy | Present | Absent |

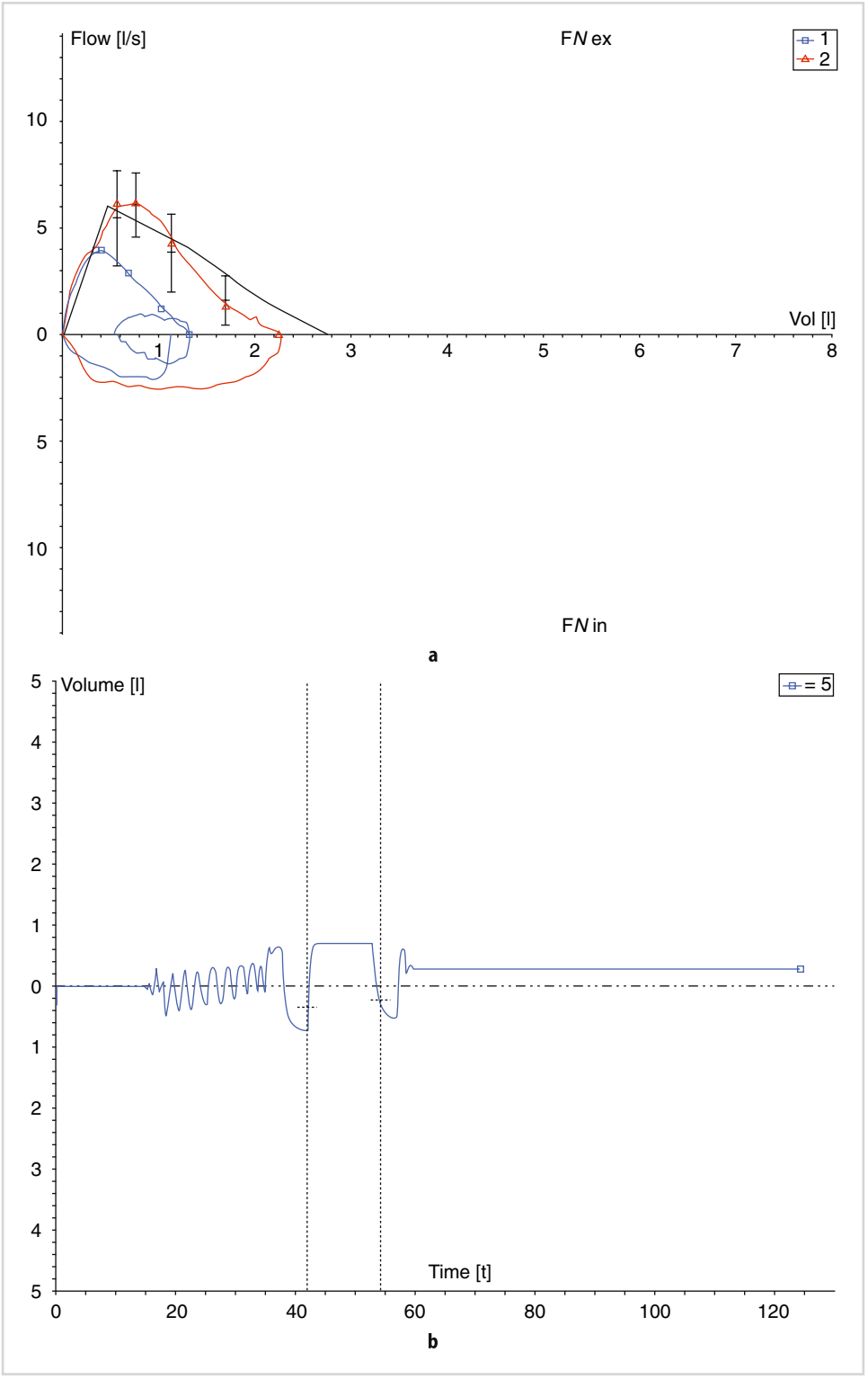


**Figure 2.8.** Physiological testing. In the ILD patient it usually reveals restrictive ventilatory changes and impaired gas exchange. Flow-volume loops before and following the corticosteroid and azathioprine therapy in a patient with ILD. Flow-volume loop shows normal shape of the expiratory (upper side) part of the loop, but whole curve is smaller than normal predicted curve. That means low forced vital capacity, seen as a fast termination of the curve, with shorter cut point (smaller volume) achieved on X-axis after forced expiration. After 8 months of treatment, flow-volume loop is no longer of restrictive pattern. Significant improvement on X-axis could be seen, due to bigger volume value, although vital capacity is still not completely normal. The lung function tests are useful not only in the recognition of restrictive disease but also they are easy to perform and a cheap follow-up (a). DLCO in interstitial lung disease often shows significantly lower value in percentage of reference value; 36% in this particular case (b). The mechanism of the hypoxemia in ILD was earlier attributed to the thickened alveolar interstitium, but it has later been recognized that the ventilation-perfusion mismatching was the major factor and that the diffusion barrier to oxygen was only important during exercise.

**Table 2.3.** Interstitial lung disease and airway obstruction.

| |
|---|
| Sarcoidosis |
| Hypersensitivity pneumonitis |
| Langerhans cell granulomatosis |
| Lymphangioleiomyomatosis |
| Tuberous sclerosis |
| Combined COPD and ILD |

## 2.1.9. Histologic Diagnosis

When and why a lung biopsy should be performed in diffuse interstitial lung disease is undefined. One should, however, attempt to obtain a lung biopsy early in the disease, particularly in a young or middle-age patient. This approach allows clinicians to get lung tissue before end-stage fibrosis obliterates any identifying disease hallmarks. Transbronchial biopsy is useful in the diagnosis of sarcoidosis, alveolar proteinosis, miliary tuberculosis, and *Pneumocystis* pneumonia (Figure 2.9). The procedure has limitations because the amount of tissue obtained is often insufficient for extensive diagnostic studies. Open lung biopsy, the gold standard for ILD, is being replaced by video-assisted thoracoscopic (VAT) lung biopsy. The diagnostic accuracy of thoracoscopic lung bi opsy is equivalent to open lung biopsy. Furthermore, perioperative morbidity, length of hospital stay, and duration of chest pain are significantly lower in patients who undergo thoracoscopic lung biopsy. Usually, idiopathic interstitial pneumonias, Langerhans cell granulomatosis, and lymphangioleiomyomatosis need either a thoracoscopic or an open lung biopsy for diagnosis.

## 2.1.10. Bronchoalveolar Lavage

Bronchoalveolar lavage (BAL; Figure 2.9) has expanded our understanding of the pathogenesis of many interstitial lung diseases including sarcoidosis, hypersensitivity pneumonitis, and idiopathic interstitial fibrosis, but the clinical indications and use of the test is far from established. In patients who have idiopathic pulmonary fibrosis, the BAL specimens contain more neutrophils and eosinophils than do normal control specimens. BAL lymphocytosis is a feature of sarcoidosis, hypersensitivity pneumonitis, drug reactions, and collagen vascular diseases (Table 2.5). BAL-IgG levels are increased in idiopathic pulmonary fibrosis, whereas IgM is increased in hypersensitivity pneumonitis

**Table 2.4.** Commonly used laboratory tests in ILD.

| Test | Finding | Disease |
|---|---|---|
| Complete blood count | Leukopenia | Sarcoidosis, brucellosis, tuberculosis |
| | Eosinophilia | Vasculitis, parasites, drug-induced disease |
| Sedimenation rate | Elevated | Collagen vascular disease, lymphangitic carcinomatosis |
| Sputum/body fluids | Acid-fast bacillus, fungi | Histoplasmosis, disseminated tuberculosis<br>Coccidioidomycosis |
| Kveim-Siltzbach tests | Positive | Sarcoidosis |
| Angiotensin converting enzyme | Elevated | Sarcoidosis |
| Antineutrophilic cytoplasmic antibody | Positive | Vasculitis |
| Serum alkaline phosphatase | Elevated | Sarcoidosis |
| Serum calcium | Elevated | Carcinomatosis, sarcoidosis |
| Serum lactic dehydrogenase | Elevated | *Pneumocystis jerovici* pneumonia, alveolar proteinosis |
| Precipitin antibody (IgG) | Present | Hypersensitivity pneumonitis |
| Beryllium lymphocyte transformation | Positive | Berylliosis |
| Antineutrophilic cytoplasmic antibody | Positive | Wegener granulomatosis |

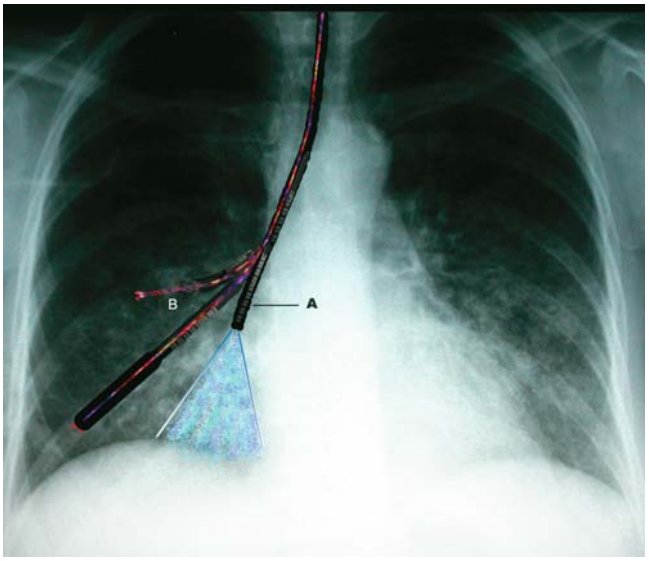


**Figure 2.9.** Bronchoalveolar lavage procedure. The fluid (saline, 200 ml) is introduced most often into the middle lobe following the wedging of the bronchoscope. After the lavage is completed, the recovery of the remaining lung lavage fluid follows. It is important that the accompanying laboratories are prepared to process this valuable material. The most important is the cell profile analysis (a). Transbronchial lung biopsy: plain radiograph shows biopsy forceps introduced into the distal branching of the bronchi (b).

patients. Both the percentage of inflammatory cells and immunoglobulins in BAL decrease during treatment with corticosteroids.

Diagnostic algorithm of interstitial lung diseases is depicted in Figure 2.10.

## 2.1.11. Differential Diagnosis

In the differential diagnosis of interstitial pulmonary disorders, sarcoidosis, collagen vascular diseases, idiopathic pulmonary fibrosis, and bronchiolitis obliterans organizing pneumonitis are the most common and are responsible for about two thirds of all cases. Other entities include drug-induced lung disease, pulmonary infiltration with

**Table 2.5.** Lung lavage cell profiles in common interstitial lung diseases.

| Disease | Alveolar Macrophages | Lymphocytes | Neutrophils | Eosinophils | Other Cells | CD4/CD8 Ratio |
|---|---|---|---|---|---|---|
| Sarcoidosis | | ++ | =/+ | =/+ | | ↓/=↑↑ |
| Idiopathic pulmonary fibrosis | | + | ++ | + | | = |
| BOOP | Foamy | + | + | + | | ↓ |
| Nonspecific interstitial pneumonia | | + | + | + | | ↓ |
| RB-ILD/DIP | Aveolar macrophages contain cigarette pigment | = | ++ | = | | = |
| Acute interstitial pneumonia | | = | ++ | = | Atypical pneumocytes type II, amorphous material: fragments of hyaline membranes | = |
| Hypersensitive pneumonitis | Foamy | ++ | + | =/+ | Sporadically plasma cells and mastocytes | ↓/= |
| Drug-induced pneumonitis | Foamy | ++ | + | + | Sporadically plasma cells and mastocytes | ↓/= |
| Connective tissue disease | | + | + | =/+ | | ↑/=/↓ |
| Eosinophilic pneumonia | | + | = | ++ | Sporadically plasma cells | ↓ |
| Diffuse alveolar hemorrhage | Siderophages | =/+ | + | =/+ | | = |
| Alveolar proteinosis | Foamy | + | = | = | | ↓ |
| Langerhans cell histiocytosis | | = | = | =/+ | Langerhans cells CD1a and protein S-100 positive | = |

BOOP, bronchiolitis obliterans organizing pneumonia; RB-ILD/DIP, respiratory bronchiolitis associated interstitial lung disease.
↓ CD4/CD8 Ratio decreases; ↑ CD4/CD8 Ratio increases; = CD4/CD8 Ratio stayes within normal range.

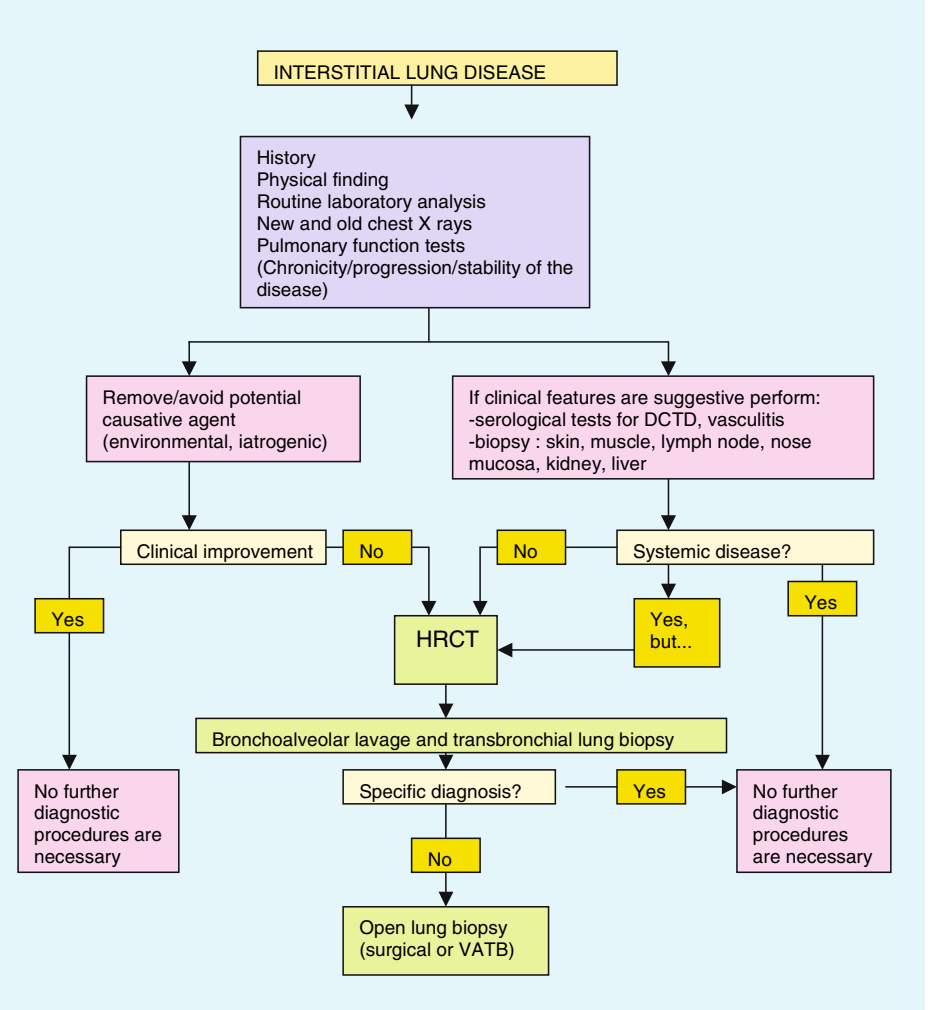


**Figure 2.10.** Diagnostic algorithm of interstitial lung diseases. Reprinted from Raghu G: Interstitial lung diseases: A clinical overview and general approach. In Fishman, Elias, Grippi, Kaiser, Senior (Eds), *Fishman's Pulmonary Diseases and Disorders*, 3rd edition. McGraw-Hill, pp. 1037–1053, 1997. © 1998 with permission of The McGraw-Hill Companies.

eosinophilia syndrome, hypersensitivity pneumonitis, Langerhans cell granulomatosis, and other granulomatous and nongranulomatous infections.

## Bibliography


1. Sharma O, Chan K. Interstitial Lung Disease. Current Practice of Medicine 1999;2:1647–1660.
2. Weibel ER. Pathway for Oxygen. Cambridge, MA: Harvard University Press; 1984.
3. Weibel ER, Gil J. Structure-function relationships at the alveolar level. In: West JB, Ed. Bioengineering Aspects of the Lung. New York: Marcel Dekker; 1977:1–88.
4. Katzenstein A, Myers J. Idiopathic pulmonary fibrosis: Clinical relevance of pathologic classification. Am J Resp Crit Care Med 1998;157:1301–1315.
5. Nagai S, Kitaichi.M, Izumi T. Classification and recent advances in idiopathic interstitial pneumonia. Curr Opin Pulm Med 1998;4:256–260.
6. Selman M, Vargas M. Airway involvement in hypersensitivity pneumonitis. Curr Opin Pulm Med 1998;4:9–15.
7. Drent M, Jacobs JA. Bronchoalveolar lavage. In: Baughman RP, du Bois R, Lynch JP, Wells AU, Eds. Diffuse Lung Disease. A Practical Approach. London: Arnold; 2004:56–64.
8. British Thoracic Society Recommendations on the Diagnosis and Assessment of Diffuse Parenchyma Lung Disease. Thorax 1999;54(Suppl.1):1–30.
9. Raghu G. Interstitial lung disease: A clinical overview and general approach. In: Fishman AP, Ed. Fishman's Pulmonary Diseases and Disorders, 3rd ed. New York: McGraw-Hill; 1998;I:1037–1053.
10. Lynch D. Imaging of diffuse parenchymal lung disease. In: Schwartz MI, King TE, Eds. Interstitial Lung Disease, Fourth Ed. Hamilton: BC Decker; 2003:75–113.

# 3

# Radiology and Nuclear Imaging in Interstitial Lung Disease

Currently, the following techniques are used to support the diagnosis, assess the severity, and monitor the course and response to treatment in patients with interstitial lung disease:

1. Gallium-67 scanning
2. Thallium-201 imaging
3. Positron emission tomography (PET)
4. Magnetic resonance imaging (MRI)
5. High-resolution computed tomography (HRCT)

*Gallium-67 citrate* is a radiopharmaceutical agent that is injected intravenously. It is excreted predominately by the gastrointestinal tract. Gallium selectively accumulates in areas of infection, inflammation, and neoplasm. The test has been used to evaluate adenopathy and parenchymal disease caused by sarcoidosis. Leung et al. showed a significant correlation between the intensity of gallium uptake and the extent of nodular disease or parenchymal consolidation. It is also helpful in assessment of the extent of extrathoracic sarcoidosis, and it could also be of diagnostic value if Panda or Lambda signs are detected (Figure 3.1).

*Thallium-201 chloride*, another radiopharmaceutical agent, is occasionally used in diagnosing pulmonary disease. It is most often used for cardiac imaging, for instance if myocardial sarcoidosis is suspected. It also accumulates in active neoplastic tissue. In an HIV patient an irregular reticulo-nodular-interstitial thallium uptake strongly suggests Kaposi sarcoma.

*Positron emission tomography* using fluorodeoxyglucose is helpful in detecting metabolically active lesions, neoplasms, infections, and noninfectious inflammation. Unfortunately, PET has had little success in evaluating interstitial lung disease.

*Magnetic resonance imaging*, unlike nuclear imaging or computed tomography, does not use ionizing radiation. It uses radiofrequency energy and an external magnetic field to induce signal from mobile protons in the body (usually hydrogen in water, fat, and other biomolecules). Large lesions such as lung carcinoma and pneumonia are easily visualized with MRI, but the subtle findings of interstitial lung disease are generally beyond MRI resolution. MRI, however, has been used successfully in the evaluation of asbestosis and progressive massive fibrosis due to silicosis. MRI delineates the extrapulmonary manifestations of interstitial lung disease including pleural plaques and mediastinal adenopathy.

*High-resolution computed tomography* is the most useful technique for evaluating interstitial lung disease. The procedure uses very-thin-section (1.0 to 1.5 mm) tomography and constructs images on a computer with a high spatial frequency reconstruction algorithm. Although HRCT is done without intravenous contrast agents, some institutions prefer to perform conventional computed tomography of the chest immediately after HRCT. This allows for the diagnosis of other lesions, particularly lung cancer that might coexist with interstitial lung fibrosis.

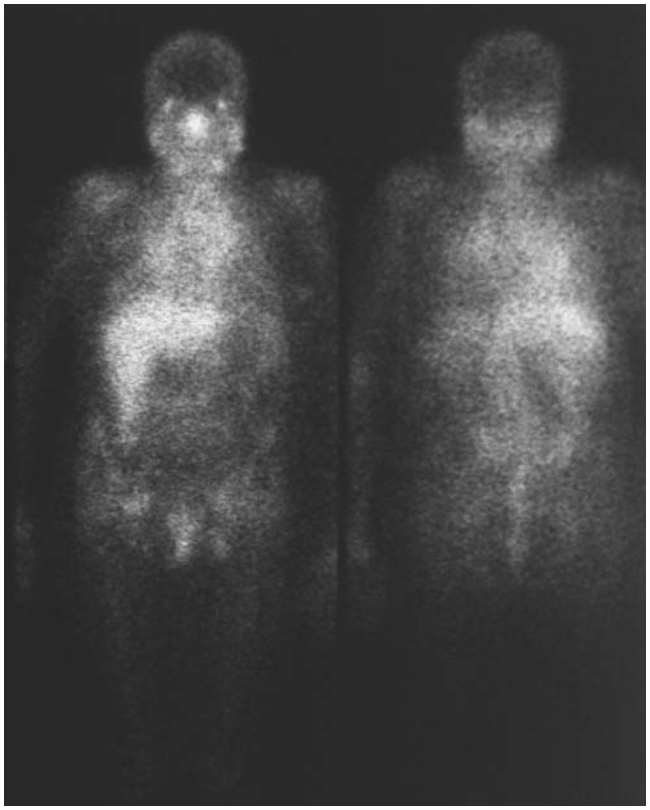

**Figure 3.1.** Gallium-67 total body scan showing accumulation in the lachrymal glands, parotid glands (positive Panda sign), and hilar lymph nodes (positive Lambda sign).

HRCT is the only radiological method that can visualize details of the secondary pulmonary lobule, the smallest lung unit that is covered with connective tissue layer. HRCT interpretation depends on understanding of its anatomy (Figure 3.2). The HRCT features of interstitial lung disease include intra- (Figure 3.3) and interlobular septal thickening (Figure 3.4), nodularity (Figure 3.5a, b), central peribronchovascular thickening (Figure

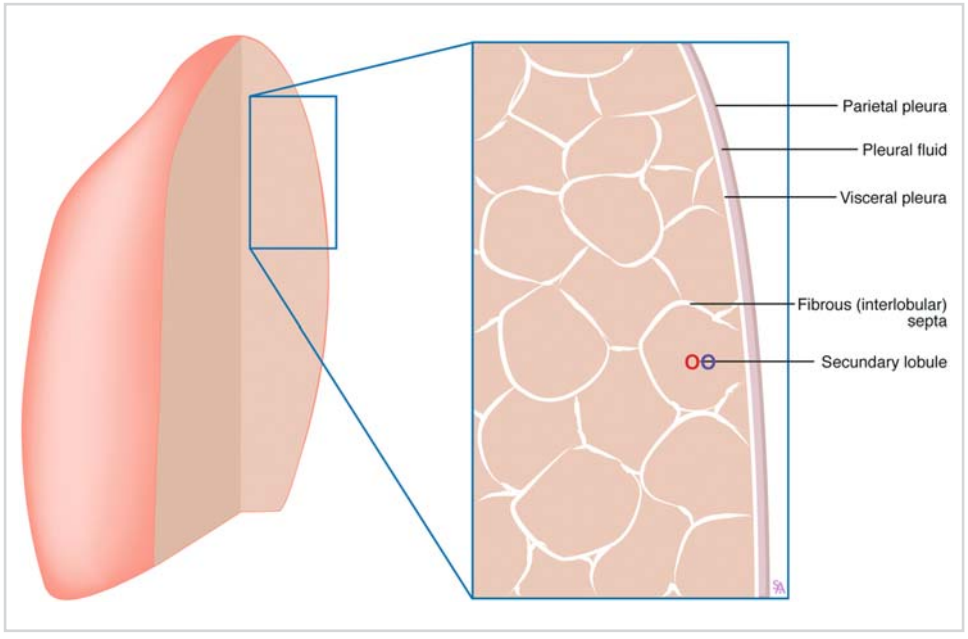


**Figure 3.2.** Scheme of secondary pulmonary lobule showing core structures, centrilobular arteries and bronchioli, and fibrous septa. These septa are sheets of connective tissue that form the boundaries of the secondary lobule that incorporates veins and the lymphatics. Lymphatics are present within the septal and centrilobular structures (not visualized with HRCT). The respiratory bronchioles, alveolar ducts, and alveoli occupy the space between the core and septal structures.

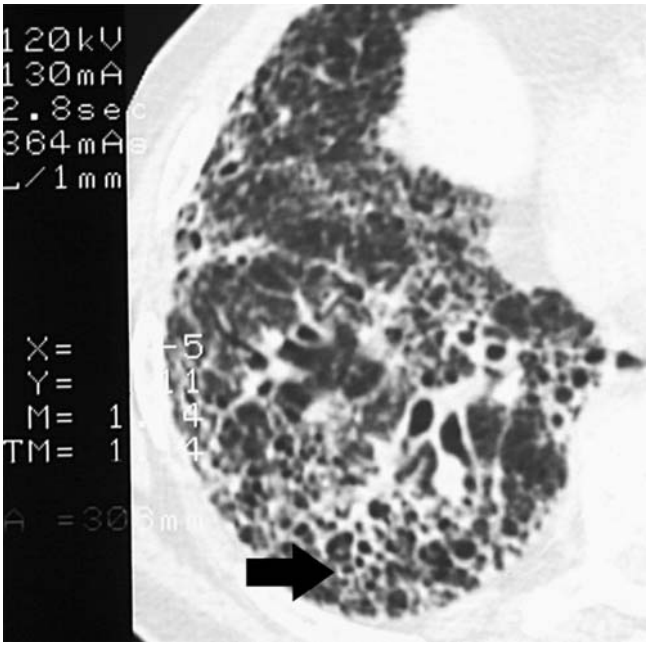


**Figure 3.3.** Intralobular thickening in idiopathic pulmonary fibrosis.

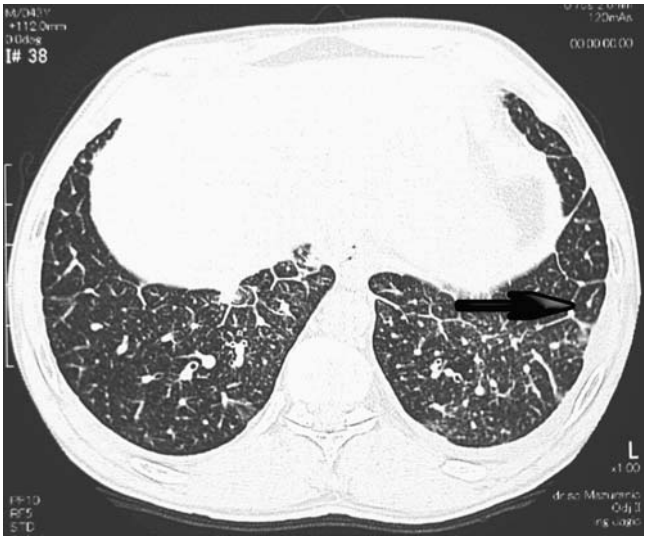


**Figure 3.4.** Interlobular, septal thickening in a patient with lymphangitic carcinomatosis.

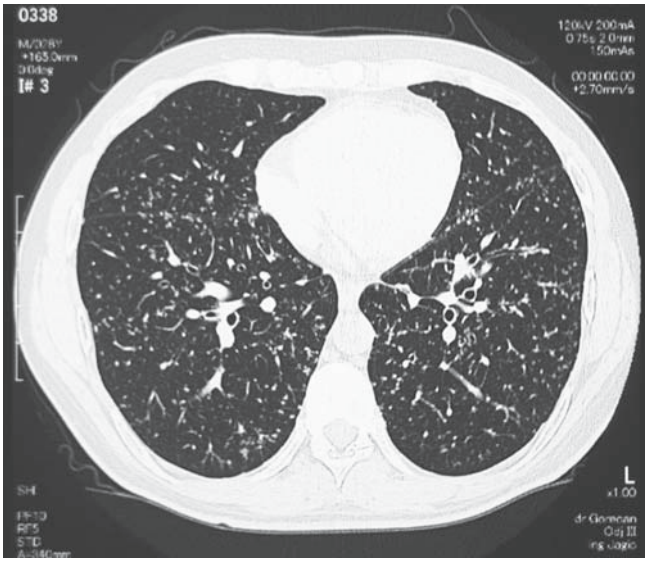


**a**

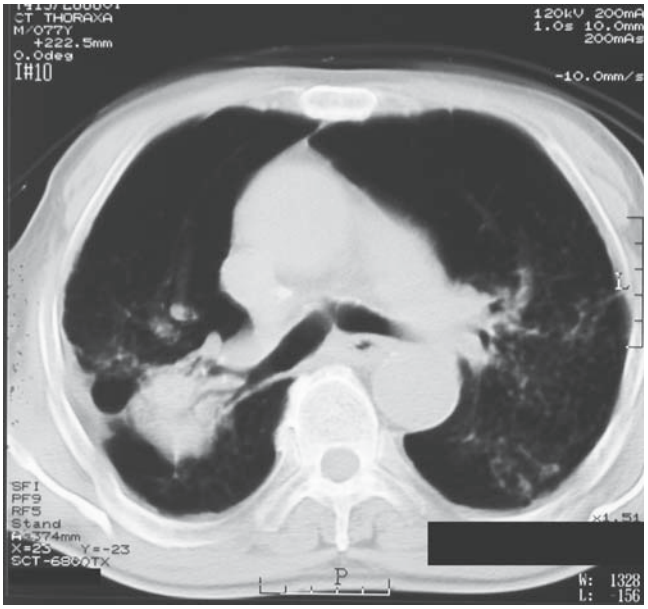


**b**

**Figure 3.5.** Small nodules in a patient with sarcoidosis (a) and large nodules in a patient with Caplan syndrome (b).

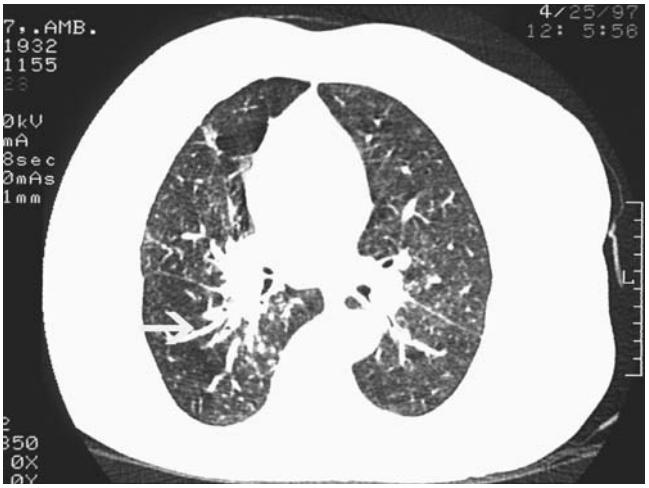


**Figure 3.6.** Consolidations and micronodules along the bronchovascular bundles in a patient with sarcoidosis.

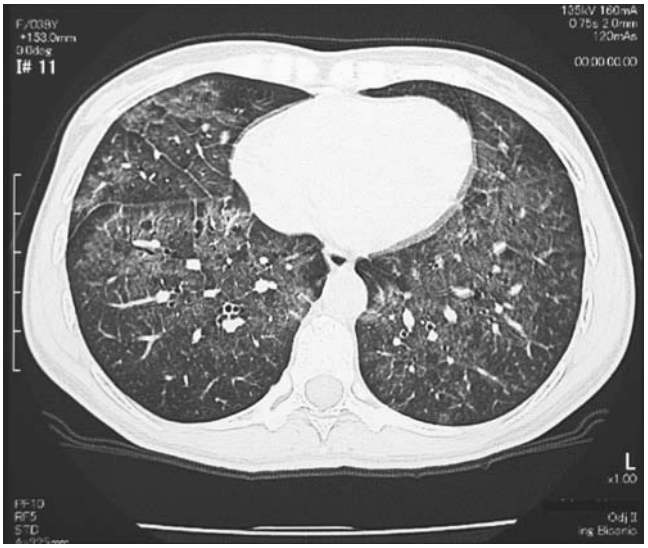


**Figure 3.7.** Ground-glass attenuation in acute hypersensitive pneumonitis.

3.6) with or without "beading," and the classic ground-glass attenuation (Figure 3.7) or consolidation (Figure 3.8). Ground-glass opacity signifies a hazy increase in lung opacity (compared with density of normal lung) not associated with obscuration of underlying vessels. Consolidation is an increase in lung opacity that results in obscuration of blood vessels. The characteristic pattern in IPF is multiple peripheral small cystic spaces or *honeycombing* (Figure 3.9), whereas in lymphangioleiomyomatosis and Langerhans cell histiocytosis, the lung parenchyma is studded with multiple, uniformly distributed thin-walled delicate cysts (Figure 3.10), sometimes forming bizarre patterns. A HRCT finding in most common interstitial lung diseases is shown in Table 3.1.

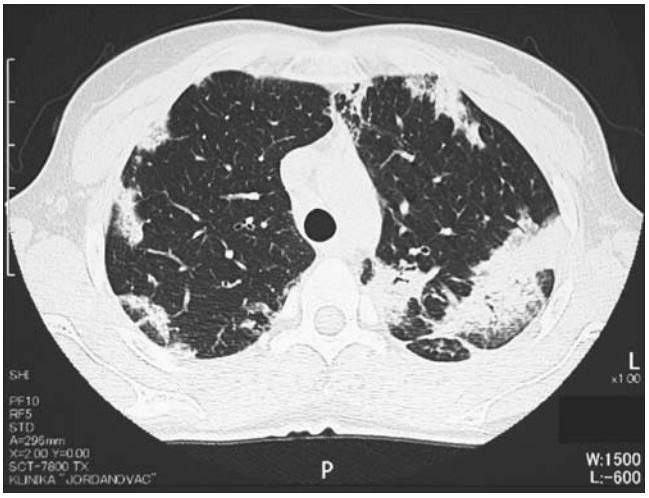


**Figure 3.8.** Consolidation in a patient with Churg-Strauss syndrome.

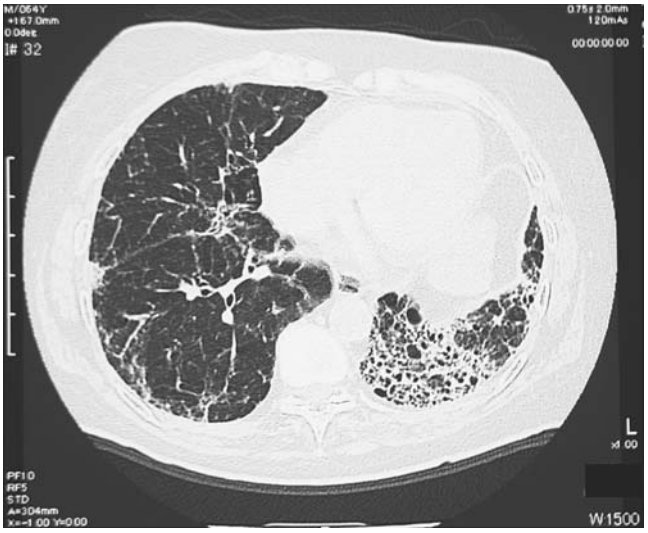


**Figure 3.9.** Honeycombing in idiopathic pulmonary fibrosis.

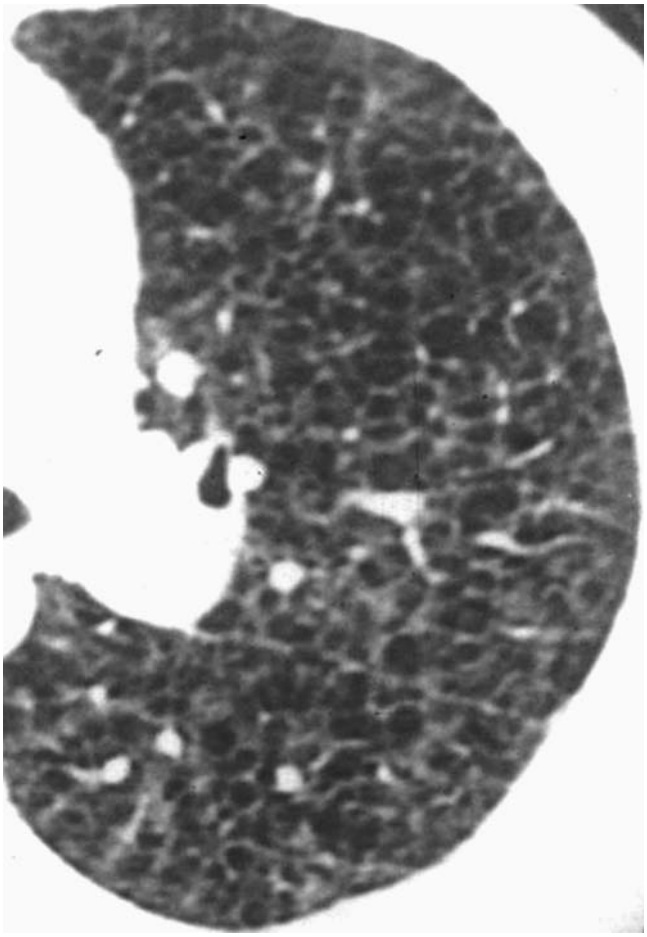

**Figure 3.10.** Uniformly distributed thin-walled delicate cysts in lymphangioleiomyomatosis (LAM).

**Table 3.1.** HRCT finding in most common interstitial lung diseases.

| Pattern | Disease |
|---|---|
| Nodules | Sarcoidosis, military tuberculosis, fungal infections, silicosis, coal worker's pneumoconiosis, asbestosis, bronchiolitis, HP, LCH, metastatic disease |
| Lines (thickened septa, intralobular or reticular lines) | IPF, lymphangitic carcinomatosis, DCTD, asbestosis, sarcoidosis, PAP |
| Ground glass | Hypersensitive pneumonitis, DIP, BOOP, AIP, DAH, PAP, eosinophilic pneumonia, drug toxicity |
| Consolidation | BOOP, eosinophilic pneumonia, bronchoalveolar carcinoma, sarcoidosis |
| Lung cysts | LAM, LCH, LIP |
| Honeycombing | IPF/UIP, DCTD, asbestosis, sarcoidosis, HP |
| Decreased lung attenuation | Pulmonary embolism, constrictive bronchiolitis |
| Mosaic pattern | Constrictive bronchiolitis, pulmonary thromboembolism |

HP, hypersensitive pneumonitis; LCH, Langerhans cell histiocytosis; IPF, idiopathic pulmonary fibrosis; DCTD, diffuse connective tissue disease; PAP, pulmonary alveolar proteinosis; DIP, desquamative interstitial pneumonia; BOOP, bronchiolitis obliterans organizing pneumonia; AIP, acute interstitial pneumonia; DAH, diffuse alveolar hemorrhage; LAM, lymphangioleiomyomatosis.

## Bibliography


1. Wilcox A. Advances in radiology for interstitial lung disease. Curr Opin Pulm Med 1999;5:278–263.
2. Leung A, Brauner M, Caillat-Vigneron N, Valeyre D, Grenier P. Sarcoidosis activity: Correlation of HRCT findings with those of gallium-67 scanning, broncho-alveolar lavage, and serum angiotensin-converting enzyme assay. J Comput Assist Tomogr 1998;22:229–234.
3. Bekkelund S, Aasebo U, Pierre-Jerome C, Holmboe J, Magnetic resonance imaging of the thorax in the evaluation of asbestosis. Eur Respir J 1998;11:194–197.
4. Pipavath S, Godwin JD. Imaging of interstitial lung disease. Clin Chest Med 2004;25:455–465.
5. Zompatori M, Bna C, Poletti V, Spaggiari E, Ormitti F, Calabro E, Tognini G, Sverzellati N. Diagnostic imaging of diffuse infiltrative disease of the lung. Respiration 2004;71:4–19.

# 4

# Sarcoidosis

Sarcoidosis, a multisystem disease, occurs worldwide. The disease has a high prevalence rate in Scandinavian countries, England, Ireland, and North America, whereas in the United States, sarcoidosis shows a predilection for African Americans. Women outnumber men, particularly in Eastern European countries. The disease most commonly occurs in the third and fourth decades of life; it is rare in children and the elderly.

Because of its multisystem nature, sarcoidosis often appears in the offices and clinics of general practitioners or family physicians, internists, chest physicians, cardiologists, dermatologists, ophthalmologists, and practitioners of other specialties (Table 4.1). In the past, syphilis was known as *the great masquerader*; now sarcoidosis may be called *la petite simulatrice*. What *causes* sarcoidosis remains unknown. A recent study found few environmental or occupational antigens playing a significant role. Agricultural employment, exposures to insecticides and pesticides at work, molds and musty odors are some exposures with positive association. Others have linked mycobacterial and propionibacterial organisms with sarcoidosis. The principal immunological alterations in the disease include peripheral depression of delayed-type hypersensitivity, imbalance of OK T4 : T8 subsets, an influx of T4 helper cells and Th1 cytokines to the sites of granuloma formation, hyperactivity of B cells, and presence of immune complexes. It appears that in genetically predisposed individuals, sarcoidosis is a manifestation of a genetically determined enhanced Th1 immune response to yet unknown microbial pathogen/s. The *diagnosis* of sarcoidosis is based on the following criteria.

*1. Recognize the clinical picture of sarcoidosis.* Lungs are the most commonly affected organs; more than 90% of the patients have an abnormal chest radiography. Other commonly involved organs include the skin (30%) (Figure 4.1a, b, c, d, e, f, g), eyes (25%) (Figure 4.2a, b, c, d, e), liver and spleen (20%) (Figures 4.3a, b), and cardiac (Figure 4.4a, b) and nervous system (Figure 4.5a, b) in about 5% each. Lymph node, salivary gland, lachrymal gland (Figure 4.6a, b, c), musculoskeletal and joint sarcoidosis (Figure 4.7a, b, c, d) is frequently seen.

Hypercalcemia is seen in about 10% of the patients, whereas hypercalciuria is three times more common.

About 20–50% of the patients complain of dyspnea, cough, chest tightness or pain. Blurring of vision, red-eye, photophobia, and loss of visual acuity occur in less than 20% of the patients. Lofgren syndrome, a combination of erythema nodosum and bilateral hilar adenopathy, is a manifestation of acute sarcoidosis and is seen mainly in Caucasian patients. The combination of bilateral parotid gland enlargement, uveitis, and facial nerve involvement is called *Heerfordt syndrome*. Lupus pernio, a typical skin lesion of chronic sarcoidosis, is often associated with bone lesions. Fatigue, polyuria, thirst, arthritis, heart block, mono- or polyneuritis, muscle weakness, or anemia may occur.

*2. Recognize the chest radiography abnormality.* Because the intrathoracic involvement may remain asymptomatic, the disease is usually discovered on a routine chest x-ray film. There are four radiographic stages of intrathoracic sarcoidosis.

**Table 4.1.** Clinical presentations of sarcoidosis.

| | | |
|---|---|---|
| Internist<br>Fever, arthritis, weight loss, parotid enlargement, lymphadenopathy | Chest Physician<br>Cough, dyspnea, abnormal x-ray, chest pain | Radiologist<br>Bilateral hilar adenopathy, lung infiltrate |
| Ophthalmologist<br>Red eye, lacrimal enlargement, papilledema | Rheumatologist<br>Arthritis, bone cysts, myopathy | Dermatologist<br>Erythema nodosum, lupus pernio, keloid |
| Endocrinologist<br>Diabetes insipidus, hypercalcemia | Neurologist<br>Cranial nerve palsies, meningitis, neuritis, headache | Cardiologist<br>Heart-block, dyspnea, heart failure |
| Hematologist<br>Anemia, leukopenia, enlarged spleen, thrombocytopenia | Nephrologist<br>Nephrocalcinosis, renal failure, hypercalciuria | Gastroenterologist<br>Gastric granuloma, hepatic granuloma, raised serum alkaline phosphatase |

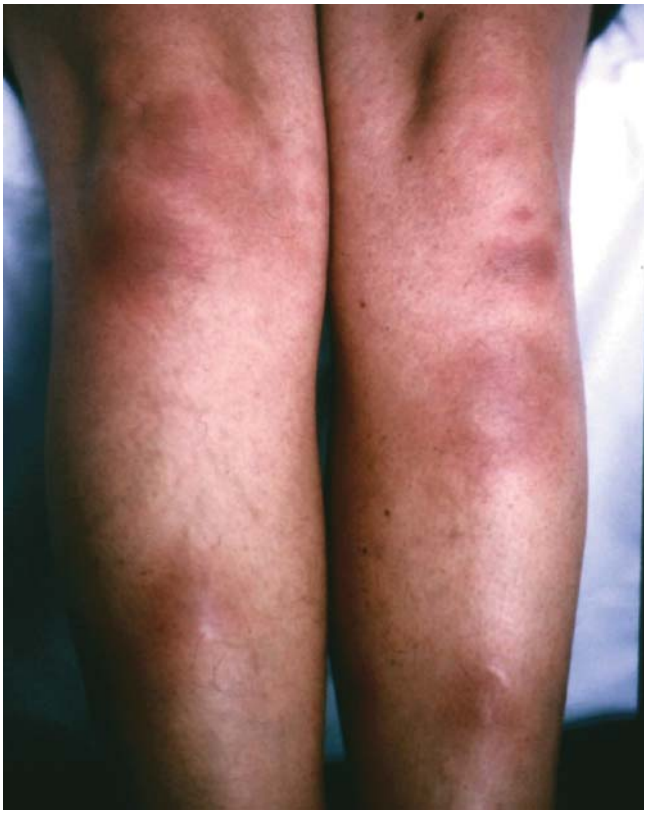

a

b

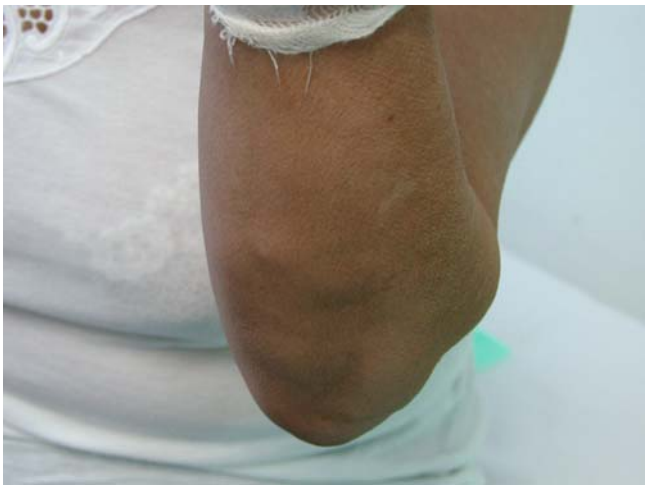

c

**Figure 4.1.** Cutaneous sarcoidosis. Erythema nodosum is the most common nonspecific manifestation of sarcoidosis (a). Skin plaques of the knee and the scar due to biopsy in a patient with chronic sarcoidosis (b). Subcutaneous nodules are also a feature of chronic sarcoidosis (c). Lupus pernio, a chronic skin sarcoidosis causing grave cosmetic problems. The lesions regressed following methotrexate therapy (d). Scar sarcoidosis in a patient who had corrective thoracotomy due to pectus excavatum (e). Fine-needle aspiration of the skin lesion shows granulomatous reaction: epitheliod cells (f), multinucleated giant cell of Langhans type (g), and some lymphocytes. Magnification ×200, MGG stain (May-Grünwald-Giemsa) (f).

(continued)

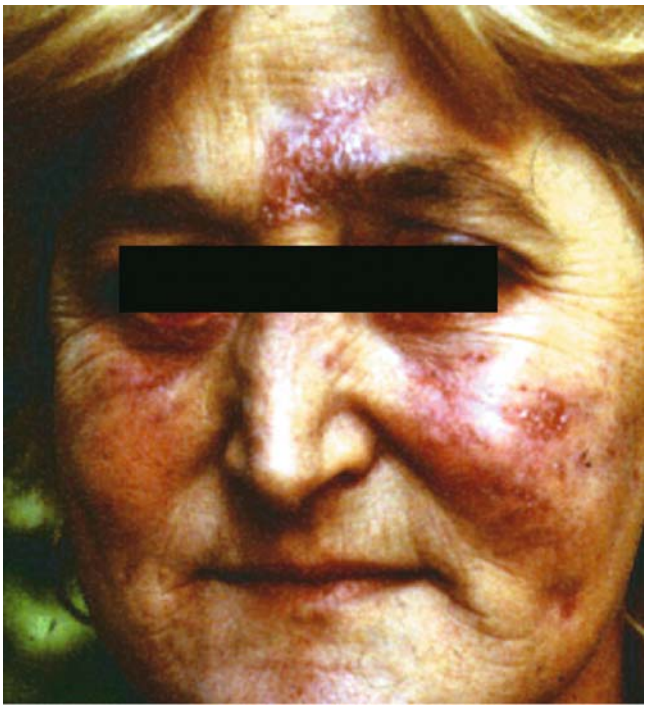

d

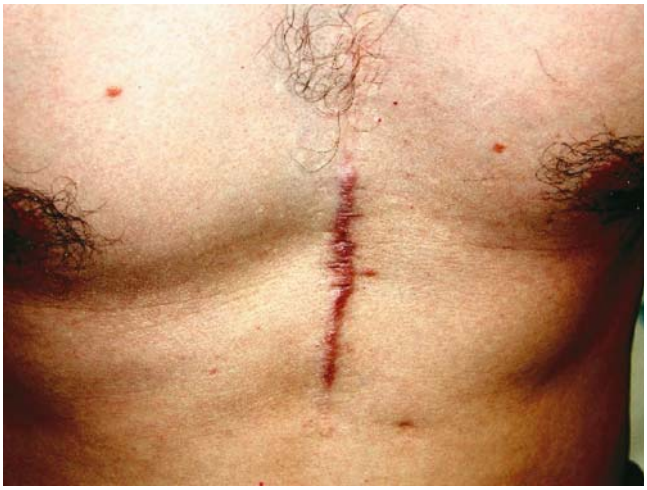

e

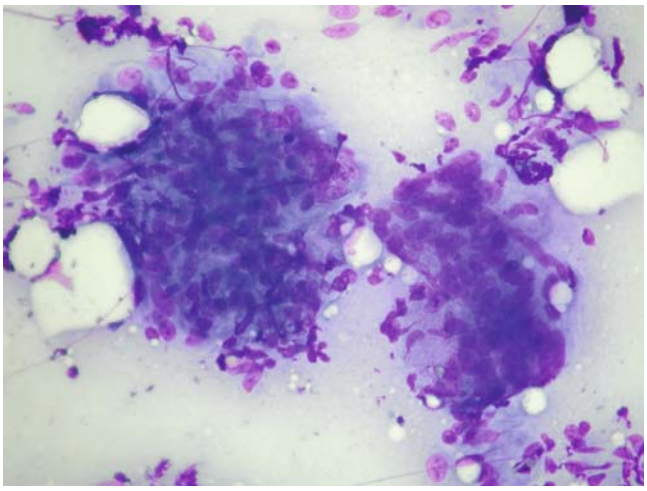

f

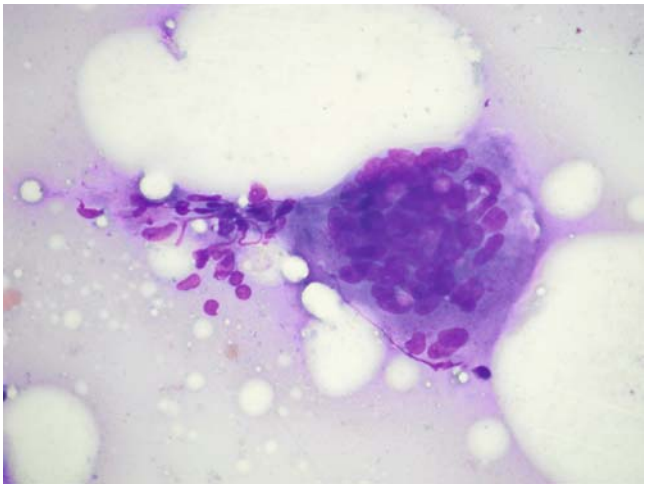

g

**Figure 4.1.** (continued)

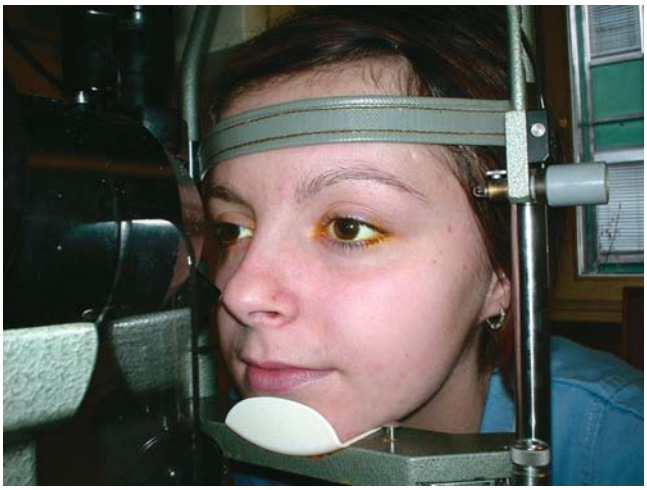

a

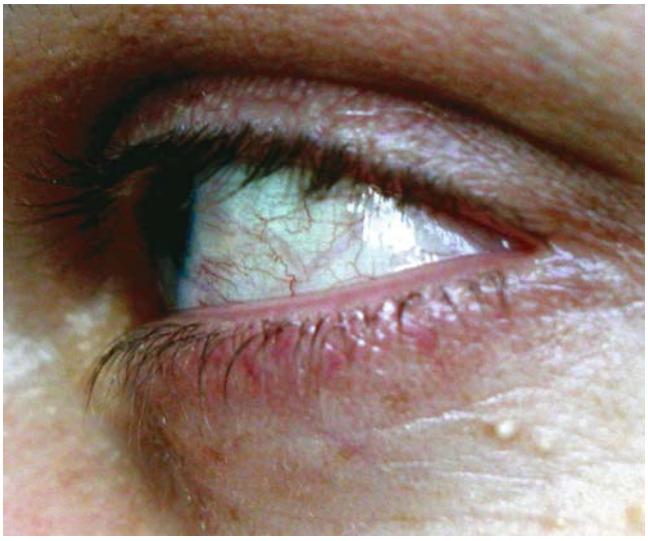

b

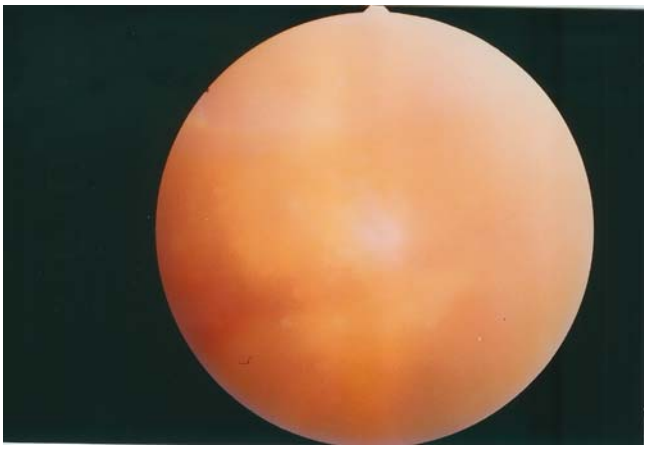

c

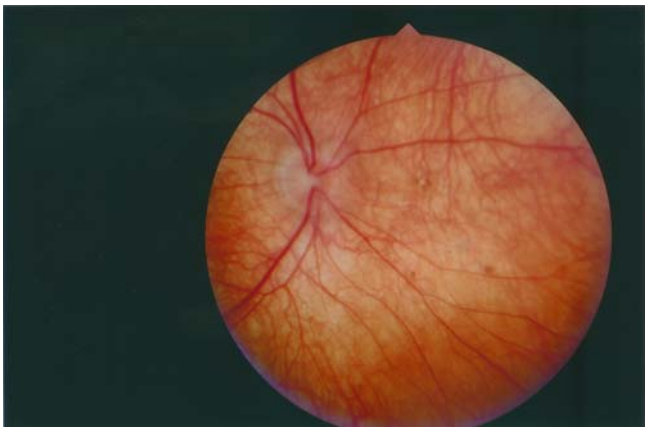

d

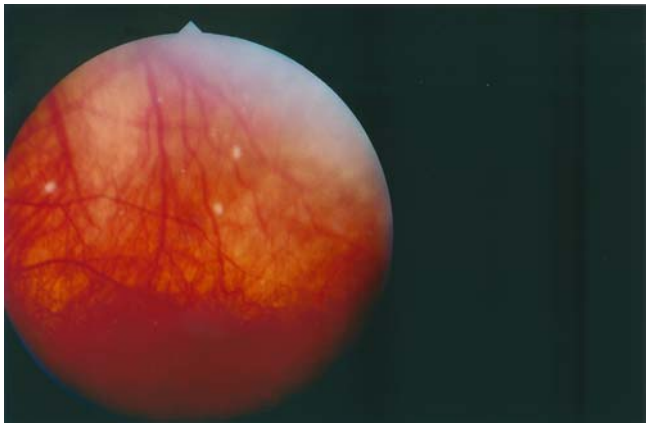

e

**Figure 4.2.** Ocular sarcoidosis. Slit-lamp analyses and staining with fluoroscein is mandatory in the examination of anterior uvea. Cornea and conjunctiva may stain with fluoresceine, bengal rose, and lissamine green in case of surface defects and irregularities (a). Iridocyclitis with blurred vision due to acute sarcoidosis, which faded away following topical steroid therapy (b). Vitritis is an inflammation of the vitreous body, in the posterior portion of the eye. Patients with vitritis may notice redness of the eye, sensitivity to light, blurred vision, or spots. The first picture was taken during acute phase of the inflammatory infiltration of the vitreous when the vision was blurred (c) and the second following therapy with consecutive clearance of the infiltrates and regaining of normal acuity of the vision (d). Posterior uveitis-chorioretinal punctiform atrophy (e).

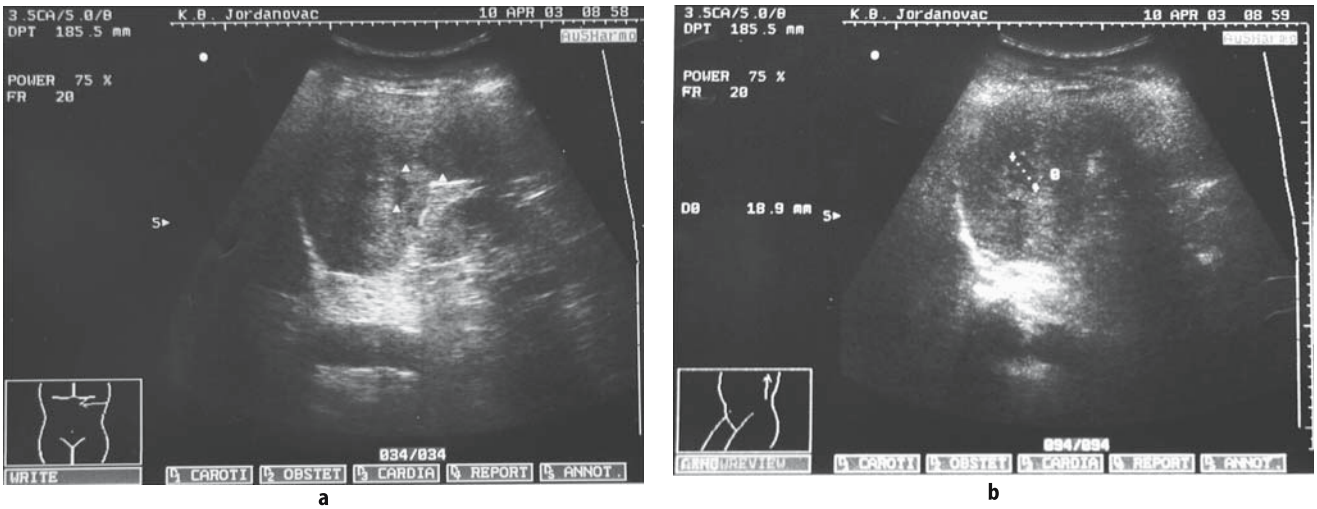


a b

**Figure 4.3.** Liver and splenic involvement in sarcoidosis. Ultrasound finding of nodules in the liver (a) and spleen; the spleen is enlarged and measures 160 mm (b).

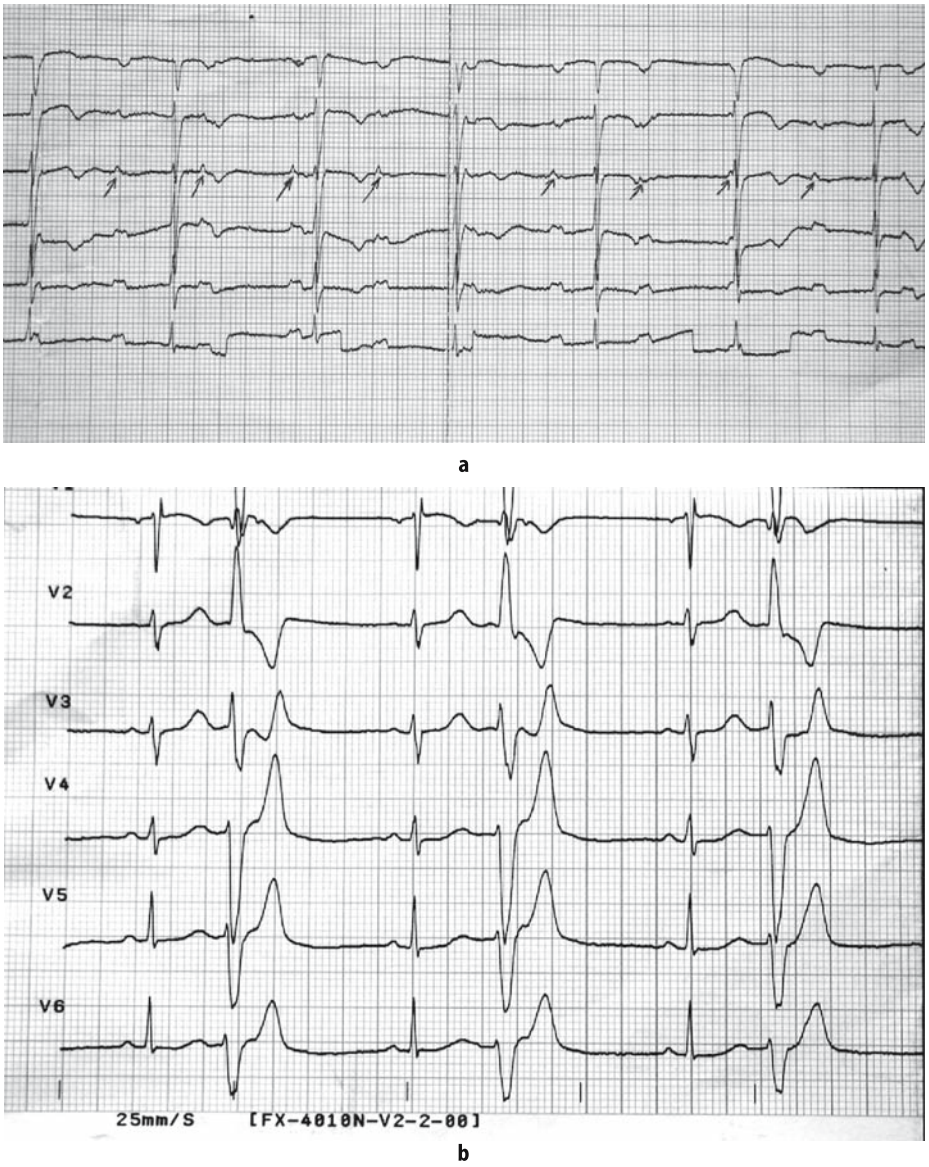


a b

**Figure 4.4.** Myocardial sarcoidosis. Electrocardiograph abnormalities are found in 50% of the patients with sarcoidosis. Most often there are conduction disturbances. The ECG shows atrioventricular dissociation in patient with chronic multiorgan sarcoidosis (a), and arrhythmias, in this particular case incomplete right bundle branch block and unifocal ventricular extrasystoli (b).

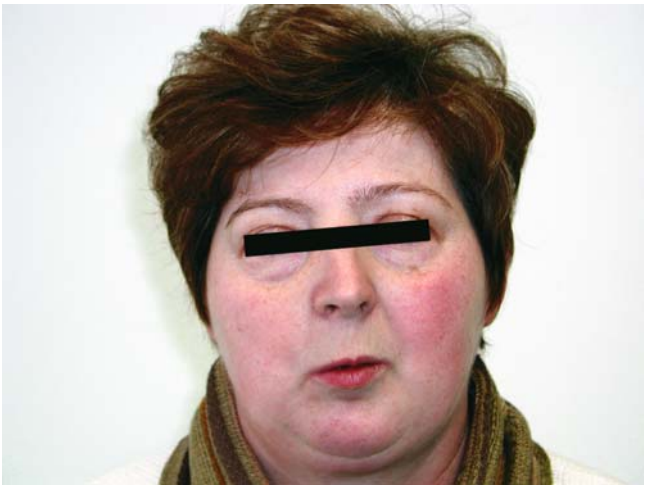

a

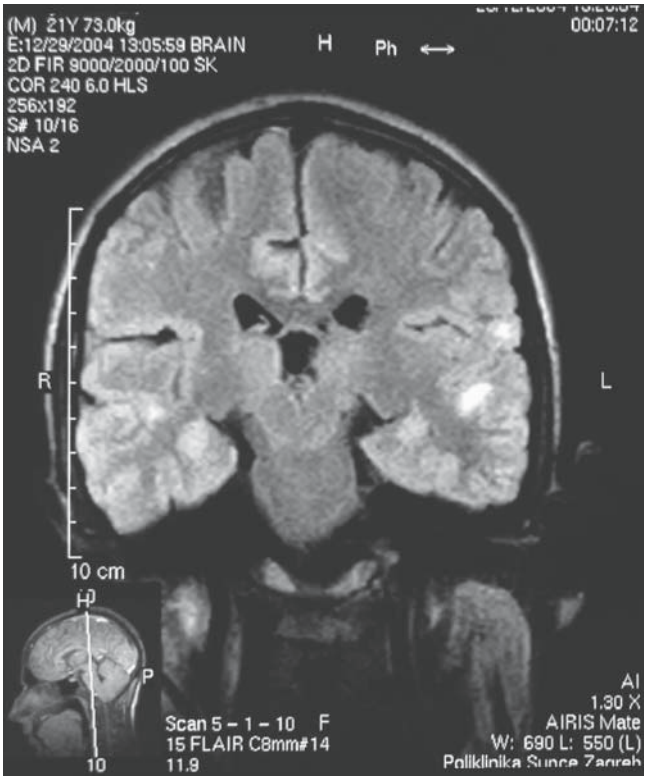


b

**Figure 4.5.** Neurosarcoidosis may present as the central or peripheral neural lesion. Most frequent manifestation of neurosarcoidosis is facial nerve palsy. This patient still has discrete facial nerve palsy following the corticosteroid therapy (a). The sarcoidosis of central nervous system by MR: Coronary section of the brain through temporal and parietal lobes in FLAIR sequence shows three hyperintense zones 5–10 mm in diameter cortically, two hyperintense zones are located in both temporal lobes, and one is located in parietal operculum. The patient's leading symptom was headache but it faded away after the course of high-dose corticosteroids (b).

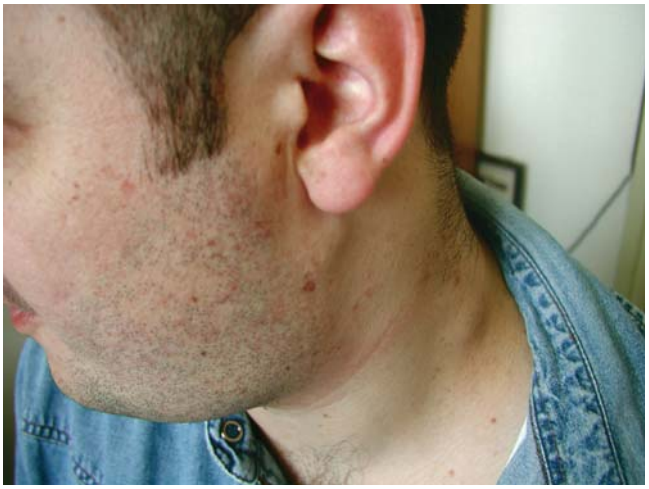

a

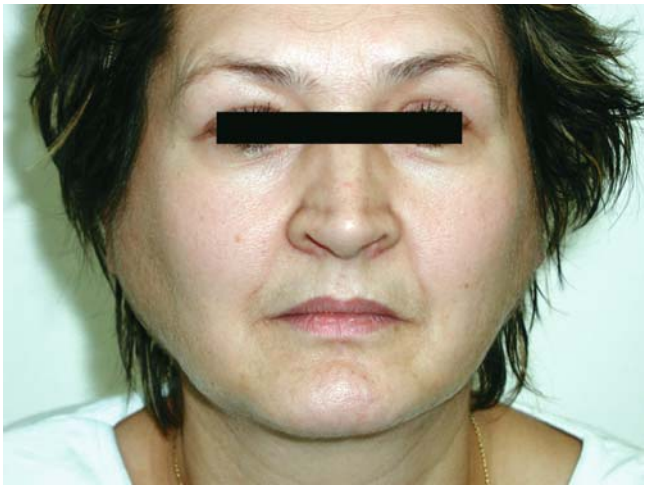

b

**Figure 4.6.** Lymph nodes, salivary and lachrymal glands in sarcoidosis. Most frequently involved are peripheral lymph nodes of the neck (a). Grave enlargement of the parotid gland due to sarcoidosis (b). Gallium-67 scanning reveals characteristic Panda sign, i.e. involvement of the parotid and lachrymal gland so the scan mimics a panda-bear's face (c).

(continued)

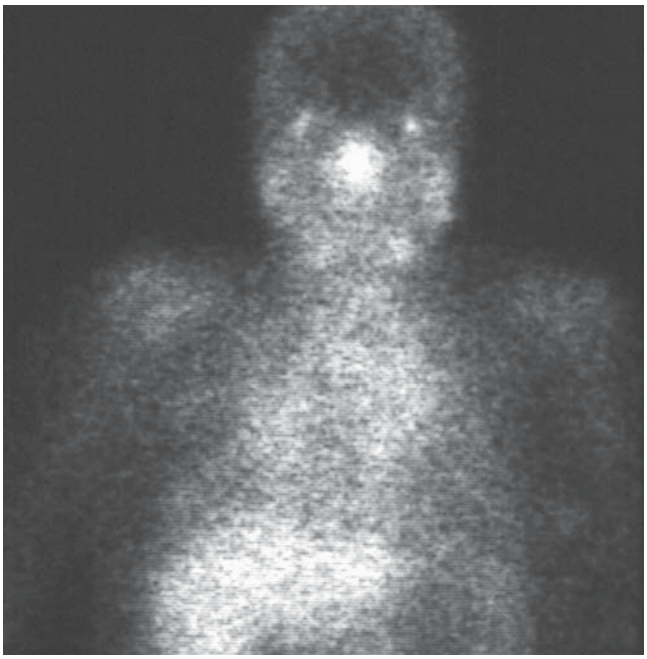

c

**Figure 4.6.** (continued)

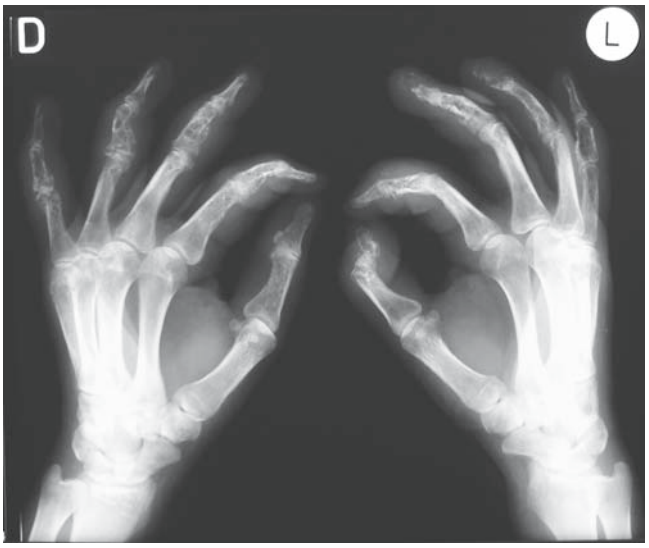


a

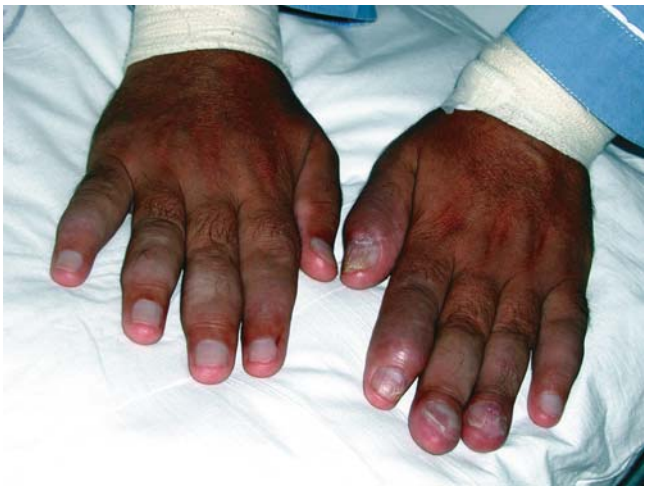

b

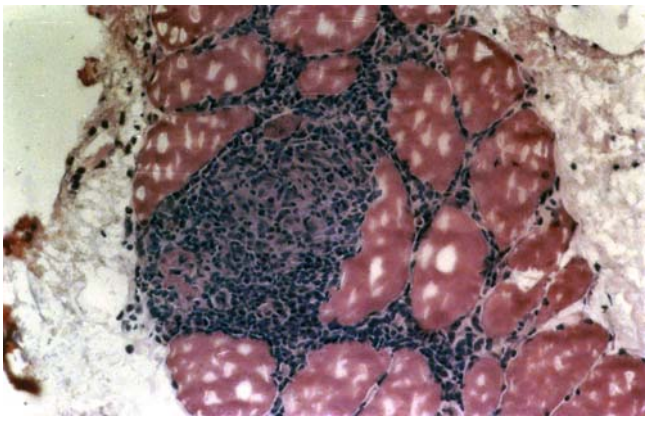

c

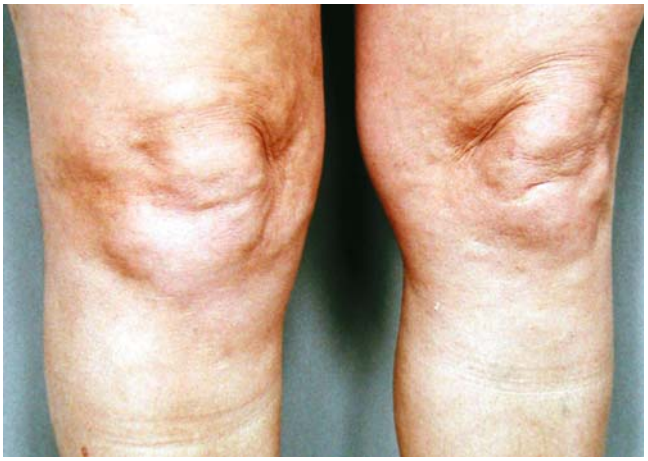

d

**Figure 4.7.** The musculoskeletal and joint involvement in sarcoidosis. Multiple bone cysts as depicted by plain radiography (a), bone cysts caused swelling of the fingers and loss of hand functions in patients who worked as a locksmith. Following the therapy he regained the function of the hands and could work again. Finger clubbing is noticed as well, but only in three fingers (b). Biopsy of the gastrocnemius muscle in a patient with suspected sarcoidosis revealed noncaseating granulomas. The symptoms were pain, itching, and tingling of the legs (c). Sarcoidosis of the right knee; swelling and pain subsided following the corticosteroid therapy (d).

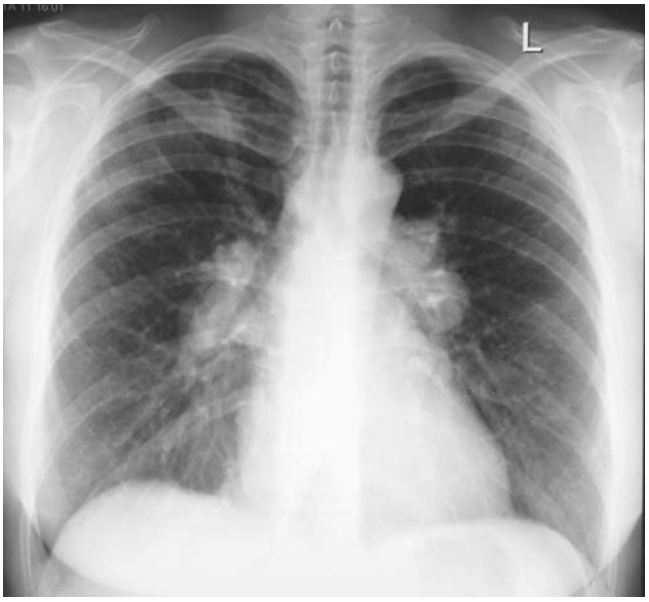


**Figure 4.8.** Sarcoidosis stage 1: bilateral hilar adenopathy.

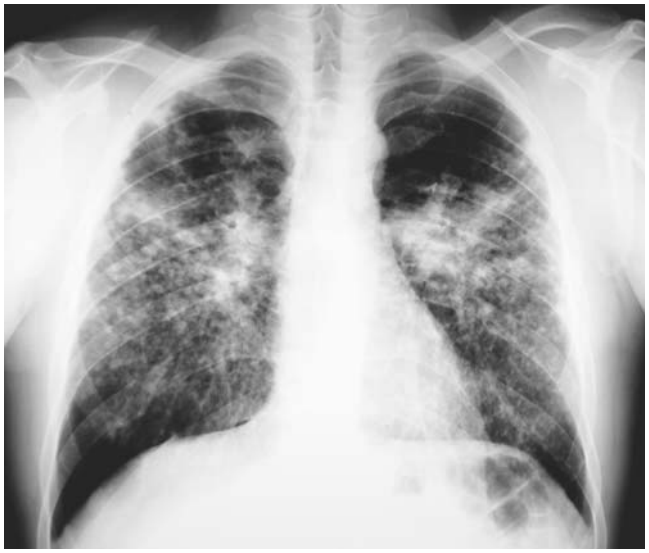

**Figure 4.9.** Sarcoidosis stage 2: bilateral hilar adenopathy with parenchymal infiltration.

Stage 1. Bilateral hilar or mediastinal adenopathy (BHL); (Figure 4.8).
Stage 2. BHL with parenchymal infiltration (Figure 4.9).
Stage 3. Parenchymal infiltration without BHL (Figure 4.10a, b).
Stage 4. Fibrocystic, bullous, and emphysematous changes (Figure 4.11a, b).

Chest computed tomography reveals more thoracic disease than can be appreciated on the plain chest radiography (Figure 4.12a, b; Figure 4.13a, b, c, d).

*3. Secure the histological evidence of noncaseating granuloma.* Once the clinical suspicion has been aroused, based on physical examination and chest radiography, the histological confirmation should be secured by obtaining a biopsy of the involved tissue. The typical lesion of sarcoidosis is a discrete round granuloma made up of densely packed epitheloid cells, a few multinucleate giant cells, and a scanty rim of lymphocytes

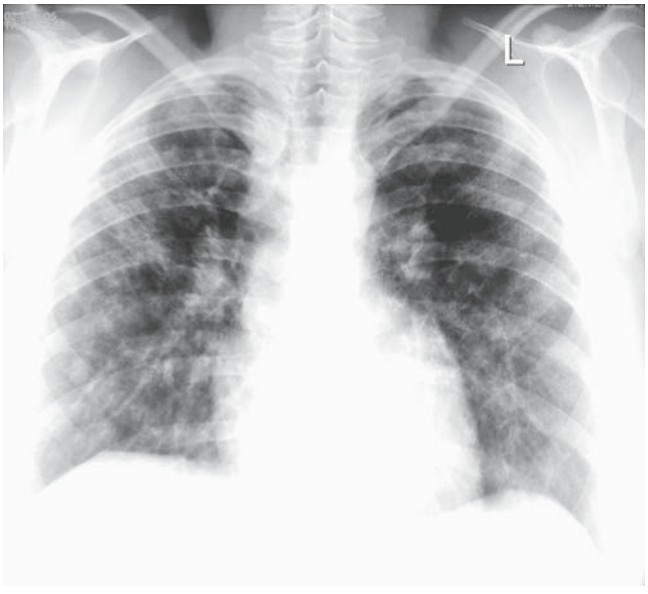


a

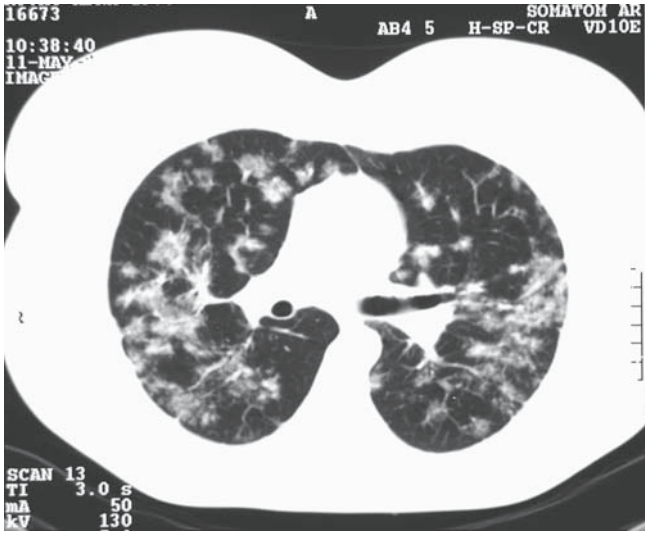


b

**Figure 4.10.** Sarcoidosis stage 3: parenchymal infiltration without bilateral hilar adenopathy (a) and HRCT scan of the same patient showing patchy ground-glass opacifications and consolidations concentrated along the bronchovascular bundles and small nodules (b).

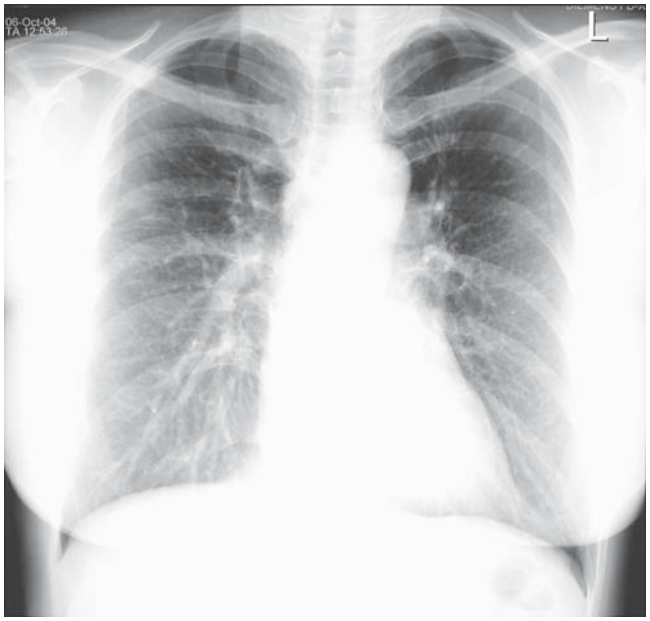


a

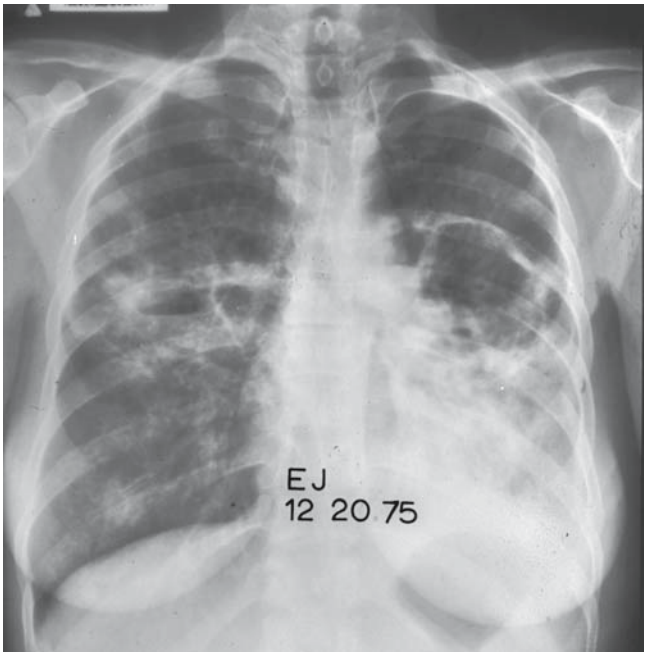


b

**Figure 4.11.** Sarcoidosis stage 4 shows minor fibrosis and increased upper lobe translucency (a). Another, advanced case of sarcoidosis stage 4 with fibrocystic, bullous, and emphysematous changes (b).

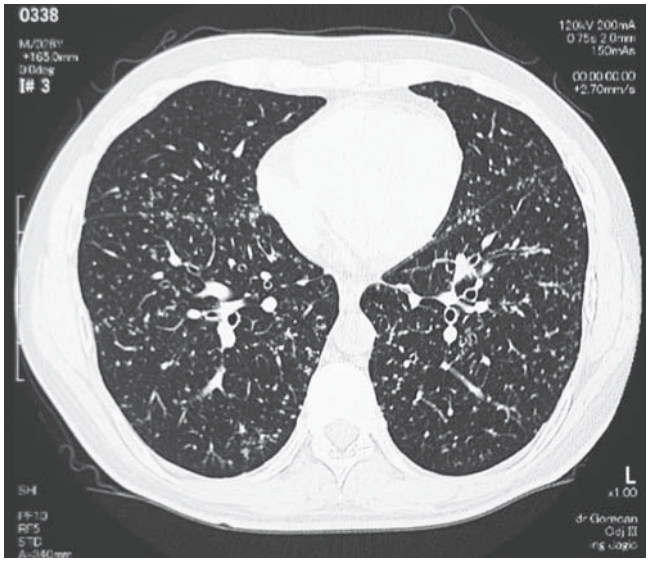


a

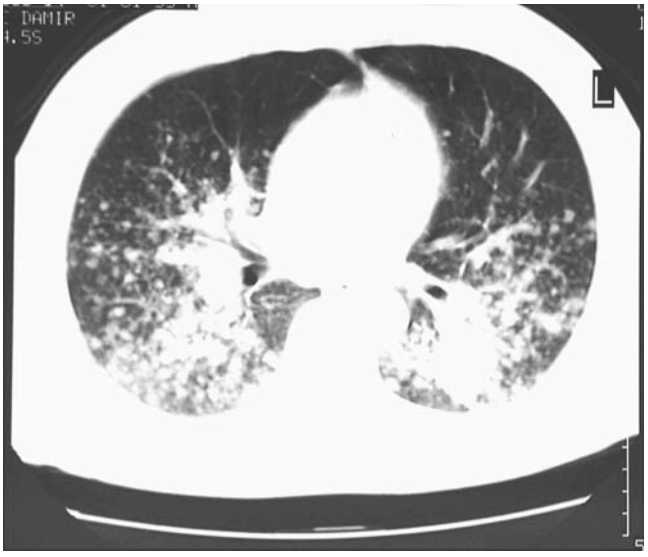


b

**Figure 4.12.** Characteristic HRCT finding in sarcoidosis are small nodules (a), or small nodules and consolidation along the bronchovascular bundles (b). In spite of gross radiological finding, both patients had no symptoms.

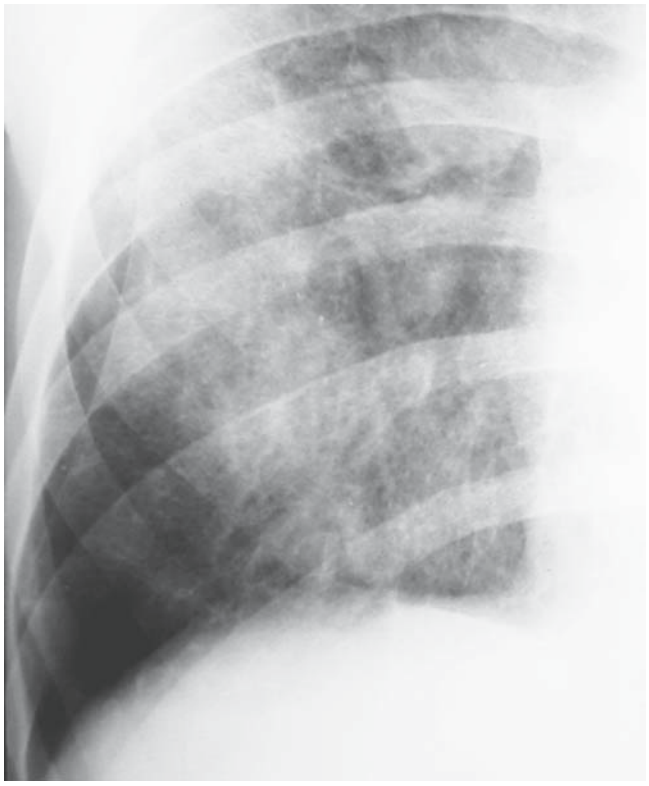

a

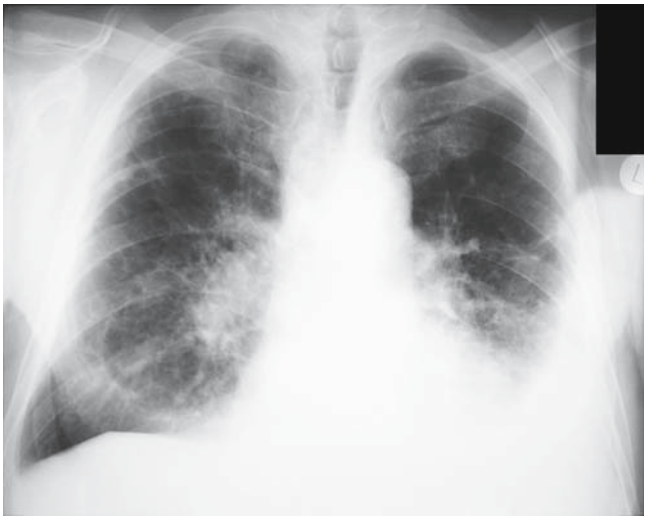

b

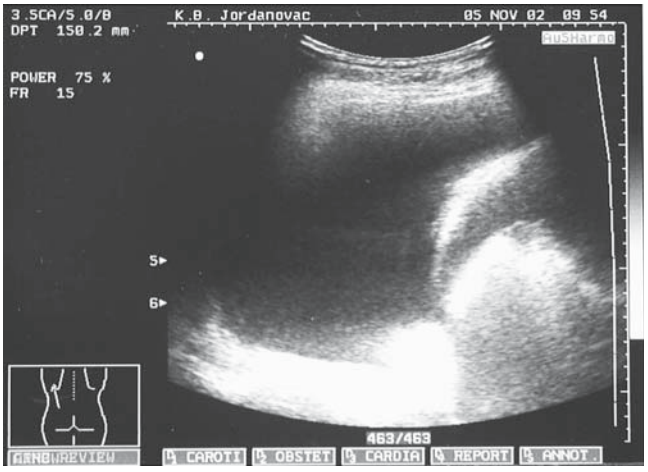


d

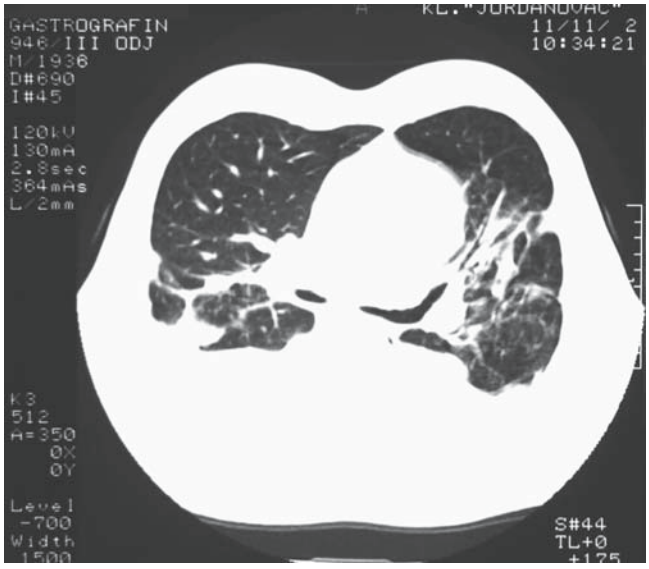


c

**Figure 4.13.** Pleural involvement in sarcoidosis. Plain radiograph of patient with chronic multiorgan sarcoidosis shows right-sided pneumothorax (a). Pleural effusion by plain radiograph (b), CT scan (c), and ultrasound analysis (d). Pleural sarcoidosis has been proved by finding of noncaseating granulomas in pleural biopsy specimen. The patient also had cardiac and chronic pulmonary parenchymal sarcoidosis.

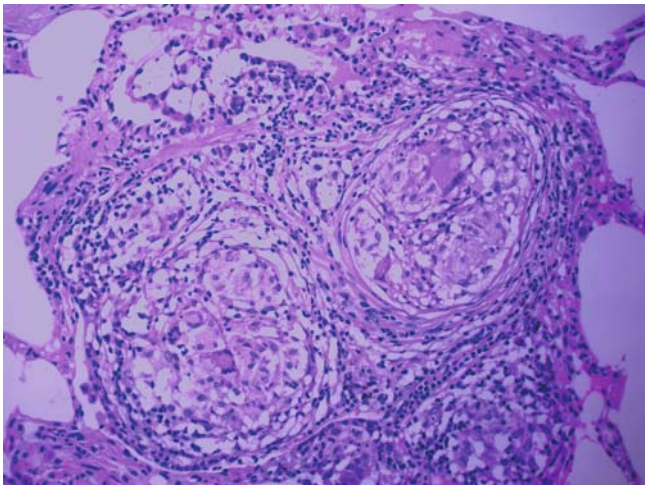

**Figure 4.14.** Pulmonary sarcoidosis. Multiple epitheloid granulomas, lymphocytes, few giant cells without necrosis.

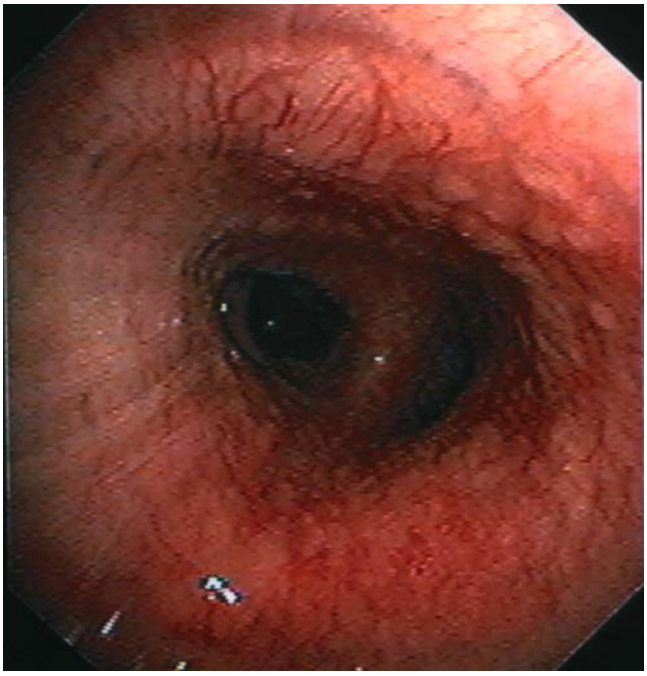

**Figure 4.15.** Typical bronchoscopic finding of the bronchial mucosa in sarcoidosis are plaques and increased vascularization.

(Figure 4.14). Granulomatous response can be found in many other conditions, and it is the clinician's responsibility to correlate clinical, radiological, and histological findings and arrive at the accurate diagnosis. Biopsy specimens should be stained for acid-fast bacilli and fungi. Specimens must be submitted for culture because tuberculosis cannot be excluded, except by negative acid-fast cultures. Lung function tests in parenchymal sarcoidosis reveal restrictive ventilatory changes and reduced diffusion capacity. Bronchoscopy often visualizes the lesions of the mucosa along the entire respiratory tract (Figure 4.15). The BAL analysis in most patients shows lymphocytic alveolitis and increased CD4/CD8 ratio (Figure 4.16a, b).

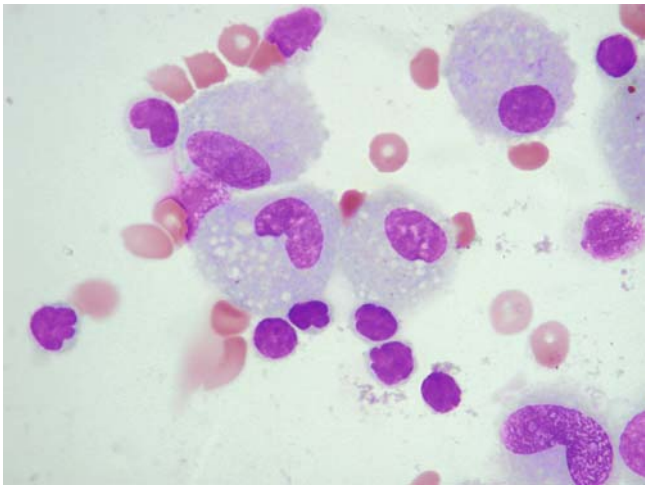

a

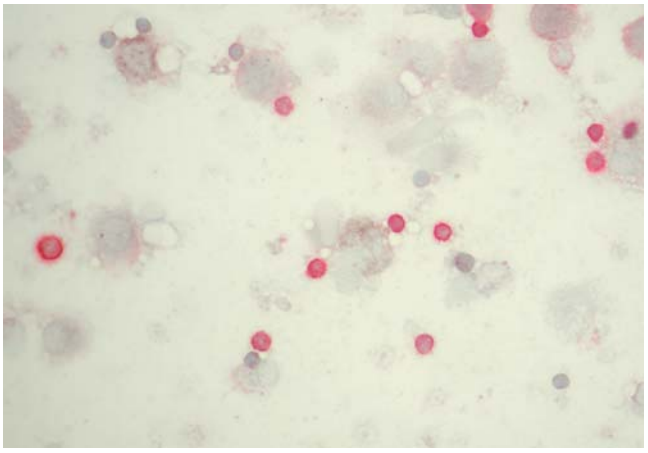

b

**Figure 4.16.** Lymphocytic alveolitis is a feature of sarcoidosis. Alveolar macrophages surrounded with small lymphocytes, BAL fluid cytology, original magnification ×1000, MGG stain (May-Grünwald-Giemsa) (a). Predominance of T-helper lymphocytes in lung lavage fluid. The technique of immunocytochemistry with monoclonal antibodies against CD4 helpers and CD8 suppressors show the ratio of more than 4 in about 50% of patients. The ratio greater than 4 is significant for the diagnosis of sarcoidosis. The figure shows CD4/CD8 ratio of 7,5 in BAL fluid cytology, positive CD4 lymphocytes stained red with immunocytochemistry; negative, gray CD8 lymphocyte, original magnification ×1000 (b).

The *treatment* of patients with sarcoidosis remains controversial. It is mandatory in cardiac, eye, neurological, or severe pulmonary sarcoidosis, but in most other instances systemic therapy is not necessary. Corticosteroids are the most effective drugs against sarcoidosis and its complications. The usual dose is 20 to 40 mg of prednisone daily for 6 to 12 months gradually reduced to maintenance levels of 5 to 10 mg daily. Hydroxychloroquine (Plaquenil) is useful in chronic skin lesions, hypercalcemia, and neurosarcoidosis. Methotrexate, azathioprine, cyclophosphamide, and chlorambucil have been used with varying success. Thalidomide, pentoxifylline, and infliximab are anti-tumor necrosis factor agents that are found to be effective in those patients with sarcoidosis who do not respond to corticosteroids or who develop severe side effects.

## Bibliography

1. Hunninghake GW, Costabel U, Ando M, Baughman R, Cordier JF, du Bois R, Eklund A, Kitaichi M, Lynch J, Rizzato G, Rose C, Selroos O, Semenzato G, Sharma OP. ATS/ERS/WASOG statement on sarcoidosis. Sarcoidosis Vasc Diffuse Lung Dis 1999;16:149–173.
2. Baughman RP, Teirstein AS, Judson MA, Rossman MD, Yeager H Jr, Bresnitz EA, DePalo L, Hunninghake G, Iannuzzi MC, Johns CJ, McLennan G, Moller DR, Newman LS, Rabin DL, Rose C, Rybicki B, Weinberger SE, Terrin ML, Knatterud GL, Cherniak R. Case Control Etiologic Study of Sarcoidosis (ACCESS) research group. Clinical characteristics of patients in a case control study of sarcoidosis. Am J Respir Crit Care Med 2001;164:1885–1889.
3. Teirstein AS, Judson MA, Baughman RP, Rossman MD, Yeager H Jr, Moller DR. A Case Control Etiologic Study of Sarcoidosis (ACCESS) Writing Group. Spectrum of biopsy sites for the diagnosis of sarcoidosis. Sarcoidosis Vasc Diffuse Dis 2005;22:139–146.
4. Gal A, Koss M. The pathology of sarcoidosis. Curr Opin Pulm Med 2002;8:445–451.
5. Moller D, Chen E. What causes sarcoidosis? Curr Opin Pulm Med 2002;8:429–434.
6. Vucinic V. What is the future of methotrexate in sarcoidosis? Curr Opin Pulm Med 2002;8:47–476.

# 5

# Introduction to Idiopathic Interstitial Pneumonias

Idiopathic interstitial pneumonias (IIPs) are heterogeneous group of nonmalignant diffuse lung diseases. *Idiopathic* means due to unknown cause, and *interstitial pneumonias* refers to the involvement of the lung parenchyma; the combination of inflammation and fibrosis is observed, contrary to the intra-alveolar processes seen for instance in bacterial pneumonias. Apart from the involvement of the interstitium, IIPs also affect the alveolar spaces, bronchioles, blood vessels, and sometimes the larger vessels. This group of diseases does not involve the COPD, bronchiolitis, pulmonary hypertension, or granulomatous diseases, diseases due to known causes, nor some "orphan" diseases.

The group could be separated from all other interstitial lung diseases on the basis of history of the disease, physical examination, radiographic imaging (plain chest x-ray and especially the HRCT scans), laboratory findings, and histopathological pattern.

ATS/ERS *classification* of idiopathic interstitial pneumonias comprises the following entities: idiopathic pulmonary fibrosis (IPF/UIP), nonspecific interstitial pneumonia (NSIP), bronchiolitis obliterans organizing pneumonia (BOOP) (synonym: cryptogenic organizing pneumonia; COP), acute interstitial pneumonia (AIP), respiratory bronchiolitis associated interstitial lung disease (RB-ILD), and desquamative interstitial pneumonia (DIP), as well as lymphoid interstitial pneumonia (LIP). The key to the classification of idiopathic interstitial pneumonias is the *histological pattern.* The new classification defines a set of histological patterns that provide the basis for final *clinico-radiologic-pathologic diagnosis* (Table 5.1).

The precise and exhausted *history of the disease* is of paramount importance. The aims are acquaintance with initial symptoms (breathlessness, dry cough), their progression, clinical course, comorbidity, and exclusion of known causes of ILD. The environmental causes, previous therapies (medications, radiation), drug abuse, and cigarette smoking should be excluded as possible causes. *Physical finding* usually reveals fine crackles (of highest frequencies of all the lung sounds!), sometimes wheezes, squeaks, or rhonchus with normal or bronchovesicular breath sounds. The extrapulmonary examination is helpful in excluding various systemic diseases (diffuse connective tissue diseases, vasculitis, some rare diseases, malignancies, infections) as the cause of ILD.

After obtaining the working diagnosis of IIP, plain chest radiograph, pulmonary function tests, and laboratory analyses are performed. If IIP is suspected, the HRCT scan is mandatory as well as bronchoscopy with lung lavage and transbronchial biopsy in most cases. Sometimes surgical biopsy has to be obtained (Figure 5.1).

In order to obtain confident diagnosis of IIP, a team of trained professionals in this area is mandatory, and it consists of pneumonologist, radiologist, and pathologist. The multidisciplinary management of patients is suggested, with highly specialized members of the team.

*Radiological imaging of the lungs*, especially the HRCT, directs the clinical reasoning and enables some conclusions to be drawn: (1) confident diagnosis of IPF with characteristic clinical features, (2) atypical clinical or CT features for IPF, (3) characteristic finding for other ILD (i.e., LCH, LAM, PAP), and finally (4) other IIP but not IPF are suspected. As IPF is most common (50% of all IIP), the radiologist has to estimate whether

**Table 5.1.** Clinico-radiologic-pathologic diagnosis of IIPs and their frequency.

| Histological Pattern | Clinico-Radiologic-Pathologic Diagnosis | Frequency |
|---|---|---|
| Usual interstitial pneumonia (UIP) | Idiopathic pulmonary fibrosis (IPF/UIP) | 55% |
| Nonspecific interstitial pneumonia (NSIP) | Nonspecific interstitial pneumonia (NSIP) | 25% |
| Organizing pneumonia (OP) | Cryptogenic organizing pneumonia (COP) or idiopathic bronchiolitis obliterans organizing pneumonia (BOOP) | 3% |
| Diffuse alveolar damage (DAD) | Acute interstitial pneumonia (AIP) | <1% |
| Respiratory bronchiolitis (RB) and desquamative interstitial pneumonia (DIP) | Respiratory bronchiolitis with interstitial pneumonia (RB-ILD) and desquamative interstitial pneumonia (DIP) | 15% |
| Lymphoid interstitial pneumonia (LIP) | Lymphoid interstitial pneumonia (LIP) | <1% |

the scan has the characteristics for IPF. If it is characteristic for IPF, with major and minor clinical criteria present, the diagnostic procedures are not necessary, especially if the patient is old, with comorbidity or respiratory insufficient. Some ILDs other then IIP that are considered in differential diagnosis have highly specific HRCT finding, for instance Langerhans cell histiocytosis (LCH), lymphangiomyomatosis (LAM), or pulmonary alveolar proteinosis (PAP), and the procedures necessary to prove the diagnosis in most cases are bronchoscopy with transbronchial lung biopsy and lavage only. Patients with atypical HRCT and clinical finding, especially if they are under the age of 50 years, should undergo open lung biopsy. HRCT findings of particular IIP are depicted in the chapters that follow.

*Bronchoalveolar lavage (BAL)* is often part of the diagnostic procedure in ILD. When IIPs are under investigation, the lung lavage is most useful in excluding the infectious and malignant processes, certificating some entities or helps in the decision to perform the open lung biopsy. The lung lavage finding is specific for Langerhans cell histiocytosis and pulmonary alveolar proteinosis. The bizarre giant multinuclear cells are often

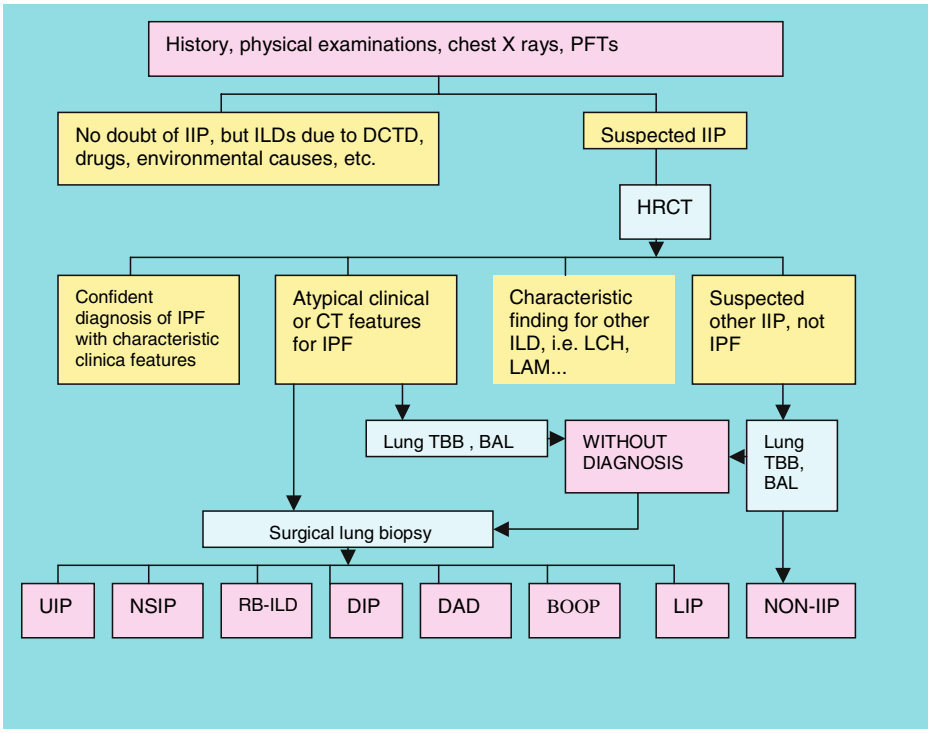


IIP – idiopathic interstitial pneumonia ; PFT – pulmonary function test; DCTD – difuse connective tissue diseases; LCH – Langerhans cell histiocytosis; LAM – lymphangioleimyomatosis; TBB – transbronhial biopsy; BAL – bronchoalveolar lavage

**Figure 5.1.** Diagnostic algorithm of idiopathic interstitial pneumonias. Adapted from data published in ATS/ERS international multidisciplinary consensus classification of the idiopathic interstitial pneumonias. *Am J Respir Crit Care Med* 2002;165:277–304.

**Table 5.2.** Course of the disease, prognosis, HRCT, and lung lavage findings in IIP.

| Clinical Entity | Course of the Disease | HRCT | Bal; Alveolitis | Prognosis |
|---|---|---|---|---|
| IPF | Chronic | Honeycombing, TB | Neutrophils | Bad |
| NSIP-cellular | Subacute | GG | Mixed | Good |
| NSIP-fibrotic | Chronic | GG, consolidation, TB | Mixed | Bad |
| BOOP/COP | Subacute | Consolidation, GG | Lymphocytes mixed | Good |
| AIP | Acute | Consolidation, GG, TB | Neutrophils, atypical pneumocytes type II, amorphous material: fragments of hyaline membranes | Bad |
| DIP | Chronic | GG | Mixed, alveolar macrophages contain cigarette pigment | Bad |
| RB-ILD | Chronic | Centrilobular changes | Neutrophils, alveolar macrophages contain cigarette pigment | Good |
| LIP | Chronic | GG | Lymphocytes | Good |

HRCT, high-resolution computed tomography; BAL, bronchoalveolar lavage; DAD, diffuse alveolar damage; GG, ground glass; TB, traction bronchiectasis.

found in histopathological sample but occasionally also in lung lavage fluid of patients with hard metal pneumoconiosis. To diagnose diffuse alveolar hemorrhage (DAH), it is necessary to have more than 90% of siderophages in BAL cell count. Lipidophages are characteristic for lipoid pneumonia. Foamy macrophages are often found in amiodarone lung. Although the analysis of lung lavage cells in differential diagnosis of IIP has no definitive diagnostic value, it is helpful because some "patterns" are indicative of certain entities. Neutrophilic alveolitis is found in IPF, lymphocytic or mixed in BOOP, and respiratory bronchiolitis and DIP (cigarette smoker's diseases!) are characterized by finding of increased percentage of alveolar macrophages and smoker's pigment. In patients with AIP, there are signs of hemorrhage, extremely increased number of alveolar macrophages, sometimes lymphocytes, atypical pneumocytes II, and amorphous material that represents the fragments of hyaline membranes.

*Transbronchial lung biopsy* sometimes is sufficient to confirm the diagnosis, for instance in patients with BOOP where granulated tissue plugs within the lumen of small airways extend into the alveolar ducts and alveoli or AIP with the histological pattern of diffuse alveolar damage (DAD).

*Open lung biopsy* is necessary for confident clinico-pathologic diagnosis except with typical clinico-radiologic picture of UIP/IPF. The procedure should be performed early in the course of the disease, from different sites, the sites that are supposed to contain active pathologically changed tissue, not definite fibrotic tissue (end-stage fibrosis). This can be estimated at site or with the help of HRCT finding. There are several benefits of obtaining a surgical lung biopsy. The establishment of a firm clinicopathologic diagnosis allows the patient and clinician to make more informed decisions about therapy. Almost all of the current treatments for IIPs have potentially serious risks and side effects, and it is not reasonable to expose patients to these risks in the presence of diagnostic uncertainty.

The diagnostic algorithm of IIP has been presented briefly. The specific entities will be described in the following chapters. Course of the disease, prognosis, HRCT and lung lavage findings in patients with IIP are briefly summarized in Table 5.2.

## Bibliogarphy


1. ATS/ERS International multidisciplinary consensus classification of the idiopathic interstitial pneumonias. Am J Respir Crit Care Med 2002;165:277–304.
2. Katzenstein AL. Katzenstein and Askin's surgical pathology of non-neoplastic disease. Philadelphia: W.B. Saunders; 1997.
3. Kandaswamy A, Kumar CS, Ramanthan RP, Jayaraman S, Malmurugan N. Neural classification of lung sounds using wavelet coefficients. Comput Biol Med 2004;34:523–537.
4. Hansell D, Kerr I. The role of high resolution computed tomography in the diagnosis of interstitial lung disease. Thorax 1991;46:77–84.
5. Costabel U, King TE. International consensus statement on idiopathic pulmonary fibrosis. Eur Respir J 2001;17:163–167.

6. Drent M, Jacobs JA, Wagenaar SS. Bronchoalveolar lavage. In: Olivieri D, du Bois RM, Eds. Interstitial lung diseases. Sheffield: ERS Journals Ltd; 2000;63–78.
7. Monaghan H, Wells A, Colby T, du Bois RM, Hansell DM, Nicholson AG. Prognostic implications of histologic patterns in multiple surgical lung biopsies from patients with idiopathic interstitial pneumonias Chest 2004;125:522–526.
8. Nagai S, Nagao T, Hoshino Y, Hamada K. Heterogeneity of pulmonary fibrosis. Curr Opin Pulm Med 2001;7:262–271.
9. Rottoli P, Bargagli E. Is bronchoalveolar lavage obsolete in the diagnosis of interstitial lung disease? Curr Opin Pulm Med 2003;9:418–425.

# 6

# Idiopathic Pulmonary Fibrosis

Idiopathic pulmonary fibrosis (IPF) (or cryptogenic fibrosing alveolitis) is an archetypal example of *lung fibrosis*. Although it is the most frequent of all, its etiology is not known, its pathogenesis only partially resolved, and its therapy quite inadequate and inefficient.

The term *idiopathic pulmonary fibrosis* refers to a specific form of chronic fibrosing interstitial pneumonia limited to the lung and always associated with histological appearance of usual interstitial pneumonia (UIP) (Table 6.1) on surgical lung biopsy. It is necessary to exclude other known causes of interstitial lung diseases and to detect abnormal pulmonary functions and characteristic abnormalities on conventional chest radiographs or high-resolution computed tomography (HRCT). In the absence of surgical biopsy, the diagnosis of IPF is uncertain, but the presence of all of the major diagnostic criteria as well as at least three of the four minor increases the likelihood of a correct clinical diagnosis of IPF (Table 6.2).

In a recent study, the prevalence of IPF was found to be 20.2 per 100,000 among men and 13.2 per 100,000 among women, which is 5 to 10 times higher than previous figures. Patients with IPF are usually 40–70 years old, and the incidence of the disease increases with age. The mean length of survival after diagnosis is 3.2–5 years.

*Clinical presentation* most often consists of slowly progressive breathlessness, tightness of the chest, and dry cough, which does not respond to antitussive agents. The symptoms are usually present for more than 6 months before presentation. Physical examination most frequently reveals bilateral, bibasilar, end-inspiratory fine crackles on auscultation and digital clubbing (Figure 6.1). The crackles extend toward the upper lobes, and lung volumes diminish with decreasing respiratory excursions as the disease progresses. Small, stiff lungs develop. Extrapulmonary involvement does not occur. Fever is rare, and its presence suggests an alternative diagnosis (BOOP, hypersensitive pneumonitis, drug toxicity, NSIP).

*Etiological agent(s)* in IPF have not been elucidated, although it has been positively associated with the exposure to metal, wood and textile dust, livestock, agricultural offending agents, stone and sand, smoking, and wood fire. It has traditionally been thought that IPF occurs as a result of an initial injury to the lung that causes the recruitment of inflammatory cells, release of cytokines, and eventually parenchymal remodeling and fibrosis. However, because inflammatory suppressive agents do not seem to be effective, it may be that IPF is not caused by inflammatory cells, but inflammatory cells are secondarily involved. Injury to alveolar epithelial cells and destruction of the subepithelial basement membrane may be the source of a number of cytokines that lead to local recruitment of fibroblasts. In this context, factors such as transforming growth factor-beta (TGF-β), platelet-derived growth factor (PDGF), tumor necrosis factor-alpha (TNF-α), and connective tissue grow factor (CTGF) seem to play a key role. Release of these cytokines may result in fibroblast proliferation and migration to various sites in the lung, followed by differentiation of the fibroblast phenotype. This differentiation of the fibroblast is likely the key to the chronic nature of IPF. The differentiated cell seems to be more resistant to apoptosis (natural cell death); the altered cells demonstrate a heightened responsiveness to fibrogenic cytokines such as TGF-β. These events would

**Table 6.1.** Clinical conditions associated with usual interstitial pneumonia pattern (UIP).

| |
|---|
| Idiopathic pulmonary fibrosis/cryptogenic fibrosing alveolitis |
| Diffuse connective tissue disease |
| Drug toxicity |
| Chronic hypersensitive pneumonitis |
| Asbestosis |
| Familial idiopathic pulmonary fibrosis |
| Hermansky-Pudlak syndrome |

**Table 6.2.** Criteria for a clinical diagnosis of idiopathic pulmonary fibrosis.

Major Criteria

(1) Exclusion of other known causes of ILD, such as certain drug toxicities, environmental exposures, connective tissue diseases.
(2) Abnormal pulmonary function studies that include evidence of restriction and impaired gas exchange.
(3) Bibasilar reticular abnormalities with minimal ground-glass opacities on HRCT.
(4) Transbronchial lung biopsy or bronchoalveolar lavage showing no features to support an alternative diagnosis.

Minor Criteria

(1) Age > 50 years.
(2) Insidious onset of otherwise unexplained dyspnea on exertion.
(3) Duration of illness ≥3 months.
(4) Bibasilar, inspiratory crackles (dry or "Velcro").

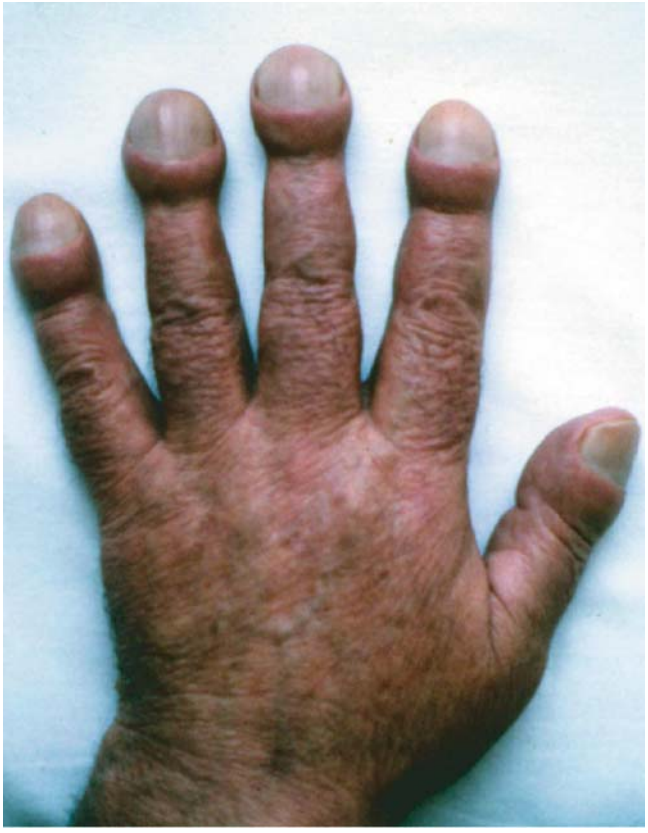

**Figure 6.1.** Finger clubbing is present in a more than 50% of the patients with IPF.

lead to prolonged retention of fibroblasts, continued connective tissue protein synthesis, and the formation of fibroblast foci, a histological hallmark in IPF. It appears that the type 2 T-cell response predominates in IPF, with an increase in IL-4 and IL-13. In summary, in IPF sequential acute lung injury is present, with aberrant wound healing, deranged epithelization, apoptosis, and remodeling of parenchyma, which results in progressive development of fixed fibrosis, which affects the normal lung architecture.

*The diagnostic approach* includes performance of radiological imaging techniques, the plain radiograph of the chest and particularly the HRCT scan, assessment of pulmonary function and laboratory tests, transbronchial biopsy and lung lavage, and open lung biopsy in those who do not fulfill the diagnostic criteria as shown in Table 6.2.

The routine laboratory tests are usually not helpful. Elevation of lactate dehydrogenase may be noted but it is a nonspecific finding. In about 10–20% of patients, low titer of anti-nuclear antibodies (ANA) and rheumatic factors are detected. High titers raise the probability of diffuse connective tissue disorder, with lung involvement.

Pulmonary function tests typically reveal restrictive ventilatory changes (reduced vital capacity [VC], and total lung capacity [TLC]) at some point in the course of the disease. The $DL_{CO}$ diffusion capacity is reduced and may precede the reduction of lung volumes. The respiratory arterial blood gases may be normal, or they may reveal mild hypoxemia. With cardiopulmonary exercise testing, early abnormalities of gas exchange could be detected. Pulmonary hypertension rarely occurs at rest, but it is common during exercise.

The plain radiograph is the screening test to detect the presence of IPF, although it may be normal in about 10% of the patients (Figure 6.2a, b). HRCT technique has changed the diagnostic procedure in these patients as it allows earlier diagnosis and helps to narrow the differential diagnosis (Figure 6.3a, b).

Bronchoalveolar lavage has limited diagnostic usefulness in IPF, but it is helpful in diagnosing numerous alternative specific entities, especially malignancies, infections, eosinophilic pneumonia, and LCH. In about 70–90 % of patients, the neutrophilic alveolitis is detected (Figure 6.4), and in 40–60% there is increased percentage of eosinophils in lung lavage fluid. Lymphocytic alveolitis is noted in about 10% of patients.

Transbronchial lung biopsy is not helpful in making the diagnosis of IPF, but it can help to exclude some other entities that are considered in differential diagnosis. The gold standard is open lung biopsy, or video-assisted thoracoscopic (VAT) lung biopsy. The usual interstitial pneumonia (UIP) is the pathological abnormality essential to the diagnosis of IPF (Figure 6.5).

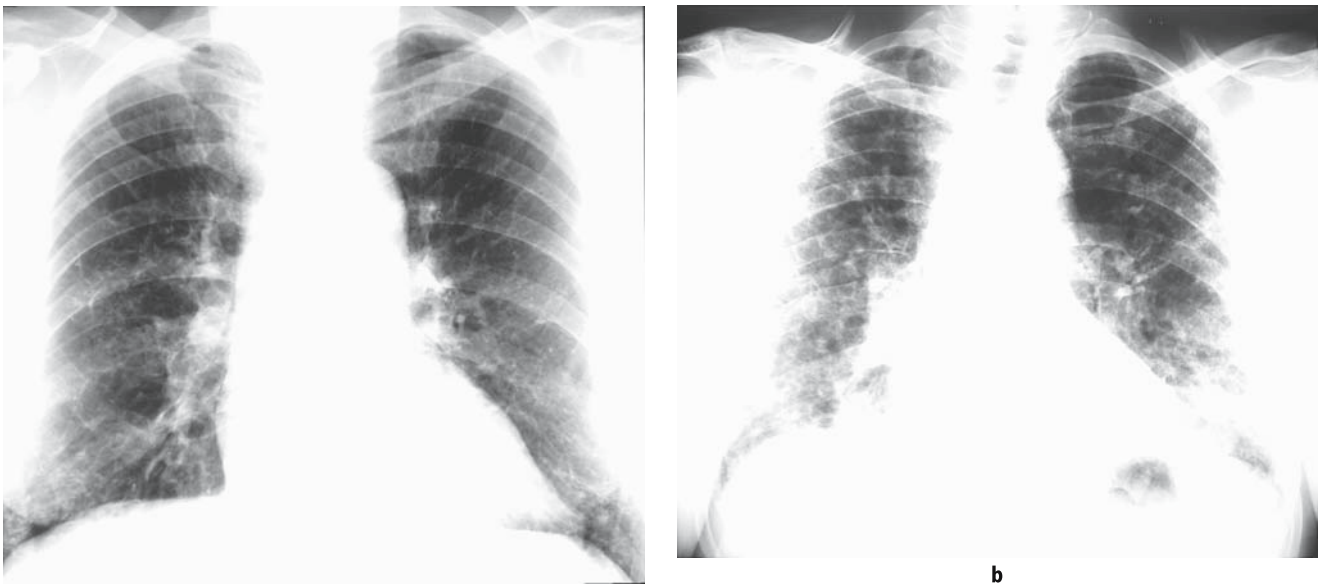

a b

**Figure 6.2.** Chest x-ray of a patient with IPF shows bibasilar fine reticular pattern in the early phase (a) and coarse in the late stage, with diminished lung volumes (b).

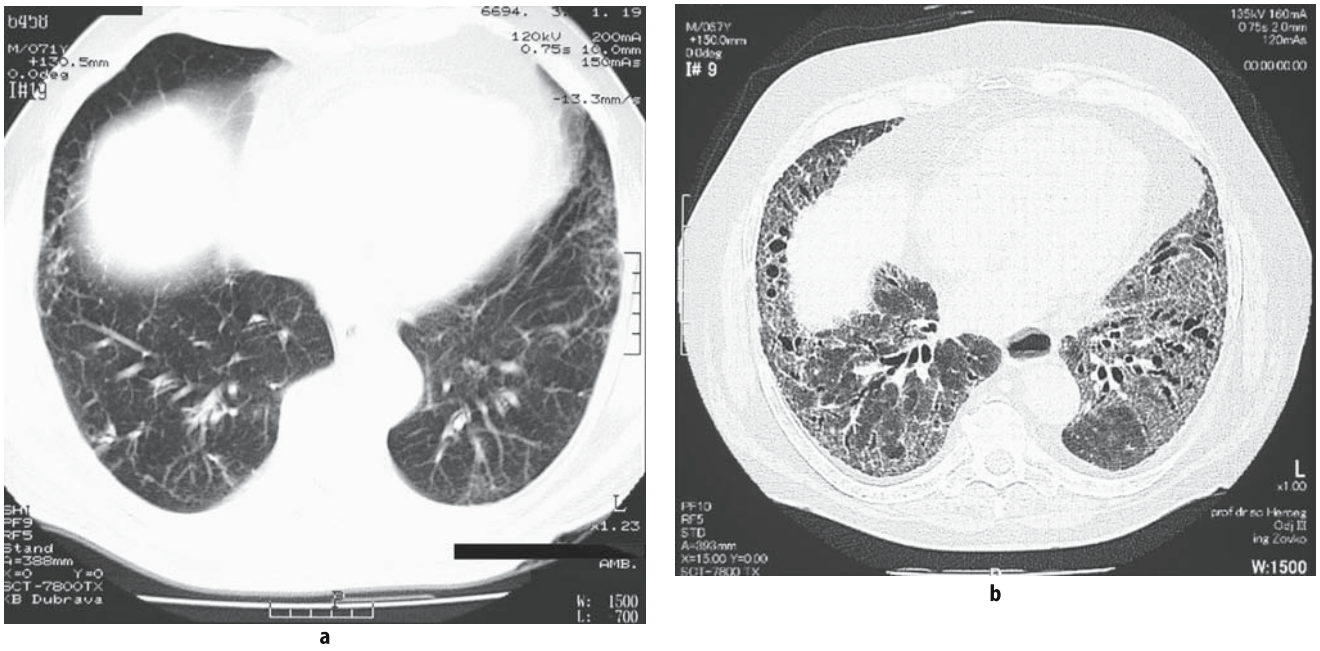

**Figure 6.3.** HRCT scan in early phase of IPF shows predominantly subpleural reticular pattern (a), and in the late phase predominantly subpleural coarse reticular pattern, septal thickening, traction bronchiectasis, and honeycombing. The ground-glass opacities are usually limited, and if extensive (>30% of the lung involved) an alternative diagnosis should be considered. This particular 70-year old patient experienced progressive dyspnea during last 8 months, quitted smoking, lost weight and was examined for suspected IPF. As he fulfilled the major and minor criteria for IPF, including the HRCT finding, the open lung biopsy was not considered necessary. As the disease progressed the corticosteroids and azathioprine were applied with insignificant efficacy (b).

Although corticosteroids have been standard *therapy* for years no evidence of benefit in survival has been established. Despite the lack of evidence, a common therapy currently used for IPF is corticosteroids in conjunction with azathioprine. The combination of prednisone (20 mg/day) and azathioprine (3 mg/kg daily but not to exceed 200 mg/day) was reported to tend to stabilize lung function in some 20% of patients.

Several studies of different medications are ongoing or have been completed. The novel medications are the result of progress in understanding of pathogenesis of this disease: pirfenidone, interferon gamma-1b, *N*-acetylcystein, colchicine, penicillamine,

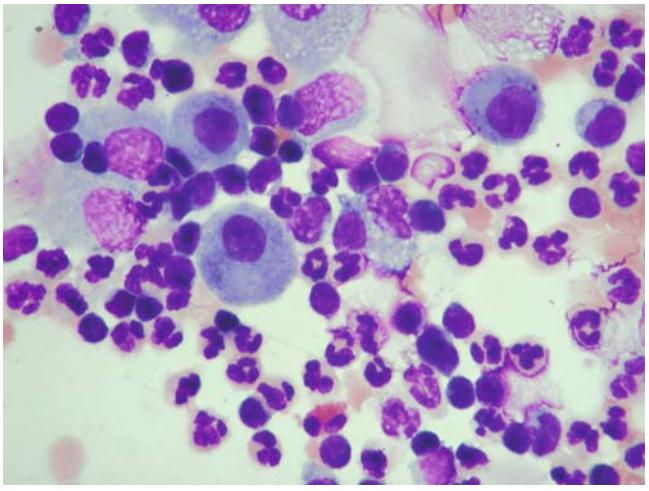

**Figure 6.4.** Neutrophilic alveolitis is a most common finding in a patient with IPF. Predominance of neutrophils and lymphocytes, few macrophages and eosinophils. BAL fluid cytology, original magnification ×1000, MGG stain (May-Grünwald-Giemsa).

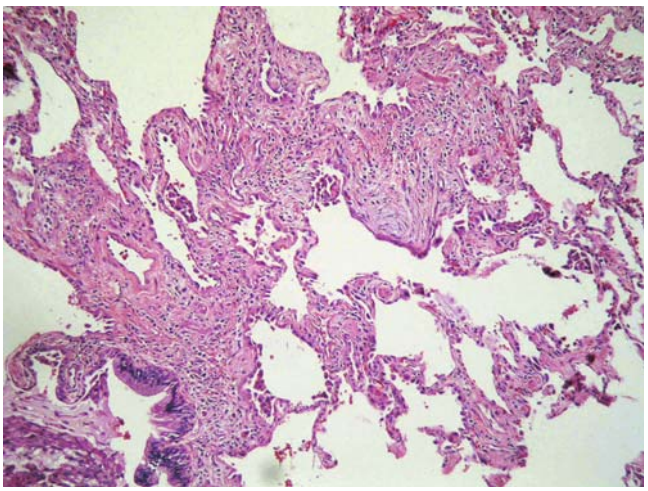

**Figure 6.5.** The histological hallmark and chief diagnostic criterion in IPF/UIP is temporal heterogeneity; alternating areas of normal lung, interstitial inflammation, fibrosis and honeycombing are seen. Scattered foci of proliferating fibroblasts "fibroblastic foci" (FF) are consistent finding. Usual interstitial pneumonia (UIP): interstitial fibrosis and fibroblastic focus in the center of the field. On the right, areas of normal or near normal septa are seen.

etanercept (anti-TNF agent), bosentane (an oral dual endothelin-1 receptor antagonist), blocking agents of connective tissue growth factor (CTGF), and others. Many of the trials used small numbers of patients, and although some patients demonstrated improved or stabilized lung function, no agent so far has had any effect on mortality.

## Bibliography

1. ATS/ERS Statement on idiopathic pulmonary fibrosis: Diagnosis and treatment. Am J Respir Crit Care Med 2000;164:646–664.
2. ATS/ERS International multidisciplinary consensus classification of the idiopathic interstitial pneumonias. Am J Respir Crit Care Med 2002;165:277–304.
3. Coultas DB, Zumwalt RE, Black WC, Sobonya RE. The epidemiology of interstitial lung diseases. Am J Respir Crit Care Med 1994;150:967–972.
4. Kawabata H, Nagai S, Hayashi M, Nakamura H, Nagao T, Shigematsu M, Kitaichi M, Izumi T. Significance of lung shrinkage on CXR as a prognostic factor in patients with idiopathic pulmonary fibrosis. Respirology 2003;8:351–358.
5. Lynch JP, Thannickal VJ. Idiopathic pulmonary fibrosis. In: Baughman RP, du Bois R, Lynch JP, Wells AU, Eds. Diffuse Lung Disease. A Practical Approach. London: Arnold; 2004:131–151.

# 7

# Respiratory Bronchiolitis Associated Interstitial Lung Disease and Desquamative Interstitial Pneumonia

Respiratory bronchiolitis associated interstitial lung disease (RB-ILD) and desquamative interstitial pneumonia (DIP) are viewed as a continuum of smoking-induced diseases. Another smoking-related condition, respiratory bronchiolitis (RB), is usually found in asymptomatic smokers and a few ex-smokers. It is unclear whether it is a disease entity or a normal response to smoking.

Characteristic histopathological finding in RB-ILD is the accumulation of alveolar macrophages within respiratory bronchioles and surrounding alveoli. Macrophages contain light-brown, finely granular pigmentation due to accumulation of smoke constituents. Chronic inflammation of neighboring bronchiolar and alveolar walls is present (Figure 7.1).

Typical histopathological features of DIP are diffuse alveolar septal thickening, hyperplasia of type II pneumocytes, and intensive accumulation of macrophages within the alveoli. The distribution of macrophages tends to be diffuse rather than bronchiolocentric as seen in RB-ILD (Figure 7.2).

*Clinical features* of RB-ILD and DIP are quite similar. Slowly progressive exertional dyspnea and nonproductive cough are frequents symptoms. Chest pain is rare, and finger clubbing is seen in 25% of the patients. End-inspiratory fine crackles over the lung bases may occur. In most cases, these diseases are benign; occasionally, extensive fibrosis supervenes.

These entities are strongly associated with *cigarette smoking*, except for a few sporadic cases of DIP in nonsmokers. The antiprotease-protease and antioxidant-oxidant imbalance plays a role in ILD. Lung fibroblasts release neutrophil and monocyte chemotactic factors in response to smoke. The lung fibroblasts modulate the inflammatory cell recruitment into the lung. Additionally, epithelial and endothelial cells contribute to the enhancement of inflammatory lung injury.

*Diagnostic procedure* includes lung function testing, chest radiological analysis, and bronchscopy with the lung lavage procedure. Lung function test often shows restrictive or mixed restrictive and obstructive pattern of pulmonary impairment. The most common pulmonary function abnormality, however, is reduced carbon monoxide (DLCO) diffusing capacity. Severe functional impairment, especially reduced DLCO, is attributable to coexistent emphysema. In patients with DIP, only restrictive pattern is detected with reduced DLCO. Severe hypoxemia is observed in advanced disease.

In RB-ILD patients, chest radiographs show parenchymal, centrilobular, ill-defined micronodules with or without ground-glass opacities (Figure 7.3a, b). Bilateral, symmetric, and predominantly basal and peripheral ground-glass attenuation is a HRCT feature of DIP, although irregular linear opacities and cystic spaces are also observed. (Figure 7.4a, b).

Bronchoalveolar lavage cell analysis in RB-ILD reveals a preponderance of brown-pigmented macrophages with a mild neutrophil increase (Figure 7.5). On the other hand, in DIP there is an increase in lymphocytes, neutrophils, and occasionally eosinophils. Transbronchial lung biopsy is not useful in diagnosing these diseases.

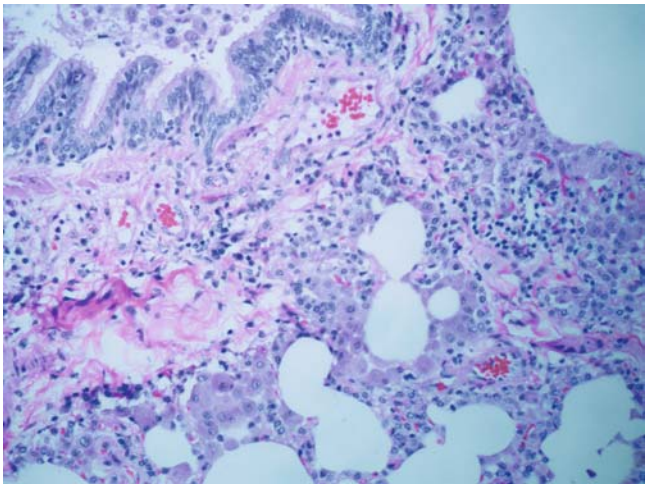

**Figure 7.1.** Respiratory bronchiolitis associated interstitial lung disease (RB-ILD). Respiratory bronchioli and adjacent alveoli are filled by macrophages containing fine granular brown pigment.

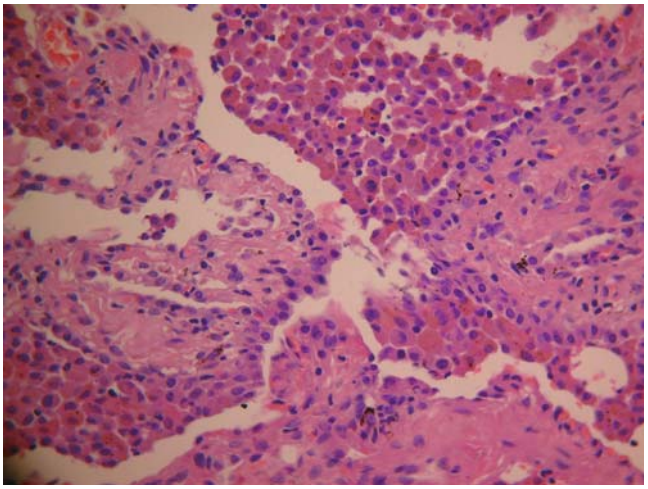

**Figure 7.2.** Desquamative interstitial pneumonia (DIP). Alveolar spaces are filled with macrophages containing fine granular brown pigment in cytoplasm. Alveolar septa with mild fibrosis.

In a smoker, the combination of typical HRCT finding, pulmonary function tests, and lung lavage analysis may allow the diagnosis of these diseases made without open lung biopsy. If there is any doubt, then an open lung biopsy should be performed (Table 7.1).

*Smoking cessation* induces spontaneous regression of these diseases. Thus, the temptation to start drug therapy should be resisted. Corticosteroid therapy induces modest clinical benefit in DIP but not in RB-ILD.

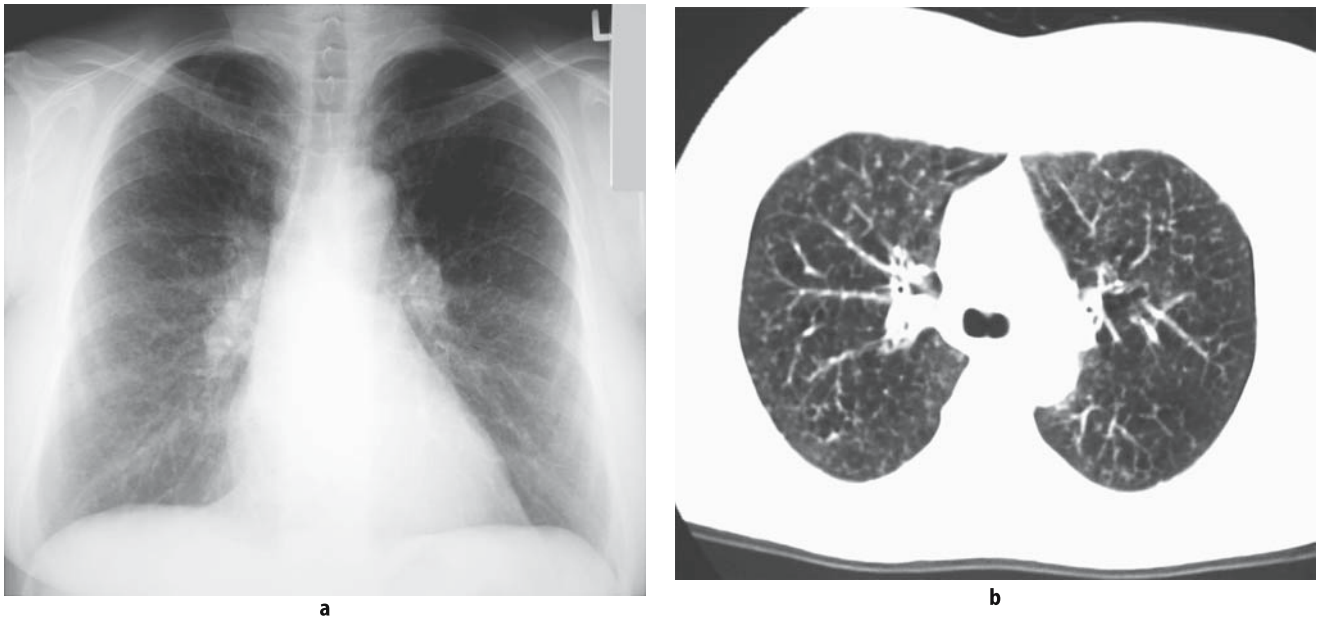

a b

**Figure 7.3.** Chest x-ray of a lady who smoked heavily for many years shows diffuse, sharpened reticular pattern (a). CT scan of the same patient shows small vague nodules and septal thickening (b). Lung lavage analyses revealed numerous brown pigmented macrophages. The final diagnosis was respiratory bronchiolitis associated lung disease and the patient was advised to quite smoking.

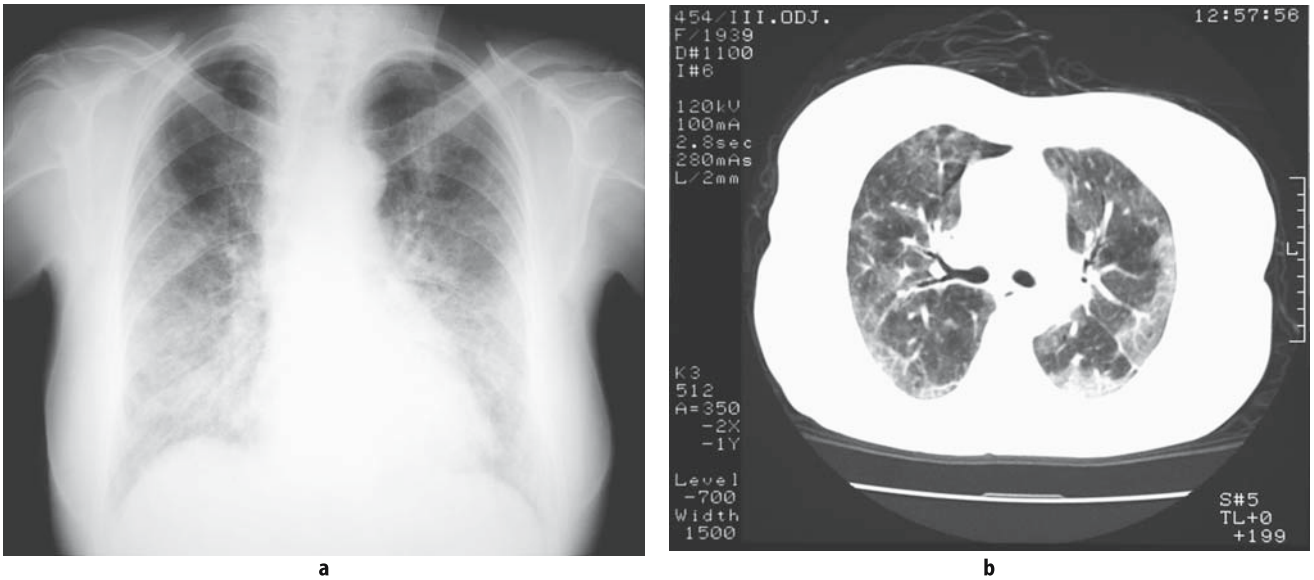


a b

**Figure 7.4.** Plain radiograph of the chest shows ground-glass opacities, distributed predominantly in the lower lobes in a patient with DIP (a). HRCT scan of the same patient shows the peripheral distribution of ground-glass opacities with no fibrotic changes (b).

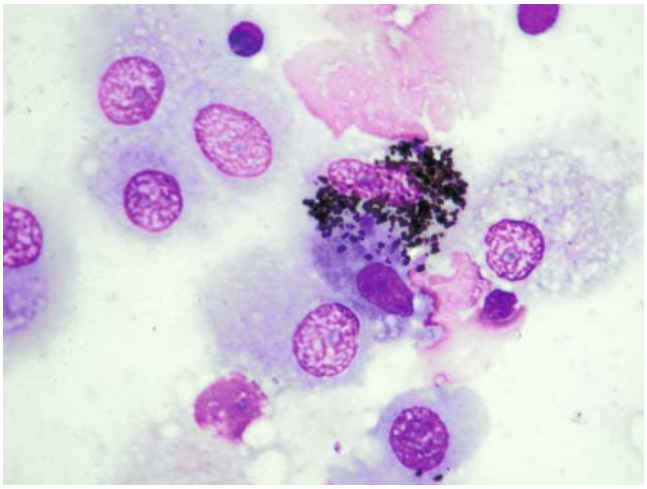

**Figure 7.5.** Brown pigmented macrophage surrounded with alveolar macrophages. BAL fluid cytology, original magnification ×1000, MGG stain (May-Grünwald-Giemsa).

**Table 7.1.** Differences between respiratory bronchiolitis associated interstitial lung disease (RB-ILD) and desquamative interstitial pneumonia (DIP).

| Feature | RB-ILD | DIP |
|---|---|---|
| Severity of lung function impairment | + | ++ |
| Histopathological finding | | |
| Pigmented macrophages within airspaces | + | ++ |
| Histological bronchocentricity | ++ | – |
| BAL | Pigmented macrophages | Pigmented macrophages, neutrophils, and eosinophils |
| HRCT | | |
| Ground glass | + | ++ |
| Alveolar septal thickening | Peribronchial | Diffuse |
| Micronodi | ++ | – |
| Honeycombing | – | – |
| Therapy | Smoking cessation alone | Smoking cessation and corticosteroids |

## Bibliography

1. Davies G, Wells AU, du Bois RM. Respiratory bronchiolitis associated with interstitial lung disease and desquamative interstitial pneumonia. Clin Chest Med 2004;25:717–726.
2. Nagai S, Hoshino Y, Hayashi M, Ito I. Smoking-related interstitial lung diseases. Curr Opin Pulm Med 2000;6:415–419.
3. Ryu JH, Myers JL, Capizzi SA, Douglass WW, Vassalo R, Decker PA. Desquamative interstitial pneumonia and respiratory bronchiolitis-associated interstitial lung disease. Chest 2005;127:178–184.
4. Park JS, Brown KK, Tuder RM, Hale VA, King Jr TE, Lynch DA. Respiratory bronchiolitis-associated interstitial lung disease: Radiological features with clinical and pathologic correlation. J Comput Assist Tomogr 2002;126:13–20.

# 8

# Nonspecific Interstitial Pneumonia

The recognition that lung biopsy samples from some patients with idiopathic interstitial disease do not fit into any well-defined histological patterns of idiopathic interstitial pneumonia led to the proposal of the term *nonspecific interstitial pneumonia* (NSIP). This attitude accelerated the identification of a group of interstitial lung diseases that had more favorable prognosis then IPF and needed to be discerned from IPF but also from other IIPs. In recent literature, the term *NSIP* is used as a clinico-radiological-pathological (CRP) form of IIP (i.e., not only as a histological pattern with a variety of etiologies as it was used previously). NSIP has been subclassified based on the extent of cellularity and fibrosis with variable etiologic backgrounds that led to heterogeneous clinical outcome.

There had been a vigorous discourse whether it is a real clinical entity and whether the idiopathic NSIP could be defined as a CRP-integrated form. At this stage of experience, based on the results, there is a definite idiopathic NSIP. Its incidence seems to be minimal. The incidence of clinical conditions associated with NSIP is much higher (Table 8.1).

*Clinical features* of patients with NSIP are not very helpful in differential diagnosis toward other IIPs. Patients with NSIP are approximately 40–50 years old, 5–10 years younger than patients with UIP. Duration of presenting symptoms ranges from a few weeks to more than 1 year. Most common symptoms are slowly progressive breathlessness, nonproductive cough, fatigue, and a history of weight loss. In a minority also fever, skin eruptions, and finger clubbing are observed. Physical examination reveals the presence of end-inspiratory fine crackles in almost all patients and, to a lesser extent, the squeaks. The prognosis of NSIP is better than usual interstitial pneumonitis (UIP). Early retrospective studies of NSIP cited favorable prognosis with short–term survival rates of 70–100%, but long-term survival data are lacking.

*The pathogenesis* of NSIP is mostly unresolved, although some data exist about possible mechanisms. Recent studies cite differences in cytokine network profiles in NSIP and UIP. There is some evidence that immune-mediated mechanisms involving T lymphocytes and dendritic cells may play a more important role in the development and perpetuation of NSIP than UIP. Fibroblasts from IPF patients have a stable phenotypic alteration marked by increased synthesis of the profibrotic cytokine TGF-β1, increased contractility, and increased collagen production, but fibroblasts from NSIP patients are lacking these characteristics. These differenced might be, partially, the cause of more extensive fibrosis in IPF.

*Diagnostic procedure* includes laboratory tests, chest radiograph analysis, bronchoscopy, and open lung biopsy. Laboratory tests are nonspecific; serum erythrocyte sedimentation rate and lactic dehydrogenase LDH are frequently increased. A restrictive ventilatory defect is present in more than 90% of patients, with mild airflow limitation in a minority and reduced $DL_{CO}$ in all (Figure 8.1d). Pulmonary function tests cannot discriminate NSIP from UIP.

Chest radiographic features in NSIP shows bilateral patchy alveolar and interstitial pulmonary infiltrates with more frequent involvement of the lower lung zones (Figure 8.1a, c; Figure 8.2a). HRCT characteristic features include ground-glass opacities with or

**Table 8.1.** Clinical conditions associated with nonspecific interstitial pneumonia (NSIP) histological pattern.

| |
|---|
| No detectable cause, i.e., idiopathic NSIP |
| Diffuse connective tissue disease |
| Hypersensitive pneumonitis |
| Drug-induced pneumonitis |
| Infections |
| Occupational |
| Immunodeficiency including HIV infection |

without consolidation with varying degrees of interstitial changes (Figure 8.1b; Figure 8.2b). Honeycomb change is uncommon in NSIP (a cardinal feature of UIP). CT features are similar in idiopathic or CTD-associated NSIP (Figure 8.3). Considerable overlap in HRCT patterns exist between NSIP and UIP.

Within limited data, most studies suggest that NSIP is associated with increased lymphocytes and neutrophils in bronchoalveolar lavage fluid. These series noted no difference in the cell profiles between the patients with NSIP and those with UIP, although the predominance of T-suppresor cells is more suggestive of NSIP. It is impossible to differentiate NSIP from other IIPs using transbronchial lung biopsies.

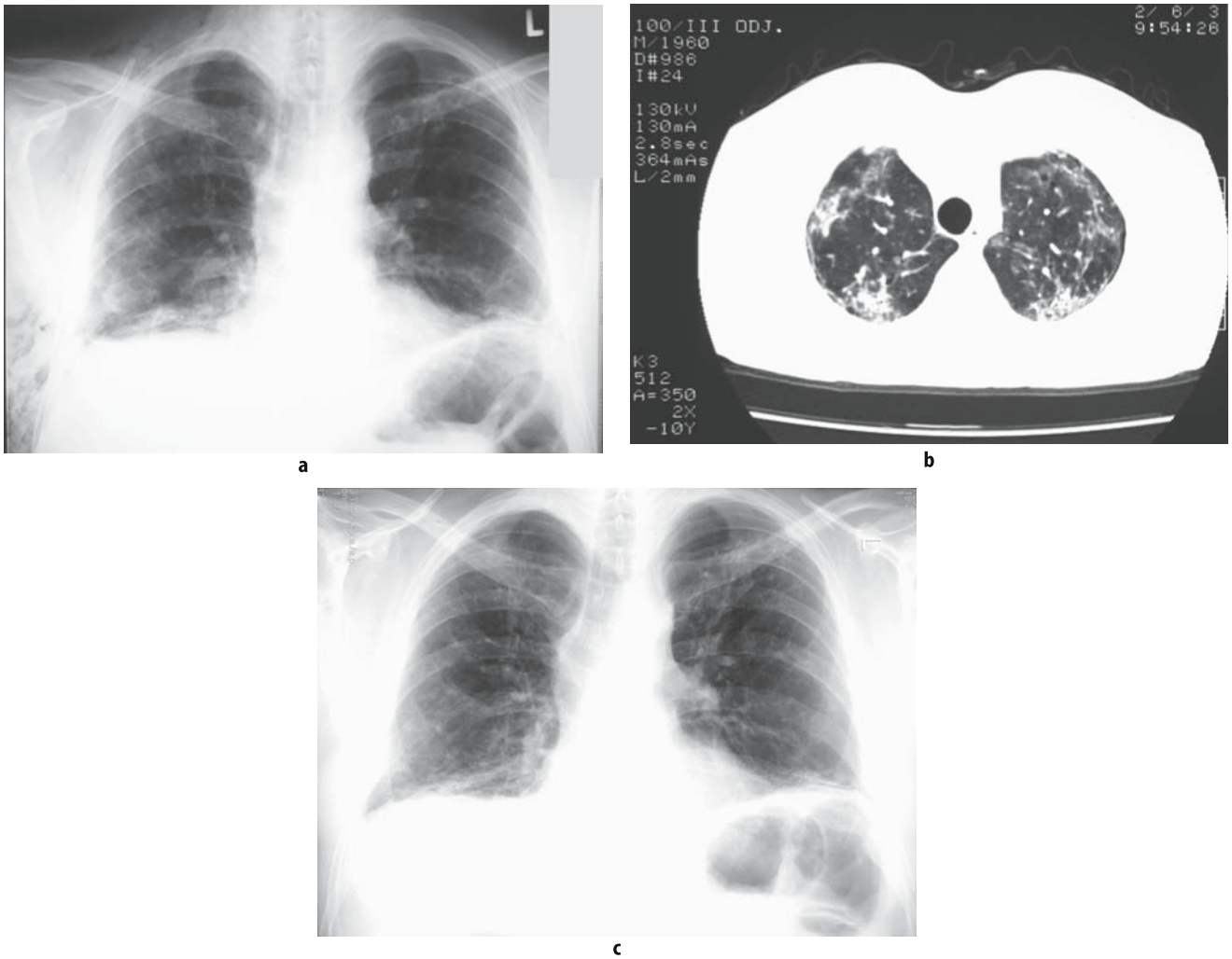


**Figure 8.1.** Plain radiograph of the chest shows bilateral patchy alveolar and reticular pattern, and no honeycombing in a patient with idiopathic cellular NSIP; the subcutaneous emphysema following the surgical open lung biopsy procedure is seen (a). HRCT scan of the chest of the same patient reveals bilateral consolidation and ground-glass pattern (b). Six-month therapy with corticosteroids and azathioprine caused regression of bilateral patchy infiltrates (c) and diminishing of restriction. Flow-volume curve shows restrictive pattern, with normal value of peak expiratory flow (PEF) resembling strong expiratory effort at the beginning of exhalation, followed with rapid graduate decrease of airflow, which finished earlier than normal. Significant improvement occurred after combined immunosuppressive treatment, with completely bigger flow-volume loop (d).

(continued)

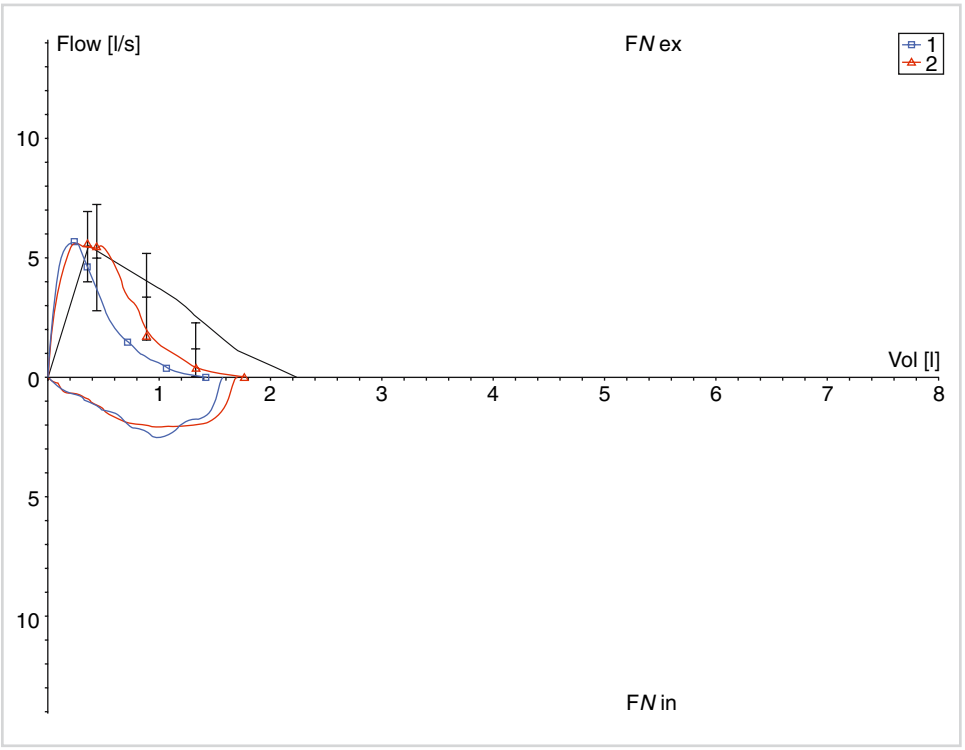


d

**Figure 8.1.** (continued)

A *surgical biopsy* is necessary for a confident diagnosis in all cases of IIP except those who demonstrate typical features of IPF. The "key" histological features of NSIP are the "temporally uniform" pattern together with a "diffuse interstitial fibrosing process" (Figure 8.4a) and virtually absent fibroblastic foci and the lack of features of IPF or other interstitial pneumonia.

The presence of fibrosis (Figure 8.4b, c) on surgical lung biopsy is associated with a worse prognosis. Five-year mortality for fibrotic NSIP was 45%; older age and reduced $D_{LCO}$ are independently associated with heightened mortality.

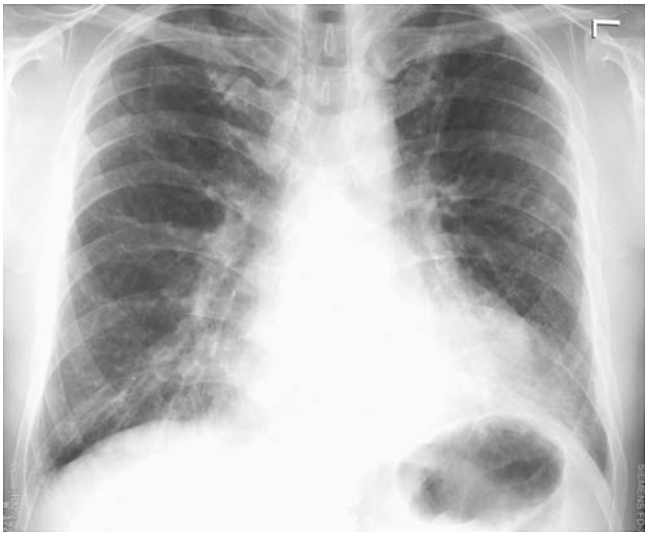

a

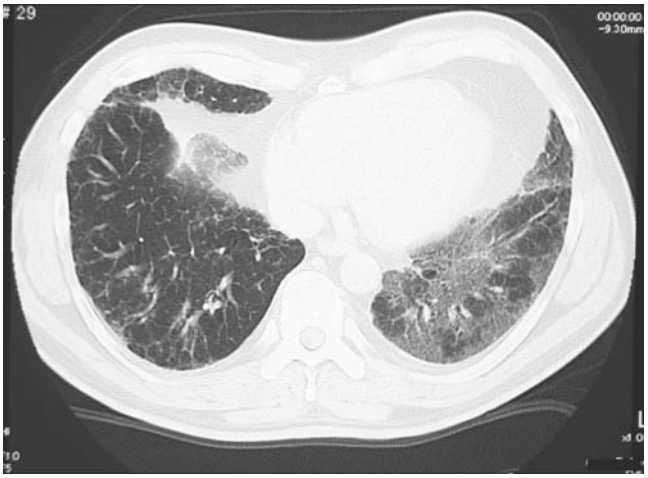

b

**Figure 8.2.** A 40-year-old patient suffered from dyspnea and cough for almost 1 year. The symptoms could not be connected with any know cause of ILD. He refused the aggressive diagnostic procedure but finely open lung biopsy was performed. The histopathological diagnosis was fibrotic NSIP. Plain chest radiograph shows coarse reticular pattern and bibasilar opacifications (a) and HRCT scan reveals some ground-glass opacifications in the left lung and interlobular septal thickening and parenchymal retraction in the right lung.

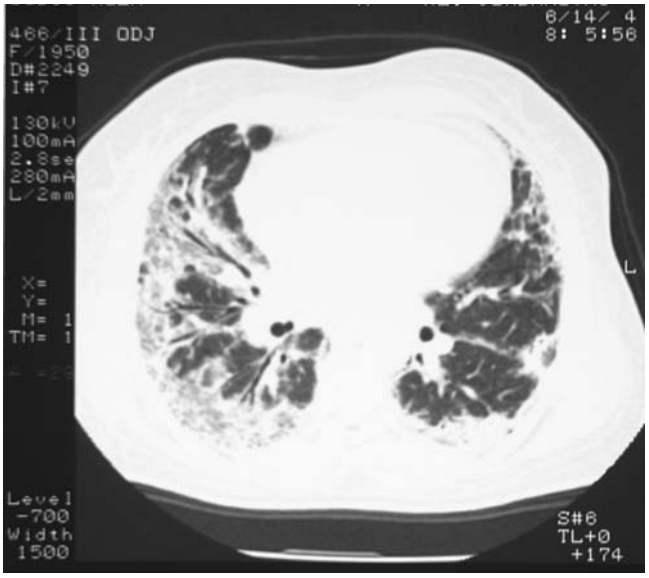


**Figure 8.3.** The HRCT scan in a patient with systemic sclerosis associated NSIP; ground-glass opacities are seen around peribronchovascular bundles.

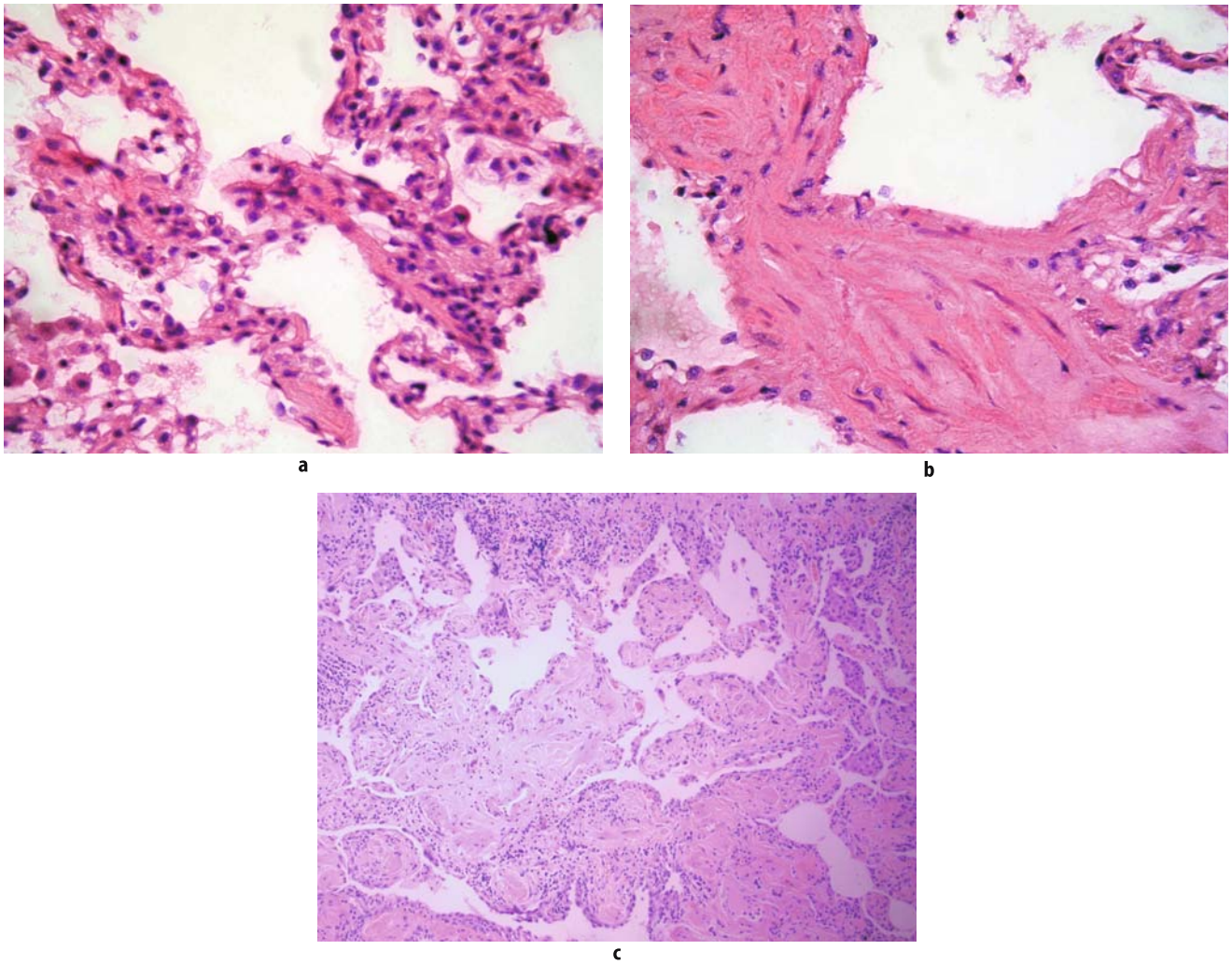


**Figure 8.4.** Nonspecific interstitial pneumonia (NSIP). Cellular NSIP: in alveolar septa there are some infiltrates of lymphocytes and plasma cells. The lesions show temporal uniformity. Lung biopsy shows prominent interstitial inflammation without significant scarring and fibroblastic foci (a). Fibrotic NSIP: alveolar walls are thickened with fibrosis, but alveolar architecture is preserved. The fibrotic form of NSIP resembles UIP and has worse prognosis than cellular NSIP (b). End-stage of NSIP: consists of dense fibrosis and the normal lung architecture is replaced by cystic spaces (c).

The *therapy* of NSIP is not uniform, and additional randomized, controlled studies are required. The initial therapy should be prednisone (60 mg daily for 1 month, 40 mg for 2 months) with gradual taper. If unsuccessful, azathioprine (2–3 mg/kg per day) is added for 6 months.

## Bibliography

1. Travis WD, Matsui K, Moss JE, Ferrans VJ. Idiopathic nonspecific interstitial pneumonia: Significance of cellular and fibrosing patterns. Survival comparison with usual interstitial pneumonia and desquamative interstitial pneumonia. Am J Surg Pathol 2000;24:19–33.
2. Nagai S, Handa T, Tabuen R, Kitachi M, Izumi T. Nonspecific pneumonia: A real clinical entity? Clin Chest Med 2004;25:705–715.
3. Drent M, du Bois RM, Poletti V. Recent advances in the diagnosis and management of nonspecific interstitial pneumonia. Curr Opin Pulm Med 2003;9(5):411–417.
4. Lynch JP, Horowitz JC, Thannickal VJ. Non-specific interstitial pneumonia. In: Baughman RP, du Bois R, Lynch JP, Wells AU, Eds. Diffuse Lung Disease. A Practical Approach. London: Arnold; 2004:153–165.
5. Shimitzu S, Yoshinouchi T, Ohtsuki Y, Fujita J, Sugiura Y, Banno S, Yamadori I, Eimoto T, Ueda R. The appearance of S-100 protein positive dendritic cells and the distribution of lymphocyte subsets in idiopathic interstitial pneumonia. Respir Med 2002;96:770–776.

# 9

# Bronchiolitis Obliterans Organizing Pneumonia

Bronchiolitis obliterans organizing pneumonia (BOOP) and organizing pneumonia (OP) are synonymous. The characteristic histopathological finding is the granulated tissue plugs within the lumen of small airways that extend into the alveolar ducts and alveoli. Numerous conditions and diseases show identical histological picture (Table 9.1), but the clinician by means of clinical, radiological, and laboratory findings establishes the final diagnosis. By eliminating the known causes and conditions of this syndrome, the diagnosis of idiopathic BOOP is made.

Idiopathic BOOP is an unequivocal *clinicopathologic entity* that is recognized in typical cases as a pulmonary infiltrate accompanied by febrile illness of a few weeks duration that is not responsive to a typical course of antibiotics. It affects men and women equally, most often between 50 and 60 years of age. Mild fever is frequent, and nonproductive cough, sweats, anorexia, fatigue, weight loss, and mild dyspnea are usually present. The symptoms are rarely severe; some patients experience acute respiratory failure even with fatal ending.

*Pathogenesis* of BOOP is not resolved thoroughly. The histological pattern of BOOP is a result of nonspecific reaction that results from alveolar damage with intra-alveolar leakage of plasma proteins, especially coagulation factors, which further undergoes a process of intra-alveolar organization. The first step consists of acute alveolar epithelial injury, with cell necrosis and denudation of the basal lamina. Organization begins with formation of intra-alveolar fibrinoid inflammatory clusters rich in coagulation factors and further intra-alveolar migration of interstitial fibroblasts through gaps in the injured basal laminae. The proliferating fibroblasts colonize the fibrin strands. They undergo phenotypic modulation into myofibroblasts and organize into fibroinflammatory buds with deposition of a loose connective matrix in which fibronectin and collagen III are abundant. The buds become progressively more fibrotic with concentric layers of myofibroblasts and connective tissue, thus giving the typical appearance of intra-alveolar buds.

*Diagnosis* rests upon typical history of the disease, chest radiological findings, and histopathological analysis. Laboratory tests are nonspecific; increased blood neutrophils, erythrocyte sedimentation rate (even above 100 mm/first hour), and C-reactive protein values can be detected.

Lung function tests show mild restrictive ventilatory defects, without obstruction. Reduced $DL_{CO}$ and mild hypoxemia are often detected.

Plain radiograph of the chest shows bilateral, bibasilar, peripheral, and sometimes migratory patchy alveolar pattern in a typical patient with BOOP (Figure 9.1a, b), but patients with diffuse BOOP show multiple alveolar and reticular infiltrates (Figure 9.2a). HRCT scan reveals consolidation and ground-glass pattern; their size may range from few centimeters to an entire lobe (Figure 9.1c and Figure 9.2b).

Broncholaveolar lung lavage differential cell count shows moderate increase of lymphocytes, neutrophils, and eosinophils (i.e., mixed alveolitis) (Figure 9.3), with decreased CD4/CD8 ratio. Foamy macrophages are often present.

**Table 9.1.** Clinical conditions associated with bronchiolitis obliterans organizing pneumonia (BOOP) histological pattern.

| |
|---|
| Idiopathic BOOP |
| Postinfectious BOOP |
| Viruses (HIV, herpesvirus, influenza virus) |
| Bacteria (*Nocardia asteroides*, *Mycoplasma pneumoniae*, *Legionella* pneumophilia, *Chlamydia pneumoniae*) |
| Parasites (*Plasmodium vivax*) |
| Fungi (*Aspergillus, Pneumocystis jiroveci* |
| Diffuse connective tissue disease |
| Polymyositis/dermatomyositis, rheumatoid arthritis, systemic sclerosis, Sjögren syndrome, systemic lupus erythematosus, polymyalgia rheumatica, Behçet disease, mixed cryoglobulinemia |
| Drugs |
| Inhalation of toxic fumes |
| Bone marrow graft, lung and liver transplantation |
| Irradiation (breast cancer) |
| Miscellaneous |
| Thyroid disease, ulcerative colitis, Crohn disease, neoplasms, myeloproliferative disorders |

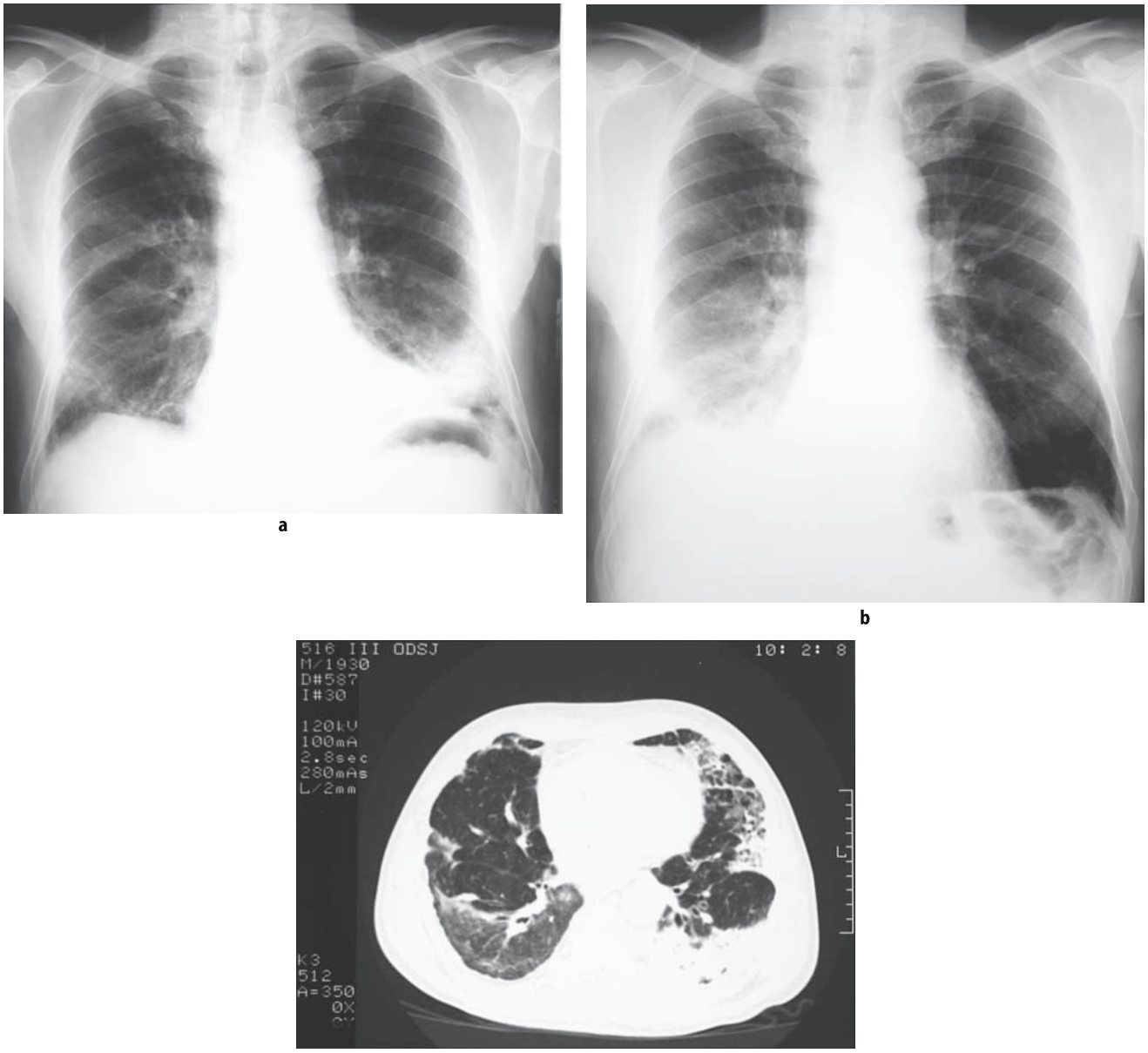


a b c

**Figure 9.1.** Plain radiograph of the chest shows bilateral, bibasilar, peripheral alveolar infiltrates, which migrated from left (a) to the right (b) lung in a patient with idiopathic BOOP. HRCT scan reveals peripheral consolidation and ground-glass opacities and air bronchogram (c). The patient presented with febrile illness of a few weeks duration. Characteristic radiological appearance of idiopathic BOOP was complemented with finding of granulated tissue plugs within the lumen of small airways that extend into the alveolar ducts and alveoli in a sample material obtained by transbronchial lung biopsy. The patient fully recovered after 6-month course of corticosteroids.

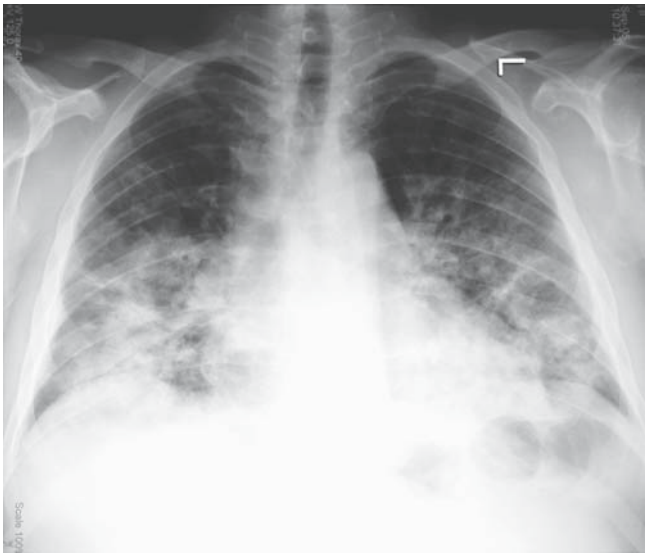

a

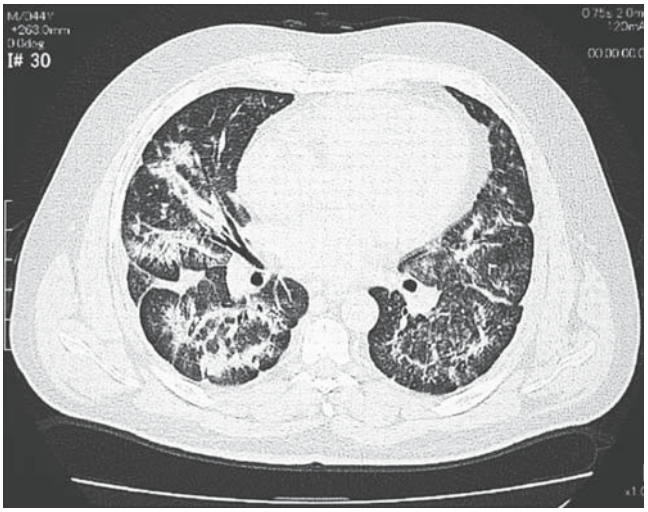


b

**Figure 9.2.** Chest x-ray finding in a patient with diffuse BOOP shows multiple alveolar and reticular infiltrates (a). HRCT scan shows multiple, patchy consolidations and scarce reticular pattern without honeycombing (b).

The method to obtain an adequate sample of lung tissue for histopathological analysis is VAT biopsy, sometimes surgical open lung biopsy, and exceptionally in characteristic clinical setting transbronchial biopsy suffices. Figure 9.4 shows the characteristic histopathological finding in BOOP.

The current reference *treatment* of BOOP is corticosteroids. There are occasional reports of spontaneous recovery or after treatment with erythromycin. Some authors propose high initial doses (1 mg $kg^{-1}$ $day^{-1}$), but most treatment protocols use lower doses of corticosteroids (i.e., 0.75 mg $kg^{-1}$ $day^{-1}$ of prednisone). Corticosteroid therapy causes the complete disappearance of pulmonary infiltrates in 65% to 85% of cases but relapses are common. The therapy of secondary BOOP is less efficient.

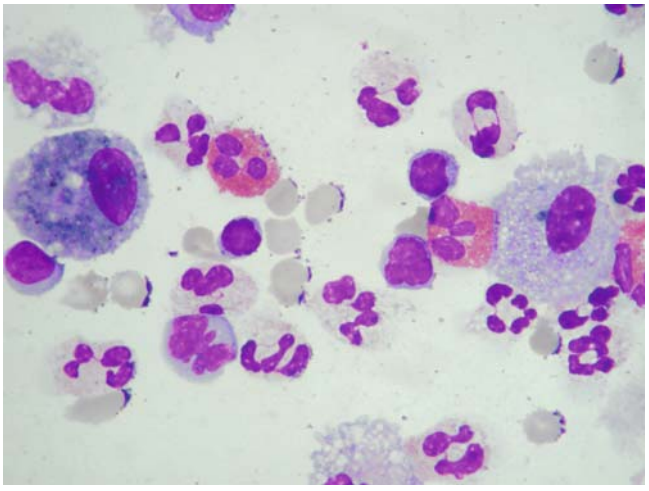

**Figure 9.3.** Lung lavage analyses most often show mixed alveolitis. Neutrophils, eosinophils, small lymphocytes, few macrophages. BAL fluid cytology, original magnification ×1000, MGG stain (May-Grünwald-Giemsa).

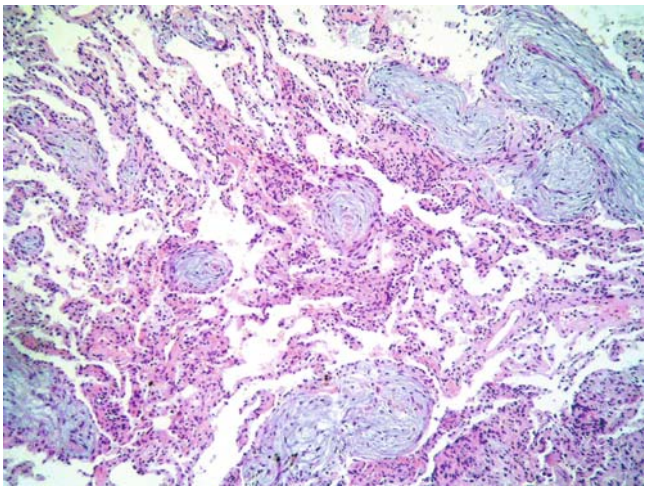

**Figure 9.4.** Bronchilitis obliterans organizing pneumonia (BOOP). The distal airway spaces are filled with granulation tissue (fibroblasts in myxoid stroma).

## Bibliography

1. Cordier JF. Cryptogenic organizing pneumonia. Clin Chest Med 2004;25:727–738.
2. Poletti V, Cazzato S, Minicuci N. The diagnostic value of bronchoalveolar lavage and transbronchial lung biopsy in cryptogenic organizing pneumonia. Eur Respir J 1996;9:2513–2516.
3. Peyrol S, Cordier JF, Grimaud JA. Intra-alveolar fibrosis of idiopathic bronchiolitis obliterans organizing pneumonia.Cell-matrix pattern. Am J Pathol 1990;137:155–170.
4. Epler GR. Bronchiolitis obliterans organizing pneumonia. Arch Intern Med 2001;161:158–164.
5. Lazor R, Vandevenne A, Pelletier A, Leclerc P, Court-Fortune I, Cordier JF. Cryptogenic organizing pneumonia. Characteristics of relapses in a series of 48 patients. Am J Respir Crit Care Med 2000;162:571–577.

# 10

# Acute Interstitial Pneumonia

In 1935, Hamman and Rich reported four cases of rapidly progressive lung fibrosis with identical histological pattern. Today, acute interstitial pneumonia (AIP) is defined as a rapidly progressive and histologically distinct form of interstitial pneumonia. The pathological pattern is an organizing form of diffuse alveolar damage (DAD) that is also found in acute respiratory distress syndrome (ARDS) and other acute interstitial pneumonias of known causes (Table 10.1). The term *AIP* is reserved for cases of unknown cause.

Histopathologically, the hallmark of early (exudative) phase of DAD is hyaline membranes. Their presence is helpful in differentiating DAD from other IIPs. The lung biopsy typically shows widespread injury with uniform temporal appearance, alveolar septal thickening, and alveolar organization. In the late (organizing) phase, loose organizing fibrosis within alveolar septa and hyperplasia of type II pneumocytes is seen (Figure 10.1).

AIP frequently starts as a flu-like illness in patients over a wide age range (average 50 years). Both sexes are equally affected. The initial *symptoms* are myalgia, headache, sore throat and cough, fever, and dyspnea. The typical signs are tachypnea, tachycardia, fine crackles, and occasional wheezes. Most patients develop hypoxemia and respiratory failure, requiring mechanical ventilation. Curiously, most of the patients are in good health when AIP appears. The occurrence of the illness is not related to any known respiratory disease. The clinical course is progressive although a few patients recover completely.

*Pathogenesis* of AIP is partially resolved. Initial alveolar epithelial cell damage and death are caused by single insult. The inflammatory mediators (TNF-α, interleukin -1β, and others) are released. The neutrophils migrate into the alveolar spaces. Injured alveolar epithelial barrier exudes proteins into alveolar space that leads to the formation of hyaline membranes. The hyaline membrane functions as a framework for migration of fibroblasts, myofibroblasts, and inflammatory cells. The result is considerable augmentation of lung collagen, with widening of interstitial spaces that often causes obliteration of air sacs.

*Diagnosis procedure* consists of radiological chest examination, lung function testing, and lung biopsy analysis. Chest radiographs show diffuse, patchy, bilateral alveolar pattern with sparing of costophrenic angles (Figure 10.2a, b). The most common HRCT findings in patients with AIP are ground-glass haziness, bronchial dilatation, intralobular linear opacities, and architectural distortion. The distribution of ground-glass opacifications is diffuse, bilateral, with areas of focal sparing of lung lobules giving a geographical appearance. Consolidation is frequently seen. Lung lavage is helpful in excluding alveolar hemorrhage, hypersensitive pneumonitis, eosinophilic pneumonia, and also serves as a source of adequate and valuable samples to perform thorough microbiological analyses. Usually neutrophilic alveolitis is associated with scattered atypical type II pneumocytes collected in clusters with extracellular amorphous material (fragments of hyaline membranes).

Other tests, especially serological tests aimed at exclusion of pulmonary vasculitis and connective tissue diseases, are necessary. The exact diagnosis is mandatory, because

**Table 10.1.** Clinical conditions associated with diffuse alveolar damage (DAD) pattern.

| |
|---|
| Idiopathic: acute interstitial pneumonia (AIP) |
| Acute hypersensitive pneumonitis |
| ARDS |
| Connective tissue disease |
| Dermatomyositis/polymyosistis, mixed connective tissue disease, microscopic polyangiitis, rheumatoid arthritis, systemic lupus erythematosus, systemic sclerosis |
| Drug-induced lung disease |
| Amiodarone, bleomycin, busulfan, carmustine, crack cocaine, nitrofurantoin |
| Infection |
| *Legionella* pneumophilia, *Mycoplasma pneumoniae*, viruses |
| Inhalants and toxins |
| Chlorine gas, nitrogen dioxide, oxygen toxicity, phosgene, paraquat |

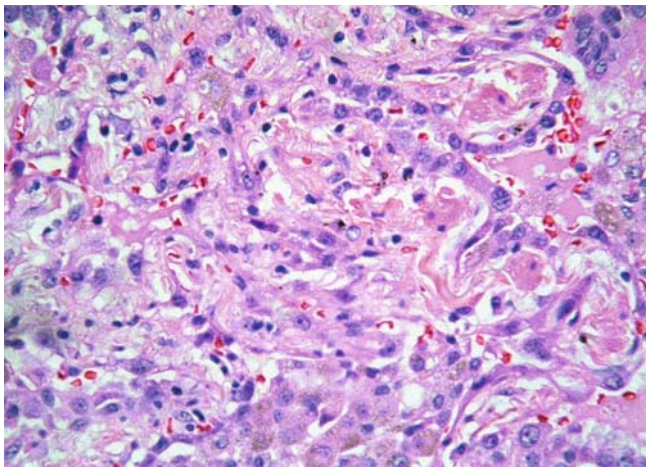

**Figure 10.1.** Acute interstitial pneumonia (AIP). The alveolar septa are widened, with myxomatous and edematous stroma; there is interstital fibroblast proliferation. Marked alveolar type II pneumocyte hyperplasia with scanty exudate in alveolar spaces.

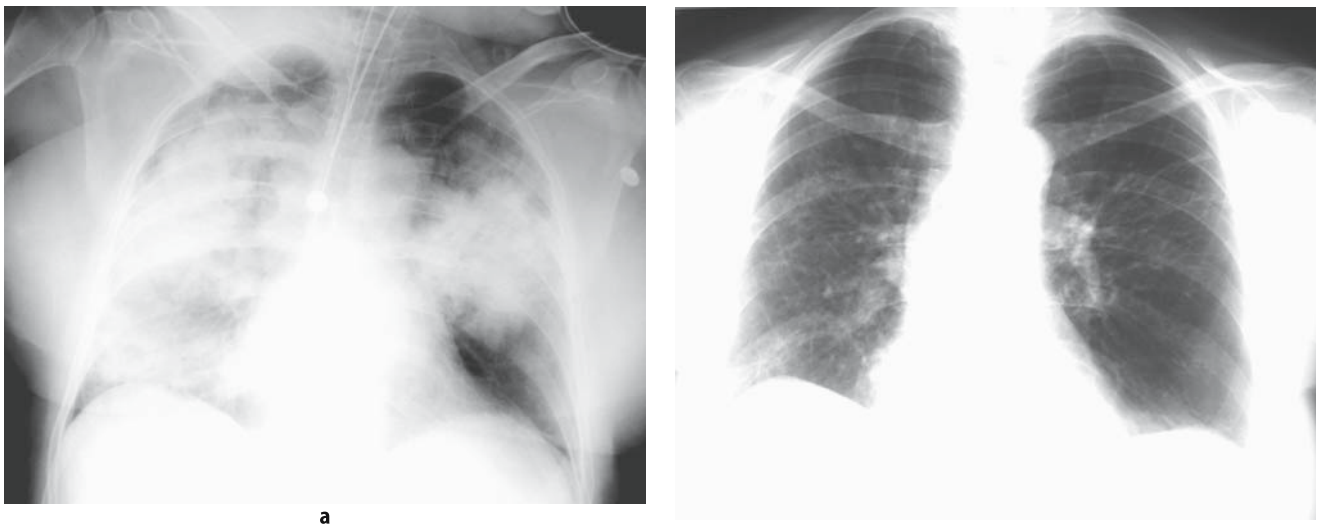

a b

**Figure 10.2.** Plain radiograph of the chest of a patient with AIP shows diffuse alveolar infiltrates (a) and almost normal finding following successful treatment in the ICU. The patient required mechanical ventilation and received high doses of methylprednisolone and azathioprine. Prior to this event she was a healthy person (b).

some of the diseases that are in the differential diagnosis are treated aggressively with immunosuppressive agents.

Open lung biopsy is the procedure that should be weighted carefully because these patients, especially if they require mechanical ventilation, are at risk of developing serious complications.

There is no effective *therapy* for patients with AIP. Most of the patients receive parenteral methylpredinsolone in high doses ($2\,mg\,kg^{-1}\,day^{-1}$ in divided doses) for several days, subsequently switching to oral preparations. There are sporadic reports on effective therapy with immunosuppressive agents.

## Bibliography

1. Vourlekis JS. Acute interstitial pneumonia. Clin Chest Med 2004;25:739–747.
2. ATS/ERS International multidisciplinary consensus classification of the idiopathic interstitial pneumonias. Am J Respir Crit Care Med 2002;165:277–304.
3. Katzenstein AA, Myers JL, Mazum MT. Acute interstitial pneumonia: A clinicopathologic, ultrastructural and kinetic study. Am J Surg Pathol 1986;10:256–267.
4. Bonaccorsi A, Cancellieri A, Chilosi M, Trisolini R, Boaron M, Crimi N, Poletti V. Acute interstitial pneumonia: Report of a series. Eur Respir J 2003;21:187–191.

# 11

# Lymphoid Interstitial Pneumonia

Lymphoid interstitial pneumonia (LIP) represents diffuse involvement of the lung parenchyma by reactive pulmonary lymphoid hyperplasia. In 1969, Liebow and Carrington coined the term. Later, it was thought that LIP represents a pre-neoplastic condition that often progresses to lymphoma, and it was excluded from the group of IIPs. Recently, immunohistochemical and molecular analysis have suggested that although malignant transformation can occur, such development is extremely rare.

Histopathologically, LIP is characterized by dense interstitial lymphoid infiltrate with variable peribronchial involvement. The infiltrates comprise mostly T lymphocytes, plasma cells, and macrophages. The alveolar septa are extensively infiltrated. Lymphoid follicles, including follicles with germinal centers, are often present (Figure 11.1a, b).

The majority of patients with LIP are female, with an average age at presentation of about 50 years. Respiratory symptoms include dyspnea, dry cough, and chest pain. Hemoptysis is rare. Night sweats, fever, and weight loss are infrequent. Lung auscultation reveals bilateral, usually bibasilar crackles. Extrapulmonary lymphatic manifestations like hilar and mediastinal lymphadenopathy and splenomegaly are not a feature of LIP; the presence of these requires search for an alternative diagnosis.

The *cause* of idiopathic LIP is not known. The spectrum of acquired benign diffuse proliferations of BALT (bronchus associated lymphoid tissue, or "pulmonary microtonsils") includes follicular bronchitis/bronchiolitis, diffuse lymphoid hyperplasia, and LIP. The cause of idiopathic LIP is not known, but the LIP histological pattern is found in numerous autoimmune diseases and viral infections and is thought to represent a nonspecific response to various stimuli in a uniquely susceptible host (Table 11.1).

*Diagnostic procedure* includes laboratory analysis, chest roentgenological examination, and bronchoscopy. Almost 80% of patients with LIP have serum dysproteinemia, polyclonal hypergammaglobulinemia, and, less frequently, hypogammaglobulinemia. Chest radiographic features consist of basilar reticular or reticulonodular infiltrate with or without honeycombing (Figure 11.2). HRCT films show areas with ground-glass opacifications and poorly defined centrilobular nodules (Figure 11.3). Subpleural nodules, thickening of bronchovascular bundles, and septal thickening are also noted.

Open lung biopsy is required. Lung lavage fluid analysis is helpful as it usually shows high-intensity lymphocytic alveolitis with an increase in the total cell count of $CD3^+$ T cells and slight increase of polyclonal $CD20^+$ B-cells in typical cases.

When the histological diagnosis of LIP is established, the search for the known cause is essential. The diagnosis of LIP is the diagnosis of exclusion.

The current reference *treatment* of LIP is corticosteroids, with or without immunosuppressive agents. Some patients respond well; others remain relatively stable for years, and still others deteriorate and die of pulmonary fibrosis.

**Table 11.1.** Clinical conditions associated with lymphoid interstitial pneumonia (LIP) pattern.

| |
|---|
| Idiopathic: lymphoid interstitial pneumonia (LIP) |
| Infections |
| *Pneumocystis jiroveci*, hepatitis B, Epstein-Barr virus, herpes virus, tuberculosis |
| Diffuse connective tissue disease |
| Sjögren syndrome, rheumatoid arthritis, systemic lupus erythematosus |
| Immunodeficiency |
| HIV, common variable immunodeficiency, agammaglobulinemia |
| Other immunological disorders |
| Autoimmune hemolytic anemia, myasthenia gravis, pernicious anemia, Hashimoto thyroiditis, chronic active hepatitis, primary biliary cirrhosis |
| Drug-induced (phenytoin, captopril) or toxic exposure |

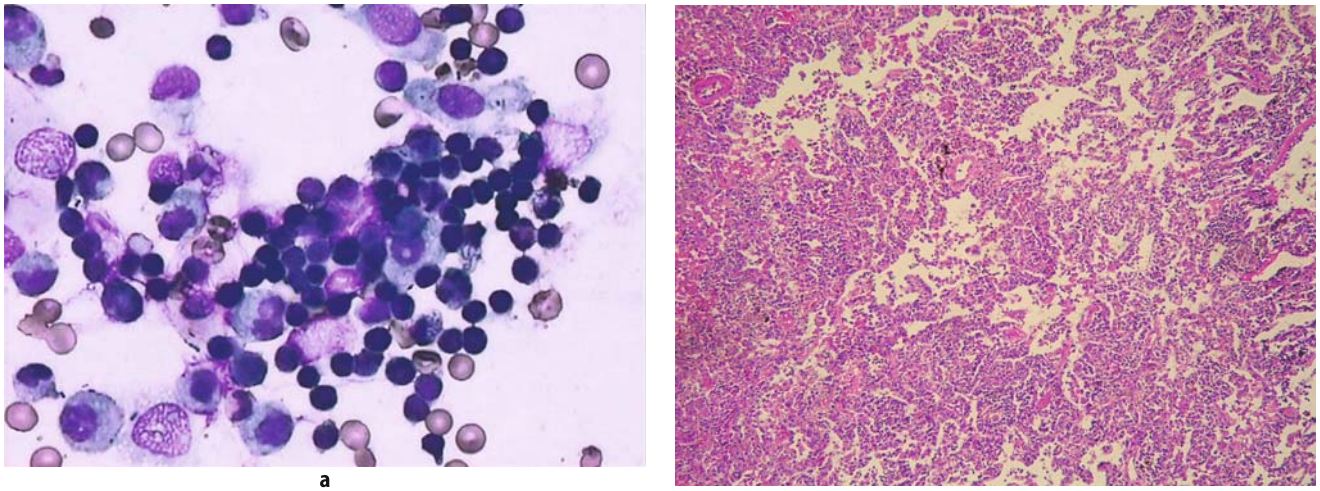

a b

**Figure 11.1.** The cytological imprint of lung biopsy shows the clusters of foamy macrophages and reactive pneumocytes, some small lymphocytes and neutrophil granulocytes (a). Histopathological finding of the same patient shows prominent interstitial widening by infiltrate of small lymphocytes. There is no prominent fibrosis (b).

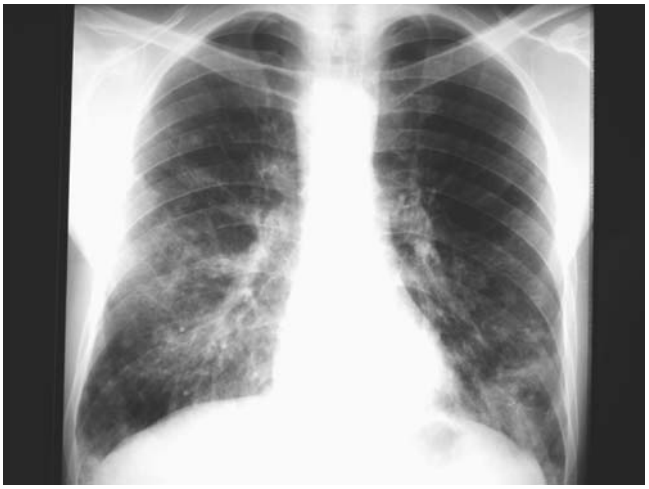

**Figure 11.2.** Plain radiograph of the chest in a patient with LIP shows characteristic basilar reticulonodular pattern.

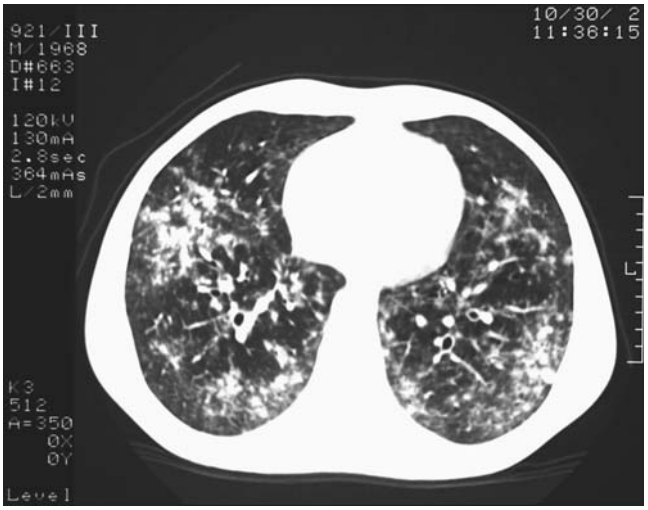


**Figure 11.3.** HRCT scan of the chest shows characteristic ground-glass pattern and nodules in the same patient with LIP. He was successfully treated with corticosteroids.

## Bibliography

1. Nicholson AG. Lymphocytic interstitial pneumonia and other lymphoproliferative disorders of the lung. Sem Resp Crit Care Med 2001;22:409–421.
2. Swigris JJ, Berry GJ, Raffin TA, Kuschner WG. Lymphoid interstitial pneumonia: A narrative review. Chest 2002;122:2150–2164.
3. Fishback N, Koss M. Update on lymphoid interstitial pneumonia. Curr Opin Pulm Med 1996;2:429–433.
4. Poletti V, Kitaichi M. Facts and controversies in the classification of idiopathic interstitial pneumonias. Sarcoidosis Vasc Diffuse Lung Dis 2000;17:229–238.

# 12

# Eosinophilic Interstitial Lung Disease

The eosinophilic lung diseases are a heterogeneous group of clinical entities characterized by an increased number of eosinophils in the blood, airways, alveoli, and/or interstitial spaces. Many attempts have been made to devise a practical and useful clinical classification. Collectively, these clinical entities are lumped together in a common term: *pulmonary infiltration with eosinophilia* (PIE) syndromes.

Common interstitial lung diseases with increased eosinophils and parenchymal infiltration include bacterial, fungal, and parasitic infections, allergy to certain fungi, diffuse connective tissue diseases, vasculitides, various drug-induced syndromes, cancer, and idiopathic pulmonary eosinophilia (of unknown cause), like chronic eosinophilic pneumonia (CEP), acute eosinophilic pneumonia (AIP), hypereosinophilic pneumonia, Loeffler syndrome, sarcoidosis, or idiopathic pulmonary fibrosis (Table 12.1) (discussed below).

Muller reported a study of 7000 eosinophil determinations in 1000 patients with tuberculosis in which the eosinophil count correlated with disease activity. Eosinophilia was present in patients who fared well, and eosinophilia was twice as frequent in men as in women; the incidence in women being 6%.

Pulmonary eosinophilia represents a hypersensitivity reaction to coccidioidomycosis and has been observed in up to 88% of patients with primary infection. A transient pneumonia and eosinophilia is also noted in histoplasmosis, cryptococcosis, and dirofilaria (Figure 12.1). Allergic bronchopulmonary aspergillosis (Figures 12.2, 12.3, and 12.4) and bronchocentric granulomatosis are two clinical syndromes cause by aspergillus organisms that have significantly elevated blood, sputum, and bronchoalveolar lavage fluid eosinophils.

Tropical eosinophilia occurs in those areas of the world where the temperature is warm and the humidity high. It affects men more often than women and most frequently young people in their twenties and thirties. Asian Indians are particularly susceptible. Symptoms include dry, irritating, and nocturnal cough. In most patients, the peripheral eosinophil count is usually more than 2000 $mm^3$ and may exceed 4000 $mm^3$. The radiographic findings include diffuse military mottling and increased hilar markings. The filarial skin and the complement-fixation tests are positive. A good clinical response to diethylcarbamazine confirms the diagnosis.

Certain drugs, such as penicillin, sulfonamides, nitrofurantoin (Figure 12.5), cromolyn sodium, *para*-aminosalicylic acid, chloropropamide, tetracycline, bleomycin, and methotrexate, may cause ill-defined patchy amd interstitial pulmonary densities. Patients usually have been taking the drug for a few weeks before the symptoms appear. The symptoms disappear rapidly if the offending drug is discontinued.

In 1932, Loeffler described a benign, self-limiting clinical syndrome. It produces fleeting pulmonary infiltration and mild eosinophilia associated with minimal or no respiratory or systemic symptoms. No cause is known; usually, no treatment is required. By definition, the disease resolves within 4 weeks. A careful search for parasitic infection or drug reaction should be pursued.

**Table 12.1.** Classification of eosinophilic interstitial lung disease.

| | |
|---|---|
| Bacterial infections | Brucellosis; mycobacterial illnesses |
| Fungal infections | Aspergillosis; coccidioidomycosis |
| Parasites | Schistosomiasis; trichinosis |
| | Tropical eosinophilia |
| AIDS associated | *Pneumocystis jiroveci* pneumonia |
| Allergy | Allergic bronchopulmonary mycoses |
| Diffuse connective tissue disease and vasculitis | Systemic lupus erythematosus; Churg-Strauss vasculitis; Wegener granulomatosis |
| Drug induced | Methotrexate, bleomycin, sulfasalazine, clarithromycin, nitrofurantoin, tetracycline |
| Cancer | Lung cancer |
| | Lymphoma |
| Idiopathic | Chronic eosinophilic pneumonia |
| | Acute eosinophilic pneumonia |
| | Hypereosinophilic pneumonia |
| | Loeffler syndrome |

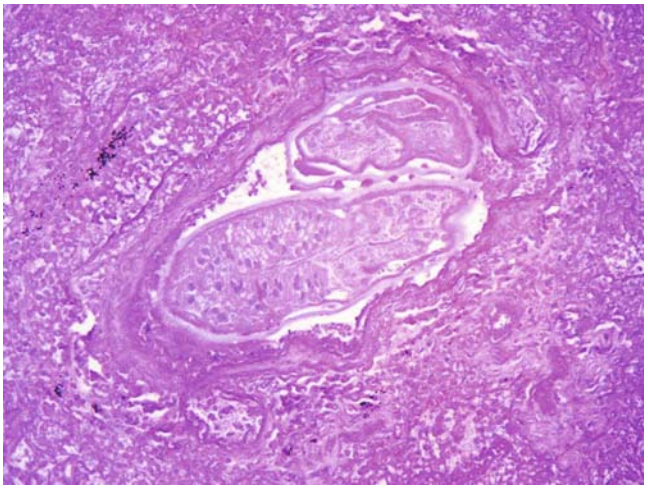

**Figure 12.1.** Histological finding of the patient with dyrophillariosis: open lung biopsy, PAS stain. In the center of an infarct there is small pulmonary artery containing two cross sections of *Dirofilaria*.

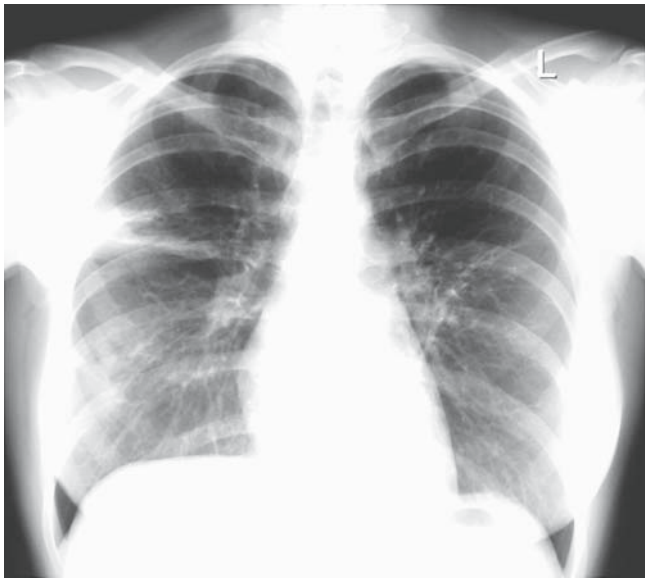

a

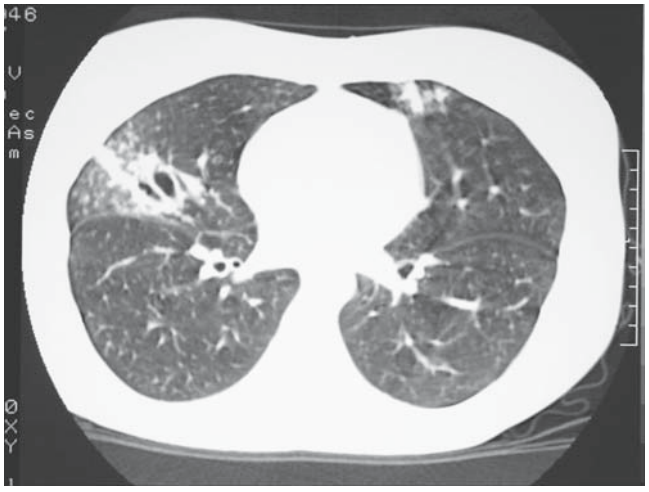

b

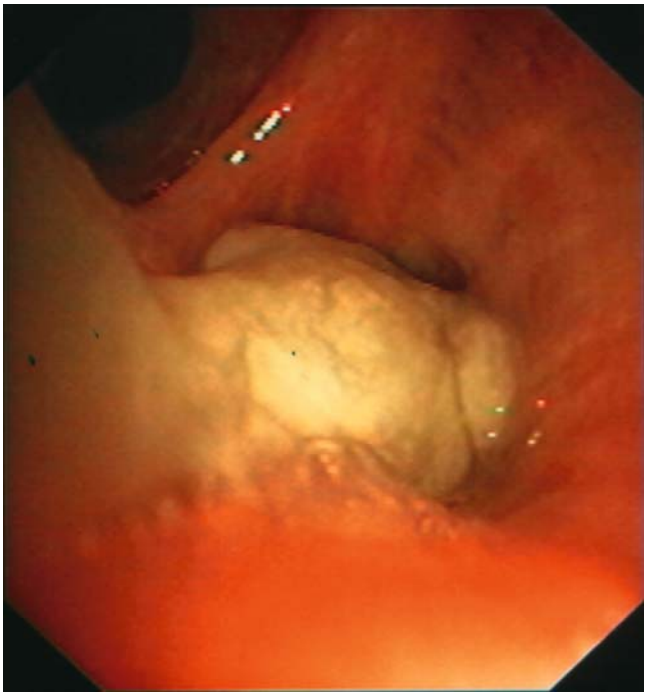

c

**Figure 12.2.** Plain radiograph of the chest shows unilateral alveolar infiltrates in a young woman suffering from asthma (a). HRCT of the same patient shows dilated lobar bronchi forming proximal bronchiectasis (b). Bronchoscopic finding in the same patient shows the lobar bronchus filled with plug of mucus (c).

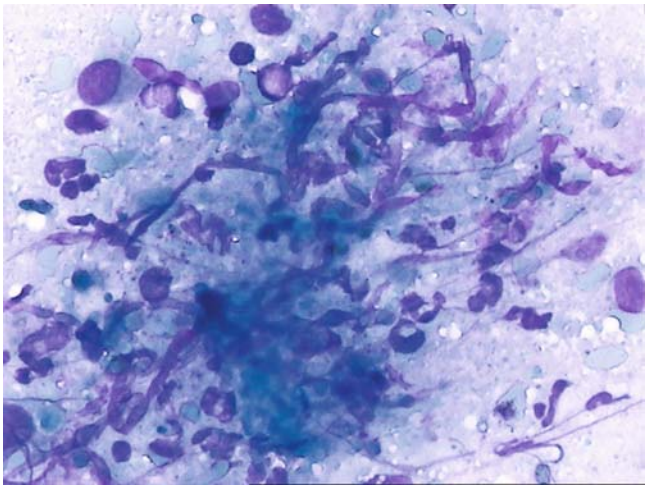

a

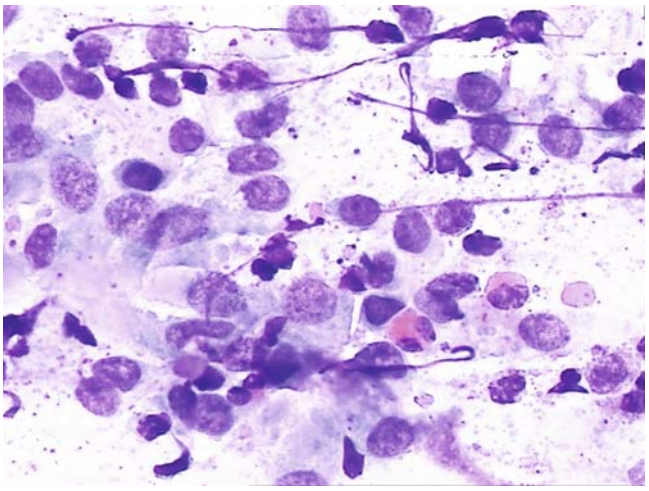

b

**Figure 12.3.** Characteristic cytological finding of ABPA are hyphae, neutrophils, detritus, and eosinophilic granulocytes. Characteristic branching septating hyphae, bronchial epithelial cells, erythrocytes. Brush bronchial smear cytology, original magnification ×400, MGG stain (May-Grünwald-Giemsa) (a). Neutrophils, detritus, and eosinophil. Brush bronchial smear cytology, original magnification ×1000, MGG stain (May-Grünwald-Giemsa) (b).

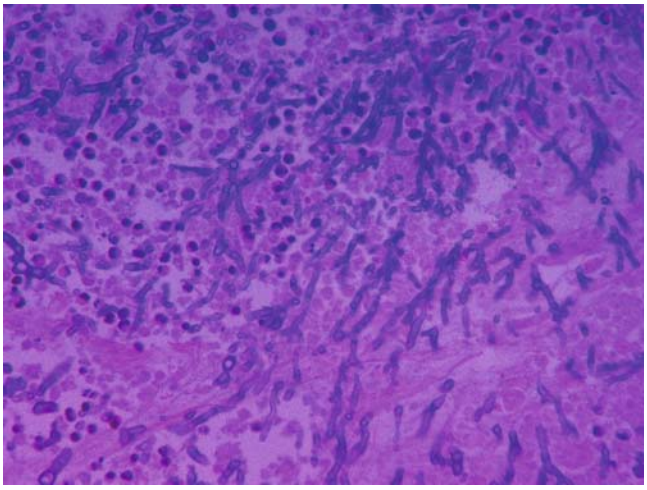

a

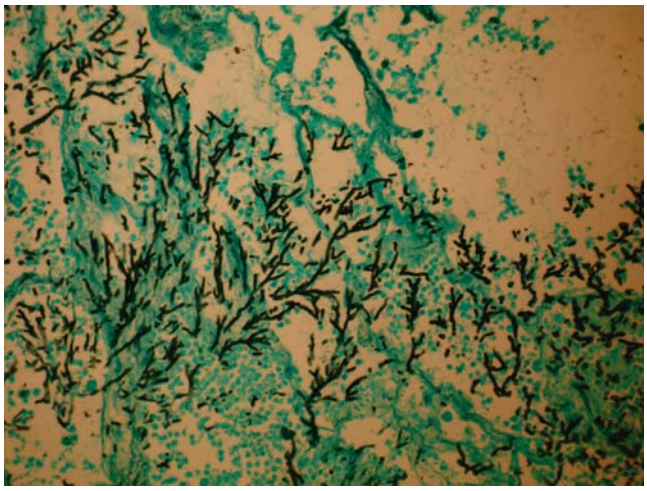

b

**Figure 12.4**. Allergic bronchopulmonary aspergillosis (ABPA). The airways are typically filled with numerous branching casts that contain eosinophils, Charcot-Leyden crystals, Curschmann spirals, and fungal hyphae. The debris, eosinophils, and branching hyphae are consistent with *Aspergillus* (a). Gomori methenamine silver stain showing branching hyphae of *Aspergillus* (b).

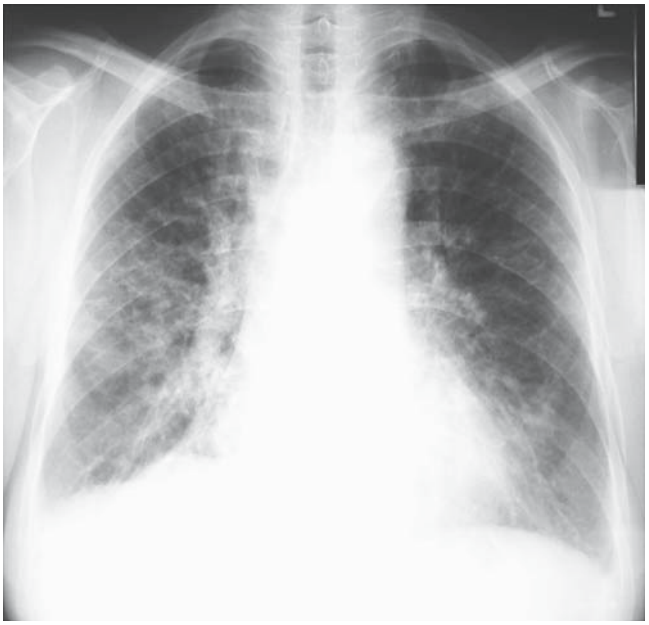

a

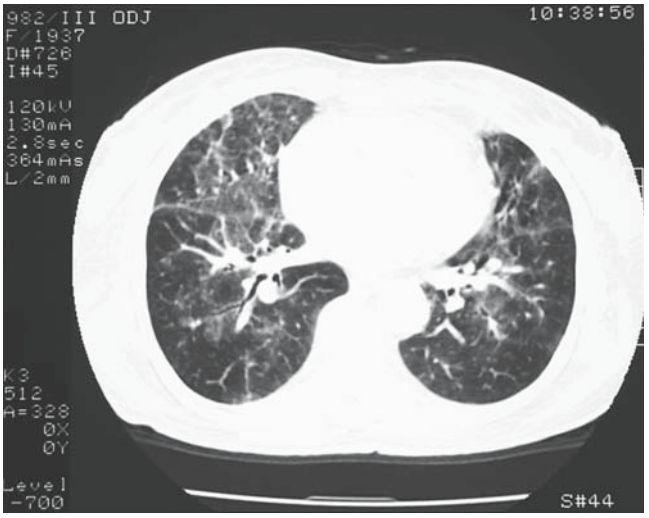


b

**Figure 12.5.** Drug-induced pulmonary eosinophilia in a patient who was treated with nitrofurantoin. The infiltrates disappeared soon after the cessation of the drug. The plain radiograph shows multiple patchy alveolar and linear interstitial opacifications (a) and CT scan ground-glass pattern (b).

Chronic eosinophilic pneumonia is a syndrome consisting of fever, cough, night sweats, weight loss, and dyspnea. The radiographic studies reveal dense infiltrate localized in the peripheral parts of the lungs. Radiographs in this condition have been described as a photographic negative of the picture seen in pulmonary edema (Figure 12.6a, b). Hilar adenopathy and cavitation are absent. The characteristic histological picture is a dense infiltrate of histiocytes, eosinophils, and plasma cells (Figure 12.6c). Increased levels of IL-5, IL-6, and IL-10 are found in bronchoalveolar lavage fluid from involved lung segments. The presence of circulating immunecomplexes, elevated levels of IgE, and a frequently positive rheumatoid factor suggest an immunopathogenic mechanism. Treatment with corticosteroids rapidly resolves all clinical and radiographic abnormalities. If a relapse occurs, pulmonary lesions are usually identical in size, shape, and location in those of the initial episode.

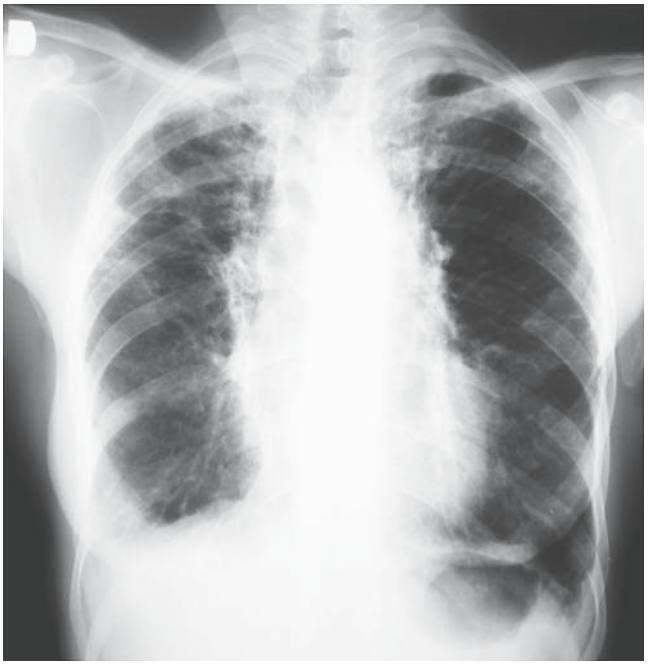

a

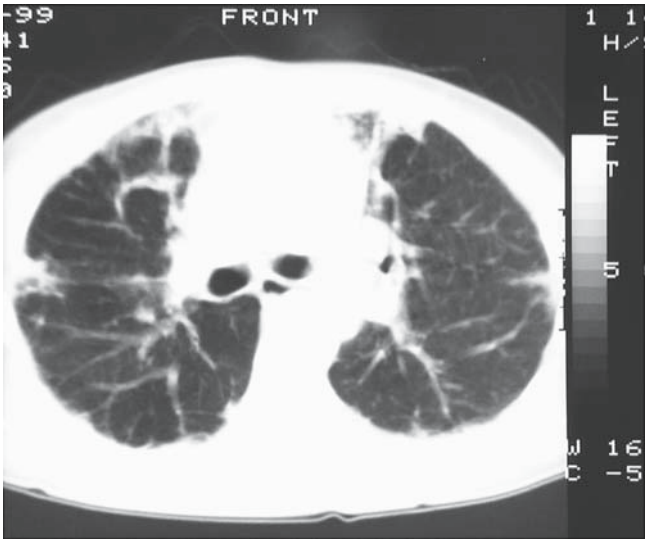


b

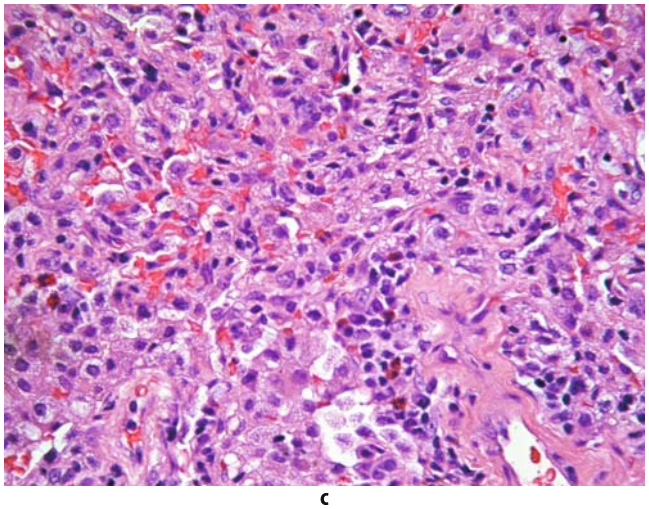

c

**Figure 12.6.** Plain radiograph of the chest shows the peripheral distribution of alveolar infiltrates, often described as the "the photographic negative of chronic pulmonary edema" (a). HRCT of the same patient revealed the peripherally distributed consolidation and ground-glass changes, with no signs of fibrosis (b). Histopathological finding was chronic eosinophilic organizing pneumonia with infiltrates of eosinophils and with some foamy cells in the alveoli (c). The patient has experienced relapses of the diseases every time the corticosteroids were abolished. Now she works as a nurse and uses permanent low-dose corticosteroid therapy.

Idiopathic hypereosinophilic syndrome is a rare multisystem illness characterized by sustained overproduction of eosinophils and unchecked T-cell secretion of IL-3, IL-5, and granulocyte macrophage colony-stimulating factor. The illness may be fatal. Corticosteroids are commonly used; about 50% of the patients respond to treatment. Other drugs such as busulfan, hydroxyurea, and imatinib have also been used.

Eosinophilia may be associated with diffuse parenchymal infiltrate that accompanies primary systemic vasculitis. It also occurs in association with rheumatological disorders, chronic infections, lymphoma, sarcoidosis, and extrinsic allergic alveolitis. Primary vascular processes affecting the lung include giant cell arteritis, pulmonary capillaritis, Takayasu arteritis, and those associated with circulating antibodies to neutrophil cytoplasmic enzymes.

Why eosinophils invade the lung tissue remains unclear. Nevertheless, the illnesses lumped together as the eosinophilic lung diseases are a heterogeneous group of clinical entities.

## Bibliography

1. Crofton J, Livingstone J, Oswald N. Pulmonary eosinophilia. Thorax 1952;7:1.
2. Gaensler E, Carrington C. Peripheral opacities in chronic eosinophilic pneumonia: The photographic negative of pulmonary edema. Am J Radiol 1977;128:1.
3. Alberts M. Eosinophilic interstitial lung disease. Curr Opin Pulm Dis 2004;10:419.
4. Savani D, Sharma O. Eosinophilic lung disease in the tropics. Clin Chest Med 2002;23:377.

# 13

# Drug-induced Lung Diseases

The first reports on adverse drug effects in the respiratory system, which appeared about 60 years ago, described nitrofurantoin-induced eosinophilia and pulmonary hypertension caused by fenfluramine, an appetite suppressant. Now it is recognized that more than 350 drugs can cause lung toxicity. Some drugs, like amiodarone, show an affinity to the lung tissue. Type II pneumocytes and Clara cells contain various microsomal enzymes that have the ability to metabolize drugs during the process of biotransformation. Disbalance of enzymatic reaction during the two phases of biotransformation may release various toxic metabolites that induce bioactivation and tissue injury (Figure 13.1). Drug-induced lung disease may involve any part of the pulmonary system (Table 13.1). The most important part of diagnostic evaluation is an accurate history of the disease. Patients should be asked about all medications, including over-the-counter preparations, vitamins, dietary supplements, herbal preparations and tea, ophthalmic solutions, and topically applied creams. It is necessary to obtain information about doses, duration of treatment, and period from the first medication until the onset of symptoms. The clinical presentation and most diagnostic findings are nonspecific, and the most helpful information pertains to resolving symptoms after the drug is discontinued. This can take a long time particularly in adverse reactions that are induced by drugs with long half-life and prolonged elimination. Definitive confirmation of drug-induced reaction is positive rechallenge test. Rechallenge test, however, is not recommended in patients with serious and life-threatening adverse reactions.

Overall prevalence of drug-induced lung diseases is not known. According to several European national epidemiological registries, 3–5% of newly diagnosed patients with interstitial lung diseases account for drug-induced reactions. The most frequent interstitial drug-induced reactions are those induced by amiodarone (Figures 13.2, 13.3, 13.4, and 13.5), cytototoxic agents (methotrexate) (Figure 13.6a, b), and psychotropic drugs (Figure 13.7a, b, c). Plain chest radiographs and HRCT scans are helpful diagnostic procedures. The bronchoalveolar lavage finding of plasma cells, mastocytes, and eosinophils are indicative of lung toxicity due to various drug exposure (Figure 13.5b). Lung biopsy is helpful in excluding other causes of ILD. In patients with amiodarone toxicity, transbronchial histopathological finding and cytological analyses of the imprint could point to the accurate diagnosis (Figure 13.5a).

It is important to be aware of possible adverse drug effects on the respiratory system.

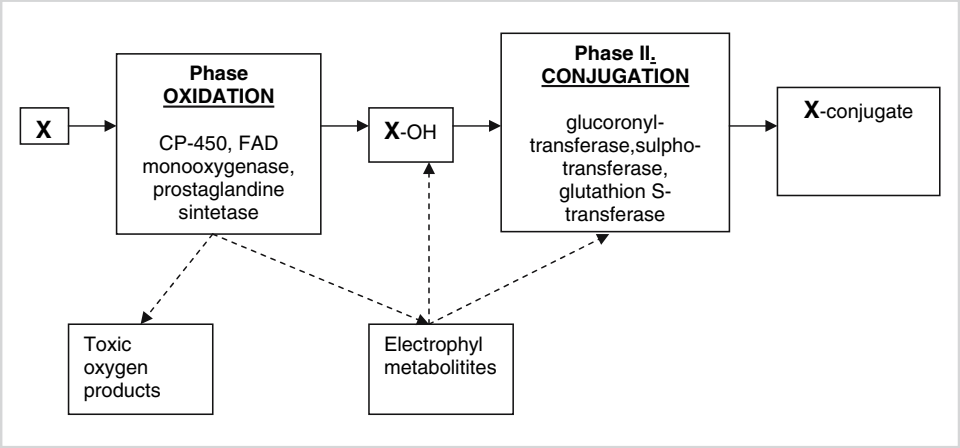


**Figure 13.1.** Biotransformation and bioactivation of xenobiotics. In the case of disbalance of enzymatic velocity between phase I (oxidation) and phase II (conjugation), process of biotransformation leads to bioactivation of drug, release of toxic metabolites and its products.

**Table 13.1.** Classification of drug-induced lung diseases according to clinical features.

| Localization | Adverse Effect |
|---|---|
| Airways | Rhinitis, cough, laryngeal edema bronchospasm acute, subacute, and chronic pneumonitis |
| Pulmonary interstitium | BOOP, DIP, LIP, pulmonary eosinophilia, pulmonary fibrosis, diffuse pulmonary calcification, lipoid pneumonia, pulmonary nodule, diffuse alveolar damage, granulomatosis |
| Capillary endothelium | Non-cardiogenic pulmonary edema |
| Vessels | Pulmonary embolism, pulmonary hypertension, veno-occlusive disease, vascultis-angiitis, fat embolism, alveolar hemorrhage, Goodpasture syndrome |
| Pleura | Pleural effusion, pleural/pericardial thickening, lupus-like syndrome, hemathothorax, pneumothorax, polyserositis |
| Mediastinum | Hilar and mediastinal lymphadenopathy, mediastinal lypomathosis, mediastinal sclerosis, thymus enlargement, mediastinal hemorrhage |
| Muscle and nerves | Hypoventilation, respiratory dyskinesia, respiratory muscle disfunction |
| Other systemic manifestations | Systemic hypersensitivity syndromes with pulmonary infiltrates, rash, eosinophilia, hepatic and mental dysfunction |

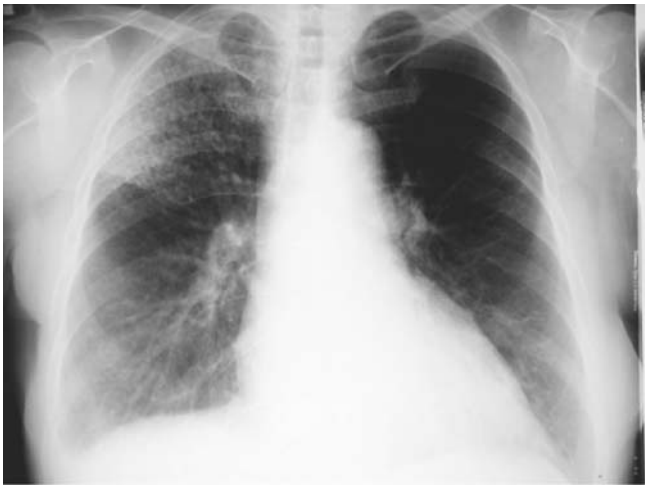

**Figure 13.2.** Amiodarone lung toxicity. Plain chest radiograph of the patient with histopathologic pattern of hypersensitive pneumonitis shows inhomogenous infiltration of right upper lobe.

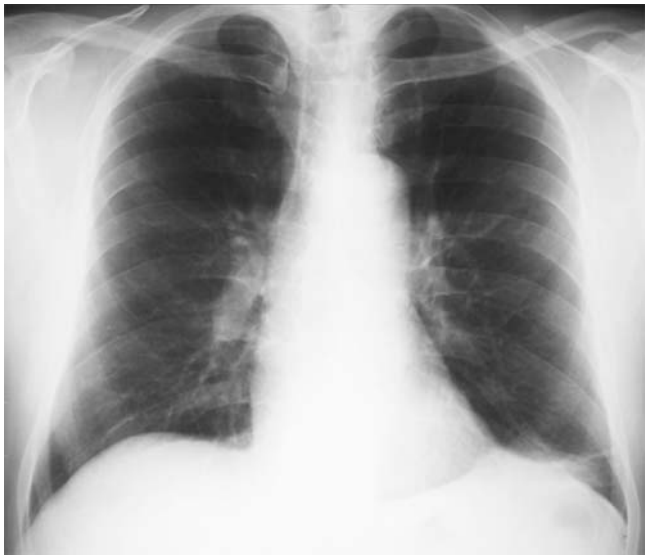

**Figure 13.3.** Amiodarone lung toxicity. Plain chest radiograph of the patient with histopathologic pattern of organizing pneumonia and pleural thickening.

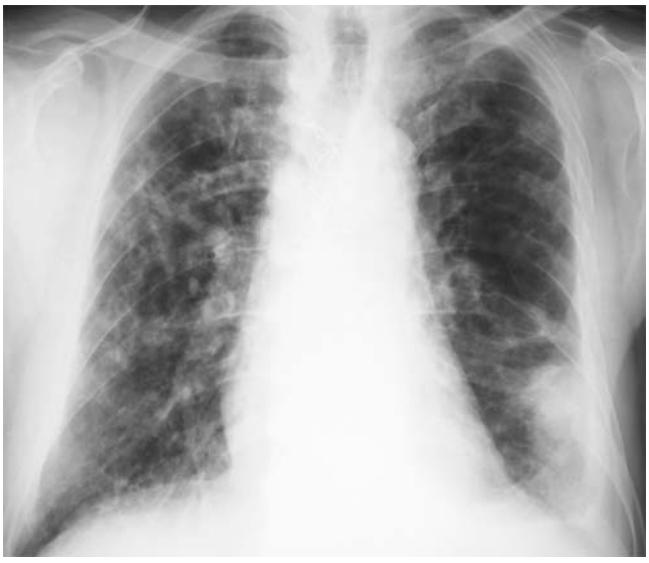

**Figure 13.4.** Amiodarone lung toxicity. Plain chest radiograph of the patient who had undergone aortocoronary bypass. Ten days after the surgery he developed acute amiodarone-induced interstitial pneumonia with histologic pattern of diffuse alveolar damage. Mechanical ventilation was trigger for amiodarone toxicity.

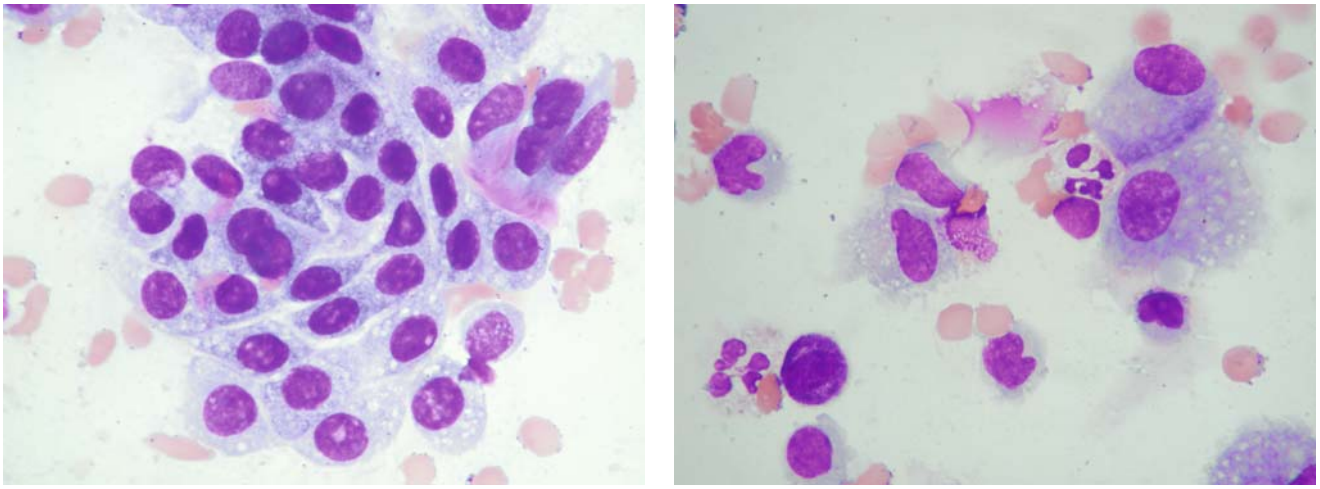

a b

**Figure 13.5.** Cytological appearance of amiodarone exposure. Foamy type II pneumocytes in transbronchial lung biopsy imprint cytology, original magnification ×1000, MGG stain (May-Grünwald-Giemsa) (a). Mastocyte in BAL fluid: mastocyte among alveolar macrophages, neutrophils, and erythrocytes. BAL fluid cytology, original magnification ×1000, MGG stain (May-Grünwald-Giemsa) (b).

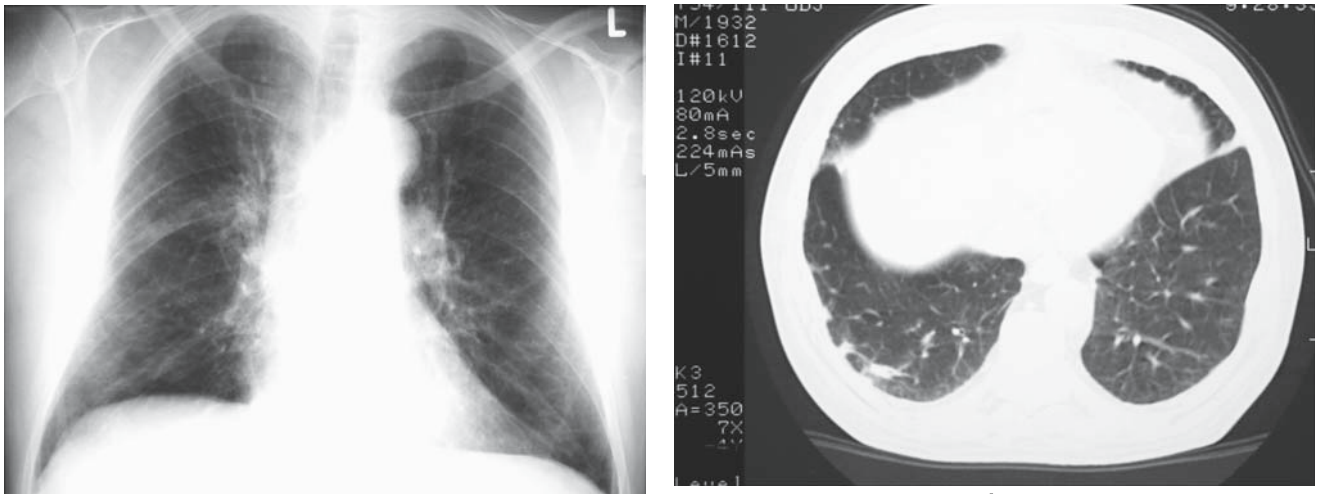


a b

**Figure 13.6.** Plain radiograph of methotrexate lung toxicity in the patient suffering from rheumatoid arthritis reveals fine linear and reticular interstitial pattern predominantly in the middle lung fields. Rheumatoid arthritis seems to be predisposing factor for methotrexate-induced lung disease (a). CT scan of the same patient (b).

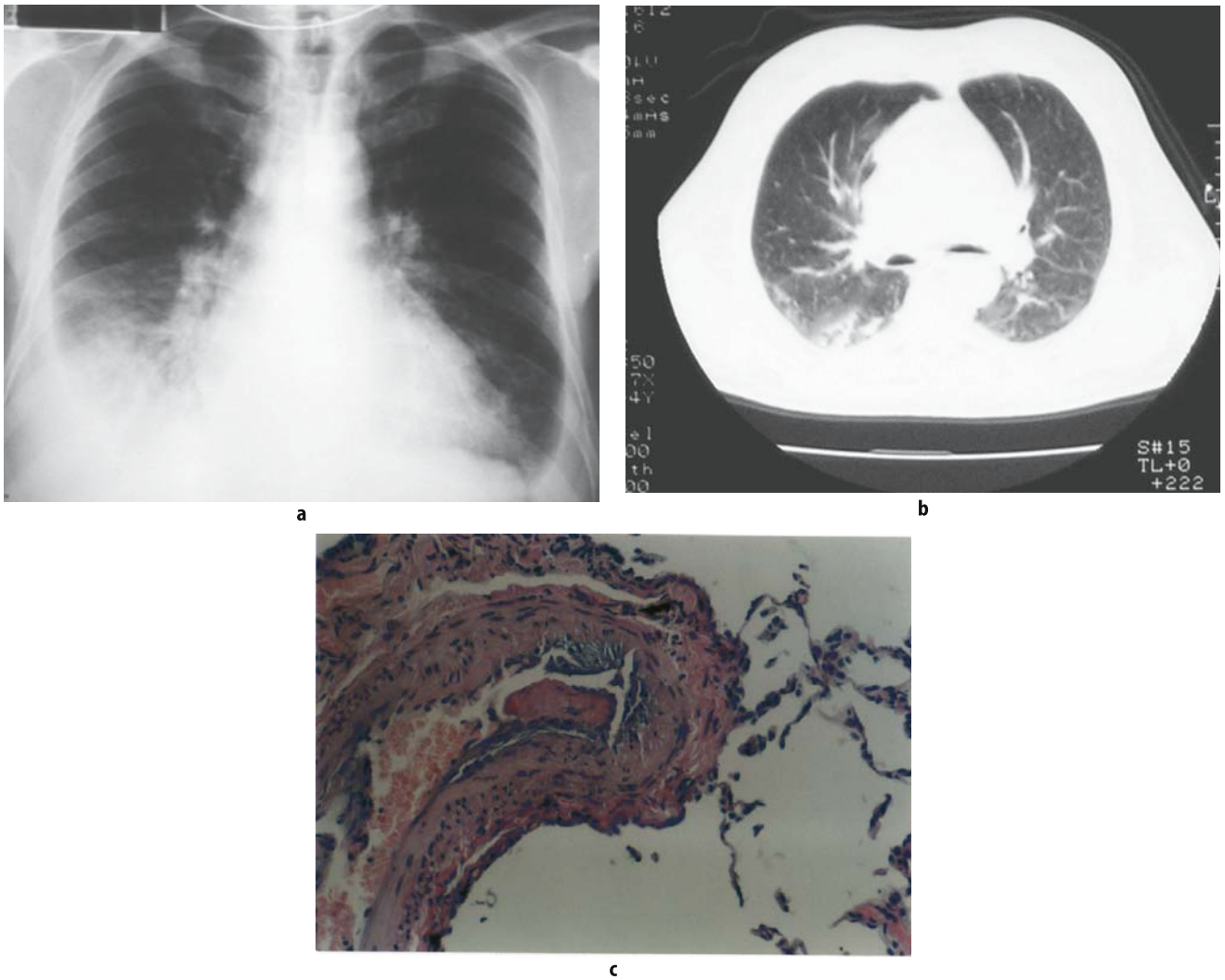


a b c

**Figure 13.7.** Plain chest radiograph of the patient with paranoid schizophrenia, two weeks after intramuscular administration of flufenazine and biperidine. The infiltration of the basal segments of the right lower lobe and bilateral pleural effusion (a). CT scan shows subpleural ground-glass opacities and consolidation (b). Histologic changes of samples obtained by transbronchial lung biopsy of the same patients revealed small vessels incompletely obstructed by organized thrombi. Perfusion scan was negative. Rechallenge test showed that adverse reaction was induced by biperidine (c).

## Bibliography

1. The Uppsala Monitoring Centre. Available at www.who-umc.org/index2.html.
2. The drug-induced lung diseases. Available at www.pneumotox.com.
3. Fishman AP. Aminorex to fen/phen: An epidemic foretold. *Circulation*. 1999;99:156–161.
4. Delaunois LM. Mechanisms in pulmonary toxicology. Clin Chest Med 2004;25:1–14.
5. Wood DL, Osborn MJ, Rooke J, Holmes DR Jr. Amiodarone pulmonary toxicity: Report of two cases associated with rapidly progressive fatal adult respiratory distress syndrome after pulmonary angiography. Mayo Clin Proc 1985;60:601–603.

# 14

# Radiation-induced Lung Diseases

Radiotherapy may cause severe adverse effects, targeting numerous organs including respiratory system. Radiation energy agitates electrons in lung tissue and produces a number of tissue-damaging free radicals. The injury may be immediate (intracellular protein denaturation, membrane disruption) or delayed (alterations of DNA) reactions in lung tissue. Several studies showed that unilateral thoracic radiation causes bilateral lymphocytic alveolitis similar to that of hypersensitivity pneumonitis. A similar immunologic reaction is responsible for producing migratory pneumonitis in patients receiving breast radiotherapy. Thus, radiation-induced lung diseases can be classified into immediate (radiation-induced bronchitis), delayed (radiation-induced pneumonitis), and immunologic (migratory pneumonitis due to breast irradiation) (Table 14.1).

## 14.1 Radiation-induced Bronchitis

This kind of injury is due to cellular membrane disruption. It appears during radiotherapy and is characterized by nonproductive cough and, less commonly, wheezing. Symptoms usually disappear soon after radiation is withdrawn. Most of the patients need no therapy. Severe radiation bronchitis during brachytherapy may result in bronchial stenosis.

## 14.2 Radiation-induced Pneumonitis

Pneumonitis, the consequence of cellular DNA injury, appears in the second generation of cells. Symptoms occur 4–12 weeks after the completion of radiation. Paroxysmal dry cough, dyspnea, and fever are the common symptoms. Clinical course varies from asymptomatic illness to severe life-threatening disease depending on the radiation dose, fractionation, volume of lung irradiated, and concurrent chemotherapy. Physical examination may reveal crackles and pleural rub. Radiation-induced pneumonitis occurs always in the field of irradiation. Radiographic features include alveolar infiltrate, consolidation, ground-glass haziness, and pleural thickening (Figure 14.1a). Asymptomatic radiographic changes, occurring in almost half of irradiated patients, are more frequent than symptomatic pneumonitis. Histopathologic changes reveal alveolar damage (Figure 14.1b). Clinical symptoms diminish within 1 to 2 months along with development of radiation fibrosis seen in all patients with radiation-induced pneumonitis. The treatment includes nonsteroidal anti-inflammatory drugs, cough suppressants, and corticosteroids. Some have proposed using anticoagulants. Supplemental oxygen is recommended in respiratory failure.

**Table 14.1.** Classification and pathogenesis of radiation-induced lung injury.

| | Free oxygen radicals | |
|---|---|---|
| Damage of nongenetic cellular structure | DNA alteration and damage | Bilateral lymphocytic alveolitis |
| Rapid cell death | The second generation cell damage | Hypersensitivity reaction |
| **Radiation-induced bronchitis** | **Acute radiation-induced pneumonitis** | **Migratory pneumonitis due to breast irradiation** |

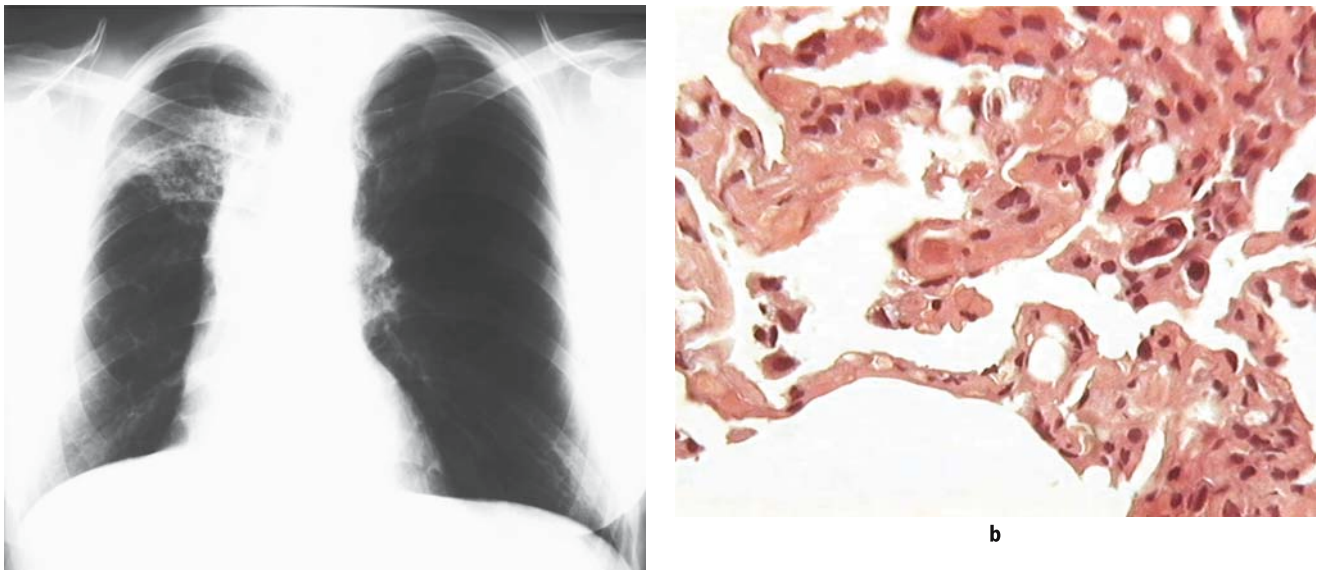

a b

**Figure 14.1.** Acute radiation pneumonitis: plain chest radiograph of the patient who underwent right upper lobectomy and radiation because of lung cancer. One month after radiation he developed fever, cough, and shortness of breath. Plain radiograph revealed new infiltrate in the field of irradiation (a). Histopathologic finding of sample obtained by transbronchial lung biopsy showed hyaline membranes, atypical, hyperplastic, and hypetrophic type II pneumocytes, and hyaline thrombi in small vessels (b).

## 14.3 Migratory Pneumonitis Due to Breast Irradiation

This uncommon disease exclusively occurs after breast irradiation. Onset of symptoms varies from 1 month to 1 year after the completion of radiation. In contrast with the usual radiation-induced pneumonitis, migratory pneumonitis appears in nonirradiated parts of lung. Clinical features include fever, sweating, fatigue, weight loss, dyspnea, and nonproductive or minimally productive cough. Radiographic changes have a tendency to migrate (Figure 14.2a, b, c). The histopathologic pattern is of BOOP. Corticosteroids

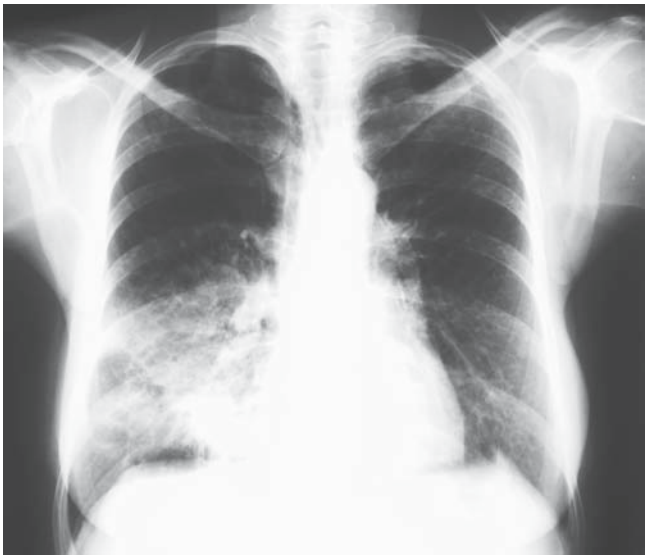

a

**Figure 14.2.** Migratory radiation pneumonitis after breast irradiation. Plain chest radiograph of the woman who complained of fever, cough, and dyspnea. Six months ago she underwent left breast segmentectomy and radiation because of breast cancer. At the time of admission she had pneumonitis on nonirradiated lung (a). HRCT scan of the same patient showed ground-glass pattern, discrete consolidation, and retraction (b). Histopathologic finding of migratory radiation pneumonitis revealed bronchiolitis obliterans organizing pneumonia (BOOP) pattern (c).

(continued)

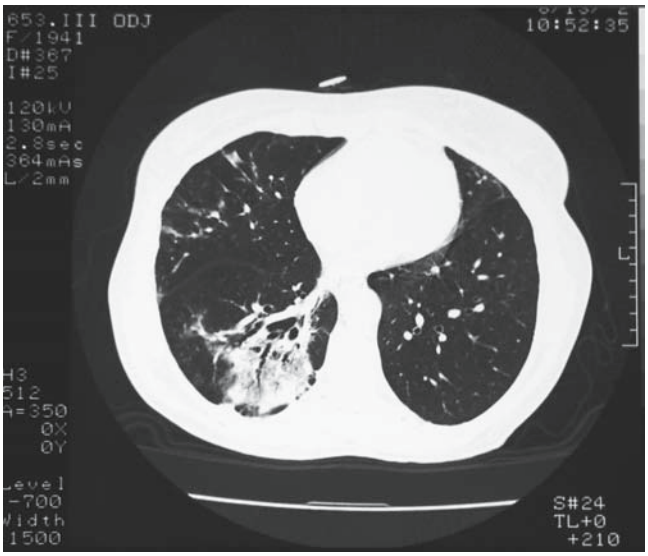


b

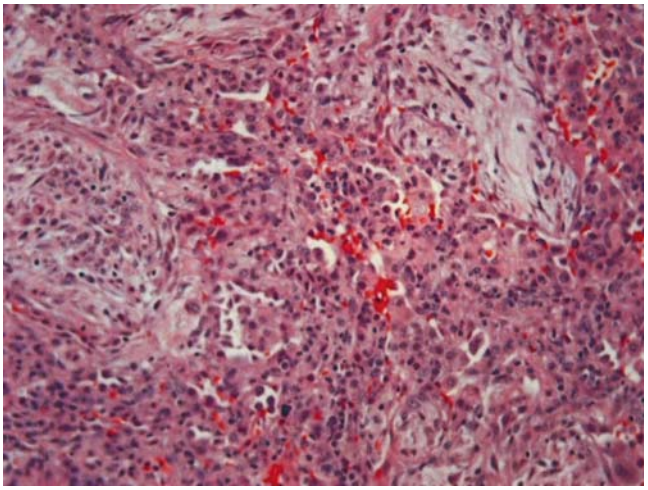

c

**Figure 14.2.** (continued)

therapy is effective in doses and tapering schedule as in idiopathic BOOP. Relapse may occur after withdrawing corticosteroids, and in such cases lifelong therapy is recommended.

## Bibliography

1. Abratt RP, Morgan GW, Silvestri G, Willcox P. Pulmonary complications of radiation therapy. Clin Chest Med 2004;25:167–177.
2. Trott KR, Herrmann T, Kasper M. Target cells in radiation pneumopathy. Int J Radiat Oncol Biol Phys 2004;58:463–469.
3. Martin C, Romero S, Sanchez-Paya J, Massuti B, Arriero JM, Hernandez L. Bilateral lymphocytic alveolitis: A common reaction after unilateral thoracic irradiation. Eur Respir J 1999;13:727–732.
4. Abratt RP, Morgan GW. Lung toxicity following chest irradiation in patients with lung cancer. Lung Cancer 2002;35:103–109.
5. Nambu A, Araki T, Ozawa K, Kanazawa M, Ohki Z, Miyata K. Bronchiolitis obliterans organizing pneumonia after tangential beam irradiation to the breast: Discrimination from radiation pneumonitis. Radiat Med 2002;20:151–154.

# 15

# Drug Addict's Lung

Illicit drug abuse is a social and medical problem worldwide, causing a broad spectrum of medical complications in the population of drug consumers. The lifestyle of addicts is associated with high risk of infections, particularly of HIV infection, tuberculosis, viral hepatitis, as well as aspiration and sepsis. The lungs are particularly vulnerable in addicts because the most common routes of drug administration are inhalation and intravenous, leading to significant respiratory morbidity and mortality. Although almost all illicit drugs impair respiratory function to some degree (Figure 15.1a, b), the most severe parenchymal disorders are caused by heroin, cocaine, and their derivates (Figure 15.1c, d).

## 15.1. Heroin

Heroin is derived from morphine, a substance extracted from the seedpod of the poppy plant. Heroin usually appears in the street as a yellow or brownish powder, depending on various additive ingredients such as talc, cornstarch, chalk, and so forth. Usual routes of administration are sniffing, snorting, smoking, and intravenous injection. Numerous lung complications of heroin abuse may be acute and chronic.

Acute complications are the consequence of the basic psychoactive substance, and include hypoventilation due to respiratory depression, noncardiogenic pulmonary edema (NCPE), and severe asthma. Heroin-related NCPE is defined as the syndrome in which a patient develops hypoxia within 24 hours of heroin overdose, accompanied with radiographic evidence of diffuse pulmonary infiltrates not attributable to other causes. Treatment is supportive with supplemental oxygen and occasionally mechanical ventilation. Symptoms usually resolve spontaneously within 48 hours, but fatal outcome is common. Some series showed that even 18% of hospitalized patients with heroin-related NCPE had died. Snorting of heroin, and especially the mixture of heroin and cocaine, seems to be an important cause of severe asthma attacks and asthma deaths.

Chronic complications of heroin abuse are numerous and are the consequence of insoluble additives to heroin, as well as nonsterile conditions during the intravenous administration. Talc causes endothelial injury and embolization of small pulmonary vessels leading to pulmonary hypertension and interstitial granulomas, which results in progressive interstitial pulmonary fibrosis. Furthermore, vascular emboli and foreign-body granulomas destroy pulmonary parenchyma, forming subpleural microbullae and finally bullous lung disease. Heroin abusers occasionally have mycotic or bacterial vegetations on tricuspid valve, due to nonsterile injection, which is the origin of pulmonary septic emboli. Impurities of heroin dose are filtered by lymphatics, causing lymphoid hyperplasia, presenting on chest radiograph as hilar or mediastinal lymphadenopathy. All pathological changes together form a special entity known as *heroin-abuser lung* (Figures 15.2a, b, c, 15.3a, b, c, and 15.4a, b).


**Figure 15.1.** Natural image of drugs that most often cause lung injury: hashish and cannabis (a, b) and cocaine and heroin (c, d).

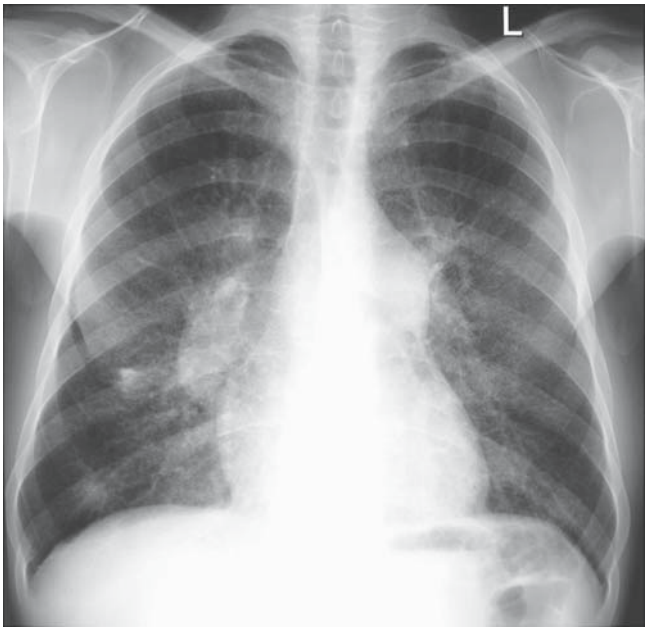


a

**Figure 15.2.** Chronic heroin toxicity. Plain chest radiograph of young male who had a 5-year history of intravenous heroin abuse reveals fine micronodular interstitial pattern, predominantly of perihilar distribution (a). CT of the same patient shows diffuse, centrilobular pin-point micronodularity (b) and small areas of consolidation (c).

(continued)

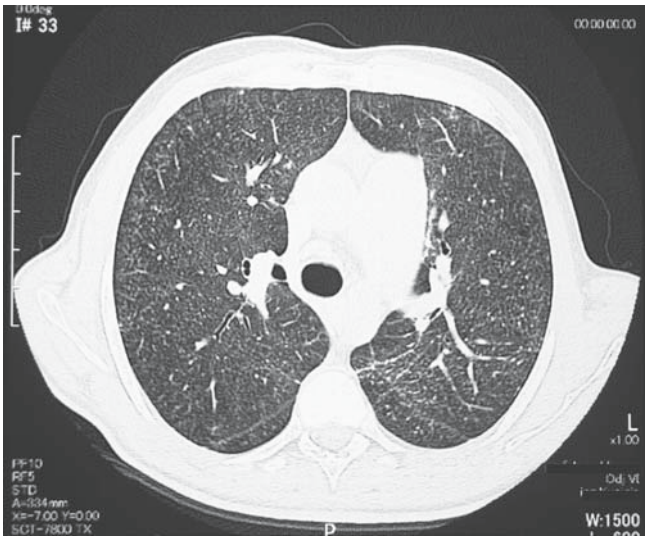


b

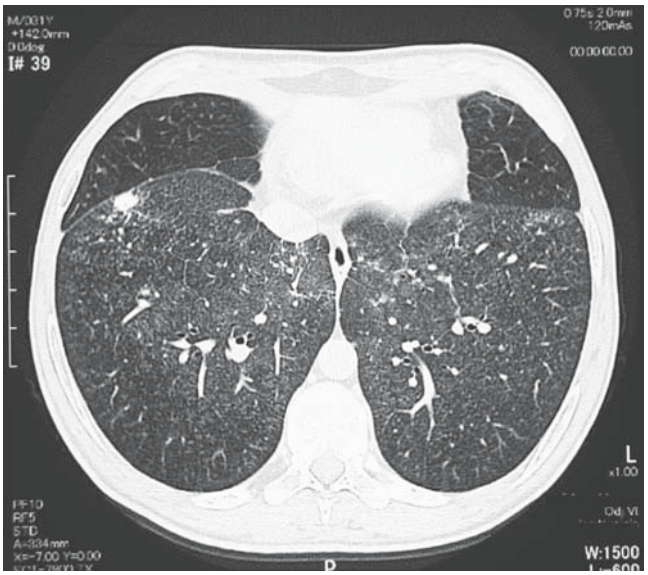


c

**Figure 15.2.** (continued)

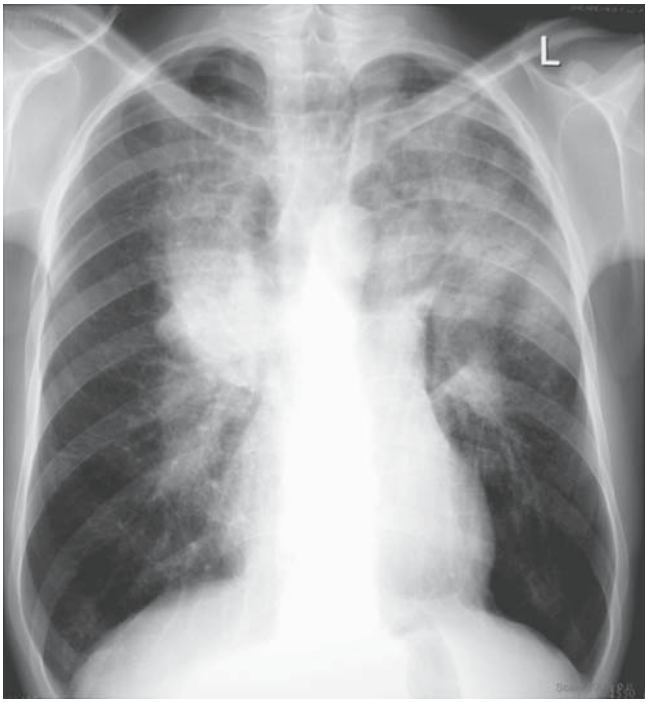


a

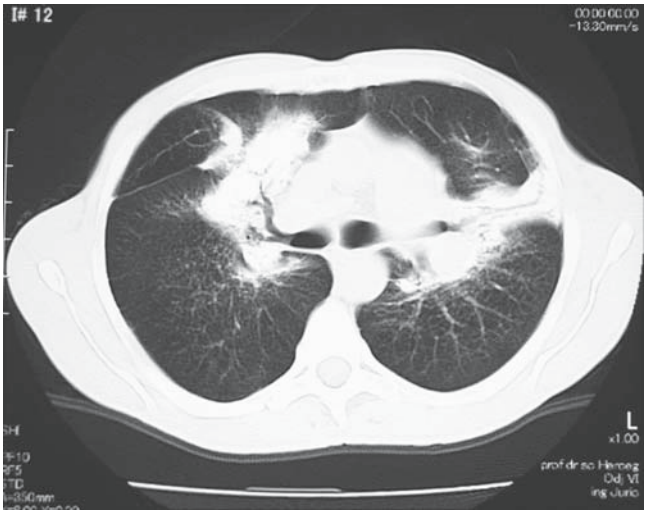


b

**Figure 15.3.** Chronic methadone toxicity. A program of detoxification of intravenous addicts includes use of oral methadone as a substitute for heroin. Talc is the major insoluble substance of tablets, and the consequence of intravenous abuse includes deposition of its particles in the pulmonary interstitium, granuloma formation, progressive pulmonary fibrosis, and pulmonary hypertension. Plain chest radiograph of heroin abuser. Patient had a 6-year history of intravenous heroin abuse. During the methadone substitution program, he used to inject intravenously a suspension of methadone tablets. Plain chest radiograph shows upper lobe conglomerate masses, infiltrates, retraction, and fibrosis (a). CT of the same patient showed massive fibrosis, lung consolidation, volume loss, and gross derangement of the lung architecture (b). Such a finding is characteristic for massive talcosis due to intravenous abuse of tablets.

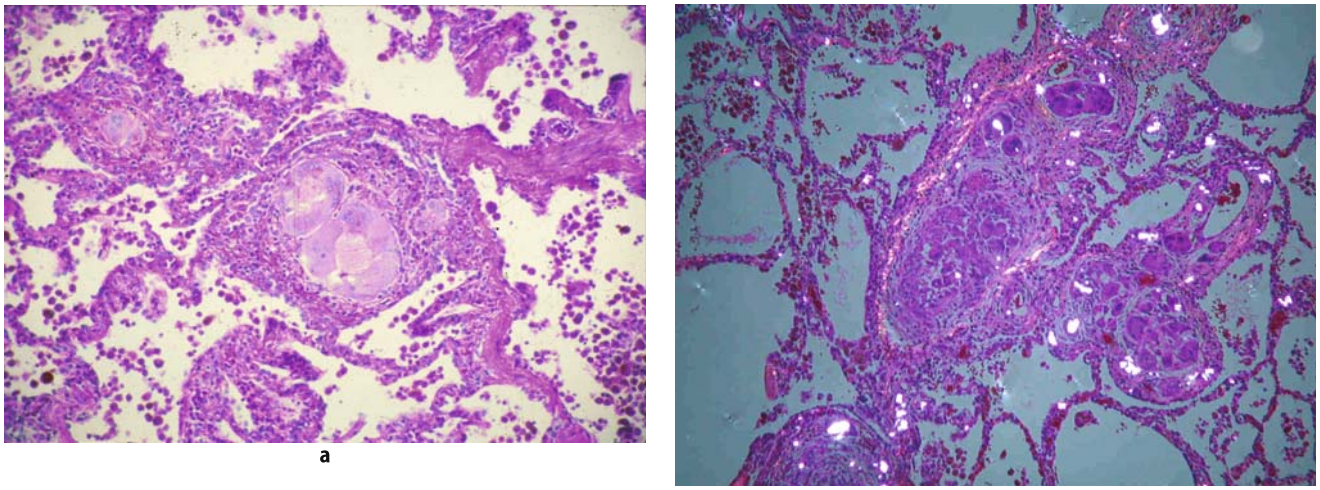

a b

**Figure 15.4.** A lung biopsy specimen shows talc-induced granulomas in a drug addict (a). A lung biopsy specimen in a drug addict showing multiple foreign-body granuloma with refractile particles in polarized light (b).

## 15.2. Cocaine

Cocaine is an alkaloid derived from coca plant. It is a white powder that is usually snorted or sniffed. Cocaine free base "crack" is also an addictive drug, processed from cocaine hydrochloride, and prepared for smoking.

Cocaine is a potent vasoconstrictor. Reduced blood flow due to vascular constriction induces endothelial injury and consequent bleeding. That is why cocaine abusers suffer from nasal and alveolar bleeding. Cocaine-induced alveolar hemorrhage may be occult, presenting by hemosiderin-laden macrophages in sputum of nearly 30% of cocaine consumers. On rare occasions, alveolar hemorrhage may be massive and life-threatening, characterized by severe respiratory failure and anemia (Figure 15.5a, b).

Occasionally, cocaine abuse may induce bronchiolitis obliterans organizing pneumonia, and crack may induce pulmonary eosinophilia syndrome. Several recent reports showed possible association between long-lasting cocaine abuse and ANCA antineutrophil cytoplasmic antibody positive vasculitis with clinical feature similar to limited Wegener granulomatosis.

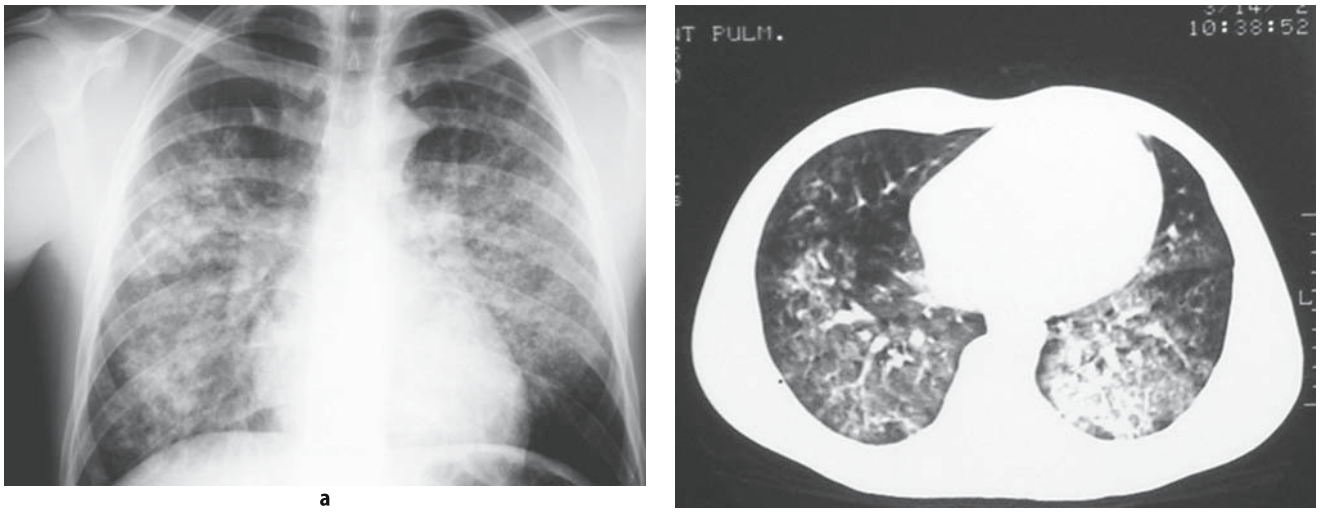


a b

**Figure 15.5.** Plain chest radiograph of the young cocaine consumer who was admitted to the hospital because of severe respiratory failure and history of hemoptysis reveals multiple patchy alveolar infiltrates. On admission his hemoglobin was 29 g/l (a). CT scan shows patchy ground-glass opacifications (b).

## Bibliography

1. National Institute on Drug Abuse (NIDA). Available at: www.drugabuse.gov/NIDAHome.html.
2. Sporer KA, Dorn E. Heroin-related noncardiogenic pulmonary edema. A case series. Chest 2001;120:1628–1632.
3. Cygan J, Trunsky M, Corbridge T. Inhaled heroin-induced status asthmaticus: Five cases and a review of the literature. Chest 2000;117:272–275.
4. Hind CRK. Pulmonary complications of intravenous drug misuse. 1. Epidemiology and non-infective complications. Thorax 1990;45:891–898.
5. Murray RJ, Albin RJ, Mergner W, Criner GJ. Diffuse alveolar hemorrhage temporally related to cocaine smoking. Chest 1988;93:427–429.
6. Gertner E, Hamlar D. Necrotizing granulomatous vasculitis associated with cocaine use. J Rheumatol 2002;29:1795–1797.

# 16

# Hypersensitivity Pneumonitis

Hypersensitivity pneumonitis (HP), or extrinsic allergic alveolitis, is an immunologically induced inflammatory disease caused by repeated inhalations of a variety of agents, including organic dusts and active chemicals. There are many types of HP, such as farmer's lung, bird fancier's lung, ventilation pneumonitis, summer-type HP, and chemical worker's lung, but the clinical features are similar irrespective of the specific causative agent (Table 16.1).

The *disease may present* in an acute, subacute, or chronic form depending on the type of antigen, amount of inhaled material, frequency of antigen exposure, and genetic susceptibility of the host. In acute HP, patients present with fever, cough, chills, malaise, and myalgia occurring approximately 4 to 6 hours after exposure to the causative antigen. The symptoms and signs subside when exposure ends (Figure 16.1a, b). In subacute HP, the onset is insidious with few if any symptoms appearing during the early stage of the disease. In the late stage of subacute HP, the patient experiences dyspnea on exertion, fatigue, cough, anorexia, and weight loss. Physical examination reveals bilateral crackles (Figure 16.2a, b, c, d, e). In chronic HP, dyspnea is the main symptom. Fibrosis now becomes indistinguishable from other forms of fibrotic disease (Figures 16.3a, b, 16.4a, b, and 16.5).

Hypersensitivity pneumonitis involves two main *pathologic mechanisms*: immune complex–mediated immune response and T cell–mediated response. The two may occur either simultaneously or at different stages of the disease, with the former mechanism initiating and mediated the acute HP syndrome and the latter modulating the subacute and chronic syndromes. Immune complex–mediated response induces acute lung injury via complement-dependent neutrophils. T-cell response, on the other hand, induces granulomatous inflammation in the alveoli as well as the small airways.

The *pathogenetic mechanism* responsible for HP is characterized by the activation and expansion of $CD8^+$ and $CD4^+$ cells. Both subsets proliferate and produce Th1 and Th2 cytokines when challenged with antigen. $CD4^+$ T cells recognize antigen presented by class II MHC molecules, whereas $CD8^+$ T cells recognize antigen presented by class I MHC molecules. The mode of antigen presentation depends on the processing of the antigen by degradation by macrophages and other antigen-processing cells. Macrophages play an important role in the granuloma formation. They participate not only in the induction phase as antigen-presenting cells but also in the development phase as effector cells through the release of proinflammatory cytokines. Macrophages suppress antigen and IL-2–induced lymphocyte transformation.

The *clinical diagnosis* of HP is based on the constellation of features: history of exposure to an offending antigen, characteristic signs and symptoms, lung function and chest radiograph abnormalities, consistent with interstitial involvement, and the presence of granulomatous inflammation. High-intensity lymphocytic alveolitis is frequently found with few plasma cells and mastocytes (Figure 16.6a), with diminished CD4/CD8 ratios (Figure 16.6b). Occasionally, a positive reaction to provocation challenge with an offending antigen is a useful test particularly in chronic HP.

**Table 16.1.** Important causes of hypersensitivity pneumonitis.

| Condition | Antigen |
|---|---|
| *Fungal causes* | |
| Farmer's lung | Thermophilic actinomycetes |
| Air-conditioner lung | Thermophilic actinomycetes |
| Bagassosis | Thermophilic actinomycetes |
| Mushroom picker's lung | Thermophilic actinomycetes |
| Maltworker's or maltbrewer's lung | *Aspergillus clavatus* |
| Cheese washer's lung | *Penicillium casei* |
| Maple bark stripper or woodworker's lung | *Cryptostroma corticale* |
| Sequoiosis | *Aurebasidium pullulans* |
| Paprika splitter or paprika slitter's lung | Mucor |
| Dry rot lung | *Merulius lacrymans* |
| Spatlese lung | *Botyris cinerea* |
| Lycoperdonosis | *Lycoperdon* spp. |
| Saxophone lung | *Candida* |
| *Animal causes* | |
| Bird breeder's or pigeon breeder's lung | Avian protein |
| Rat handler's lung | Rat protein |
| Wheat or grain weevil disease | Weevil protein |
| Furrier's lung | Animal fur |
| Pituitary snuff taker's lung | Ox and pork proteins |
| *Chemical causes* | |
| Isocyanate lung | TDI, MDI |
| Pauli's reagent lung | Pauli's reagent |
| Vineyard sprayer's lung | Bordeaux mixture |
| Hard-metal disease | Cobalt |
| Cromolyn sodium lung | Cromolyn sodium |
| *Bacterial causes* | |
| Detergent or washing powder lung | *Bacillus subtilis* enzymes |
| *Uncertain causes* | |
| Sauna lung | ? |
| New Guinea lung | Hut thatch (?) |
| Ramin lung | Ramin wood |
| Insecticide lung | Pyrethrum |

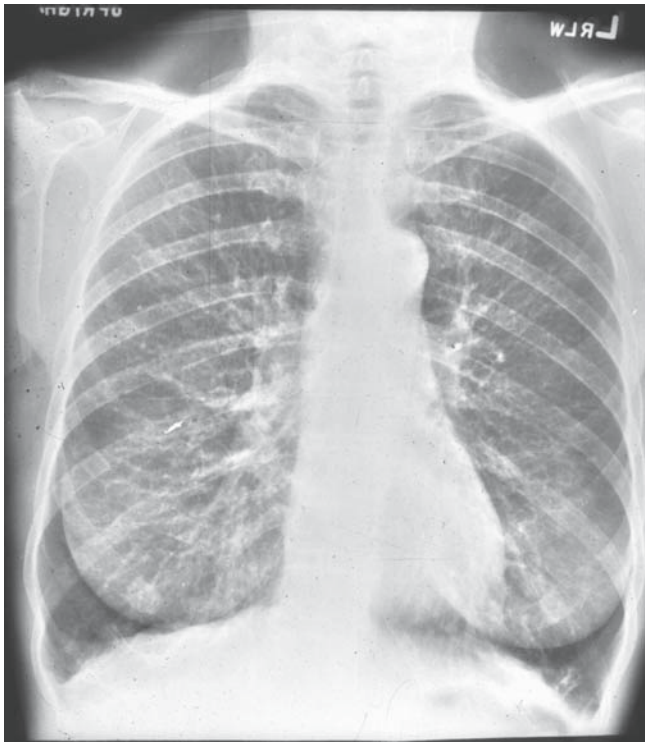

a

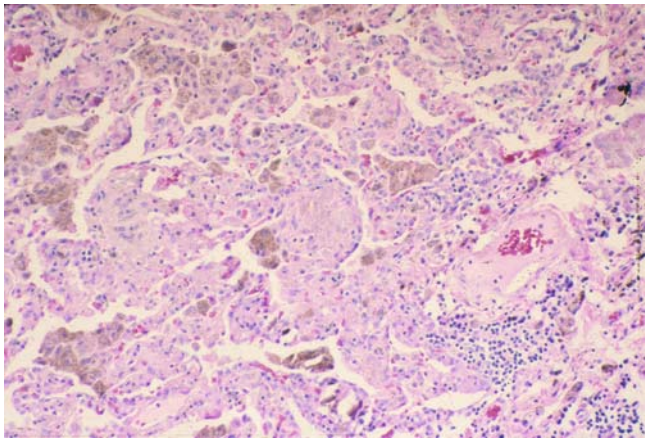

b

**Figure 16.1.** Acute HP. Posterior-anterior view of the chest in a patient with pigeon breeder's lung shows ground-glass haziness and associated air-trapping. Hypersensitivity pneumonitis is one of many interstitial lung diseases that involve the airways (a). A lung biopsy specimen showing mixed cellular alveolitis with lymphocytes and plasma cells consistent with acute hypersensitivity pneumonitis (b).

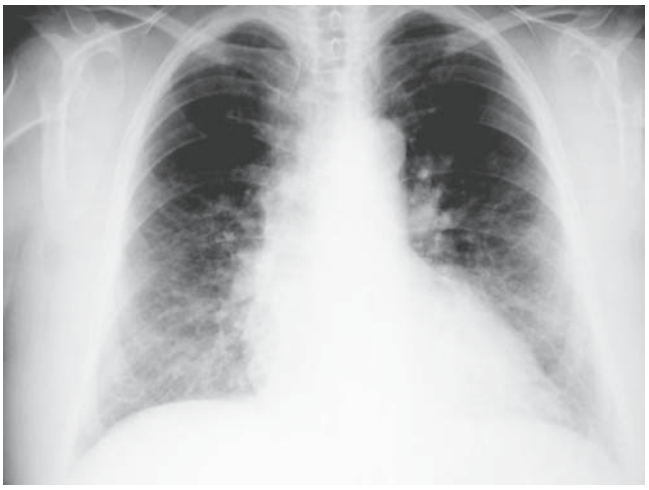

a

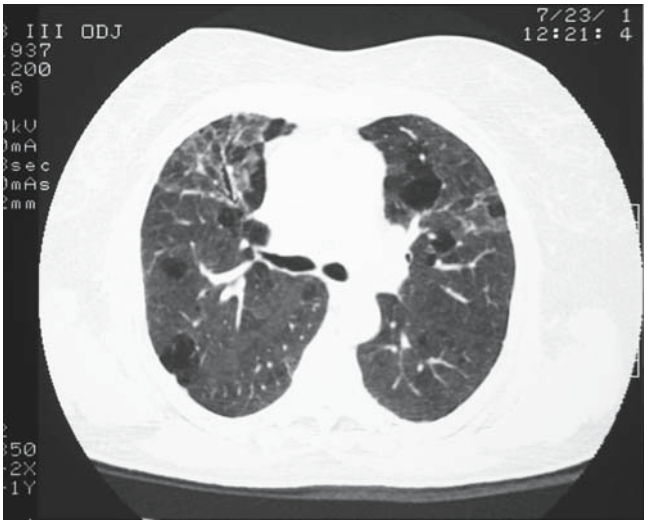


b

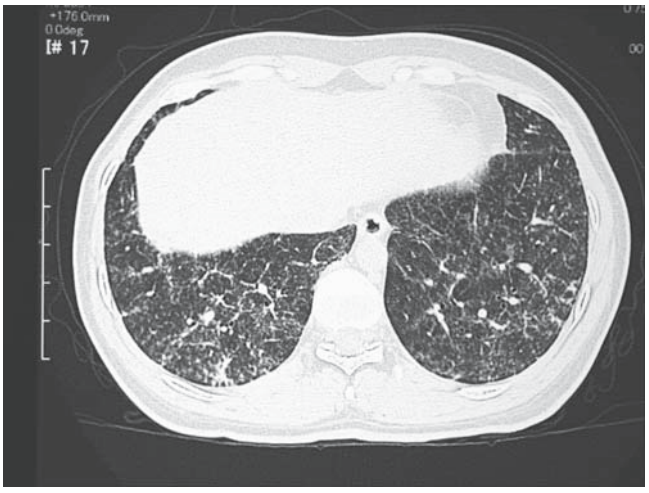


c

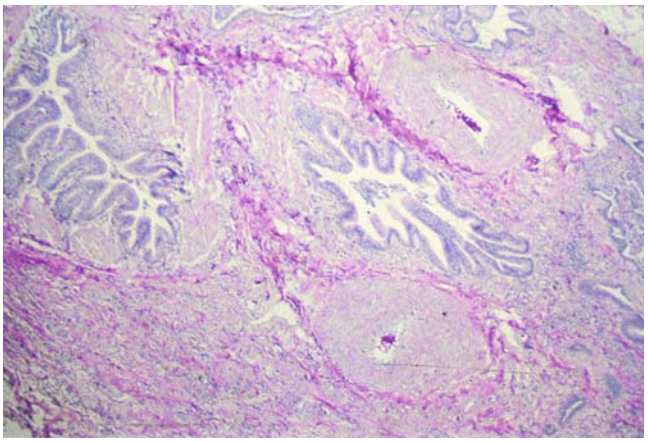

d

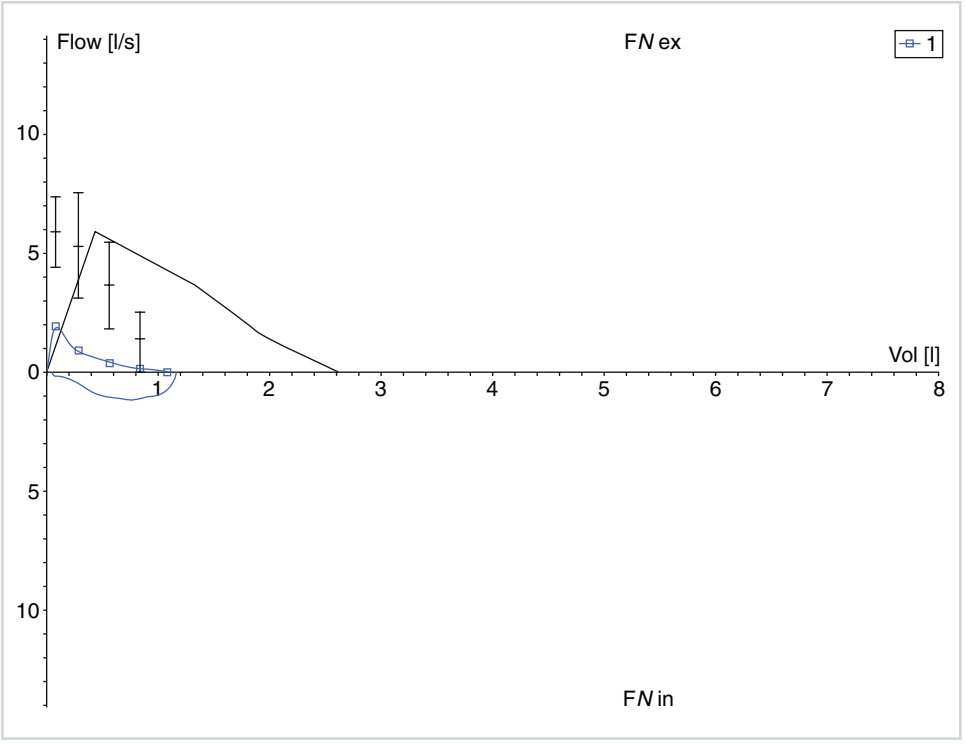


e

**Figure 16.2.** Subacute HP. Plain chest radiograph showing bilateral alveolar and reticular pattern (a). HRCT scan of the same patient; the ground-glass pattern of "geographic" distribution is seen. (b) HRCT scan of another patient with subacute HP shows thickening of the interlobular septa and vague micronodi (c). Granulomatous infiltration and fibrosis involving the lung parenchyma and airways in a patient with farmer's lung disease (d). Restrictive but also obstructive ventilatory changes are detected in HP. Flow-volume loop shows lower volume on X-axis, but also concave shape of upper side of the loop, which means obstructive limitation of air flow while a person expires (e).

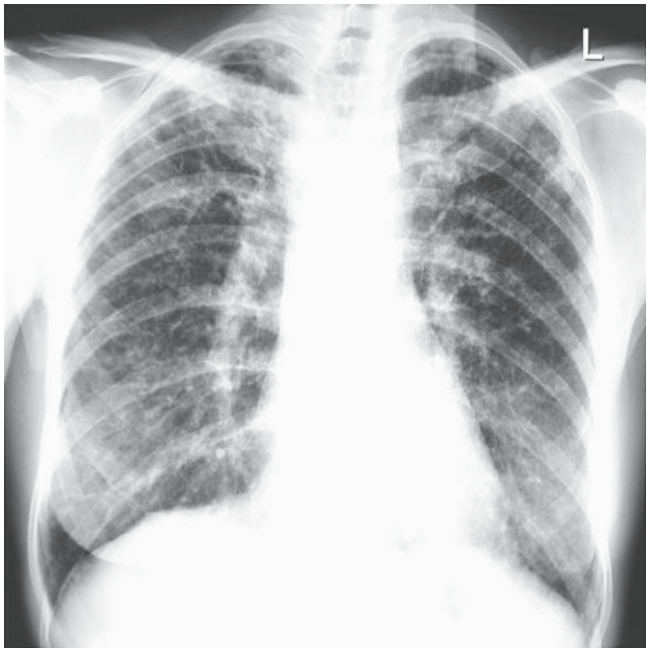


a

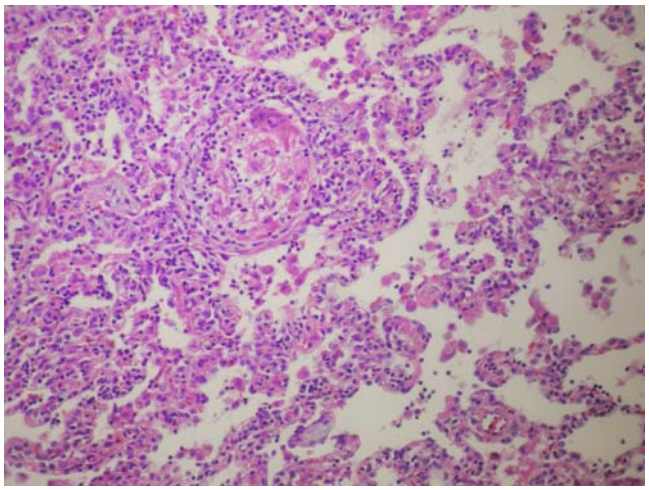

b

**Figure 16.3.** Chronic HP. Plain chest radiograph in a patient with chronic HP (detergent lung, positive precipitins to *B. subtilis*), showing upper lobe fibrosis. The duration of the disease is 8 years, and now the patient is respiratory insufficient (a). Histopathological finding at the time when the disease was first confirmed showed "poorly formed" noncaseating granuloma and interstital pneumonitis (b).

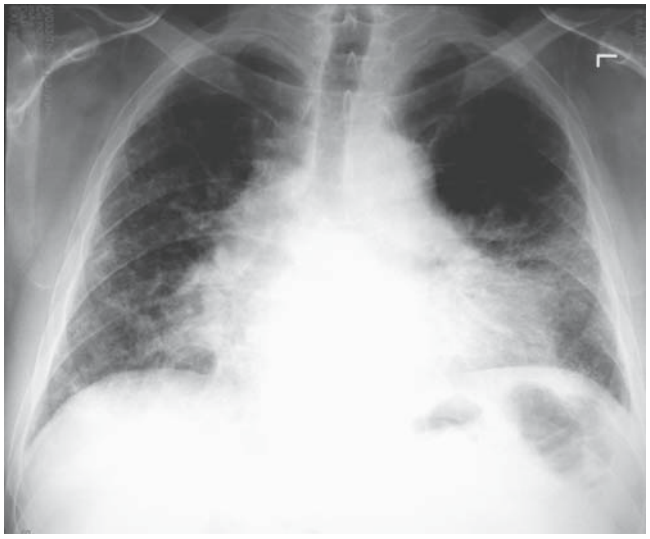

a

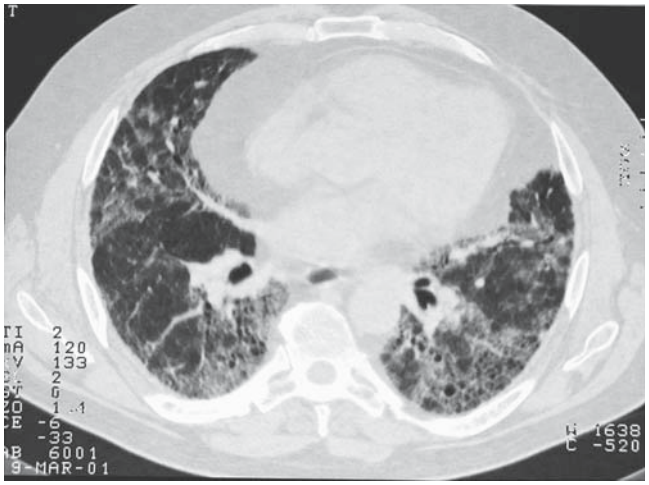


b

**Figure 16.4.** Chronic HP. A patient with farmer's lung disease showing bibasilar end-stage fibrosis on plain radiograph (a) and HRCT scans showing honeycombing, intralobular and septal fibrosis, and architectural distorsion (b). He is respiratory insufficient, and has been listed for lung transplantation. He worked for years at a milk farm, and his disease was considered occupational.

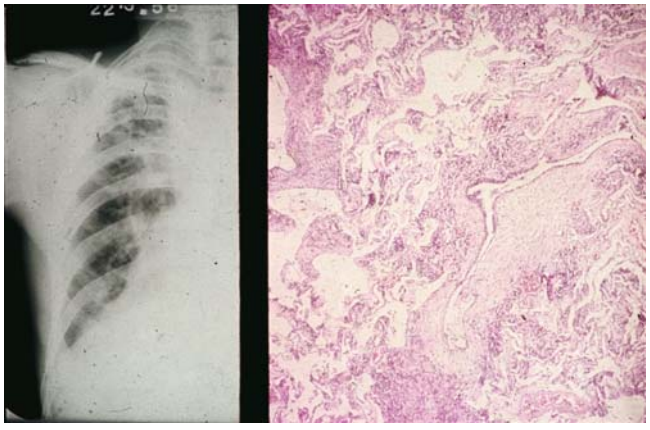

**Figure 16.5.** A patient with chest x-ray film and the histological specimen revealing chronic fibrosis and honeycombing principally involving the upper lung fields.

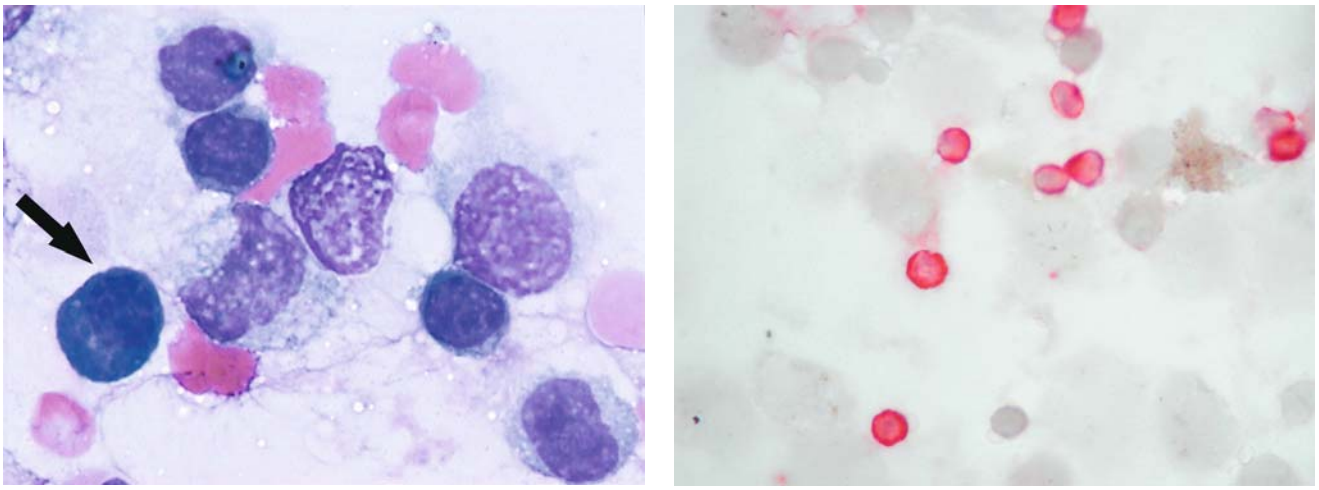

a b

**Figure 16.6.** Lung lavage analysis is helpful in the management of HP. High-intensity lymphocytic alveolitis with few plasma cells; plasma cell (arrow) and small lymphocytes. BAL fluid cytology, original magnification ×1000, MGG stain (May-Grünwald-Giemsa) (a), with predominance of $CD8^+$ T cells, a characteristic feature of HP. BAL fluid cytology, positive CD8 lymphocytes stained red with immunocytochemistry; negative, gray CD4 lymphocytes, original magnification ×1000 (b).

The *avoidance of exposure* to the causative antigen is the most important step in preventing and managing HP. Acute, recurrent episodes of HP are usually self-limiting and do not require specific therapy. Corticosteroids are indicated for severe symptoms and progressive radiological or physiological impairment. Miyajima has reported that erythromycin is effective in suppressing acute neutrophilic influx and Arthus reaction in experimental HP.

## Bibliography


1. Ando M, Suga M, Kohrogi H. A new look at hypersensitivity pneumonitis. Curr Opin Pulm Med 1999;5:299–304.
2. Kalish R, Askenase P. Molecular mechanisms of CD8+ T-cell mediated delayed hypersensitivity: Implications for allergies, asthma, and autoimmunity.J Allergy Clin Immunol 1999;103:192–199.
3. Salgame P, Abrams J, Clayberger C, Goldstein H, Convitt J, Modlin R, et al. Differing lymphokine profiles of functional subsets of human CD4 and CD8 cell clones. Science 1991;254:279–282.
4. Miyajima M, Suga M, Nakagawa K, Ito K, Ando M. Effects of erythromycin on experimental extrinsic allergic alveolitis. Clin Exp Allergy 1999;29:253–261.
5. Mohr L. Hypersensitivity pneumonitis. Curr Opin Pulm Med 2004;10:401–411.
6. Sennekemp H-J. Extrinsic Allergic Alveolitis/Hypersensitivity Pneumonitis. Ed. Dustri-Verlag Dr. Karl Feistle, Munchen, Germany: Orlando, Florida, 2004.

# 17

# Pneumoconioses

Pneumoconioses are interstitial diseases caused by chronic exposure to substantial amounts of airborne anorganic particles and their permanent deposition in the lung tissue. It is usually of occupational or environmental origin. Pneumoconioses may range from relatively harmless forms to the destructive fibrosis, depending on fibrogenic ability of particles to induce immunologic tissue reaction (Table 17.1). Besides that, severity of pneumoconiosis also depends on duration and intensity of exposure and immunologic factors of host as well.

***Silicosis*** is a progressive fibrogenic pneumoconiosis caused by inhalation of dust containing quartz (silicon dioxide). Workers on any mining, quarrying, tunneling, pottery, sandblasting, and foundry site are under special risk of permanent exposure. Particles of quartz are fibrogenic and induce granulomatous formations in pulmonary interstitium (Figure 17.1). Clinical features of silicosis depend on the stage and type of disease at the time of diagnosis. *Simple silicosis* is usually asymptomatic but has tendency to progress regardless of exposure break-off (Figure 17.2). Patients with *complicated silicosis* usually have symptoms: breathlessness on exertion, fatigue, and intermittent subfebrile episodes. At this stage, silicosis is commonly associated with tuberculosis: silicotuberculosis (Figure 17.3). Tuberculosis and other mycobacteriosis may accelerate the course of disease. *Accelerated silicosis* is a form of disease associated with connective tissue diseases like rheumatoid arthritis, progressive systemic sclerosis, or systemic lupus erythematosus (Figure 17.4). Almost half of patients in this stage have atypical mycobacterial superinfection. *Acute silicoproteinosis* is a rapidly progressive form of disease caused by massive silica exposure and characterized by weight loss, weakness, severe hypoxemia, and heart failure. Almost all patients suffering from silicoproteinosis have superinfection due to atypical mycobacteria.

***Coal miner's pneumoconiosis*** is a disease caused by deposition of coal dust in the lung tissue. It is not a progressive form of pneumoconiosis unless the coal dust contains more than 15% quartz. In that case, prognosis is similar to that of complicated and accelerated silicosis (Figure 17.5a, b).

***Asbestosis*** is a disease caused by asbestos exposure to cement products, asbestos paper for insulation, thermal and fireproofing products, spray for decorative and acoustical purposes, and so forth. Clinical features of asbestosis include interstitial and pleural disease and depend on intensity of exposure, type of asbestos fibers, age, and anatomical characteristics (Figures 17.6 and 17.7a, b). Asbestos exposure is associated with an increased risk of lung carcinoma and mesothelioma. During the past 30 years, asbestos has been replaced in many products by non-asbestos mineral fibers like carbide, carborundum, kevlar, zeolite, mineral wool, attapulgite, and so forth. According to recent reports, it seems that exposure to some of these materials may cause similar problems as exposure to asbestos.

***Talcosis*** is a disease caused by deposition of talc (magnesium silicate) in pulmonary interstitium, forming granulomas and fibrosis. According to type of exposure, several forms of talcosis have been defined. Talcosilicosis appears in miners of talc with

**Table 17.1.** Classification of pneumoconiosis.

| Pattern of Response | Disease |
|---|---|
| Retention ("benign pneumoconiosis") | Coal (<15% silica) miner pneumoconiosis |
| | Siderosis |
| | Stannosis |
| | Baritosis |
| | Antimoniosis |
| Fibrosis | Silicosis |
| | Coal (>15% silica) mine pneumoconiosis |
| | Asbestosis |
| | Talcosis |
| | Hard-metal pneumoconiosis |
| | Berylliosis |

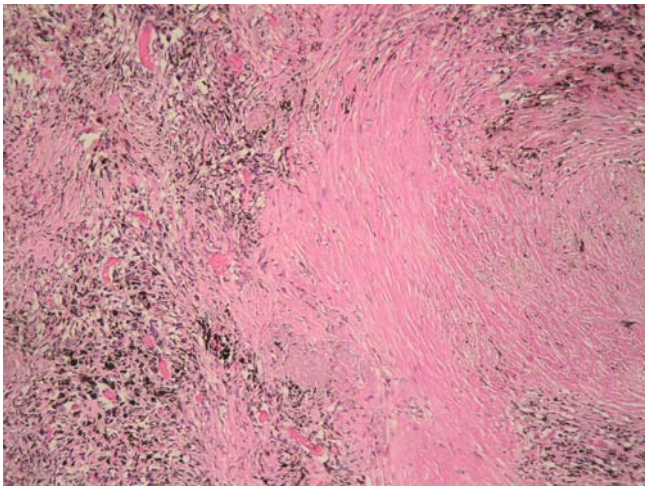

**Figure 17.1.** Silicotic nodule (maturing) exhibits virtually acellular, hyalinized collagen and peripheral dust laden macrophages.

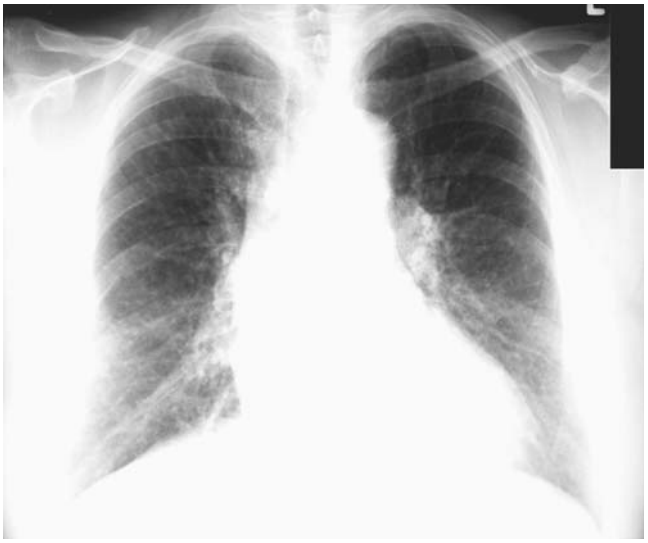

**Figure 17.2.** Plain chest radiograph of a patient with simple (uncomplicated) silicosis, manifested by micronodular polygonal interstitial pattern and eggshell calcifications in mediastinal and hilar lymph nodes.

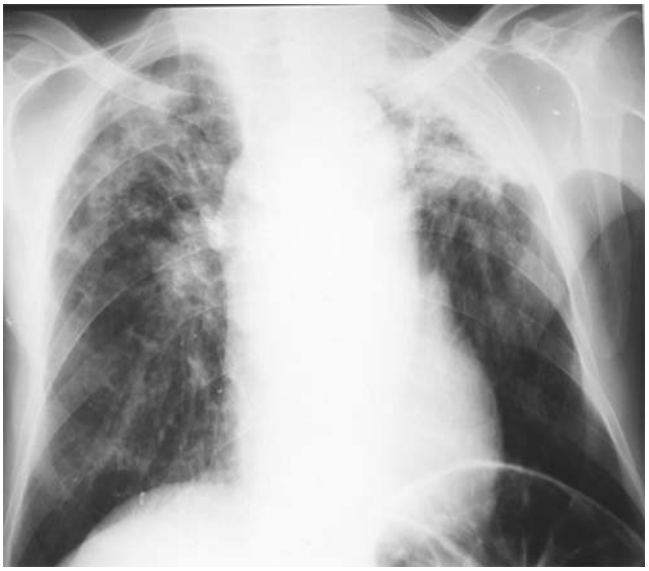

**Figure 17.3.** A patient with complicated silicosis associated with tuberculosis who was employed as a facade worker for 30 years. The radiograph shows fibrous retractive changes of hilipetal distribution, which leaves the periphery bullous or "empty." Disseminated polygonal granulomas are seen as well as eggshell calcifications of mediastinal and hilar lymph nodes.

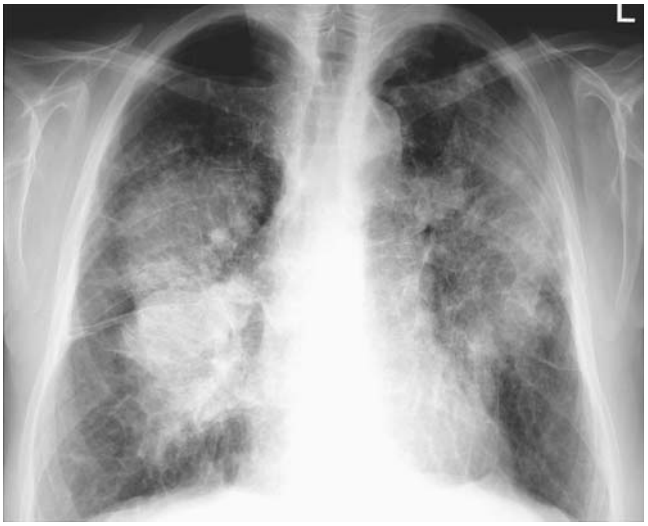

**Figure 17.4.** Accelerated silicosis associated with rheumatoid arthritis. Plain chest radiograph showing tumor-like masses consistent with massive fibrosis, coarse reticular retractive changes, and small polygonal patchy opacifications.

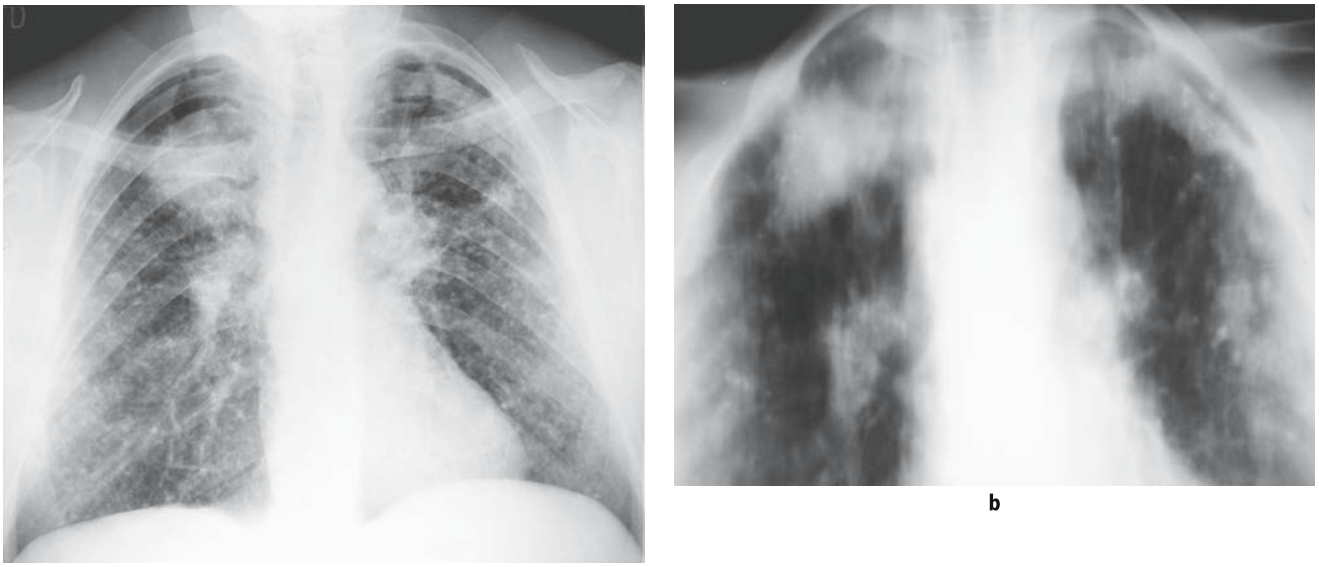

a b

**Figure 17.5.** Coal miner pneumoconiosis. Plain radiograph showing upper lobe fibrosis and consolidations of nodules (a). Frontal thin layer section of the same patient (b).

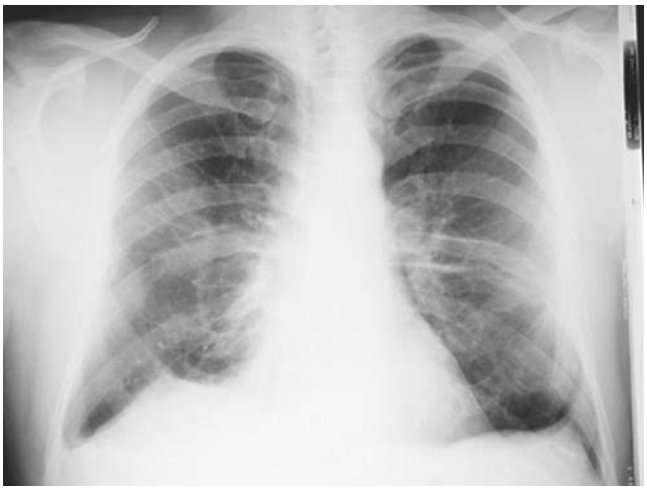

**Figure 17.6.** Plain chest radiograph of the patient suffering from asbestosis reveals reticular interstital pattern and pleural plaques. He worked for 20 years in cement production.

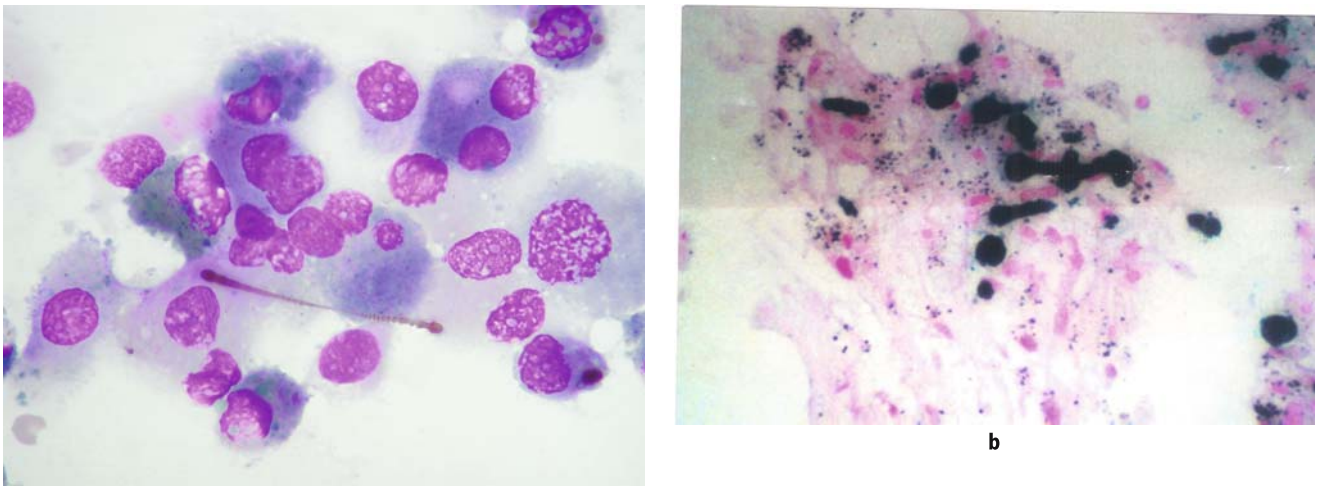

a b

**Figure 17.7.** Diagnosis of asbestosis is based on the consistent history of exposure to asbestos and definite evidence of lung fibrosis. Identification of sufficient concentration of asbestos bodies in BAL or lung biopsy specimens comprises further evidence of asbestos exposure. Asbestos body in brochoalveolar lavage fluid cytology. Single asbestos body among alveolar macrophages, original magnification ×1000, MGG stain (May-Grünwald-Giemsa) (a) and histopathological finding (b).

high-silica content, resembling silicosis. If the talc deposit contains a high amount of asbestos, exposed miners may suffer from talcoasbestosis. High degree of exposure to purified talc (quartz/asbestos-free talc) in the rubber and cosmetic industries causes small airway obstruction and granulomatous interstitial reaction with micronodular pattern on chest radiograph.

A special form of talcosis in intravenous addicts due to intravenous abuse of heroin and oral medications is associated with production of vascular granulomas, consolidations, large nodules, and masses on chest x-ray examination and with rapid deterioration.

***Hard-metal pneumoconiosis*** is a disease caused by exposure to particles of cobalt, tungsten, and their alloys, which are constituents of hard metal and diamond abrasives. Disease is typically characterized by finding of giant-cell pneumonia (GIP) in lung biopsy specimens (Figure 17.8a, b, c).

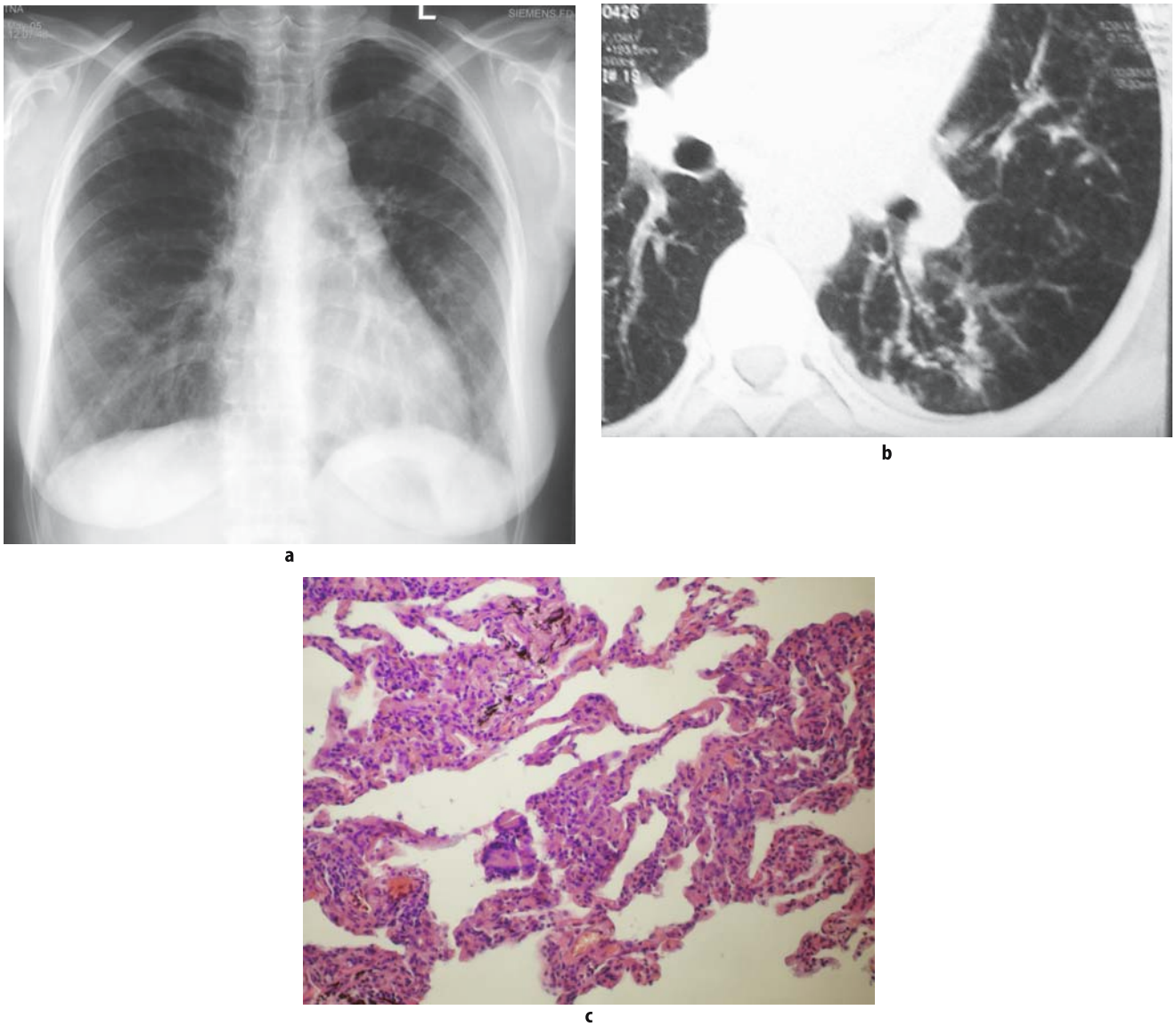

**Figure 17.8.** "Diamond polisher lung": chronic exposure to fine particles of cobalt. It is also known as hard-metal pneumoconiosis. Plain chest radiograph and CT of patient who had been employed as a diamond grinder during a period of 6 months and was exposed to high amounts of fine particles of cobalt shows middle and lower zone interstitial reticular pattern (a), and CT scan shows ill-defined basilar nodular opacities (b). Histopathologic finding of the lung biopsy specimen of the same patient reveals giant cell pneumonitis (GIP). Mild interstitial fibrosis, infiltrates of lymphocytes and macrophages and macrophages and multinucleated giant cells within the alveolar spaces are found. Specific morphologic clue is the finding of multinucleated giant cells, termed "cannibalistic" because they contain phagocytosed histiocytes within their cytoplasm (c).

***Berylliosis*** is a disease caused by exposure to beryllium, which is used in several sectors of modern technology, such as aircraft, electronics, computers and communications, and the nuclear power industry. Acute exposure to high concentrations of beryllium fumes may cause noncardiogenic pulmonary edema, and chronic exposure is associated with epitheloid granuloma formation in the lung tissue. According to clinical feature and histopathologic findings, chronic beryllium disease resembles sarcoidosis.

***Benign pneumoconiosis*** is caused by exposure to non-fibrogenic dust. This group of diseases includes siderosis, stannosis, baritosis, and antimoniosis. Non-fibrogenic anorganic particles are retained in the lung tissue without impairment of pulmonary function, in spite of radiological findings.

## Bibliography

1. Ng TP, Chan SL, Lam KP. Radiological progression and lung function in silicosis: A ten year follow up study. BMJ 1987;295:164–168.
2. Glazer CS, Newman LS. Occupational interstitial lung disease. Clin Chest Med 2004;25:467–478.
3. Rimale B, Greenberg AK, Rom WN. Basic pathogenetic mechanisms in silicosis: Current understanding. Curr Opin Pulm Med 2005;11:169–173.
4. Feign DS. Talc: Understanding its manifestations in the chest. AJR Am J Roentgenol 1986;146:295–301.
5. De Vuyst P, Camus P. The past and present of pneumoconioses. Curr Opin Pulm Med 2000;6:151–156.

# 18

# Inhalation Fever and Chemical Pneumonitis

Due to its basic function, lung parenchyma may be exposed to various toxic gases and fumes from the environment (Table 18.1). It can occur during professional exposure but also during incidents such as fire or explosion. The type of effects depends on many factors relating to duration of exposure, condition of exposure, concentration and physicochemical properties of toxic substances, degree of ventilation at the time of exposure, and preexisting respiratory capacity. Physicochemical properties, particularly solubility of inhaled substance, determine site and type of injury. Whereas the very soluble substances cause irritation and inflammation of nasal mucosa and upper airways, less soluble substances injure distal parts of the respiratory system causing bronchiolitis, pneumonitis, and alveolar damage.

Acute exposure to high concentration of toxic fumes causes diffuse alveolar damage resulting in adult respiratory distress syndrome. It is commonly related to inhaled toxic products of combustion from fire but also to careless handling of toxic substances (Figure 18.1a, b) or accidental inhalation (Figure 18.2a, b, c, d). Treatment is supportive, with supplemental oxygen and, depending on severity, intubation with ventilatory support.

Chronic exposure to small amounts of toxic fumes does not provoke an immediate reaction, so prolonged exposure leads to interstitial pulmonary fibrosis (Figure 18.3a, b). Patients have progressive dyspnea. Corticosteroids and other immunosuppressive therapy are usually not effective, and most patients require chronic supplemental oxygen or lung transplantation.

Some substances become toxic when used as aerosol. It was first noted in 1993 after a new spray paint had been introduced in textile factories in Spain and Algiers, causing an epidemic of bronchiolitis obliterans organizing pneumonia among workers. Response to immunosuppressive treatment and outcome of disease were variable.

Some workers exposed to metal fumes (especially zinc oxide) during galvanization process experience metal fume fever—a flu-like illness that includes fever, chills, myalgia, malaise, leukocytosis in peripheral blood, and sometimes pulmonary infiltrates with neutrophilic alveolitis. Symptoms occur 4–8 hours after heavy exposure and usually resolve spontaneously in a few days but may occur again when a patient returns to work after a few days off (e.g., after holidays). Similar symptoms may occur in workers inhaling breakdown products of polytetrafluoroethylene and similar synthetic polymers, causing polymer fume fever. The pathogenesis of disease has not yet been delineated.

Toxic inhalation injuries lead to a wide variety of syndromes that depend on various conditions of either the host, duration of exposure, or chemical characteristics of the inhaled substance. Some of those syndromes, associated with professional exposure, are preventable. Unfortunately, severe alveolar damage due to massive exposure is commonly accidental, with advanced tissue lesions at the time of diagnosis.

**Table 18.1.** Most common causative agents of inhalation fever and chemical pneumonitis.

| Type of Injury | Causative Agents |
|---|---|
| Metal fume fever | Zinc oxide (galvanization process) |
| Polymer fume fever | Polytetrafluoroethylene (Teflon) |
| Bronchiolitis obliterans organizing pneumonia | Acamin FWN (compound of spray paint) |
| Diffuse alveolar damage | Acetaldehyde |
| | Acrolein |
| | Ammonium |
| | Boranes |
| | Chlorine |
| | Isocyanate |
| | Nitrogen dioxide |
| | Hydrogen cyanide or sulfide |
| | Phosphine |
| | Phosgene |
| | Sulfur dioxide |

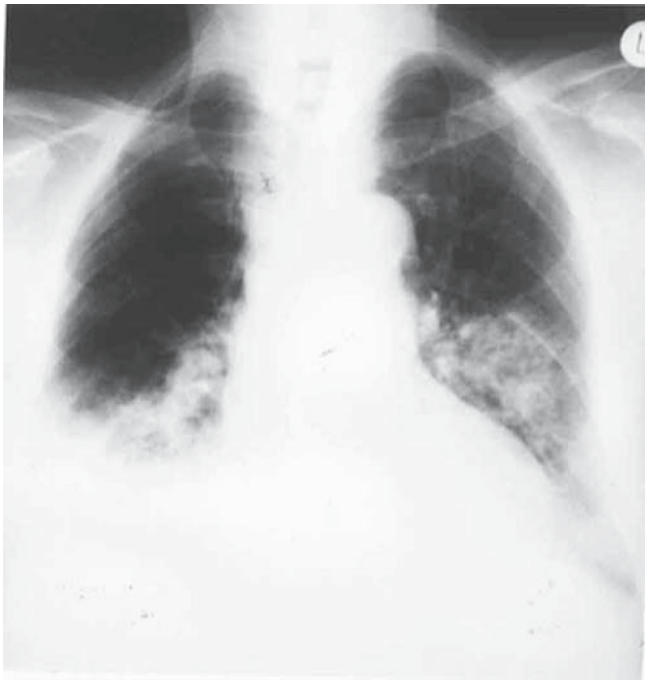

a

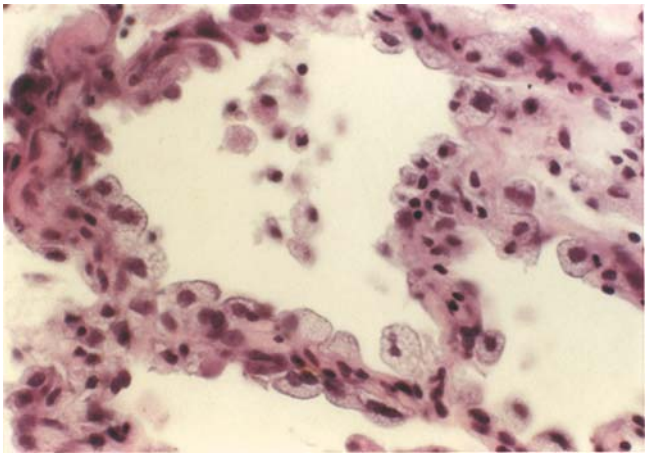

b

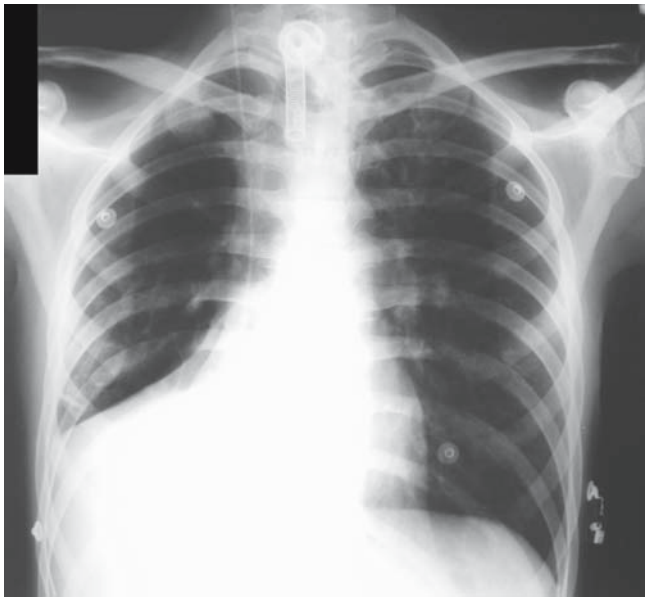

a

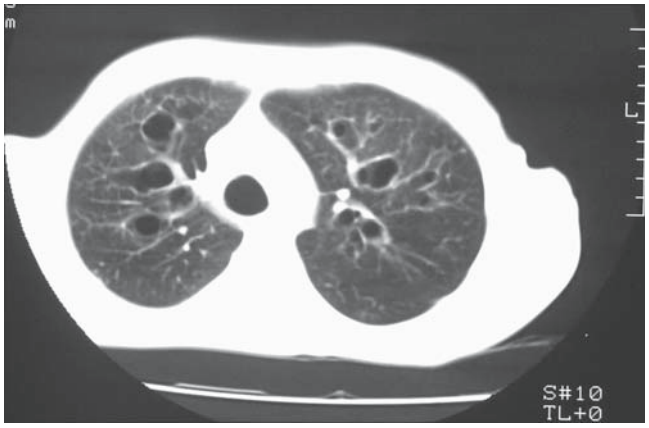


b

**Figure 18.2.** A 19-year-old worker inhaled large amounts of ammonium when the pipe of the cooling system exploded. Chest radiograph in acute phase showed atelectasis of the right lower lobe (a). CT scan shows bronchiectasis and bullae in the upper lobes (b, c) and retraction and chronic pneumonia in the right lower lobe (d). Due to grave respiratory insufficiency, lung transplantation was indicated and successfully completed.

(continued)

**Figure 18.1.** Plain chest radiograph of the patient with acute inhalation injury due to an insecticide (cholinesterase inhibitor) shows bilateral basilar confluent infiltrates with right pleural effusion (a). Histopathologic finding of transbronchial lung biopsy specimen of the same patient revealed diffuse alveolar damage pattern, with complete loss of type I pneumocytes that were replaced with atypical and hyperplasic type II pneumocytes (b).

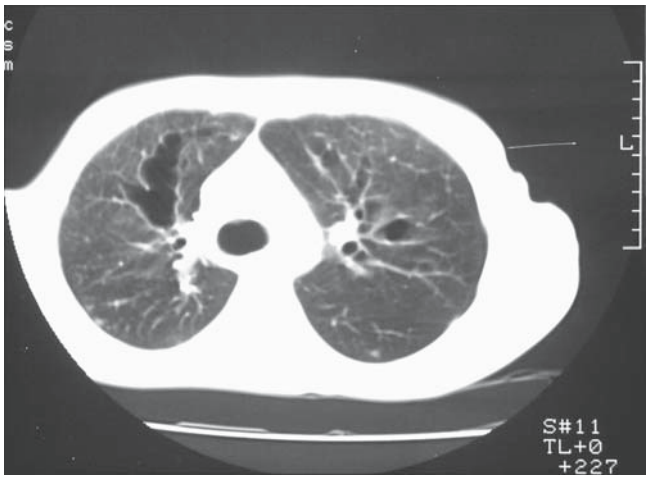


c

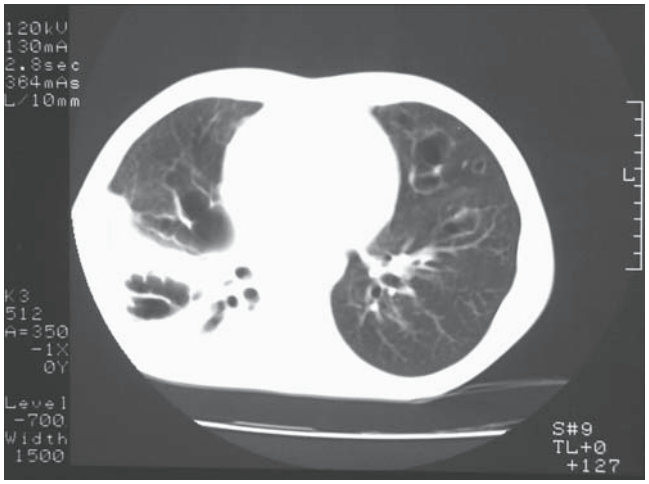


d

**Figure 18.2.** (continued)

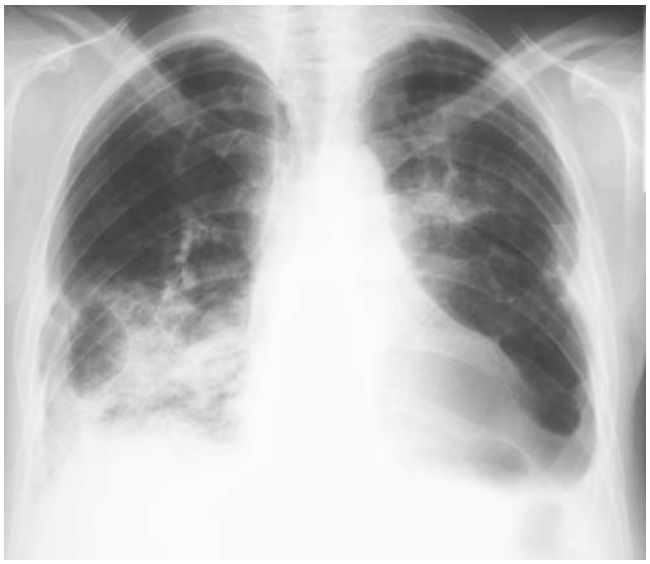

a

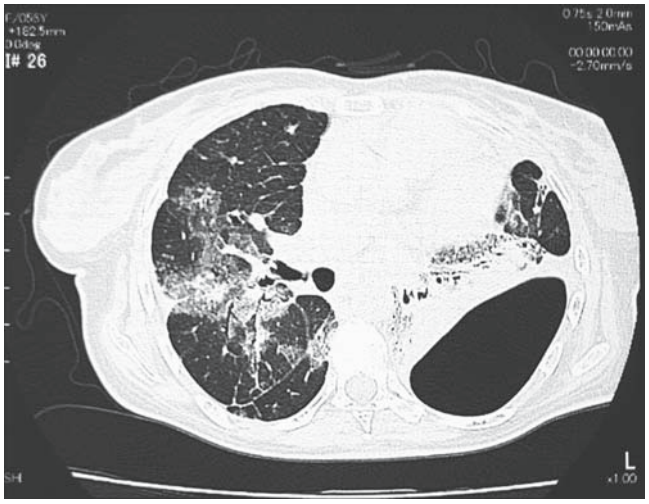


b

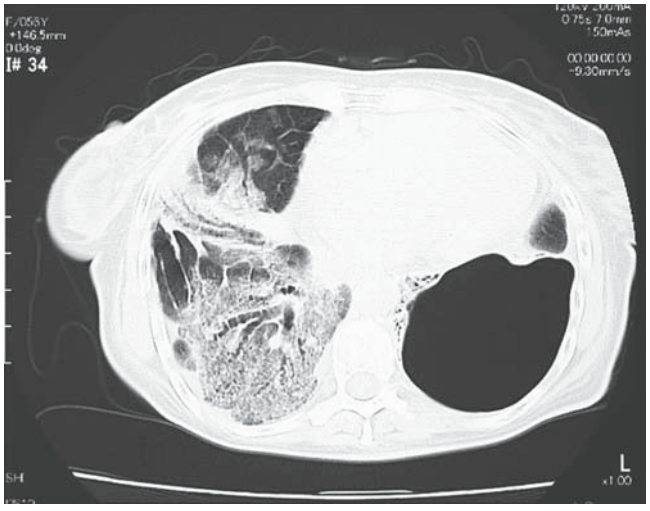


c

**Figure 18.3.** Plain chest radiograph of the woman who had professionally investigated physical characteristics of tetramethylammonium hydroxide shows diffuse, but predominantly in the lower lung fields, alveolar and reticular coarse pattern, with diminished lung volumes and a giant bullae in the left lung. Her breathlessness worsened after the explored substance had been warmed up to 90°C, releasing $NO_2$ (a). HRCT scans of the same patient show interstitial pulmonary fibrosis, focal parenchymal distortion, and destructions with formation of giant bullae (b, c).

## Bibliography

1. Swift DL. Generation and respiratory deposition of therapeutic aerosol. Am Rev Respir Dis 1980;122:71–77.
2. Mengel RG, Bernard W, Barth P, Von Wichert P, Muller B. Impaired regulation of surfactant phospholipid metabolism in the isolated right lung after nitrogen dioxide inhalation. Toxicol Appl Pharmacol 1993;120:216–223.
3. Leduc D, Gris P, Lheureux P, Gevenois PA, De Vuyst P, Yernault JC. Acute and long term respiratory damage following inhalation of ammonia. Thorax 1992;47:755–777.
4. Camus P, Nemery B. A novel cause for bronchiolitis obliterans organizing pneumonia: Exposure to paint aerosols in textile workshops. Eur Respir J 1998;11:259–262.
5. Vandenplas O, Binard-Van Cangh F, Gregoire J, Brumagne A, Larbanois A. Fever and neutrophilic alveolitis caused by a vanadium based catalyst. Occup Environ Med 2002;59:785–787.

# 19

# Pulmonary Involvement in Rheumatoid Arthritis

Rheumatoid arthritis (RA), the most common chronic connective tissue disease, is a symmetrical erosive polyarthritis that afflicts women more frequently than men. Pleuro-pulmonary involvement, however, is more common in men, particularly in those with severe, deforming joint disease, subcutaneous nodules, and high titers of rheumatoid factor (Figure 19.1a, b, c). Other risk factors include smoking, alpha-1 antitrypsin variants, extensive extra-articular disease, and the class II MHC HLA-DR4 phenotype.

In 1948, Ellman and Ball first described the pulmonary involvement in rheumatoid arthritis. The pleuro-pulmonary abnormalities associated with rheumatoid arthritis can be classified into primary and secondary. The primary pulmonary manifestations are due to the systemic inflammation inherent to RA, whereas the secondary manifestations are related to environmental exposure, drugs, infections, and malignancy (Table 19.1).

In Walker and Wright's series of 516 patients with rheumatoid arthritis, only 8 (2%) had radiographic evidence of interstitial lung disease. Men with subcutaneous nodules and high rheumatoid arthritis titers more often develop interstitial lung disease than women. Immune complex deposition in the blood vessels probably initiates the inflammation.

The prevalence of symptomatic parenchymal interstitial lung disease detected by chest radiographic screening is low, but abnormal lung functions are frequent in the presence of normal chest x-ray films. Frank et al. reported an incidence of 41%. Lung function tests show a restrictive pattern with impaired carbon monoxide transfer factor. Lung function tests may be influenced by the patient's occupation, hobbies, smoking, drug and medicine use, and hemoglobin concentration.

Joint manifestations precede interstitial lung disease in most the cases. When lung disease precedes joint disease, it is usually associated with a positive rheumatoid factor. Breathlessness and dry cough are common symptoms. Crepitations or crackles may be heard in about 10% of the patients; finger clubbing is infrequent. Sometimes skin and eye lesions could be seen (Figure 19.2a, b). Hoarseness may develop due to the involvement of the larynx (Figure 19.3).

The chest radiograph shows widespread, reticulo-linear-nodular infiltrate, honeycombing, and bronchiectasis, most marked at the lung bases (Figures 19.4a and 19.5a). Abnormal CT findings are found in 29% of the asymptomatic and 69% of the symptomatic patients. Much higher prevalence of the parenchymal abnormality is found by high-resolution computed tomography (HRCT) (Figures 19.4b and 19.5b).

Lung biopsy features in patients with pulmonary disease consists of UIP, NSIP, and inflammatory airway disease with organizing pneumonia patterns, but most of the findings are nonspecific (Figure 19.6a, b). As pleura is often involved, the biopsy is occasionally performed (Figure 19.7). Neutrophilic alveolitis is the most frequent finding in BAL although the lymphocytic pattern is sometimes detected (Figure 19.8).

Patients with pulmonary involvement in rheumatoid arthritis should be aggressively treated. The combination of methotrexate, chloroquine (or hydroxychloroquine), and sulfasalazine is the current reference treatment in progressive forms of RA as well as the pulmonary involvement.

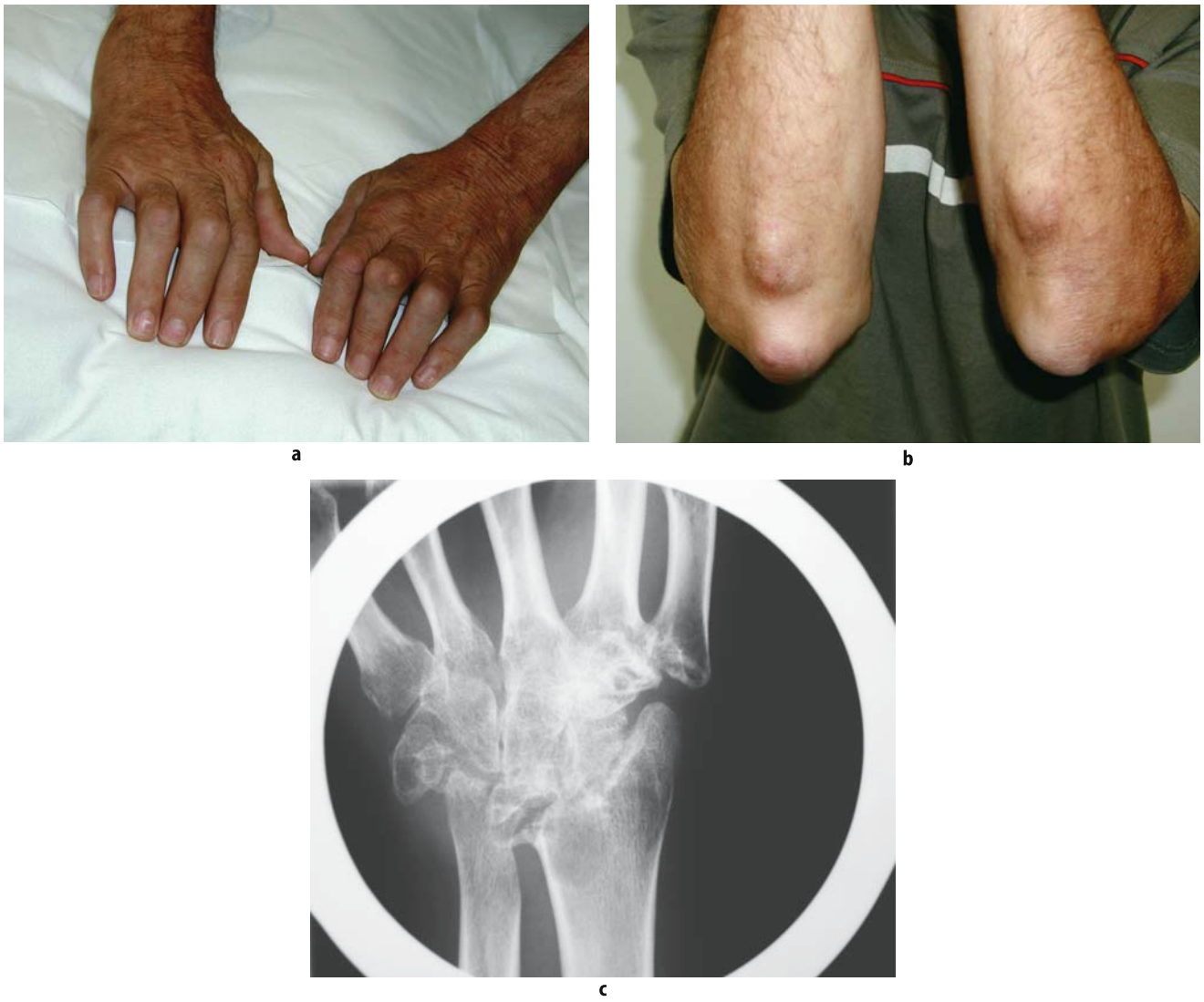

**Figure 19.1.** The hands show symmetrical arthropathy, consisting of swelling of the phalangeal joints (the swelling is caused by synovial swelling) with swan neck deformity, ulnar deviation of metacarpophalangeal joint and volar subluxation of the palm (a) and gross subcutaneous nodules typically located to the elbows, to the side that is prone to pressure, all in the same patient (b). Plain radiograph of the radiocarpal joint showing joint space narrowed and the contours of the joint surface rough with erosions. The carpal bones are almost of erased contours, with gross bone atrophy. The ulna is subluxated with erosions and its distal (styloid) ending almost resorbed (c).

**Table 19.1.** Pulmonary manifestations of rheumatoid arthritis.

| Tissue Involved | Primary | Secondary |
|---|---|---|
| Pleura | Effusion, empyema | Effusion empyema |
| | Thickening/fibrosis | |
| | Calcification | |
| | Pneumothorax | |
| Parenchyma | Nodules | Caplan syndrome |
| | Alveolitis/fibrosis | Pneumonia |
| | Pneumonitis | Eosinophilic infiltrate |
| | BOOP | |
| Airways | Bronchiolitis, bronchiectasis | Bronchospasm |
| Blood vessels | Vasculitis, pulmonary hypertension | |

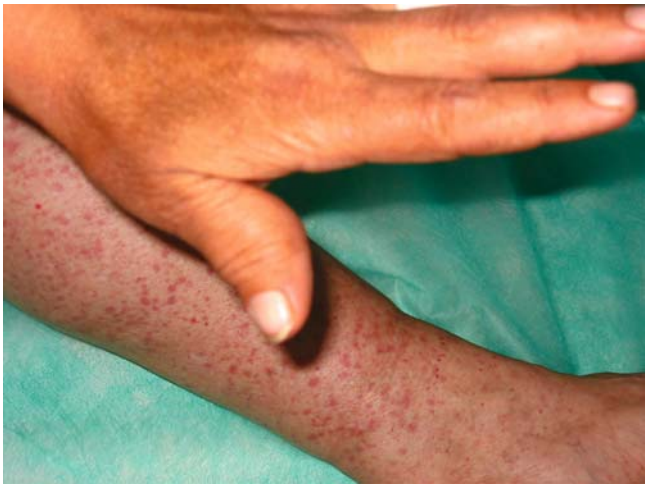

a

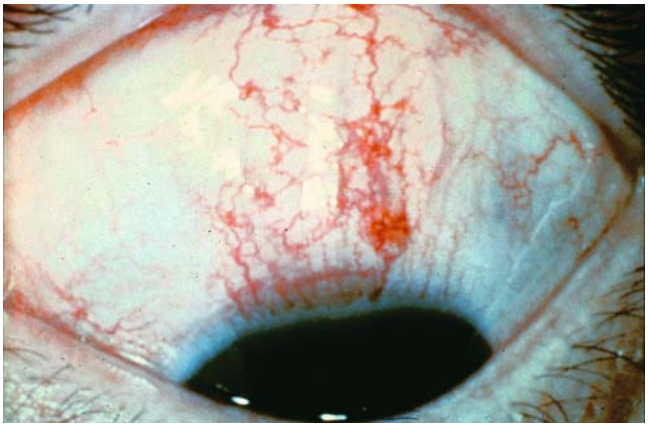

b

**Figure 19.2.** Leukocytoclastic vasculitis purpura in a patient with mild disease with few arthritic complaints (a). Scleritis is a feature of some of the patients with systemic rheumatoid arthritis. The eye is red, but the vision is preserved (b).

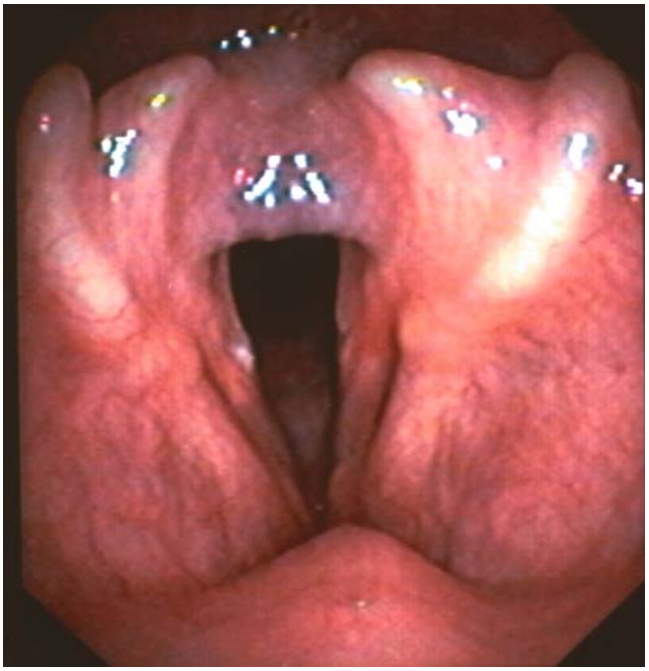

**Figure 19.3.** Laringoscopy showing laryngeal rheumatoid nodule that caused hoarseness.

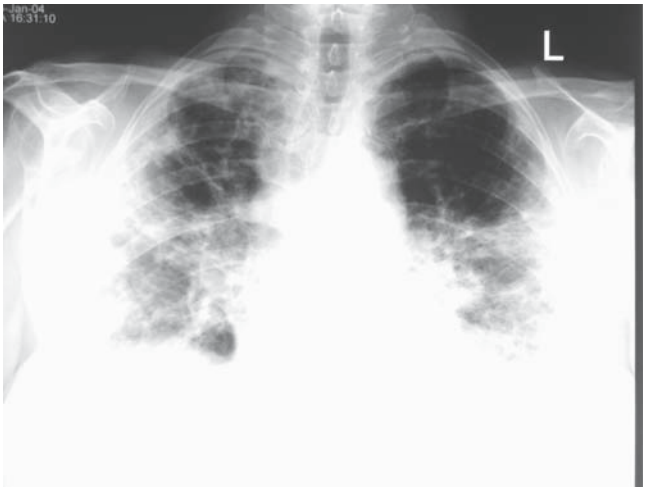


a

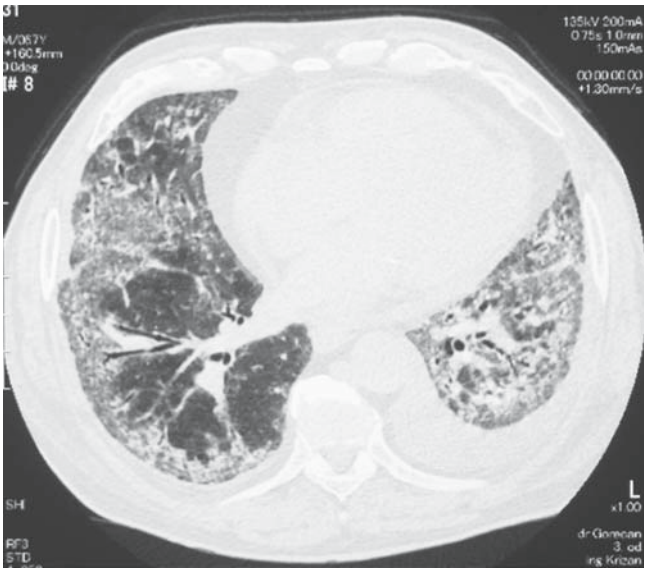


b

**Figure 19.4.** Chest radiograph shows bibasilar coarse reticular and retractive pattern and bilateral basal extensive pleural opacification, predominantly fibrothorax (a). HRCT scan in the same patient reveals mainly bibasilar and peripheral reticular pattern, thickening of the interlobular septa, intralobular interstitial thickening, and distortion of the lung parenchyma. Bilateral pleural effusion is present, predominantly on the left side with the thickening of the visceral and parietal pleura (b). The patient was treated with corticosteroids, sulfasalazine, and methotrexate with success, this is, he is not respiratory insufficient any more and does not need supplemental oxygen as it was prior to introduction of the drugs other than nonsteroidal anti-inflammatory agents.

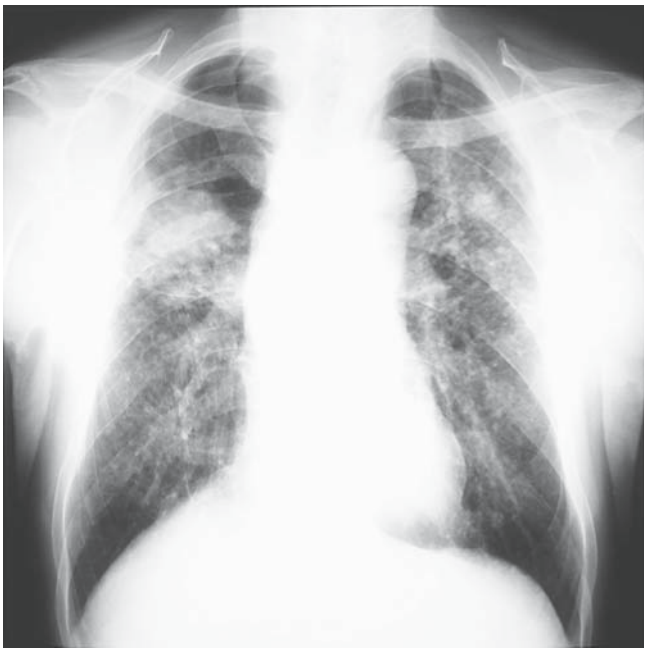

a

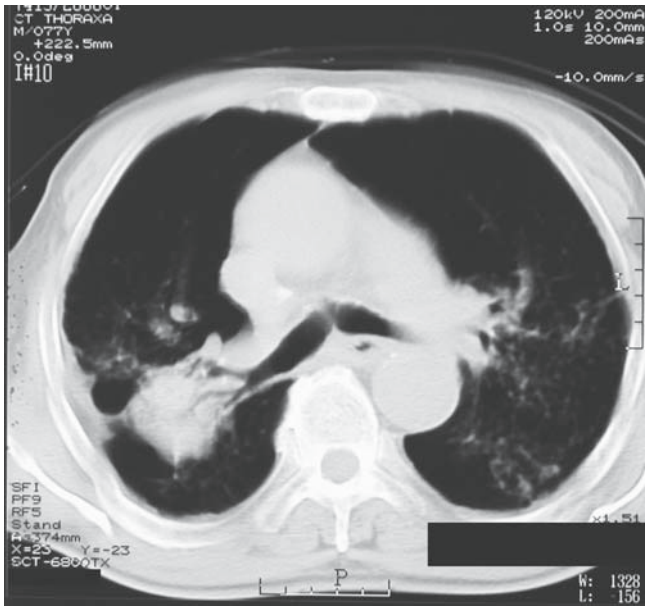


b

c

**Figure 19.5.** Rheumatoid nodules, sometimes in the form of Caplan syndrome could be seen, which connects RA with pulmonary nodules and pneumoconiosis, in this particular case with silicosis. Plain radiograph shows gross nodules predominantly in the upper lobes (a), shown also by CT scanning (b). Rheumatoid nodule and honeycombing may occur simultaneously as shown by this lung from a male patient who died of renal failure due to secondary amyloidosis (c).

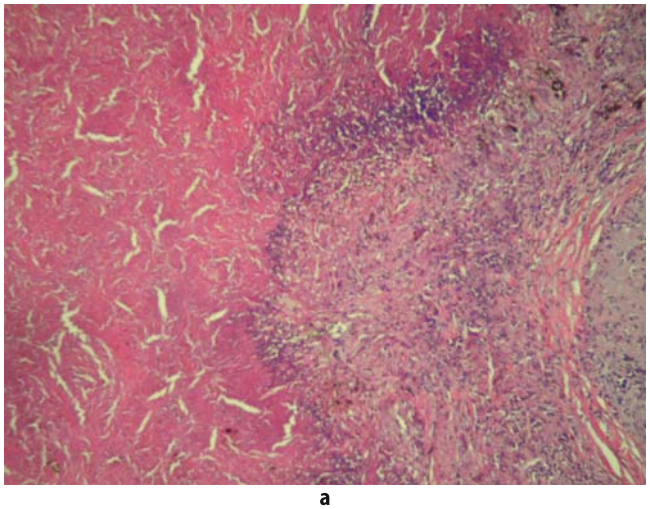

a

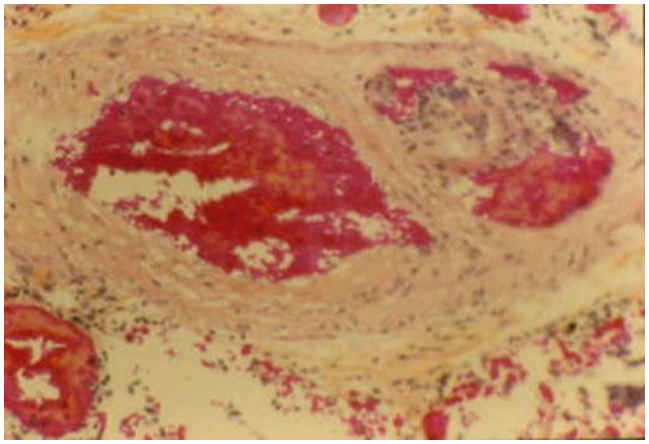

b

**Figure 19.6.** The histopathological finding of the transbronchial or open lung biopsy is diverse in RA; the pattern of usual interstitial pneumonia (UIP) is most common and the nodule in Caplan syndrome is typically rheumatoid. Rheumatoid nodule with fibrinoid necrosis and palisading histiocytes and few lymphocytes (a). Plexiform lesion. Pathological finding of pulmonary arteries in some cases of RA are compatible with plexiform lesion. This finding is not a characteristic of rheumatoid arthritis (b).

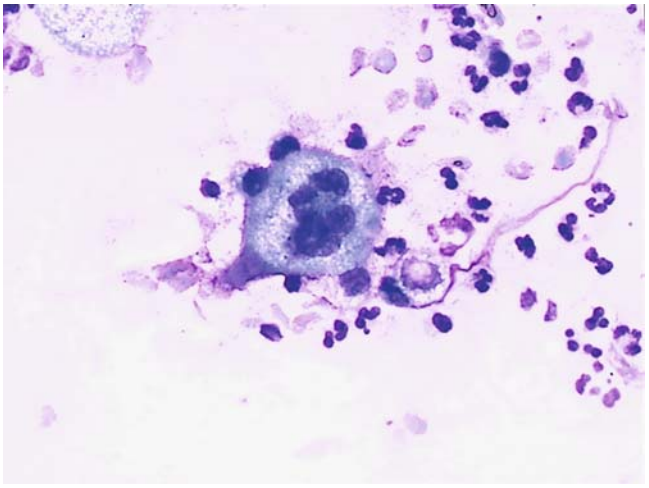

**Figure 19.7.** As the pleural effusion is a very frequent finding, pleural fluid cytoanalysis is often performed. Multinucleated, elongated giant cells and neutrophils in "dirty background" are often seen in pleural fluid of RA patients. Pleural fluid cytology, original magnification ×400, MGG stain (May-Grünwald-Giemsa).

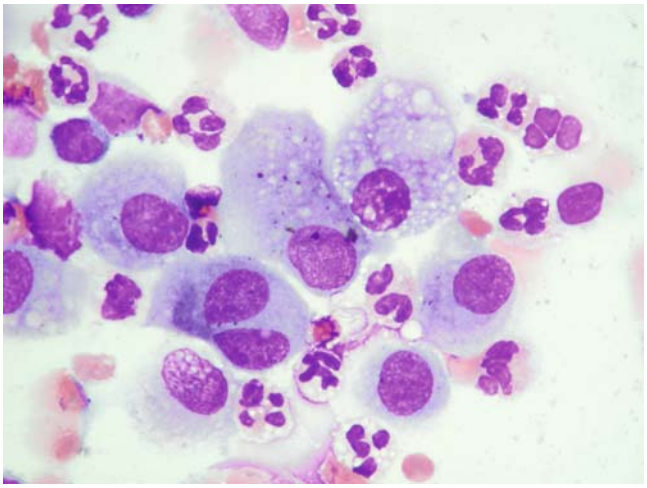

**Figure 19.8.** Neutrophilic alveolitis is a frequent finding in patients with RA. Neutrophils, few alveolar macrophages and erythrocytes are seen. BAL fluid cytology, original magnification ×1000, MGG stain (May-Grünwald-Giemsa).

## Bibliography


1. Lee H-K, Kim DS, Yoo B, Seo JB, Rho J-Y, Colby T, Kitaichi M. Histopathologic patterns and clinical features of rheumatoid arthritis associated interstitial lung disease. Chest 2005;127:2019–2027.
2. Dawson J, Fewins H, Desmon J, et al. Fibrosing alveolitis in patients with rheumatoid arthritis as assessed by high resolution computed tomography, chest radiography, and pulmonary function tests. Thorax 2001;56:622–627.
3. Ellman P, Ball R. Rheumatoid disease with joint and pulmonary manifestations. Br Med J. 1948;2:816–820.
4. Walker W, Wright V. Pulmonary lesions and rheumatoid arthritis. Medicine 1968;47:501–520.
5. Frank S, Weg J, Harkelrod L. Pulmonary dysfunction in rheumatoid arthritis. Chest 1973;63:27–34.
6. Dawson JK, Graham DR, Desmond J, Fewins HE, Lynch MP. Investigation of the chronic pulmonary effects of low dose oral methotrexate in patients with rheumatoid arthritis: A prospective study incorporating HRCT scanning and pulmonary function tests. Rheumatology (Oxoford) 2002;42:262–267.

# 20

# Systemic Sclerosis and the Lung

Systemic sclerosis (SSc; scleroderma) is a poorly understood connective tissue disease that involves the skin, gastrointestinal tract, musculoskeletal system, kidneys, heart, and the lungs (Figures 20.1, 20.2, and 20.3). The earliest inflammatory changes occur in the microcirculation with endothelial cell activation, followed by perivascular infiltration of monocytes and lymphocytes. Subsequently, fibroblasts become activated and deposit increased extracellular matrix in affected tissue systems. There is evidence to support genetic factors in the development of SSc, but few candidate susceptibility or severity genes have yet been found.

Most patients affected with this disease are 30 to 60 years in age; women are three times more frequently affected than men. Prognosis is usually poor, and the cause of death is renal, cardiovascular, or pulmonary failure. Five-year survival in patients with SSc who have lung disease is less than 40%. The risk of developing pulmonary manifestations of SSc are diffuse cutaneous forms and anti Scl-70 antibodies (Figure 20.4).

The lungs are the second most commonly affected organ in systemic sclerosis (Table 20.1), the esophagus being the most common (Figure 20.5). Clinical or autopsy evidence of pulmonary involvement is found in more than 70% of cases. Dyspnea and cough are the most frequent symptoms present in more than 50% of cases, whereas the most frequent physical sign is fine basilar crackles. Chest radiograph is abnormal in only 25% of all cases. The most common abnormality on the chest radiograph is linear-reticular pattern affecting the lung bases. Fine reticular pattern is the initial abnormality (Figure 20.6a). As the disease progresses, reticulo-nodular, nodular, and honeycomb patterns emerge (Figure 20.6b). High-resolution CT of the chest reveals the thickening of the intra-alveolar interstitium and alveolar septa, traction bronchiectasis, ground-glass pattern, consolidation, and diminished lung volumes (Figure 20.7a, b).

Restrictive lung function impairment with reduction in diffusing capacity is the usual physiological abnormality. A small number of patients have airway obstruction. Diffusing capacity is markedly reduced in patients with CREST Calcimosis Raynaud's phenomenon Oesophageal dysmotility Sclerodactily Teleangiectasia syndrome.

Bronchoalveolar lavage reveals neutrophilic, rarely eosinophilic alveolitis. Pulmonary fibrosis (histopathologically most frequently NSIP is found!) (Figure 20.8a) and pulmonary hypertension are the two most common pathological features of scleroderma (Figure 20.8b). Alveolitis may be the initial step in the disease process, but it is usually not observed without fibrosis in pathological specimens. As the disease progresses, diffuse fibrosis involves local capillaries, producing an endarteritis and distortion of alveolar spaces and the peripheral airways causing cyst formation and bronchiectasis. Patients with scleroderma can develop secondary pulmonary hypertension due to the extensive pulmonary parenchymal changes or as a primary vascular process. In any case, the presence of pulmonary hypertension carries poor prognosis (Table 20.2).

Sudden worsening of symptoms, hypoxemia, and diffusing capacity in patients with pulmonary fibrosis indicate the presence of pulmonary hypertension. Long-term survival of patients with combined interstitial lung disease and pulmonary hypertension is worse than that in isolated interstitial lung disease. Medical treatment remains unsatisfactory and experimental.

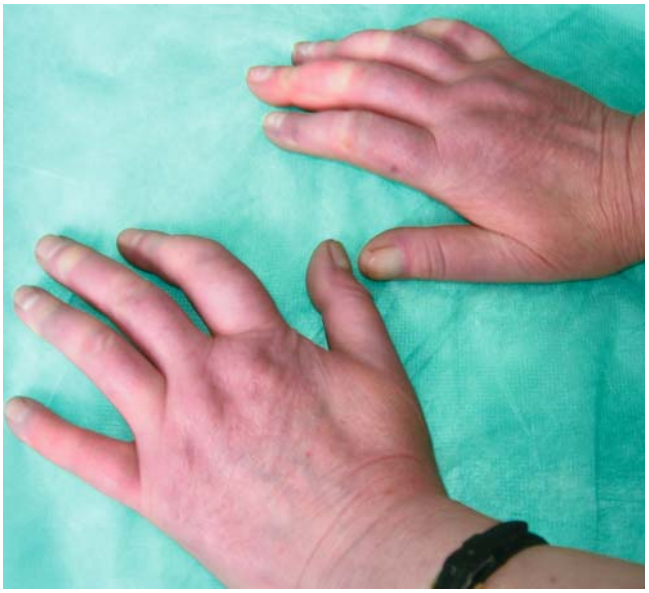

**Figure 20.1.** The hands are stiff and the skin is thickened and shiny in a patient with SSc ("sausage like").

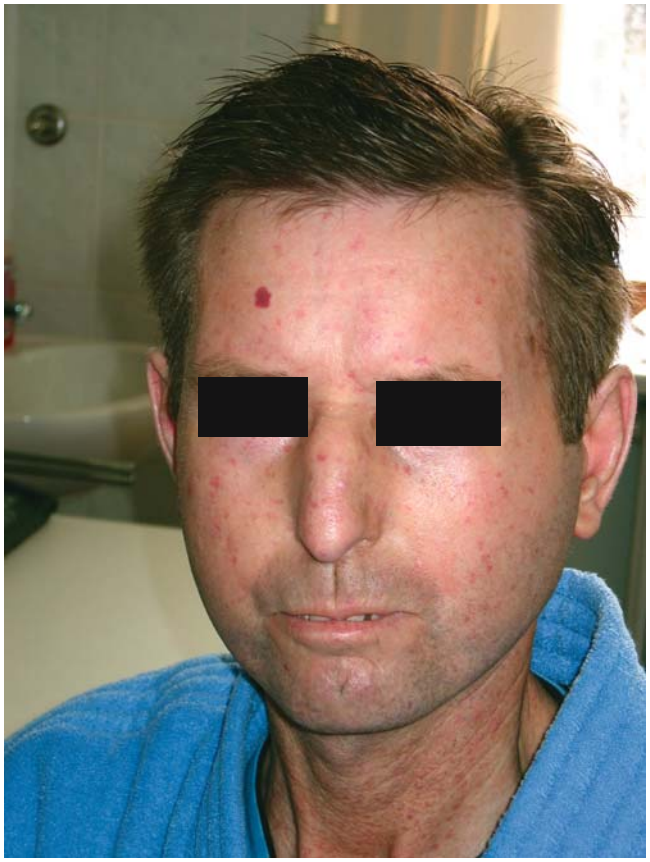

a

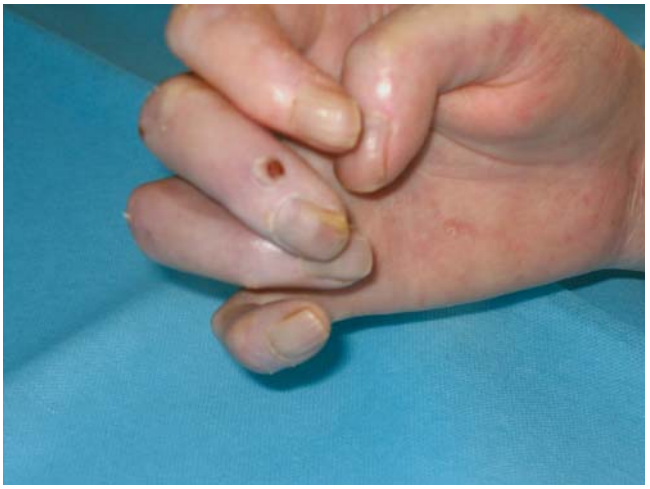

b

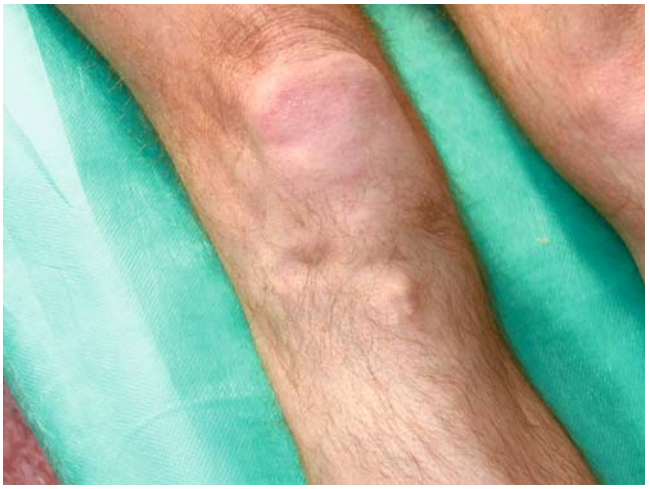

c

**Figure 20.2.** Here we present a patient with disease progression. The skin became shiny and taut with telangiectasias, the face masklike (a), the flexion contractures and trophic ulcers overlying the finger joints developed (b), as well as the subcutaneous calcification over bony eminence of the knee (c).

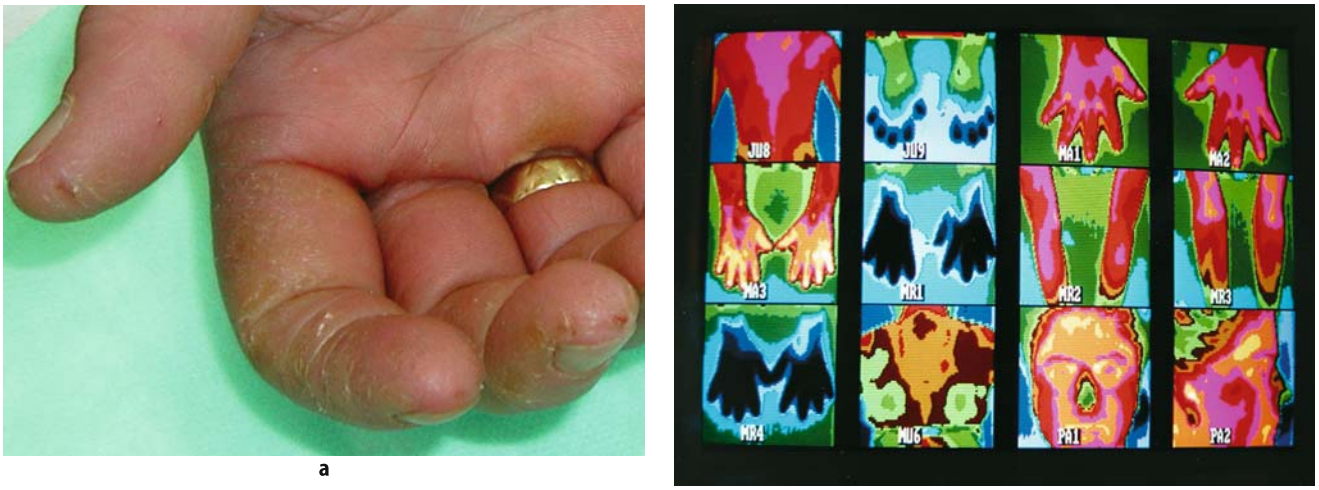


a b

**Figure 20.3.** Raynaud phenomenon is frequent in patients with SSc. This is a condition in which the smallest arteries that bring blood to the fingers or toes constrict when exposed to cold or from an emotional upset. The small veins are usually open, so the blood drains out of the capillaries. The result is that the fingers or toes become pale, cold, and numb. If there's a spasm in the small veins and blood is trapped in the capillaries, the fingers or toes turn blue as the blood loses its oxygen. The ulcerations at the tip of the fingers are sometimes seen. (a) CCTT (color computed tele thermography) test to trace Raynaud phenomenon. Images MA1 and MA2 are right and left hand of a healthy person. Following the cryoactivation (hand rests for 1 minute in the water at 4°C) the hyperemia develops and that is depicted by image MA3; the color is lighter. Image MR1 is from the patient with Raynaud syndrome; the image is dark, the "thermal amputation" is at work. Following the cryoactivation (MR4), the image is still worse due to absence of vasodilatation (b).

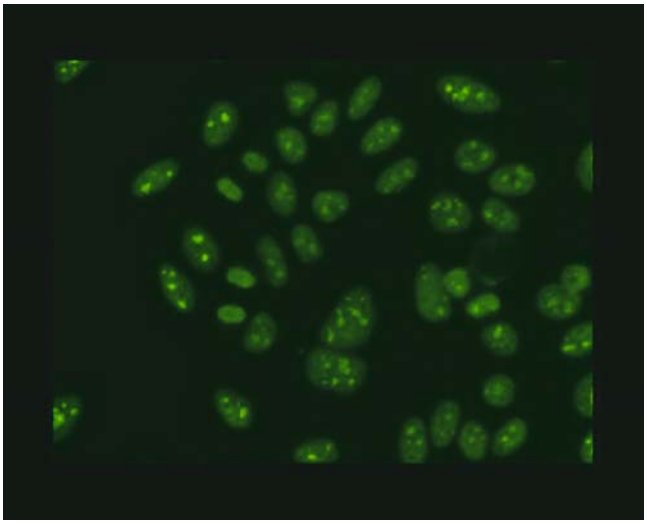

**Figure 20.4.** Antibody directed against DNA topoisomerase 1 (Scl-70). Homogeneous or fine nuclear speckled pattern. The chromosomal region in mitotic cells also staining. Nucleoli are usually stained homogeneously because of mixed patterns in systemic sclerosis but negative and ring nucleolar patterns are frequent (HEp-2 cells; Euroimmun, Lubeck, Germany; objective ×40).

**Table 20.1.** Systemic sclerosis: Pulmonary complications.

| | | |
|---|---|---|
| Primary | Fibrosing alveolitis | Affects the lower and middle lobes bilaterally and is more extensive in the peripheral than in the central areas of the lungs. More widespread reticulo-nodular infiltration and honeycombing on the chest radiograph as the disease progresses. |
| | Pleural involvement | Symptomatic pleuritis is relatively uncommon. Adhesions, thickening, and fibrous pleurisy are found in 90% of patients at postmortem examination. Large pleural effusions are unusual. |
| | Vascular changes | Pulmonary hypertension is common. It is mild in half of the patients and does not cause clinical symptoms; in the remaining patients, cor-pulmonale develops. Vascular changes can occur and progress independently of pulmonary fibrosis but are common in CREST syndrome. |
| Secondary | Infections | Pulmonary infections are frequent and related to the degree of structural damage and recurrent aspirations particularly in patients with severe disturbance of esophageal motility. |
| | Malignancy | Alveolar-cell or bronchiolar carcinomas may occur in scleroderma particularly in women with long-standing fibrosis. |

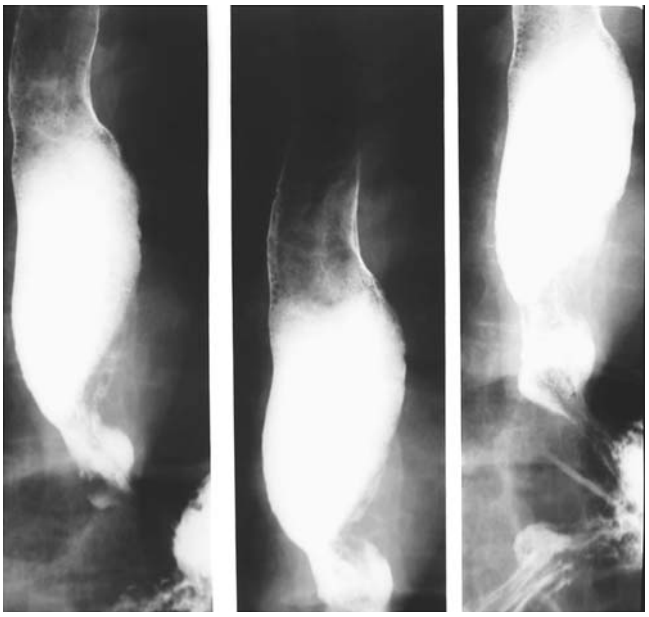

**Figure 20.5.** Esophagus disease in scleroderma is characterized by poorly functioning muscle of the lower two thirds of the esophagus. This can lead to an abnormally wide esophagus, which allows stomach acid to backflow into the esophagus to cause heartburn, inflammation, and potentially scarring. Weight loss and inanition in a patient with SSc should raise a concern of gastrointestinal involvement. Double-contrast esophagography following a barium swallow reveals dilated esophagus with reduced mucosal folds.

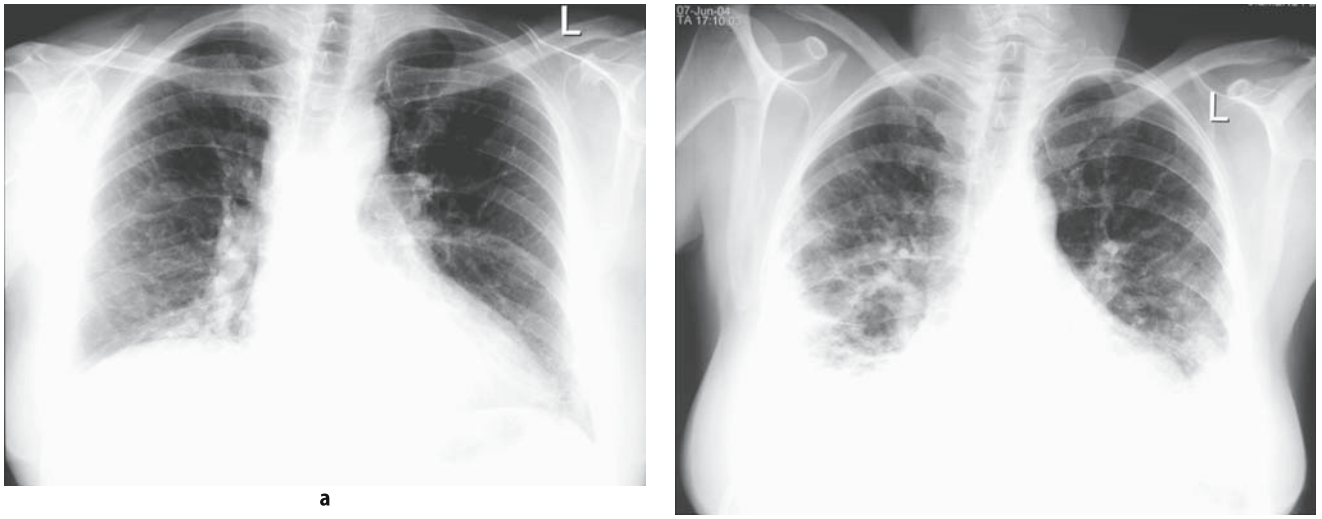


a b

**Figure 20.6.** The chest radiograph in systemic sclerosis. It shows discrete bilateral, bibasilar, and peripheral linear and reticular pattern in a patient with recent desease. The patient referred to the pulmonologist because of dry cough that persisted for several months, in spite of different medications used. She or her physician did not connect respiratory and symptoms of Raynaud syndrome that developed during the same time (a). The long-lasting SSs showing also the shrinkage of the lungs ("small, stiff lung") (b).

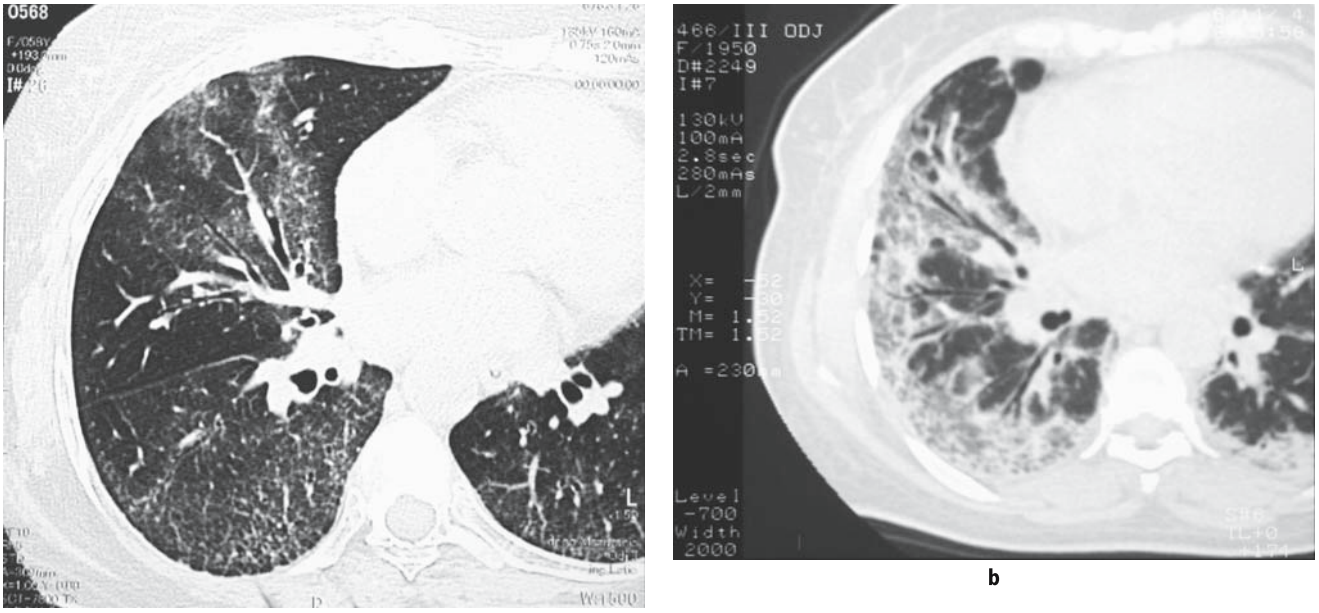


a b

**Figure 20.7.** HRCT scan in a patient with recent onset of systemic sclerosis whose chest radiograph was already shown (Figure 20.6a) reveals the thickening of the intra-alveolar interstitium and alveolar septa (a), and another in a patient with advanced disease showing incipient bronchiectasis, ground-glass pattern, consolidation, and diminished lung volumes (b).

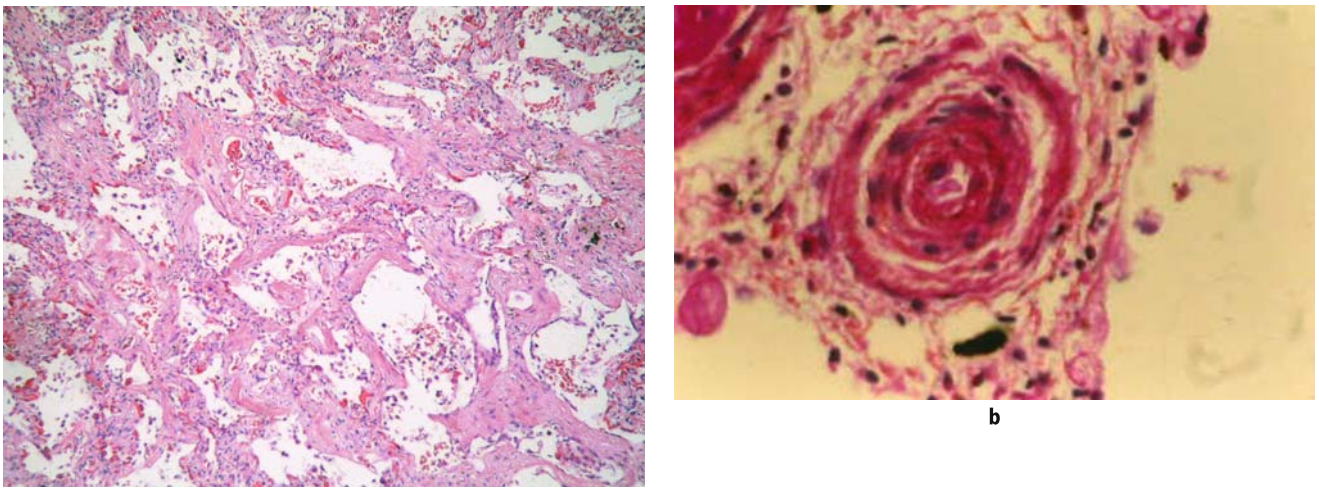

a b

**Figure 20.8.** The histopathological pattern most often is of nonspecific interstitial pneumonia (NSIP) type. In this particular case of SSc, we found features of fibrotic NSIP (a). Vascular involvement in pulmonary SSc consists of concentric fibrosis of small arteriole (b).

**Table 20.2.** Agents for treatment of pulmonary hypertension in systemic sclerosis (SSc).

| Agents for Treatment of Pulmonary Hypertension in SSc |
|---|
| 1. Calcium channel antagonists |
| 2. Prostanoids |
| 3. Sildenafil |
| 4. Nitric oxide |
| 5. Endothelin antagonists |
| 6. Oxygen |

The patients with pulmonary systemic sclerosis have an increased incidence of lung cancer. The course of pulmonary fibrosis is more indolent than IPF. Prednisone is generally not beneficial. Cyclophosphamide and recombinant alpha-interferon have been used.

## Bibliography

1. Veeraghavan S, Sharma O. Progressive systemic sclerosis and the lung. Curr Opin Pulm Med 1998;4:305–309.
2. Schurawitzki H, Stiglbauer R, Graninger W, Herold C, Polzleitner D, Burghuber OC, Tscholakoff D. Interstitial lung disease in progressive systemic sclerosis: High resolution CT versus radiography. Radiology 1990;176:755–759.
3. Johnson DA, Drane WE, Curran J, Cattau EL Jr, Ciarleglio C, Khan A, Cotelingam J, Benjamin SB. Pulmonary systemic sclerosis: A complication of gastro-esophageal reflux and occult aspiration. Arch Intern Med 1989;149:589–593.
4. Chang B, Wigley F, White B, Wise R. Scleroderma patients with combined pulmonary hypertension and interstitial lung disease. J Rheumatol 2003;30:2398–2405.
5. Kim DS, Yoo B, Lee JS, Kim EK, Lim CM, Lee SD, Koh Y, Kim WS, Kim WD, Colby TV, Kitiaichi M. The major histopathologic pattern of pulmonary fibrosis in scleroderma is nonspecific interstitial pneumonia. Sarcoidosis Vasc Diffuse Lung Disease 2002;19:121–127.
6. Ho KT, Reveille JD. The clinical relevance of autoantibodies in scleroderma. Arthritis Res Ther 2003;5:80–93.

# 21

# Systemic Lupus Erythematosus and the Lung

Systemic lupus erythematosus (SLE) is an autoimmune disease which can affect almost any organ system (Figure 21.1). In all SLE patients, the anti-nuclear antibodies (ANA) can be detected (Figure 21.2a, b, c), but the most characteristic are antibodies directed against double-stranded deoxyribonucleic acid and antibodies directed against Sm and U1-sn RNP (Figure 21.3).

Pulmonary manifestations of SLE are due to immune complex lung injury. Almost any pulmonary structure can be affected in SLE (Table 21.1).There are other causes of pulmonary injury in SLE, like pneumonias, thromboembolic incidences, and edema due to cardiac failure. All these conditions may cause acute respiratory illness with respiratory insufficiency. Acute course of the disease is also a feature of acute lupus pneumonitis and sometimes diffuse alveolar hemorrhage.

*Acute lupus pneumonitis* is a clinical syndrome detected in 1–5% of patients with a mortality of 50%. Histopathologically, diffuse alveolar damage and nonspecific interstitial pneumonia are revealed. It resembles the clinical course of acute pneumonia. Plain radiograph of the chest shows bilateral or unilateral alveolar infiltrates, sometimes with pleural effusion or atelectasis (Figure 21.4c). As the mortality is extremely high, the aggressive diagnostic and therapeutic approach is recommended. The infectious agents have to be excluded as they are the most frequent cause of lung infiltrates in SLE. High doses of corticosteroids and immunosuppressive agents (intravenous cyclophosphamide) are efficient in some cases.

*Diffuse alveolar hemorrhage (DAH*) is a serious and life-threatening pulmonary complication in SLE. It is a rare event, and it occurs in about 2% of patients with a mortality of 50–90%. Women are more frequently affected than men; usually nephritis, nephrotic syndrome, renal failure, and positive anti-DNA antibodies are present. Histopathologically, acute inflammation and necrosis involving capillaries, arterioles, and small muscular arteries has been described. The dominant symptom is dyspnea, with or without hemoptysis, fever, and anemia. Chest radiograph shows bilateral alveolar opacities (Figure 21.4a, b). The reduction of hemoglobin concentrations gives rise to the possibility of pulmonary hemorrhage. The lung lavage fluid becomes macroscopically more bloody during the procedure, and cytologically the hemosiderin-laden macrophages (siderophages) are detected. Bronchoscopy also allows for a search for infectious agents.

High doses of corticosteroids are reported to be effective, but sometimes immunosuppressive agents have to be introduced. Plasmapheresis should be reserved for patients with multiorgan SLE and severe DAH refractory to corticosteroids and cyclophosphamide.

*Chronic forms of interstitial lung disease* in SLE are uncommon, although HRCT scanning has shown that 30% of the patients have some form of the disease albeit the normal plain radiograph of the chest. Pulmonary function tests were abnormal in about 50% of the patients with abnormal HRCT. Chronic forms of lung disease in SLE present with slowly progressive dyspnea. Histopathological analysis reveals UIP, NSIP, BOOP, or LIP (Figure 21.5). Most investigators believe that there is an evolution from acute to chronic forms of ILD in SLE. Plain chest radiographic (Figure 21.6a, b) and HRCT (Figure 21.6c)

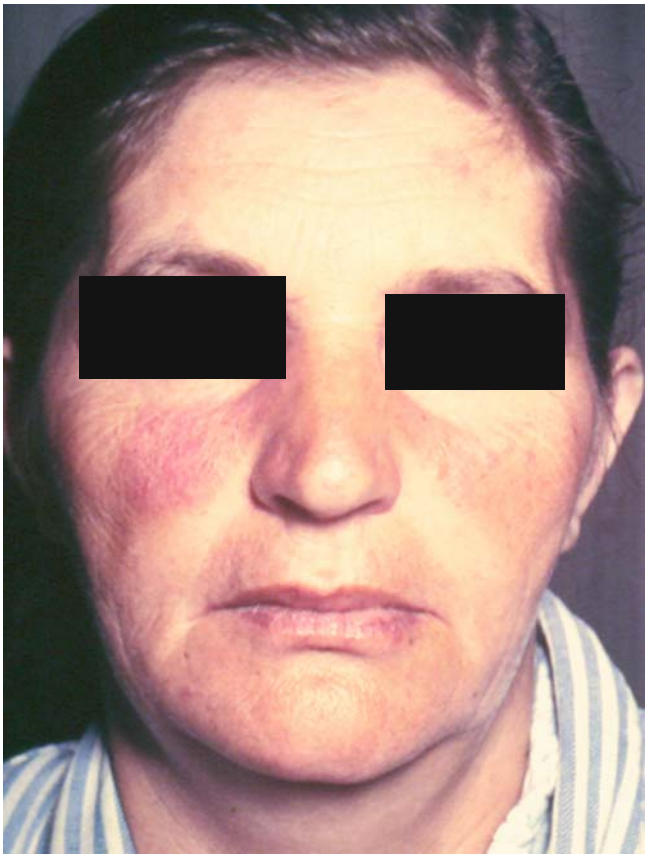

**Figure 21.1.** Butterfly rash on the face of a person with SLE.

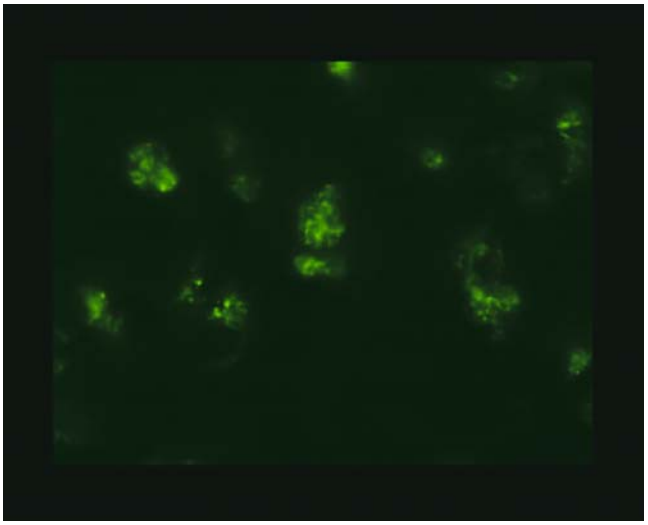

a

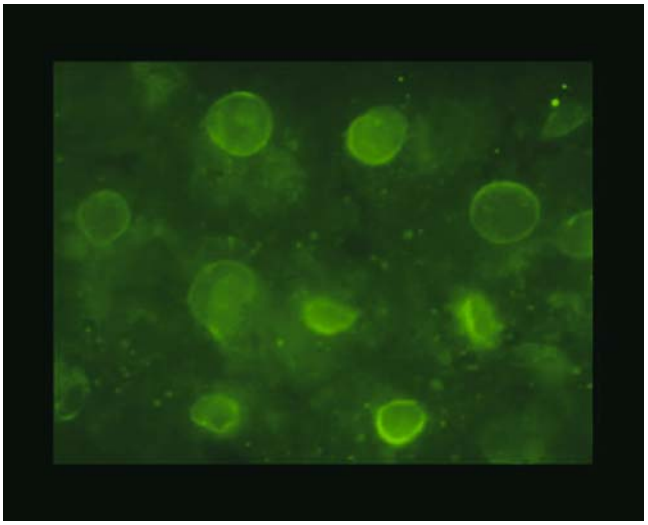

b

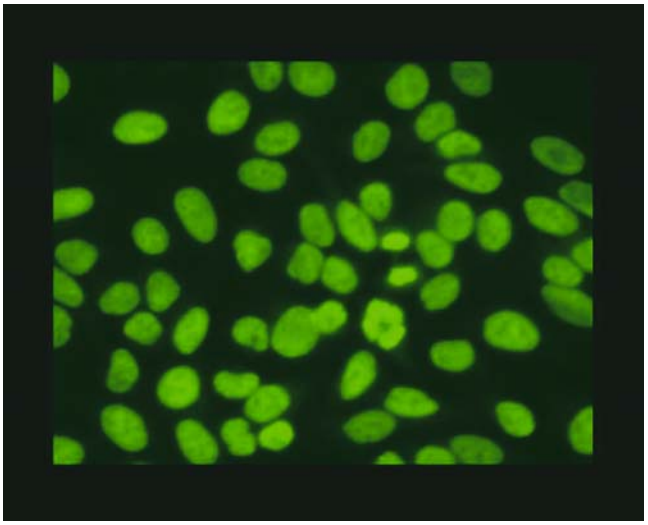

c

**Figure 21.2.** Fluorescence of the nuclei in the tissue shows the presence of anti-nuclear antibodies (ANA); the fluorescence may be speckled, perinuclear, or homogeneous. Speckled nuclear fluorescence (on home-made rat liver; objective ×100) cause antibodies directed against various target antigens (hn-RNP, U1-RNP, Sm, SS-A, SS-B) (a), perinuclear fluorescence of the nucleus (on home-made rat liver; objective ×100) cause antibodies directed against nuclear membrane laminins (b), but homogeneous is typical of SLE, though it also occurs in a range of other autoimmune and connective tissue diseases. These are antibodies directed against ds-DNA. Homogeneous diffuse fluorescence of the entire nucleus of interphase cells and the chromosomal region in mitotic cells (Hep-2 cells; Euroimmun, Lubeck, Germany; objective ×40) (c).

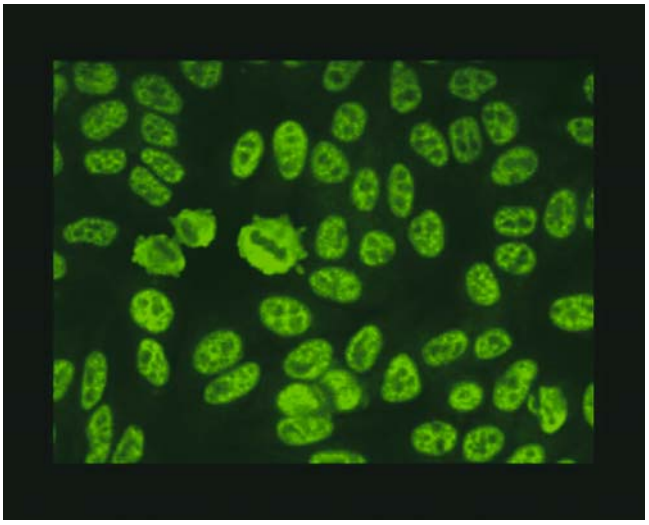

**Figure 21.3.** Antibodies directed against Sm and U1-sn RNP. Typical coarse speckled pattern with nucleolar sparing and occasional slight cytoplasmic staining (Hep-2 cells; Euroimmun, Lubeck, Germany; objective ×40).

**Table 21.1.** Pleuropulmonary manifestations of systemic lupus erythematosus.

| Pleuropulmonary Manifestations | Frequency |
|---|---|
| Parenchymal disease | |
| Usual interstitial pneumonia (UIP) | ± |
| Nonspecific interstitial pneumonia (NSIP) | + |
| Bronchiolitis obliterans organizing pneumonia (BOOP) | ± |
| Lymphoid interstitial pneumonia (LIP) | ± |
| Diffuse alveolar damage (DAD) | + |
| Diffuse alveolar hemorrhage (DAH) | + |
| *Acute lupus pneumonitis*, combination of DAD and NSIP | + |
| Airway disease | |
| Upper airway dysfunction | + |
| Bronchiolitis obliterans | ± |
| Bronchiectasis | ± |
| Pleural disease | |
| Pleural effusion | +++ |
| Diaphragmatic disease | |
| Diaphragmatic dysfunction | + |
| "Shrinking lung syndrome" | ± |
| Pulmonary vascular disease | |
| Thromboembolic disease | + |
| Vasculitis | + |
| Pulmonary hypertension | ++ |
| Miscellaneous | |
| Weakness of respiratory muscles | ++ |
| Mediastinal lymphadenopathy | + |

+++, common; ++, fairly frequent; +, occasional; ±, rare.

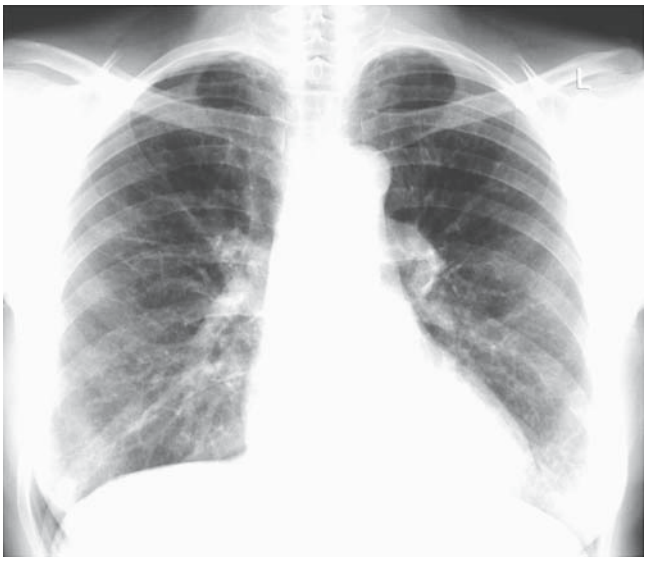

a

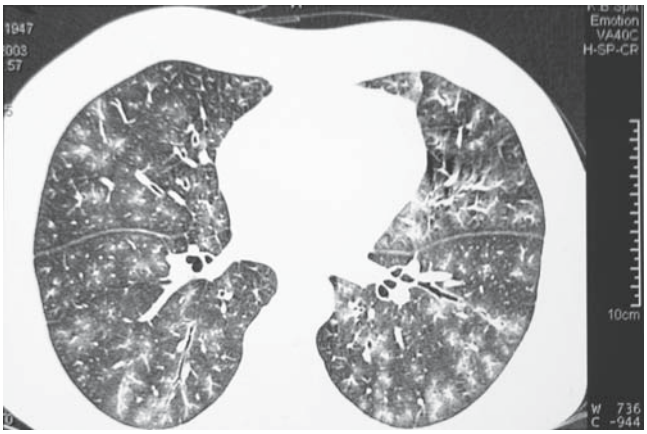


b

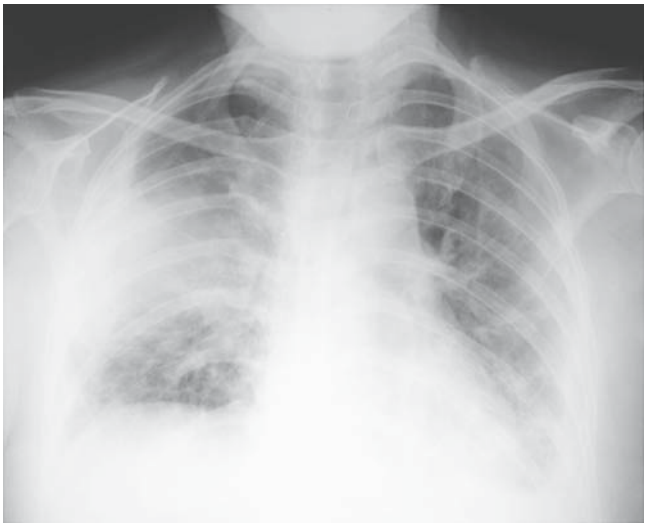

c

**Figure 21.4.** The radiological chest analysis in SLE is diverse. Diffuse alveolar hemorrhage presents as reticular interstitial and focal alveolar pattern in the left lower lobe by plain radiograph (a). HRCT scan of the same patient who presented with hemoptysis reveals centrilobular, perivascular patchy ground-glass pattern with no vessels affected. This was the only initial manifestation of SLE, which was later confirmed by identification of positive ANA, anti-dsDNA antibodies, and antibodies directed against Sm (b). Lupus pneumonitis showing bilateral alveolar pattern (c) is another acute serious event that can be seen in SLE patients.

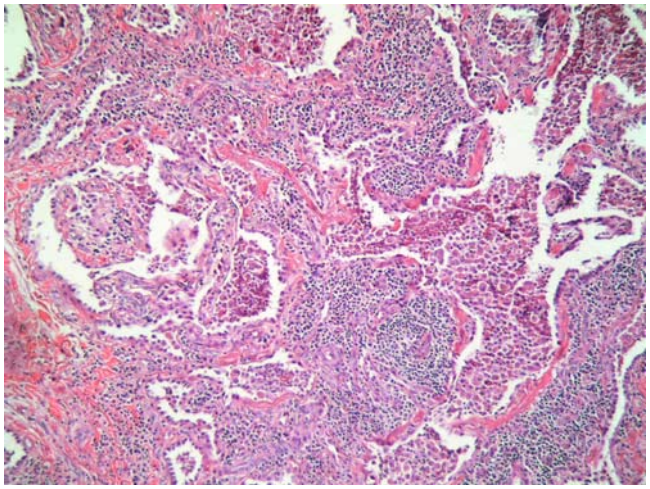

**Figure 21.5.** Systemic lupus erythematosus histology shows widening of septa with dense lyphocytoid infiltrates—nonspecific interstitial pneumonia—and accumulation of macrophages in alveolar spaces.

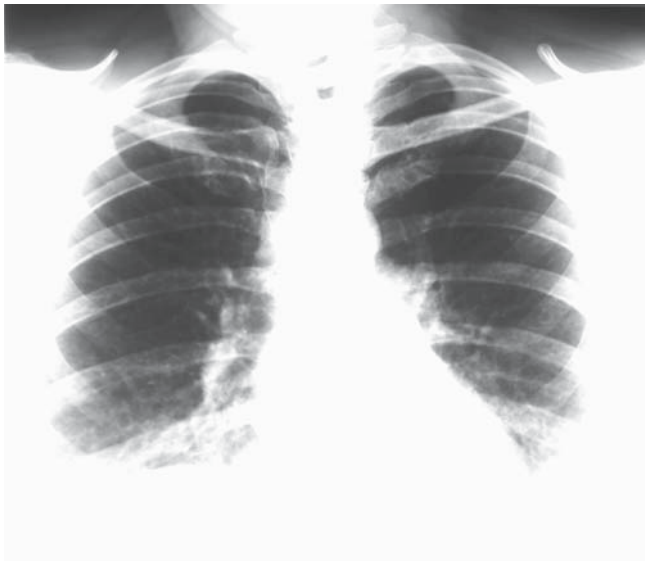

a

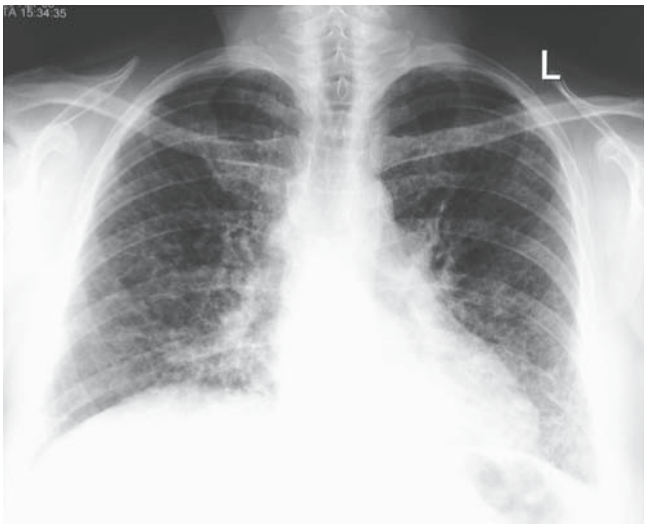


b

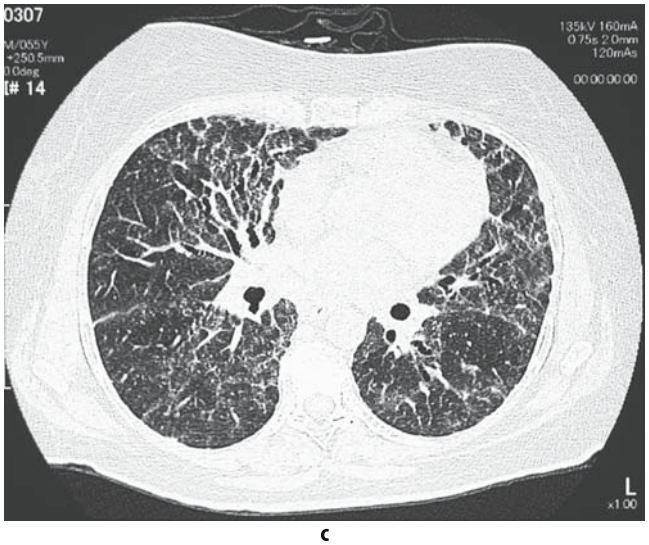


c

**Figure 21.6.** Chest radiograph in chronic form of interstitial lung disease in SLE shows bilateral and bibasilar coarse reticular changes most frequently due to usual interstitial pneumonia. This is a radiogram of a female 9 years ago; then changes were mild (a), and they slowly progressed to diffuse reticular pattern (b), and now the HRCT scan reveals the reticular pattern, intralobular thickening, patchy ground-glass opacities, traction bronchiectasis, and architectural distortion, predominantly in the lower lobes. The fibrous pleural changes are seen (c).

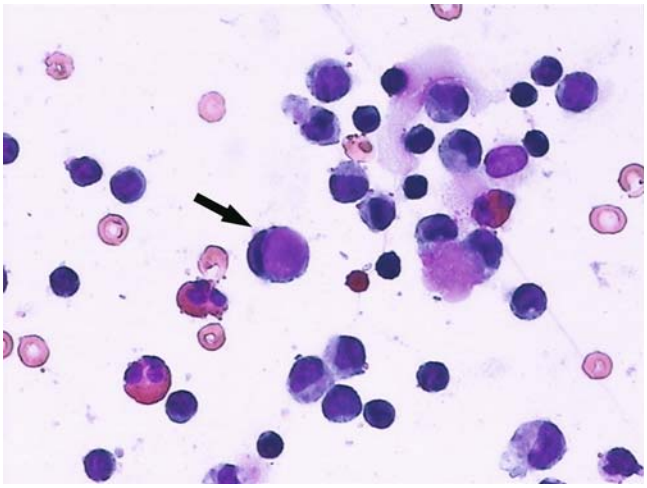

**Figure 21.7.** Frequently, pleural effusion is found in patients with SLE. The predominant cells in pleural exudate are lymphocytes, but occasionally LE cells can be found. LE cell (arrow), small lymphocytes, eosinophils, and erythrocytes are seen. Pleural fluid cytology, original magnification ×400, MGG stain (May-Grünwald-Giemsa).

findings are almost identical to the finding in IPF. The most common physiological deficit is the reduction in diffusing capacity. Restrictive ventilatory changes are frequently detected. Bronchoalveolar lavage is helpful in exclusion of the infections and alveolar hemorrhage, but less in the procedure of evaluation of the SLE lung changes. As pleural effusion is common, the exudate is sometimes analyzed (Figure 21.7). Open lung biopsy is seldom indicated. Treatment of chronic forms of ILD in SLE is poorly evaluated. Patients treated with corticosteroids improve in the majority of cases. Improvement with oral methotrexate has been reported.

Serious complications of SLE are *antiphospholipid syndrome* and pulmonary hypertension. Antiphospholipid syndrome occurs as a feature of SLE or as an independent, primary disorder. In 30–40% of patients with SLE, the antiphospholipid antibodies are found. The presence of these antibodies increases 3–4 times the incidence of thromboembolic events but also the development of thrombotic and nonthrombotic pulmonary hypertension, pulmonary arterial thrombosis, pulmonary microemboli, ARDS, and alveolar hemorrhage. Moderate-intensity warfarin for thromboprophylaxis in patients with antiphospholipid antibodies and previous thrombosis is appropriate, with the target International Normalized Ratio (INR) from 2.0 to 3.0.

## Bibliography


1. Santos-Ocampo AS, Mandell BF, Fessler BJ. Alveolar hemorrhage in systemic lupus erythematosus: Presentation and management. Chest 2000;118(4):1083–1090.
2. Fink SD, Kremer JM. Successful treatment of interstitial lung disease in systemic lupus erythematosus with methotrexate. J Rheumatol 1995;22:967–969.
3. Crestani B. The respiratory system in connective tissue disorders. Allergy 2005;60:715–734.
4. Strange C, Highland K. Interstitial lung disease in the patient who has connective tissue disease. Clin Chest Med 2004;25:549–560.
5. Bankier AA, Kiener HP, Wiesmayr MN, Fleischmanu D, Kontrus M, Herold CJ, Graninger W, Hubsch P. Discrete lung involvement in systemic lupus erythematosus: CT assessment. Radiology 1995;196:434–439.
6. Crowther MA, Ginsberg JS, Julian J, Denburg J, Hirtsh J, Douketis J, Laskin C, Fortin P, Anderson D, Kearon C, Clarke A, Geerts W, Forgie M, Green D, Consfantini L, Yacura W, Wilson S, Gent M, Kovacs MJ. A comparison of two intensities of warfarin for the prevention of recurrent thrombosis in patients with the antiphospholipid antibody syndrome. N Engl J Med 2003;349:1133–1138.

# 22

# Polymyositis/Dermatomyositis and the Lung

Polymyositis is a rare autoimmune disease, characterized by inflammation and degeneration of the skeletal muscles. If the skin is involved it is called dermatomyositis (Figure 22.1a, b, c). The incidence is 2–6 patients per 1 million inhabitants. In polymyositis, clonally expanded $CD8^+$ cytotoxic T cells invade muscle fibers that express MHC class I antigens, which leads to fiber necrosis via the perforin pathway. Dermatomyositis is a microangiopathy affecting skin and muscle; activation and deposition of complement causes lysis of endomysial capillaries and muscle ischemia. The causative autoantigen has not yet been identified.

*Pulmonary manifestations* of polymyositis/dermatomyositis (PM/DM) are numerous and present in about 50% of patients. They intensely influence the outcome of the disease; the overall mortality is 24%, and in patients with pulmonary involvement it rises to 62%. Specific pulmonary manifestations are diverse (Table 22.1), but most frequent are interstitial changes due to nonspecific interstitial pneumonia, complications due to aspiration pneumonia secondary to pharyngeal and esophageal disorder, and hypostatic pneumonia and respiratory failure secondary to respiratory muscle dysfunction and hypoventilation. Opportunistic infections and drug-induced pneumonitis are considered in differential diagnosis.

*Interstitial lung disease* is more frequent in women and can precede the onset of muscle or skin disease in 25% of cases. The initial symptoms are cough and dyspnea. Plain radiograph of the chest reveals bilateral, lower lobe reticulonodular pattern (Figure 22.2), and HRCT scan reveals bibasilar septal thickening, ground-glass opacities, and consolidation (Figure 22.3). Honeycombing is quite rare. Lung function tests show restrictive ventilatory changes and reduced DLco. Respiratory muscle weakness is demonstrated by a decrease in maximal inspiratory pressure and flow rates. Patients who have PM/DM and interstitial lung disease have more frequently an extractable nuclear antigen to RNA synthetase that is called the Jo-1 antibody (Figure 22.4) than those without ILD. As the causes of pulmonary disease in PM/DM patients are diverse, bronchoscopy and lung lavage are aimed to solve the differential diagnosis, especially if opportunistic infection is assumed or if respiratory failure of undefined etiology develops. Open lung biopsy is seldom performed.

Progressive and nonprogressive disease needs to be distinguished by clinical and physiologic monitoring to avoid overtreatment. Patients with ongoing functional deterioration mostly benefit from aggressive therapy. Cyclophosphamide together with corticosteroids is beneficial in many patients.

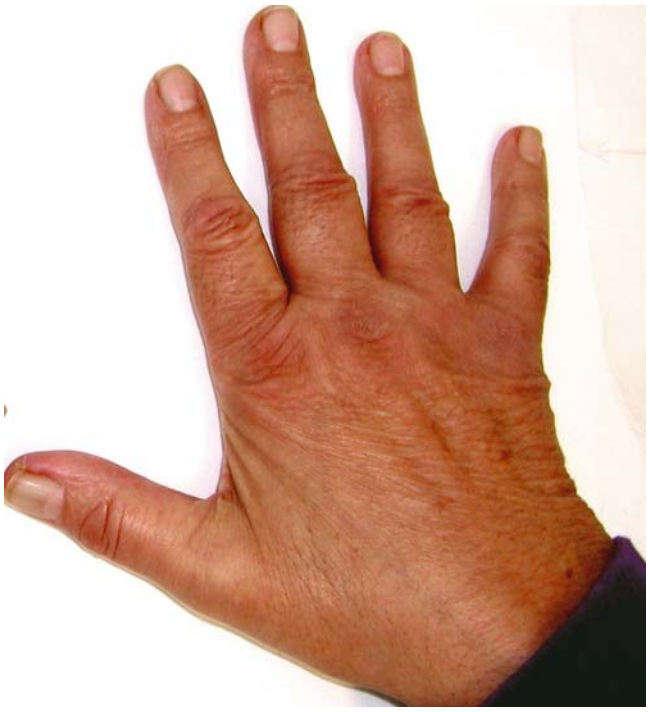

a

b

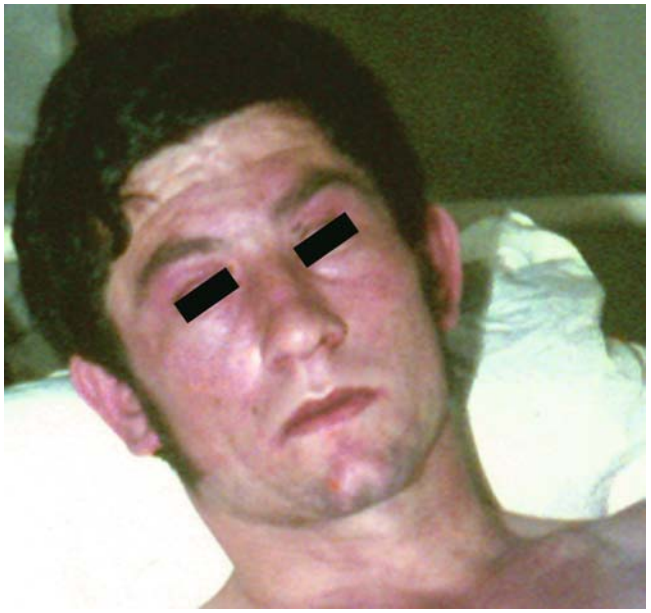

c

**Figure 22.1.** Gottron plaques, red-purple keratotic, atrophic erythema are found on the surface of finger joints, in this case most prominent over the metacarpophalangeal joints (a). A composite showing diffuse interstitial lung disease in a patient with dermatomyositis with violaceous or heliotrope rash of the face. The rash is named after the flower called Heliotrope because it follows the course of the sun (b). In this patient the skin rash is also located in a fairly characteristic distribution, including around the eyes and face, where it is edematous and red (c). Of note is that the skin lesions can occur well before the muscle manifestations.

**Table 22.1.** Pulmonary manifestations of polymyositis/dermatomyositis (PM/DM).

| | Frequency |
|---|---|
| Parenchymal disease | |
| Nonspecific interstitial pneumonia (NSIP) | +++ |
| Usual interstitial pneumonia (UIP) | ++ |
| Bronchiolitis obliterans organizing pneumonia (BOOP) | ++ |
| Lymphoid interstitial pneumonia (LIP) | ± |
| Diffuse alveolar damage (DAD) | ± |
| Complications of PM/DM: aspiration pneumonia secondary to pharyngeal and esophageal disorder and hypostatic pneumonia and respiratory failure secondary to respiratory muscle dysfunction and hypoventilation | +++ |
| Pleural disease | |
| Pleural disease | ± |
| Spontaneous pneumothorax | ± |
| Miscellaneous | |
| Weakness of respiratory muscles | +++ |
| Malignancy (primary or metastatic) | + |
| Pulmonary hypertension | + |
| Diffuse alveolar hemorrhage | ± |

+++, common; ++, fairly frequent; +, occasional; ±, rare.

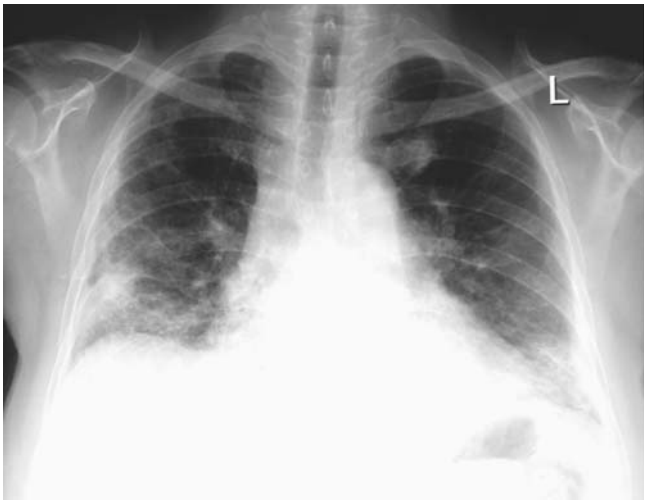


**Figure 22.2.** Chest radiograph in a patient with PM/DM shows coarse reticulomicronodular and alveolar pattern.

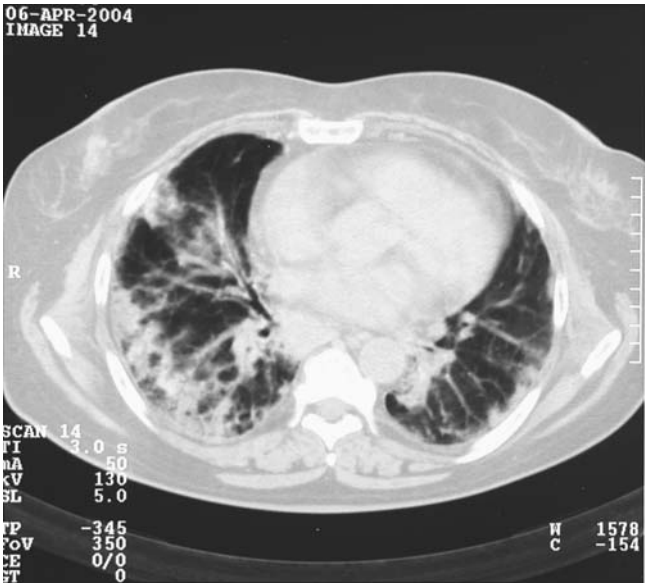


**Figure 22.3.** HRCT scan shows bibasilar and peripheral thickening of the interlobular septa, ground-glass pattern and consolidation of asymmetric distribution with pleural fibrosis.

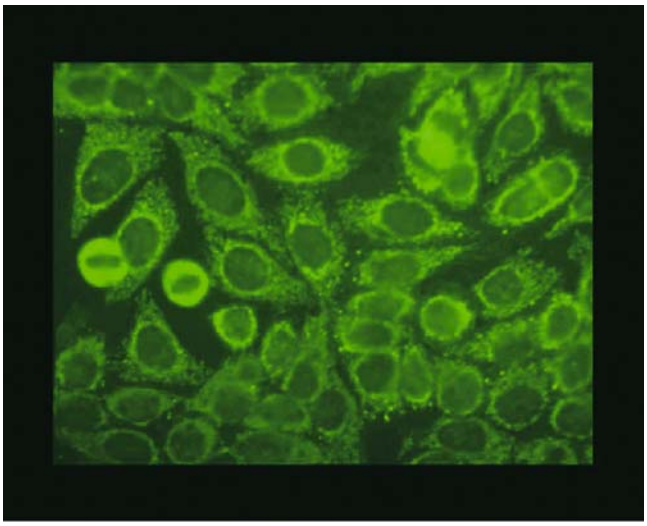

**Figure 22.4.** Antibody directed against Jo-1. Fine granules condensed around the nucleus, which diminish toward the periphery of the cytoplasm (HEp-2 cells; Euroimmun, Lubeck, Germany; objective ×40).

## Bibliography

1. Douglas WW, Tazelaar HD, Hartman TE, Hartman RP, Decker PA, Schroeder DR, Ryu JH. Polymyositis-dermatomyositis-associated interstitial lung disease. Am Rev Respir Crit Care Med 2001;164:1182–1185.
2. Fathi M, Dastmalchi M, Rasmussen E, Lundberg IE, Torling G. Interstitial lung disease, a common manifestation of newly diagnosed polymyositis and dermatomyositis. Ann Rheum Dis 2004;63:297–301.
3. Schnabel A, Hellmich B, Gross WL. Interstitial lung disease in polymyositis and dermatomyositis. Curr Rheumatol Rep 2005;7:99–105.
4. Dalakos MC, Hohlfeld R. Polymyosistis and dermatomyosistis. Lancet 2003;362:971–982.

# 23

# Sjögren Syndrome and the Lung

Sjögren syndrome (SS) is a chronic autoimmune disorder of the exocrine glands and extraglandular organs, in which the dryness of the eyes (*xerophthalmia)* (Figures 23.1a, b, c, d and 23.2a, b, c) and mouth *(xerostomia*) (Figure 23.3) dominate along with symptoms of polyarthritis (Figure 23.4). It is an autoimmune exocrinopathy with accumulation of lymphocytes and plasma cells; the similar perivascular lymphocytic infitrates could be found in various organs, including the lungs. It can be encountered alone (primary Sjögren syndrome) or in the presence of another autoimmune disorder (60% of cases), most frequently rheumatoid arthritis. Women are more frequently affected than men. Rheumatoid and anti-nuclear factors are positive in a majority of patients; the finding of anti-Ro (SS-A) and anti-La (SS-B) antibodies being specific for SS (Figure 23.5). Despite extensive research, the pathogenesis of SS remains unknown. Certain disturbances of the immune system (i.e., B-cell hyperreactivity and enhanced levels of B cell–activating factor/B-lymphocyte stimulator) probably play a central role in this entity. Whether this is a primary abnormality or the result of predisposing factors remains uncertain.

*Pulmonary manifestations* of SS are numerous and frequent but rarely cause severe symptoms. (Table 23.1). The airways are often involved; trachea (*xerotrachea)* and bronchi due to lymphocytic infiltrates of tracheobronchial submucose. It causes hoarseness and cough, and complications such as atelectasis, recurrent pneumonias, and bronchiectasis.

*Interstitial lung disease* is uncommon in primary SS but more common in secondary disease, probably as the complication of accompanying diffuse connective tissue disease lung changes. The most frequent histopathological finding is lymphoid interstitial pneumonia (LIP) (Figure 23.6a, b).

Plain radiograph shows linear or reticular changes in about 22% of patients (Figure 23.7). HRCT reveals ground-glass opacities and interlobular thickening in about 58% of SS patients (Figure 23.8a, b).

Bronchoalveolar analysis reveals lymphocytic alveolitis with some granulocytes. Lung biopsy should be performed if minimal doubt exists toward the malignant lymphoproliferative alteration. It is usually suspected on the grounds of radiological finding of solitary or multiple round opacities, alveolar infiltrates, or hilar or mediastinal lymphadenopathy.

The *therapy* of pulmonary manifestations of SS includes steroidal and nonsteroidal anti-inflammatory agents, disease-modifying agents, and cytotoxic agents. Therapy should also include topical agents to improve moisture and decrease inflammation.

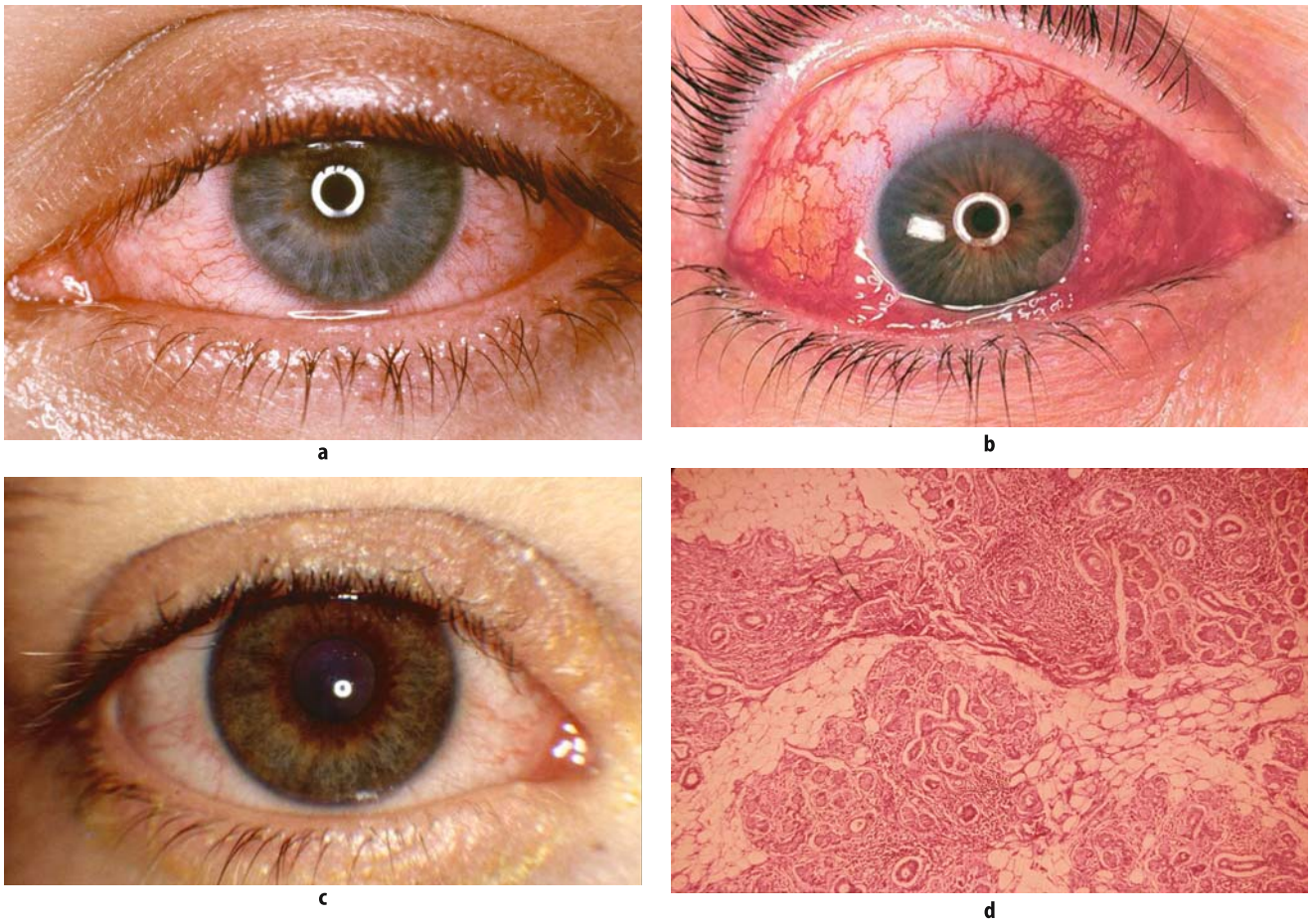

**Figure 23.1.** Dry eye. Typically, patients complain of sandy, gritty feeling, soreness and scratchiness. Other symptoms include heaviness of the lids, foreign body sensation, discomfort while blinking, stinging, and photophobia. Most prevalent are intolerance of longer watching of TV or working on computer, irritation worsening in air-conditioned spaces (cars, offices) and during colder season of the year. Also, there may be marked difference between the extent of symptoms and clinical signs, which point to dry eye. Dry eye does not have to be red, while patients may still have dry eye symptoms needing treatment. Clinical appearance of decompensated dry eye; the dry eyes are red and inflamed (a); advanced keratoconjunctivitis (b). Most frequent clinical appearance of dry eye: no or minimal redness (c). A lachrymal gland biopsy showing typical lymphocytic infiltration in a patient with Sjögren syndrome (d).

**Figure 23.2.** Primary test for tear film dysfunction is TBUT (tear break-up time) test, as tear film instability, together with hyperosmolality, are two signs common to all forms of dry eye. If TBUT is lower than 10 s, tear film is considered unstable. TBUT: tear film stained by sodium fluorescein breaks up (a). If the tear film is established to be unstable by TBUT, Schirmer test is performed. In case of values lower than 10 mm of wetted paper in 5 min, diagnosis of hyposecretory dry eye is established. Schirmer test values above 10 mm/5 min indicate tear hyperevaporation as the cause of dry eye. (b)

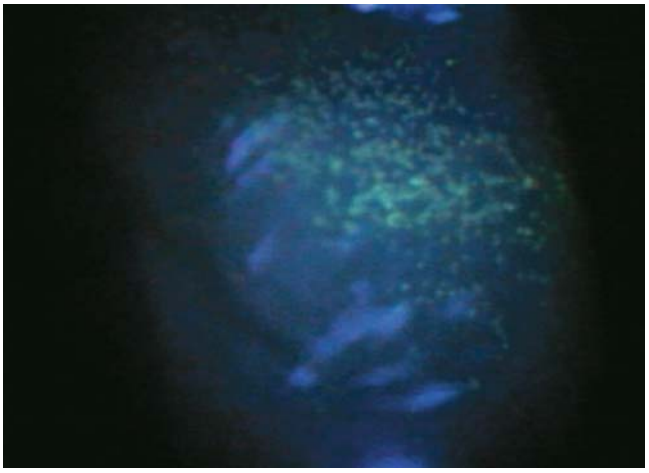

c

**Figure 23.2c.** Cornea stained by sodium fluorescein: in dry eye staining is typically located in lower (more exposed) portions of cornea.

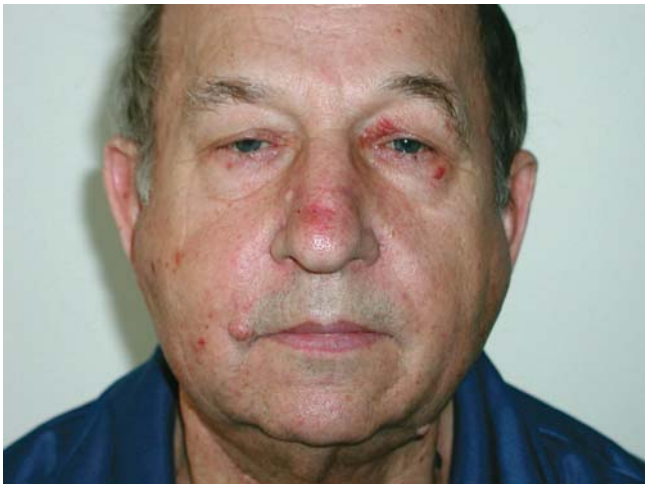

**Figure 23.3.** Dry mouth can present without or with parotid glands enlargement; in this patient the parotids are enlarged and hardened. The characteristic skin teleangiectasis are also seen.

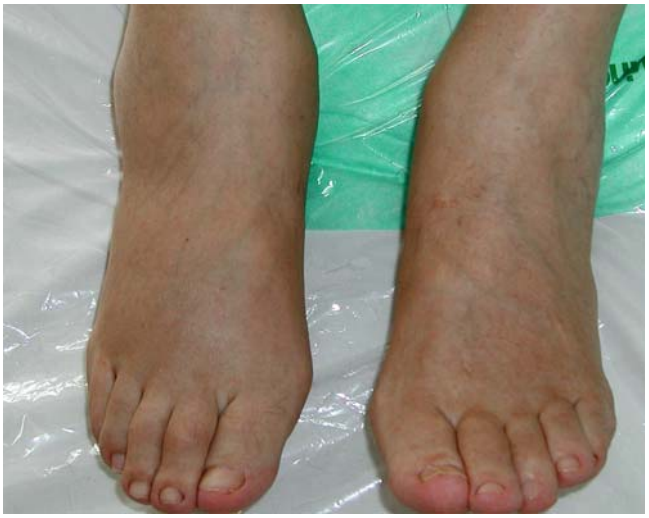

**Figure 23.4.** Painful and inflamed joints are frequent complaints in patients with Sjögren syndrome; the ankles are painful and swollen.

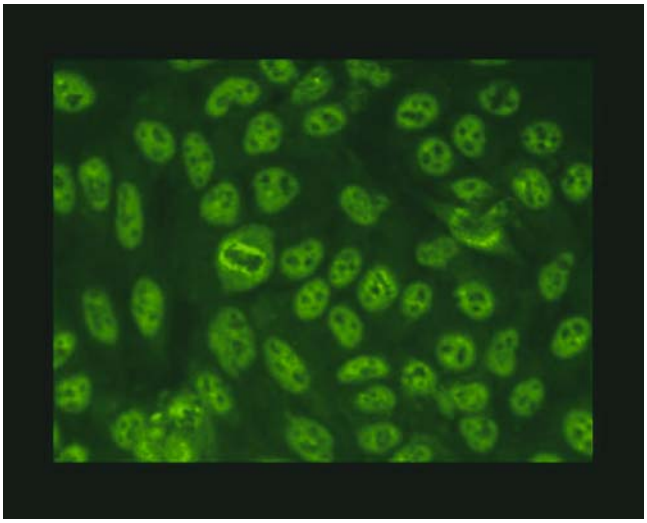

**Figure 23.5.** Antibodies directed against SS-A and SS-B. Coarse to fine speckles in interphase cells (Hep-2 cells; Euroimmun, Lubeck, Germany; objective ×40).

**Table 23.1.** Pleuropulmonary manifestations of Sjögren syndrome (SS).

| Sjögren Syndrome | Frequency |
|---|---|
| Parenchymal disease | |
| Lymphoid interstial pneumonia | +++ |
| Nonspecific interstitial pneumonia | + |
| Bronchiolitis obliterans organizing pneumonia | + |
| Usual interstitial pneumonia | ± |
| Amyloidosis | + |
| Recurrent bronchopneumonia | ++ |
| Airway disease | |
| Atrophic rhinitis | ++ |
| Xerostomia, xerotrachea | +++ |
| Chronic bronchitis | ++ |
| Bronchiolitis | ++ |
| Bronchiectasis | + |
| Pleural disease | |
| Pleural disease | ± |
| Pulmonary vascular disease | |
| Pulmonary hypertension | ± |

+++, common; ++, fairly frequent; +, occasional; ±, rare.

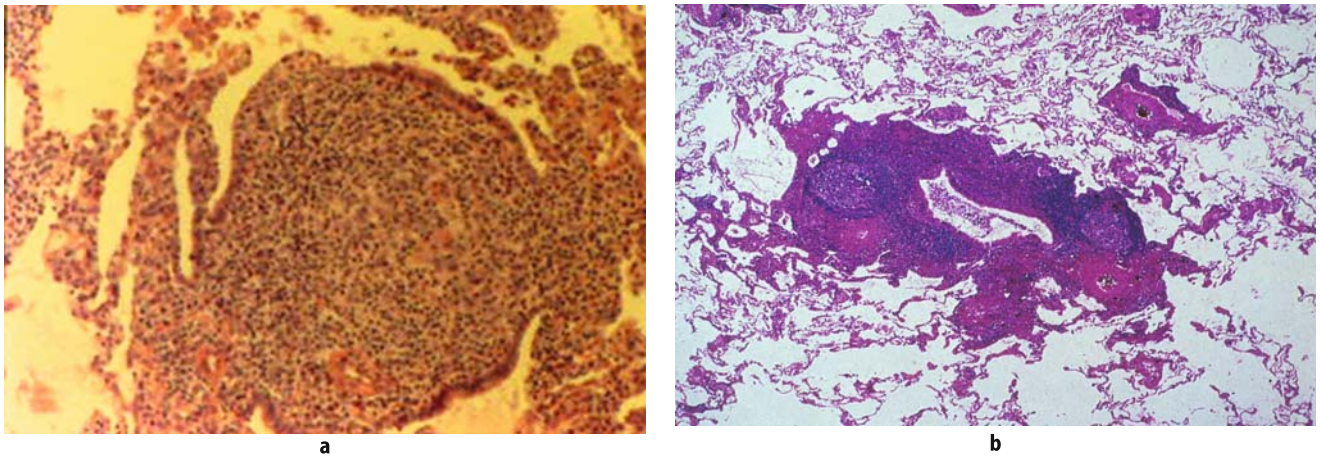

a b

**Figure 23.6.** Histopathological finding of the lung biopsy in a patient with SS and ILD shows lymphocytic interstitial pneumonia; malignant alteration can proceed so if there is a slightest possibility of such event, the transtracheal or open lung biopsy is advised. Marked lymphoid aggregates in the bronchial wall are seen (a). A lung biopsy sometimes shows bronchiolitis, as well as numerous lymphocytes (b).

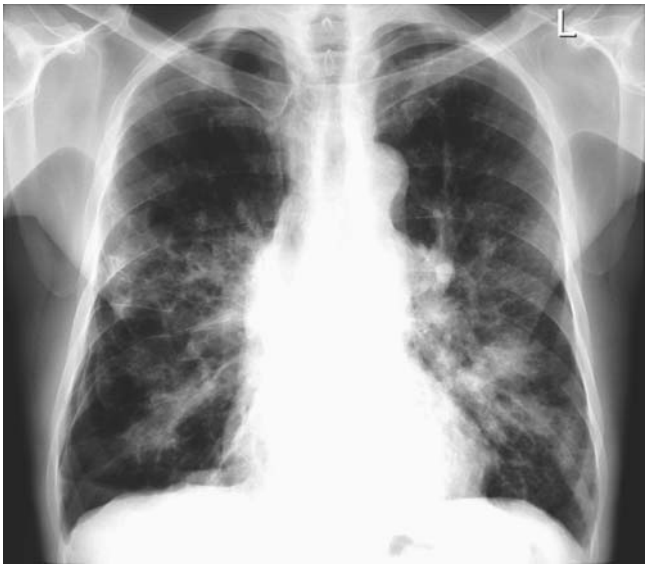

**Figure 23.7.** Chest radiograph in a patient with SS shows linear and reticular pattern, superimposed with patchy alveolar opacities, predominantly in the lower half of the lung. Right pneumothorax as a complication of transbronchial biopsy procedure is seen.

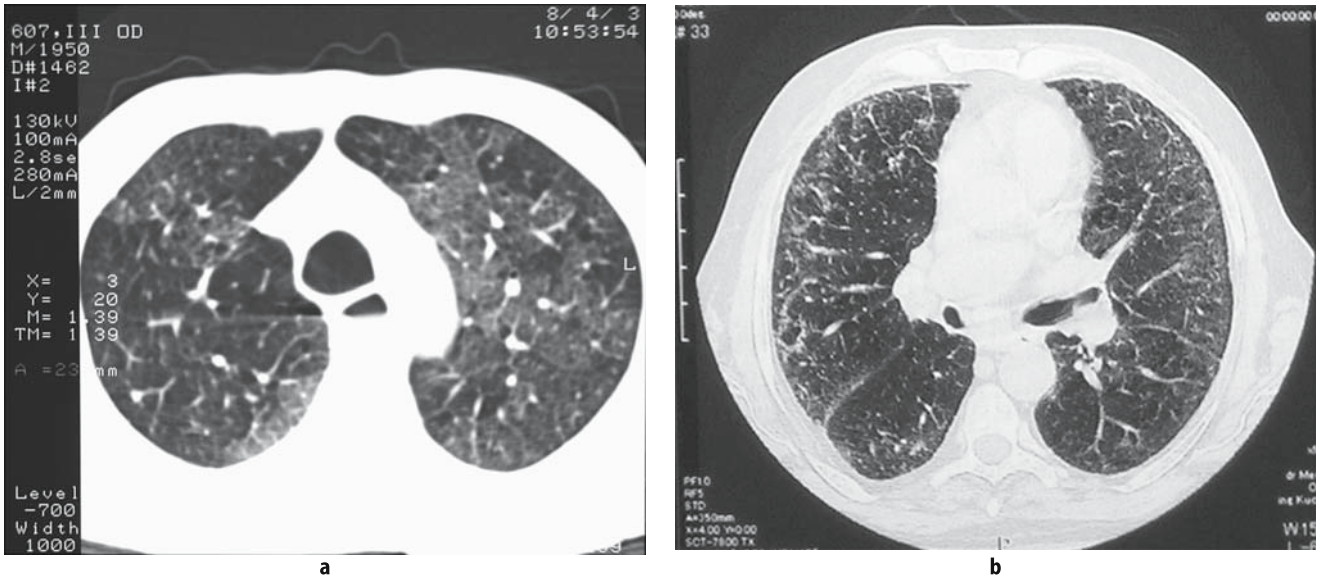


a b

**Figure 23.8.** HRCT scan shows ground-glass pattern and thickening of the interalveolar septa in geographical distribution (a). Another case of SS showing peripheral intralobular and interlobular thickening with peripheral peribronchovascular micronoduli (b).

## Bibliography

1. Fox RI. Sjögren's syndrome. Lancet 2005;366:321–331.
2. Matsuyama N, Ashizawa K, Okimoto T, Kadota J, Amano H, Hayashi K. Pulmonary lesions associated with Sjögren's syndrome: Radiographic and CT findings. Br J Radiol 2003;76(912):880–884.
3. Kassan SS, Thomas TL, Moutsopoulos HM, Hoover R, Kimberly RP, Budman DR, Costa J, Decker JL, Chused TM. Increased risk of lymphoma in sicca syndrom. Ann Intern Med 1978;89:888–892.
4. Hansen A, Lipsky PE, Dorner T. Immunopathogenesis of primary Sjogren's syndrome: Implications for disease management and therapy. Curr Opin Rheumatol 2005;17:558–565.

# 24

# Wegener Granulomatosis

Wegener granulomatosis (WG) is the most common pulmonary idiopathic vasculitis. Pulmonary idiopathic vasculitides are a group of rare diseases. Most of them are linked to the presence of anti-neutrophil cytoplasmic autoantibodies (ANCAs) (Table 24.1), less frequently to the presence of anti-glomerular and/or pulmonary basal membrane (anti-GMB) antibodies. It is a great challenge to diagnose these diseases and differentiate them from other diseases, infections, adverse drug reactions, and several other entities. It is of utmost importance to make timely confirmation of the diagnosis because it is necessary to institute the therapy as soon as possible in order to prevent the lethal outcome due to fatal pulmonary hemorrhage or acute renal failure. The connoisseurship of the clinical features and differential diagnosis as well as rapid screening tests for ANCAs and anti-GMB antibodies are of extreme importance.

Wegener granulomatosis is a systemic disease of uncertain cause. It usually begins as a localized granulomatous inflammation of upper or lower respiratory tract and may progress into generalized necrotizing granulomatous vasculitis and glomerulonephritis.

The annual incidence is 10–15 cases per million adult population. The peak incidence is in the fourth through sixth decades, and there is no gender preponderance.

*Clinical features* of Wegener granulomatosis are diverse. It is disease with a biphasic course; in one third of patients the initial phase with few complaints lasts for years and it may suddenly progress into generalized, disseminated form (Table 24.2).

Initially, patients most frequently complain of fatigue, fever, arthralgias, weight loss, symptoms of the upper respiratory tract like epistaxis, nasal crusting, sinus pain, ulcerations of the mucous membranes, deafness, and earache (Figures 24.1, 24.2a, b, and 24.3a, b, c). Destruction of the nasal cartilage can lead to saddlenose deformity and retroorbital masses to proptosis (Figure 24.4). The lower respiratory tract is almost always involved, most frequently the lung parenchyma. The symptoms are hemoptysis, cough, chest pain, and dyspnea. The subglottic inflammation can lead to stenosis and airway obstruction; the symptoms are dyspnea, cough, and stridor (Figure 24.5a, b). Kidneys are involved almost in all cases, usually late in the course of the disease. Skin (Figure 24.6), joints, central nervous system, and heart are often involved also late in the course of the disease.

*The cause* of WG is unknown, but the pathological features suggest an exaggerated cellular immune or hypersensitivity response. Predominant upper and lower respiratory tract affection suggests that inhalation antigens may play a role. The infiltrate in WG mainly consists of neutrophils, monocytes, and T lymphocytes suggesting that both cell-mediated and neutrophil-mediated immune mechanisms are active. At the onset, the injury is possibly mediated by neutrophils but the vasculitic phase most probably by mononuclear phagocytes and lymphocytes. The granuloma in WG is mediated by $CD4^+$ T cells. Circulating c-ANCAs suggests a role of neutrophils and these autoantibodies in the pathogenesis and evolution of WG. Chronic suppurative disease of the respiratory tract (upper and lower) may provide an antigenic source leading to an aggravated immune response mediated by c-ANCAs. Infection may also amplify the inflammation in WG; frequent relapses are observed in chronic nasal carriers of *Staphylococcus aureus*.

**Table 24.1.** Frequency of lung involvement in various vasculitides and frequency of ANCA positivity.

| | Lung Involvement | ANCA % Positive |
|---|---|---|
| Wegener granulomatosis | Common | c-ANCA >> p-ANCA 80–90% |
| Microscopic polyangiitis | Common | p-ANCA > c-ANCA 80% |
| Churg-Strauss syndrome | Common | p-ANCA > c-ANCA 30–50% |
| Goodpasture syndrome | Common | p-ANCA 10% |
| Takayasu arteritis | Common | Negative |
| Diffuse connective tissue disease | Common | Negative |
| Necrotizing sarcoid granuloma | Common | Negative |
| Isolated pulmonary pauci-immune capillaritis | Common | p-ANCA |
| Behçet disease | Occasional | Negative |
| Gigantocellular arteritis | Rare | Negative |
| Polyarteritis nodosa | Rare | p-ANCA Rarely positive |
| Kawasaki disease | Rare | Negative |
| Cryoglobulinemic vasculitis | Rare | Negative |

**Table 24.2.** The involvement of different organs at the onset and during the course of Wegener granulomatosis (WG).

| | Frequency at the Onset of WG (%) | Frequency During the Course of WG (%) |
|---|---|---|
| Upper respiratory tract | 73 | 92 |
| Lower respiratory tract | 48 | 90 |
| Trachea | | 30 |
| Lung | | 90 |
| Kidneys | 17 | 85 |
| Joints | 32 | 67 |
| Eyes | 14 | 50 |
| Skin | 13 | 46 |
| Central or peripheral nervous system | 4 | 40 |
| Cardiac | ? | 15 |
| Gastrointestinal | 4 | 10 |

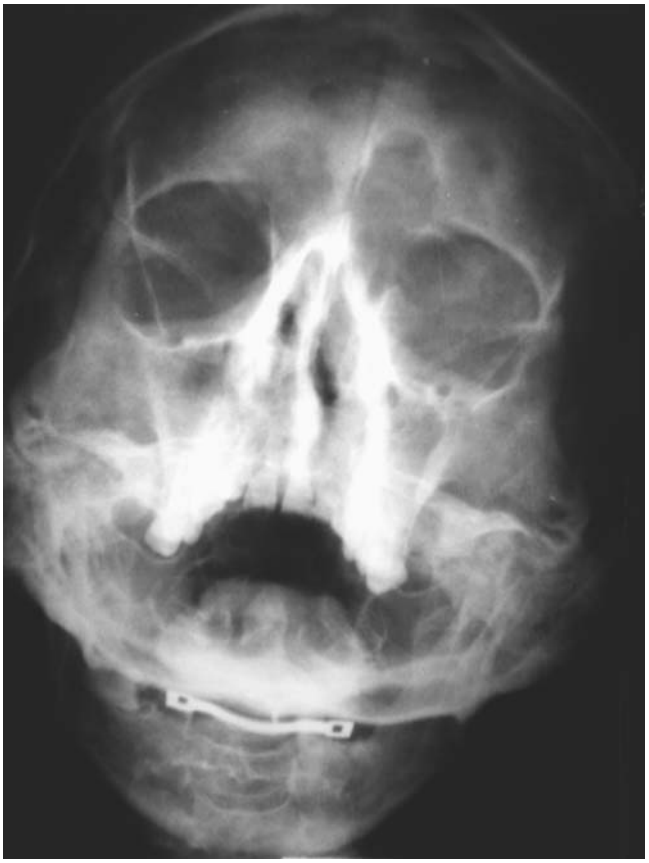

**Figure 24.1.** Plain radiograph of sinuses shows shadowing of the maxillary cavities, nasal passages, and frontal sinuses. Continuous infiltration from left frontal sinus to the left orbit, with the destruction of the bone orbital structures is seen.

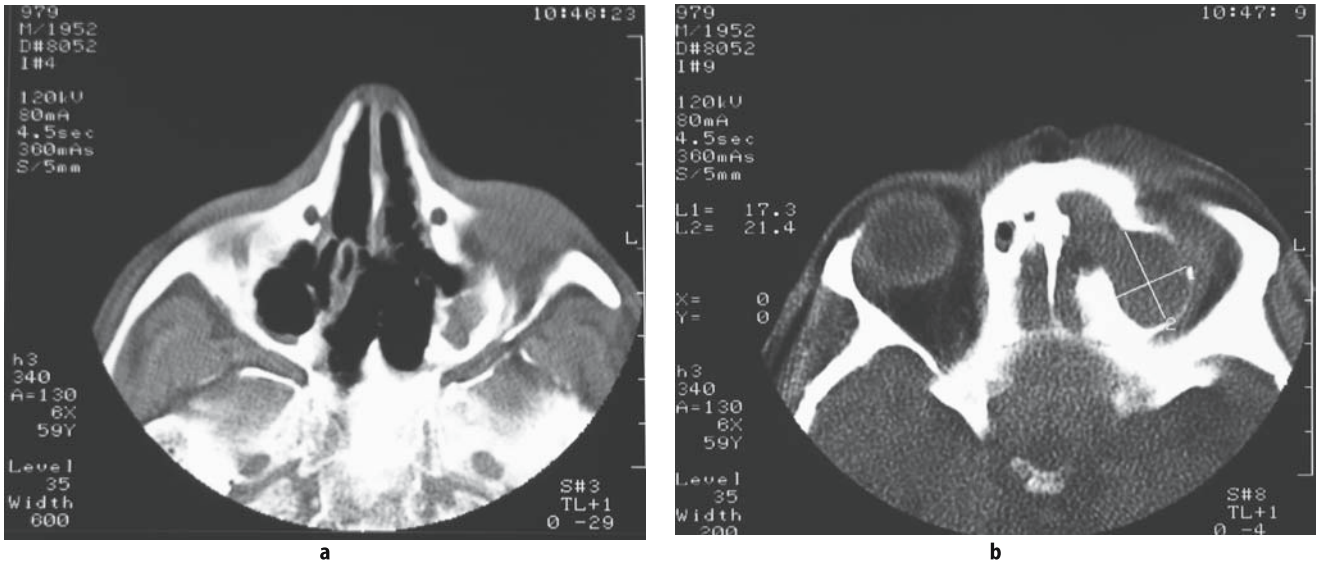


a b

**Figure 24.2.** Transversal section of CT of the orbit shows shadowing of the maxillary sinuses with inflammatory masses spreading from left maxillary sinus to the nasal passage (a) and frontal sinus filled with inflammatory masses; from the left sinus the masses spread into left orbit destroying the bone (b).

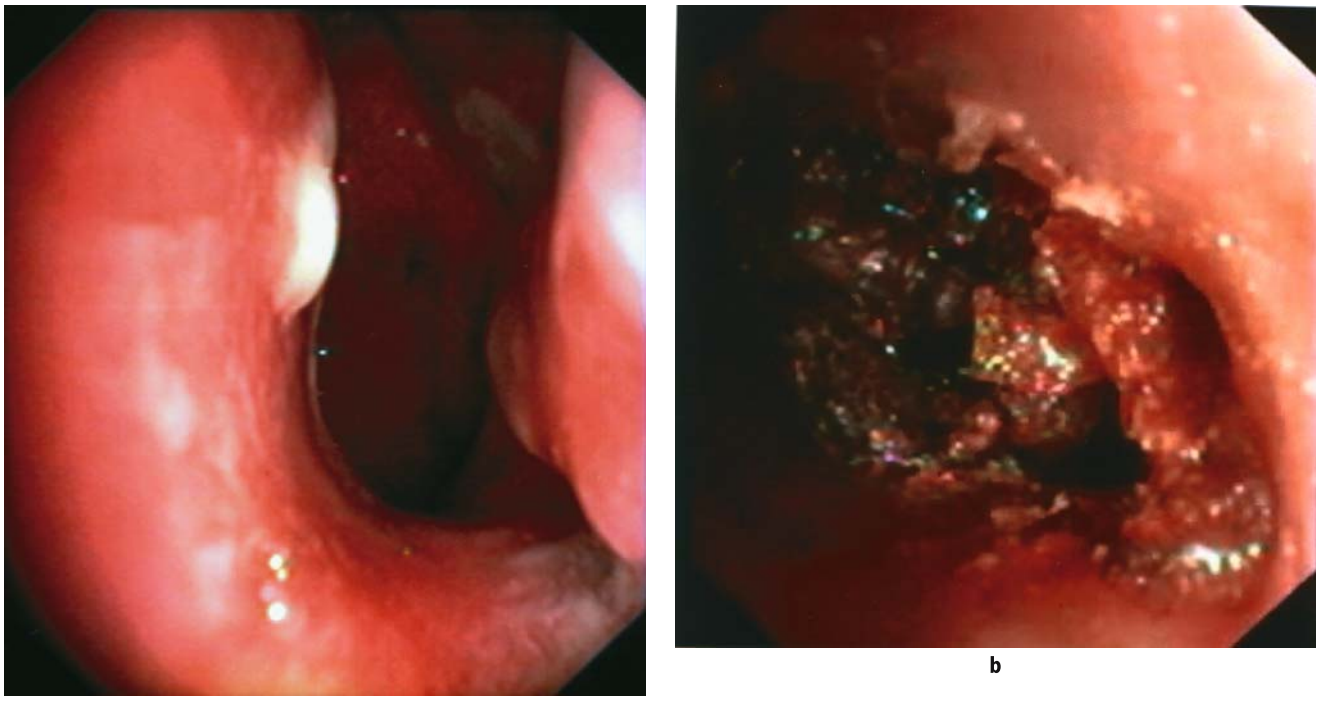

a b

**Figure 24.3.** Bronchoscopic finding in upper respiratory tract WG; granuloma in the middle nasal passage (a), necrosis and destruction of the nasal turbinate cartilage before the treatment (b), and 2 months following the introduction of cyclophoshamide (c).

(continued)

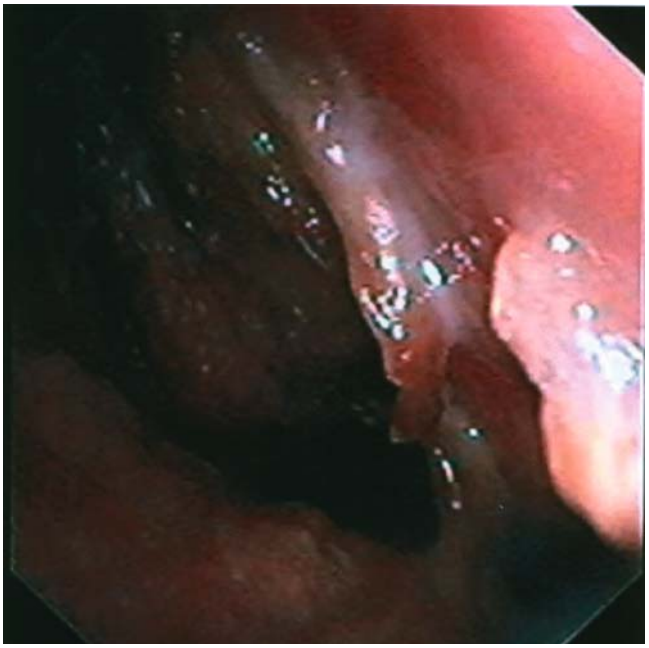

c

**Figure 24.3.** (continued)

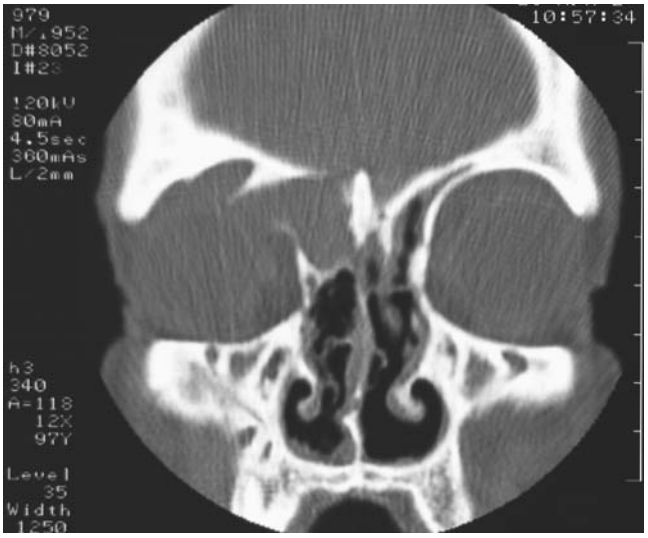


**Figure 24.4.** Coronary section of CT showing orbital granuloma suspected to penetrate intracranially. The orbital masses cause proptosis.

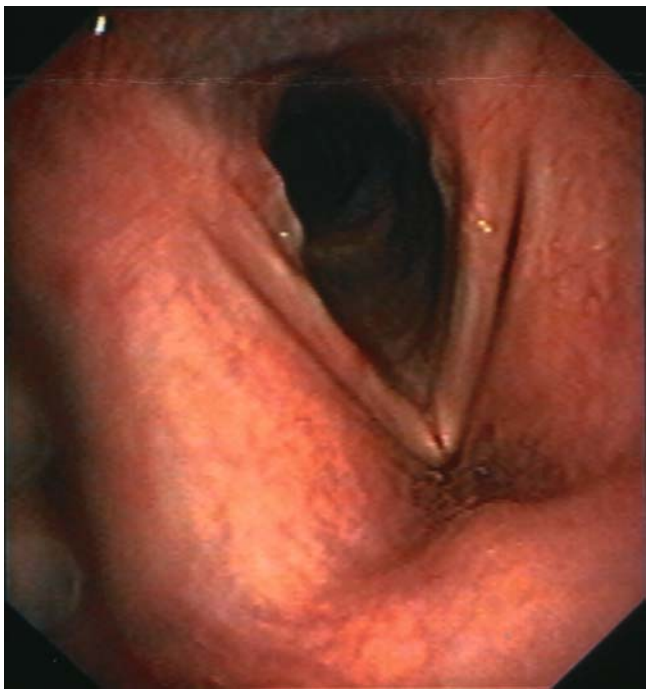

a

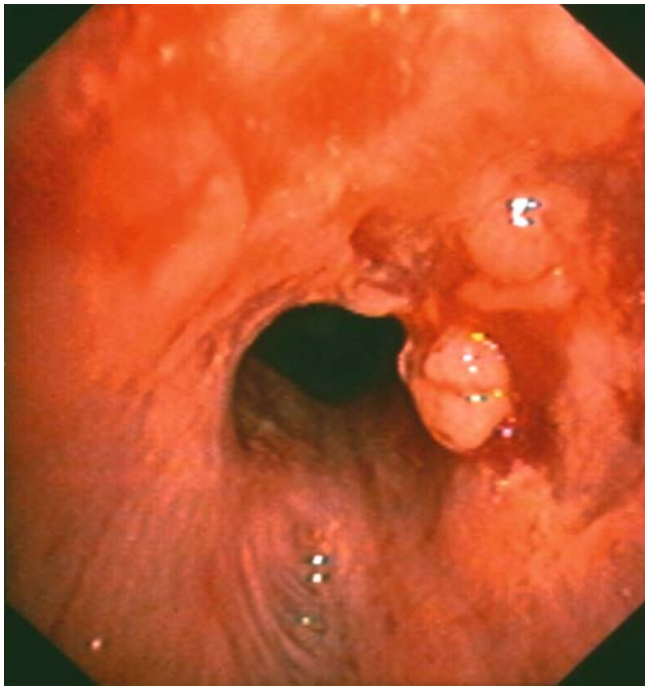

b

**Figure 24.5.** Bronchoscopic finding in WG of the tracheobronchial tree. Bilateral subglotic granuloma (a) and necrotic granuloma in the main bronchus (b).

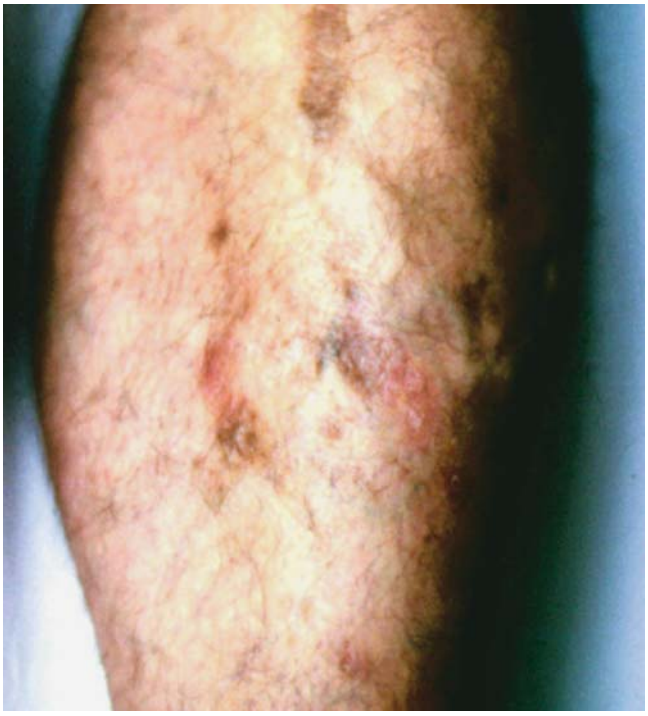

**Figure 24.6.** Characteristic skin changes in a patient with WG show intracutaneous nodules and skin defects. The skin defects are the result of the healing processes following the exulceration of nodules.

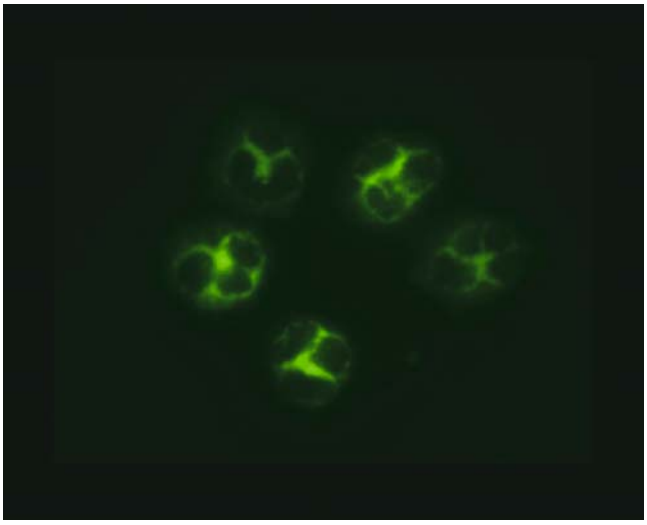

**Figure 24.7.** Antibodies directed against proteinase 3 (PR3-ANCA). Cytoplasmic c-ANCA: a coarse granular fluorescence present throughout the cytoplasm and with accentuation between nuclear lobes (on home made ethanol fixed human neutrophils, objective ×40).

*Diagnosis* rests upon characteristic clinicaI features, radiological and histopathological findings, and in most cases proof of serum anti-neutrophil cytoplasmic antibodies.

Serum c-ANCAs are a sensitive and specific marker for WG. c-ANCAs can be detected in 70% of all the cases and in almost 90% of disseminated forms of the disease (Figure 24.7). In active disease, elevated erythrocyte sedimentation rate, C-reactive protein, anemia, and thrombocytosis are detected. Urinary tests reveal erythrocituria and proteinuria. In advanced cases, the serum laboratory tests of kidney function are deranged showing renal insufficiency. Characteristic chest radiological findings are nodular infiltrates, which often cavitate (Figures 24.8a, b, c, d and 24.9). Pleural effusion, endobronchial process with atelectasis, bronchopulmonary fistula, calcification, and hilar lymphadenopathy are sometimes described. Diffuse alveolar opacities indicate diffuse alveolar hemorrhage. Diffuse alveolar hemorrhage (DAH) in WG has a grave prognosis, and it has to be confirmed and treated immediately.

Lung function tests should be a part of initial evaluation. Diffusion capacity is usually reduced, but in DAH it could be increased. Flow-volume loops are helpful to detect subglottic, tracheal, or endobronchial stenosis.

The diagnosis of WG is confirmed by histological sample analysis. The biopsy sites are lungs, upper respiratory tract, kidneys, skin, or any other organ involved. The bronchoscopy is not only useful in establishing the diagnosis (biopsy of endoluminal upper and lower respiratory tract lesions, transbronchial biopsy) but also in ruling out alveolar hemorrhage and infection. Open lung biopsy has the highest diagnostic yield but should be performed only if more accessible biopsy sites are not available. Bronchoalveolar lavage analysis shows neutrophilic alveolitis, sometimes lymphocytes. It is useful in confirmation of DAH and infection.

The hallmark of histopathological findings are necrotizing vasculitis affecting arterioles, venules, and capillaries, granulomatous inflammation, foci of necrosis (irregularly shaped "geographic"), microabscessses, and areas of fibrosis with acute and chronic inflammation (Figure 24.10a, b, c, d, e).

Disseminated, generalized disease should be *treated* with standard regimen for remission induction; that is, oral cyclophosphamide, $2\,mg\,kg^{-1}\ day^{-1}$ for 6 months and

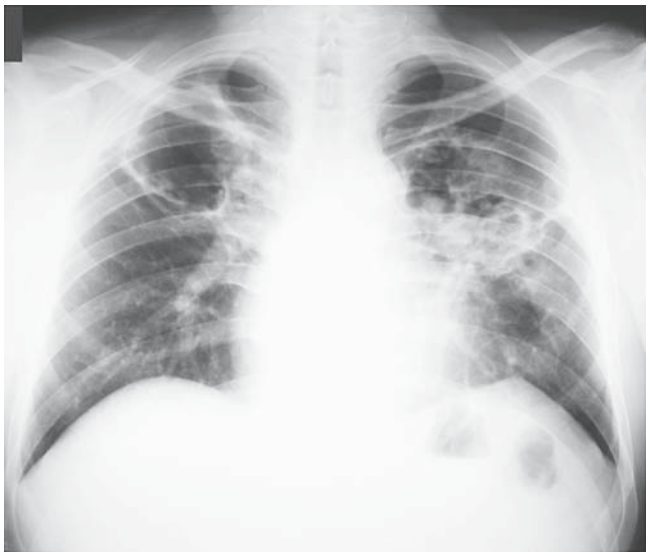

a

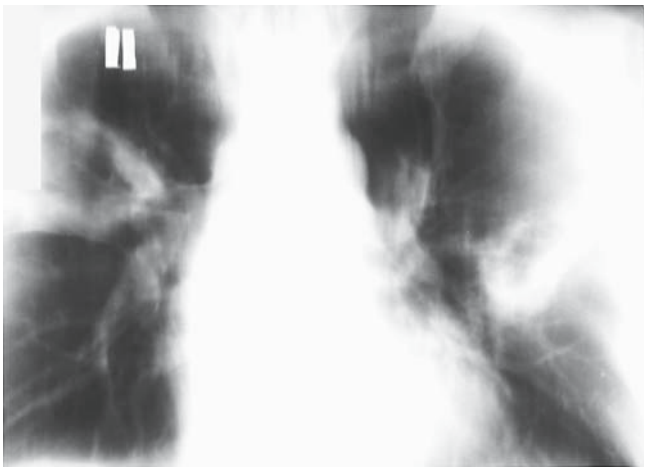

b

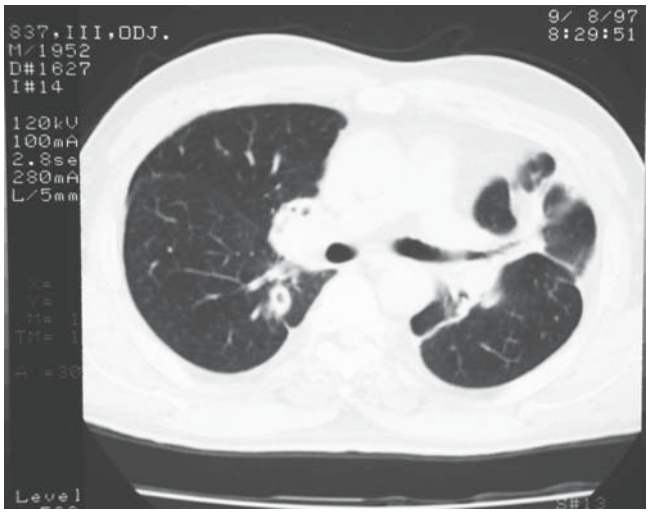


c

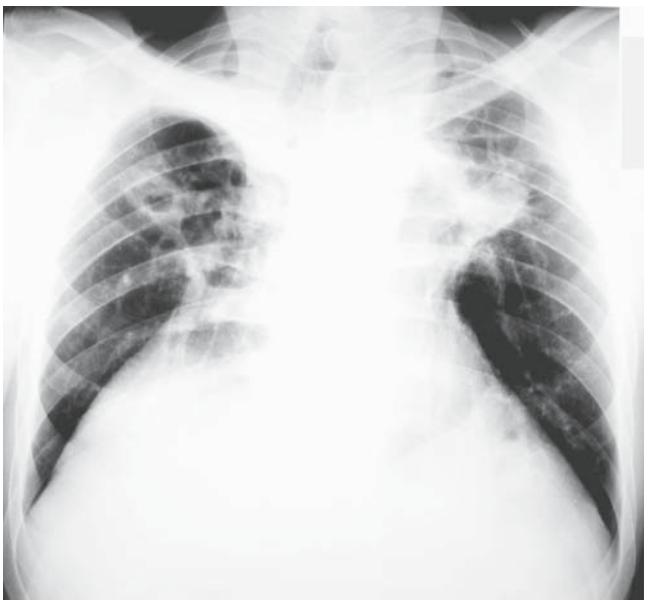

d

**Figure 24.8.** Characteristic chest radiograph (a), thin section (b), and CT scan (c) in a patient with WG all show giant macronodular infiltrates of different size, with destruction forming cavities. Control plain radiograph following the therapy with cyclophosphamide and corticosteroids, showing shrinking of the cavities and regression of the infiltrates (d). The patient lived for 12 years and died due to renal insufficiency. The enclosed CT scans of the sinuses, nose, and orbit belong to the same patient.

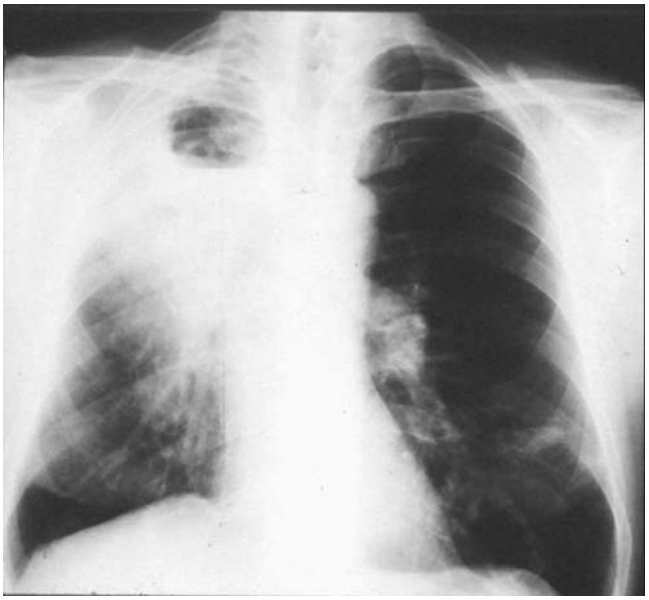

**Figure 24.9.** Fatal outcome of the patient with WG. Lobar infiltration with giant destruction and *niveau* in the right upper lobe is shown on plain radiograph of the chest. The patient was admitted to the hospital because of fever, cough, and hemoptysis. The diagnosis was not confirmed and he underwent the operative procedure. He died soon due to severe lung and pleural suppurative process.

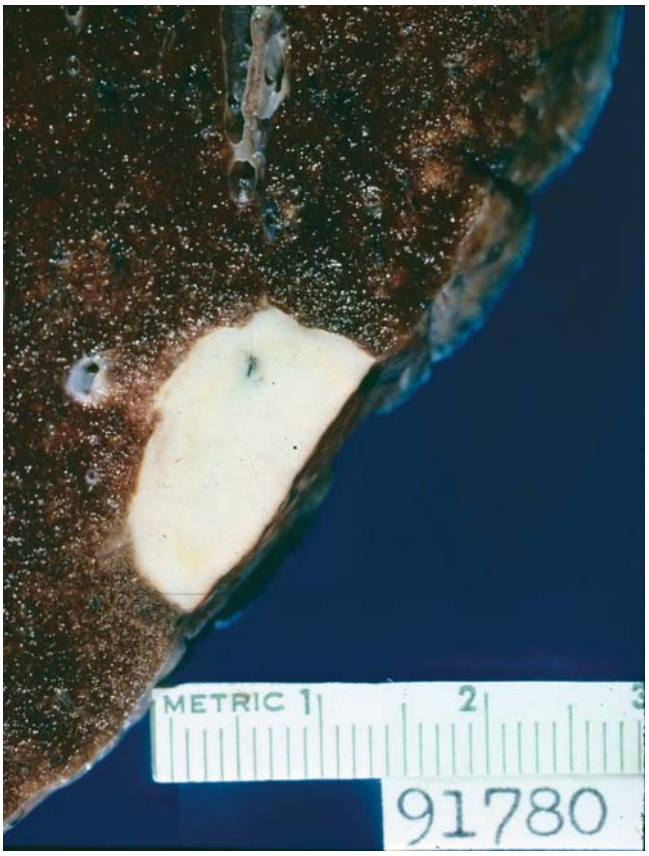


a

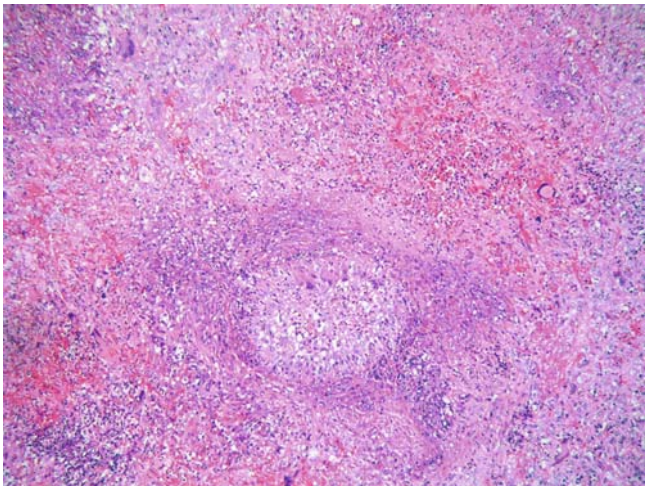

b

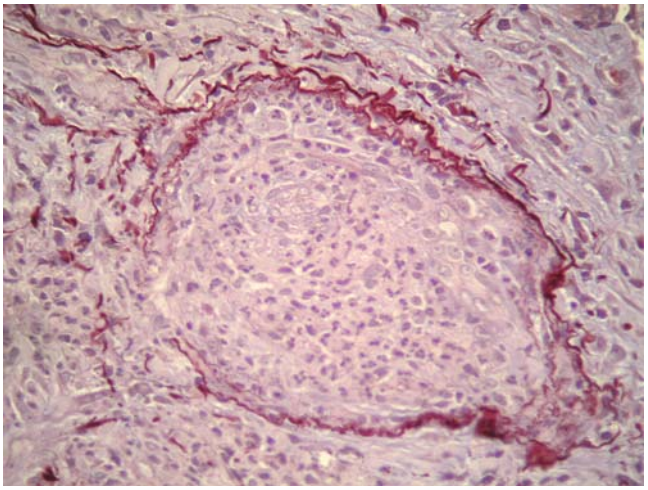

c

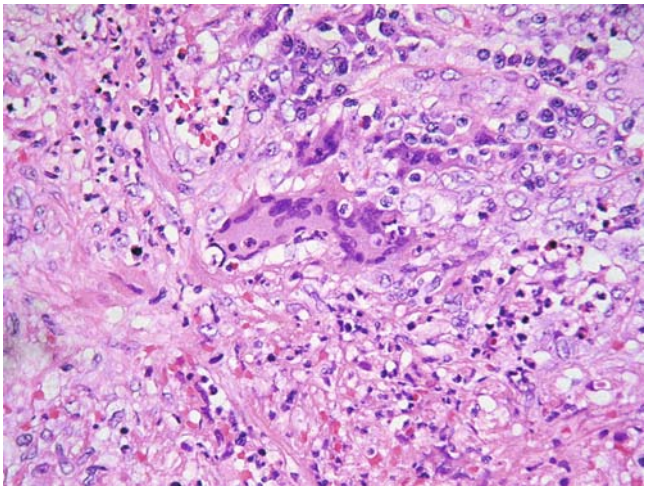

d

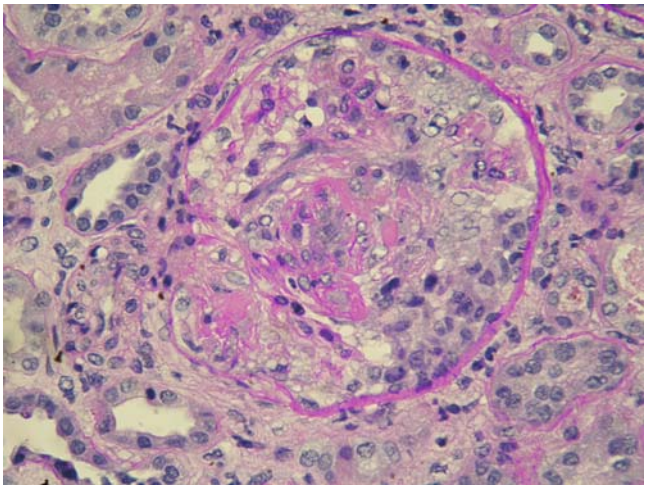

e

**Figure 24.10.** Characteristic histopathological finding in WG is necrosis, vasculitis of medium and small vessels (capillaries, venules, arteriolas, and arteries), and vague granuloma. Gross specimen of the lung showing a nodule in a patient with Wegener granulomatosis (a). Medium-sized artery with vasculitis and necrosis of vessel wall (b). Transmural inflammatory chronic infiltrate has severely fragmented the inner and outer layers of elastic lamina of the small artery and completely occluded the lumen (elastic stain) (c). The inflammatory infiltrate consists of mononuclear cells, granulocytes, and multinucleated giant cells (d). Glomerulus from a patient with Wegener granulomatosis shows segmental thrombosis and fibrinoid necrosis with large cellular crescent (PAS; ×400) (e).

prednisone 1 mg $kg^{-1}$ $day^{-1}$ for 3 months. When remission is achieved, maintenance therapy should consist of less toxic agents, methotrexate or azathioprine. In limited disease, methotrexate, target dose of 25 mg once a day, and corticosteroids are used for remission induction. The use of *trimethoprim/sulfamethoxazole* is efficient in limited disease. Aggressive, combined immunosuppressive therapy has altered the prognosis of WG, which once was a disease with high mortality.

## Bibliography

1. Seo P, Stone JH. The cytoplasmic antibody-associated vasculitides. Am J Med 2004;117:39–50.
2. Radica A, Sinico RA. Antineutrophil cytoplasmic antibodies (ANCA). Autoimmunity 2005;38:93–103.
3. Lynch JP, White E, Tazelaar H, Langfors C. Wegener's granulomatosis: Evolving concepts in treatment. Sem Resp Crit Care Med 2004;25:491–522.
4. Keogh K, Specks U. Pulmonary vasculitis. In: Baughman RP, du Bois R, Lynch JP, Wells AU, Eds. Diffuse Lung Disease. A Practical Approach. London: Arnold; 2004:184–202.
5. Goek ON, Stone JH. Randomized controled trials in vasculitis associated with anti-neutrophil cytoplasmic vasculitis. Curr Opin Rheum 2005;17:257–264.

# 25

# Microscopic Polyangiitis

Microscopic polyangiitis (MPA) is a systemic necrotizing vasculitis affecting small- and medium-sized vessels (capillaries, venules, and arterioles) associated with necrotizing glomerulonephritis and pulmonary capillaritis. Granulomas are not a feature of MP.

The annual incidence is 8 cases per million population. The peak incidence is in the fifth and sixth decades, and there is no gender preponderance. As in Wegener granulomatosis, necrotizing glomerulonephritis is very common and it occurs in majority of patients (79%) (Figure 25.1a) (Table 25.1). Pulmonary capillaritis with consecutive alveolar hemorrhage is the *clinical feature* in 30% of cases with MP (Figure 25.1b). The symptoms are hemoptysis and breathlessness. Frequently, patients complain of fever and weight loss. Around 30% of patients suffer from gastrointestinal symptoms such as abdominal pain, diarrhea, and bleeding, as opposed to Wegener granulomatosis in which these complaints are rare. The skin symptoms, such as purpuric rash (Figure 25.2), nail bed infarct, and splinter hemorrhages may be seen in 30% of patients. Neurological involvement is seen in up to 30%, most frequently in the form of mononeuritis multiplex. Upper respiratory tract and eyes and ears involvement is much less frequent than in Wegener granulomatosis.

The *diagnosis* of MPA is based on characteristic clinical picture, positive assay for perinuclear antineutrophil cytoplasmic antibodies (p-ANCA) (MPO Myeloperoxidase-ANCA) (Figure 25.3) and biopsy analysis. p-ANCA (MPO-ANCA) is preferentially associated with microscopic polyangiitis (MPA) and is detected in around 80% of MPA cases, although it can be found in other vasculitides. It seems that ANCAs are involved directly in MPA pathogenesis.

Plain radiograph most often reveals diffuse alveolar opacities as the consequence of DAH (Figure 25.4a, b) but pleural effusion and pulmonary interstitial fibrosis may be seen.

The differentiation between Wegener granulomatosis (WG) and MPA is based on finding of granulomas in patients with WG. Granulomas are almost always found in lung biopsy specimens of patients with WG but seldom in other samples. As the kidney biopsy is most frequently performed, Wegener ganulomatosis may be overlooked and thus the assessed prevalence of MPA overestimated.

The *therapy* of MPA does not differ from that of WG; most frequently the combination of corticosteroids and cyclophosphamide is used. Remission is achieved in 75% of patients.

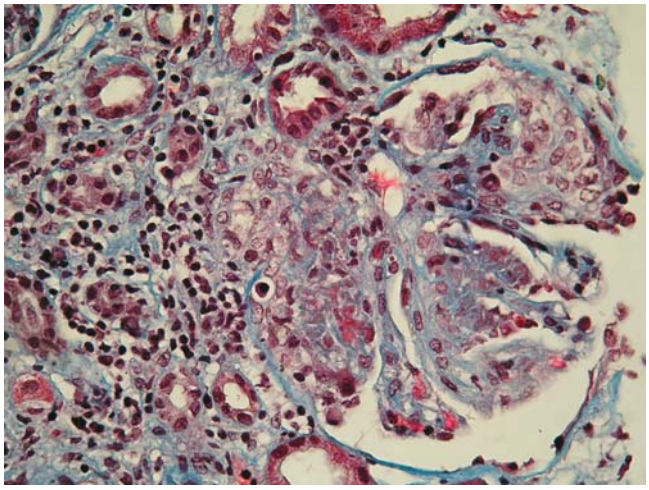

a

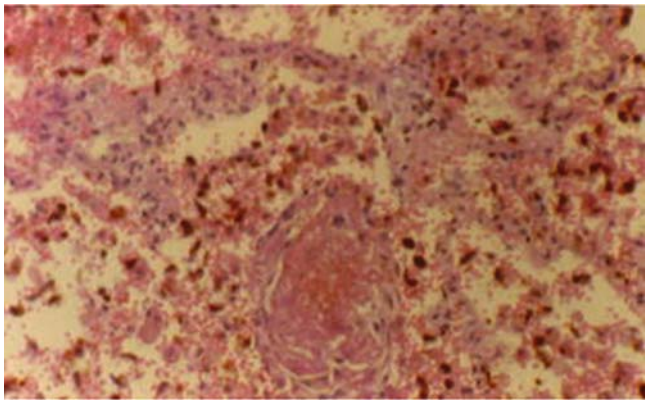

b

**Figure 25.1.** Glomerulus from a patient with microscopic polyangiitis shows an area of segmental fibrinoid necrosis with adjacent crescent formation. There is interstitial cellular infiltrate and tubular atrophy (Masson's trichrome stain; ×400) (a) and the lung biopsy in the same patient shows intra-alveolar bleeding (b).

**Table 25.1.** Differential diagnosis of pulmo-renal syndromes.

| |
|---|
| Vasculitides |
| Wegener granulomatosis |
| Microscopic polyangiitis |
| Churg-Strauss syndrome |
| Takayasu arteritis |
| Behçet disease |
| Anti-GBM disease |
| Vasculitis in diffuse connective tissue disease |
| Systemic lupus erythematosus |
| Systemic sclerosis |
| Anti-phospholipid syndrome |
| Rheumatoid arthritis |
| Drugs and poisons |
| Penicillamine |
| Hydralazine |
| Paraquat |
| Other causes of renal failure and DAH |
| Pulmonary edema with acute renal failure |
| Severe pneumonia (*Legionella* spp.) |
| Infections (hemorrhagic fever) |
| Thrombosis of renal veins and pulmonary emboli |

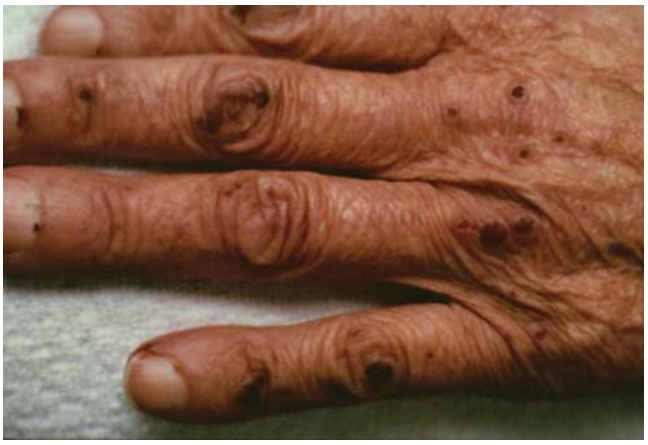

**Figure 25.2.** Vasculitic skin rash (bleeding beneath the skin that does not disappear following the pressure) and some crusts in a patient with microscopic polyangiitis. The lesions were scattered over the face, upper and lower extremities.

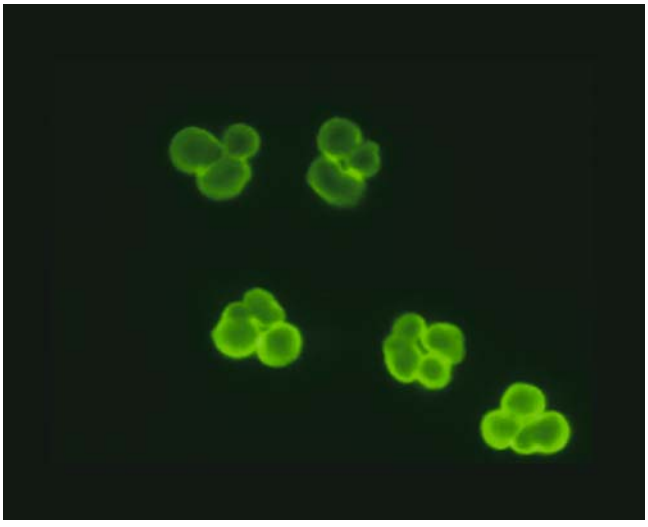

**Figure 25.3.** Antibodies directed against myeloperoxidase (MPO-ANCA). Perinuclear-pANCA: a typical perinuclear fluorescence with some nuclear extension (on home-made ethanol-fixed human neutrophils, objective ×40).

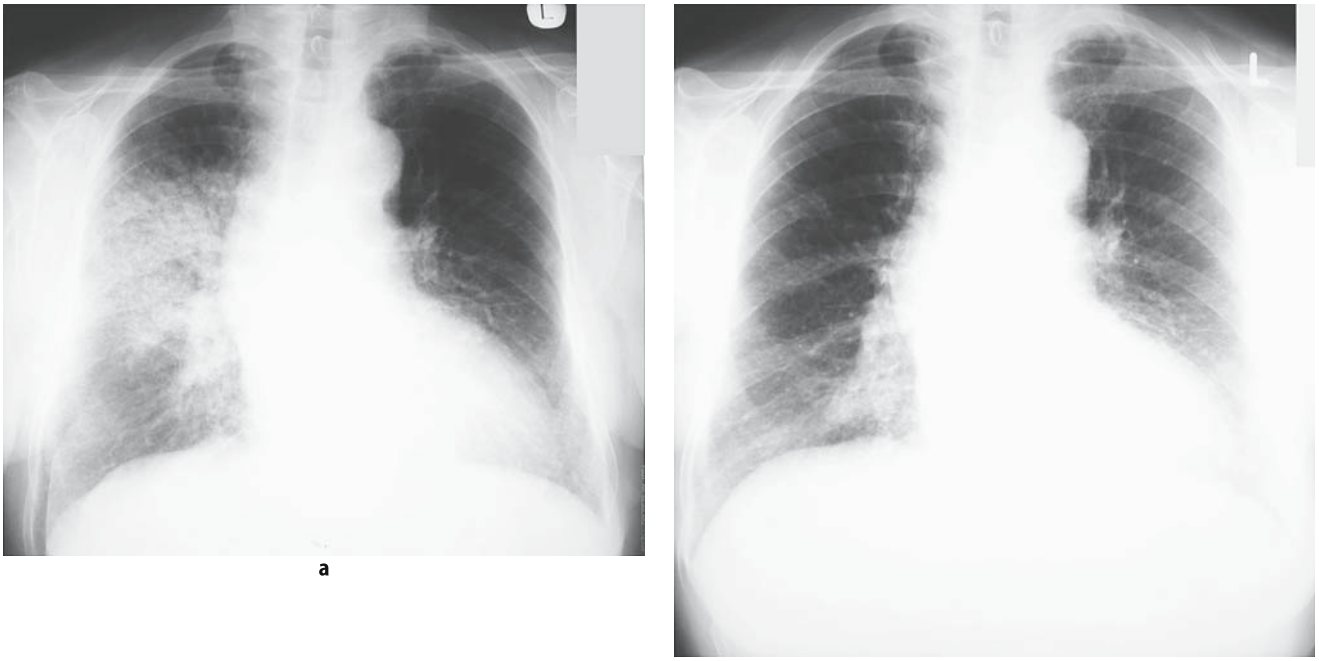

a b

**Figure 25.4.** Plain chest radiograph of a 63-year-old female patient presenting with hemoptysis due to microscopic polyangiitis shows alveolar pattern due to diffuse alveolar hemorrhage (a). The control radiograph taken 7 days following the institution of cyclophosphamide and corticosteroid therapy reveals significant clearing of the infiltrate (b).

## Bibliography


1. Guellevin L, Durand-Gasselin B, Cevallos R, Gayraud M, Lhote F, Callard P, Amouroux J, Casassus P, Jarrouse B. Microscopic polyangiitis. Clinical and laboratory findings in eighty-five patients. Arthritis Rheum 1999;42:421–430.
2. Eschun GM, Mink SN, Sharma S. Pulmonary interstitial fibrosis as a presenting manifestation in perinuclear antineutrophilic cytoplasmic antibody microscopic polyangiitis. Chest 2003;123:297–301.
3. Smyth L, Gaskin G, Pusey CD. Microscopic polyangiitis. Sem Resp Crit Care Med 2004;25;523–533.
4. Collins CE, Quismorio FP. Pulmonary involvement in microscopic polyangiitis. Curr Opin Pulm Med 2005;11:447–451.

# 26

# Churg-Strauss Syndrome

Churg-Strauss syndrome (CSS) is a small-vessel systemic necrotizing vasculitis that commonly affects the lungs, with high prevalence of asthma and peripheral blood and tissue eosinophilia.

The annual incidence is 3.1 cases per million population. Mean age of time of diagnosis is around 50 years, with equal distribution among both sexes. The cause of CSS is not known, but it seems that several triggering factors may be implicated in the pathogenesis, like leukotriene-receptor antagonists, vaccination, and desensitization.

*Three distinct phases of CCS* have been described. Asthma, allergic rhinitis, nasal polyposis, and sinusitis are usually the first symptoms. In the second eosinophilic phase blood and tissue eosinophilia are present. The signs of vasculitis characterize the third phase. Each phase may last for years but it is not necessary that each patient experiences all the phases or that they occur in this order.

Apart from respiratory and general symptoms that are found in almost 100% of patients, the symptoms and signs of other organs are present. Mononeuritis multiplex is found in 70% of patients, skin involvement in 50%, and gastrointestinal involvement in 40%. Arthritis, arthralgias, myalgias, and renal involvement have all been described. The most serious prognosis has relatively common cardiac involvement because it represents cardinal cause of mortality of patients with CSS. The granulomatous eosinophilic myocarditis and coronary vasculitis cause coronary disease and heart failure. The eosinophilic pericardial effusion may be present.

*Diagnosis of CSS* is based on characteristic clinical features, hypereosinophilia (>10% eosinophils in peripheral blood), and histopathological confirmation of tissue eosinophilia or small-vessel necrotizing granulomatous vasculitis (Figure 26.1a, b; Table 26.1). Positive anti-neutrophil cytoplasmic antibodies that recognize myeloperoxidase (MPO-ANCA or p-ANCA) (Figure 26.2) are present in 30–50% of patients; negative assay does not rule out the diagnosis.

Plain chest radiograph shows bilateral, multiple, sometimes migratory alveolar infiltrates, which rarely cavitate, and HRCT scan shows ground-glass opacities and sometimes consolidation (Figure 26.3a, b, c, d). Most frequently eosinophilic infiltrates, seldom DAH, are the cause of radiologically detected opacifications.

Bronchoalveolar lung lavage reveals eosinophilic alveolitis (>25% of eosinophils in BAL) (Figure 26.4). Biopsy of the affected organ should be performed.

Corticosteroids are the mainstay of *therapy* but relapses frequently occur after the cessation of the drug. In patients with cardiac or neurological involvement, cyclophosphamide should be added, as in WG or MPA. After the introduction of corticosteroids into therapy, the prognosis of CSS has dramatically improved.

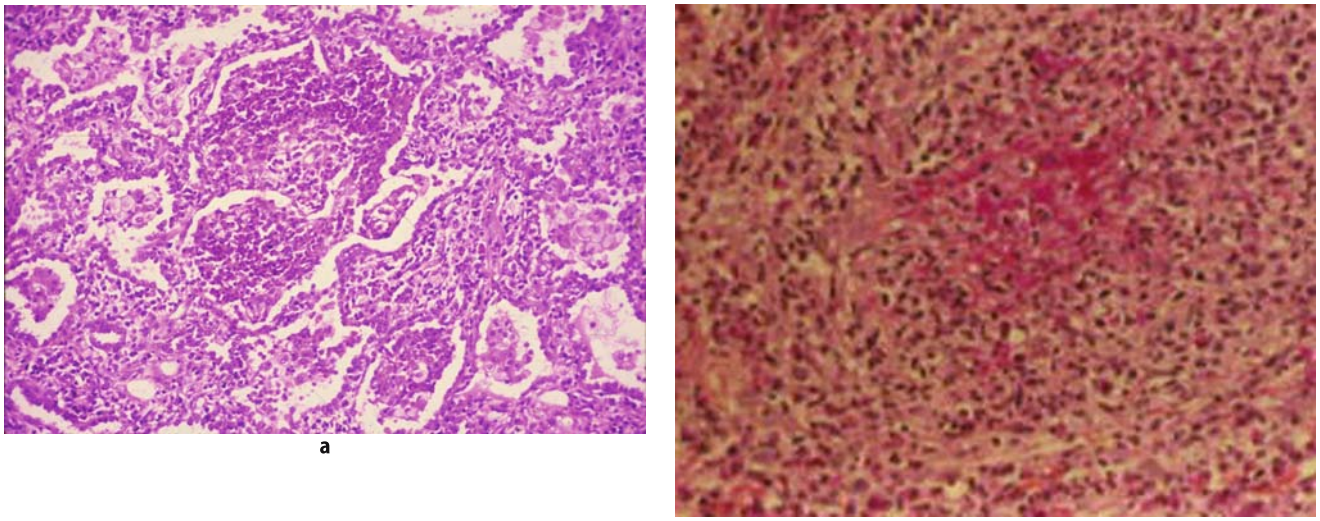

a b

**Figure 26.1.** A lung biopsy showing intense eosinophilic infiltrate filling the alveoli and occupying the interstitial spaces (a). Churg-Strauss cytoclastic vasculitis of small blood vesel in the dermis, with numerous eosinophils (b).

**Table 26.1.** American College of Rheumatology criteria for the classification of Churg-Strauss syndrome.

| Criterion | Definition |
|---|---|
| 1. Asthma | History of wheezing or diffuse, high-pitched rales on expiration |
| 2. Eosinophilia | Eosinophilia >10% of white blood cells differential count |
| 3. Mononeuropathy or polyneuropathy | Development of mononeuropathy, multiple mononeuropathies, or polyneuropathy (i.e., glove/stocking distribution) attributable to vasculitis |
| 4. Pulmonary infiltrates, nonfixed | Migratory or transition pulmonary infiltrated on radiographs (not including fixed infiltrates), attributable to systemic vasculitis |
| 5. Paranasal sinus abnormality | History of acute or chronic paranasal sinus pain or tenderness, or radiographic opacification of the paranasal sinuses |
| 6. Extravascular eosinophils | Biopsy including artery, arteriole, or venule, showing accumulation of eosinophils in extravascular areas |

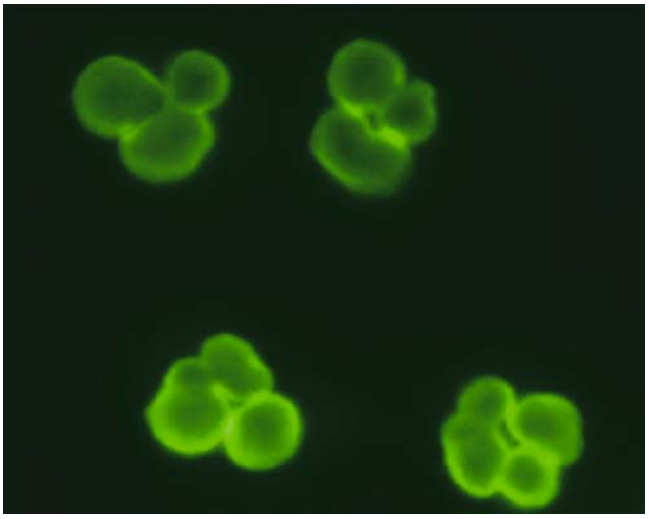

**Figure 26.2.** Antibodies directed against myeloperoxidase (MPO-ANCA) are found in 30–50% of patients with CSS. Perinuclear-pANCA: a typical perinuclear fluorescence with some nuclear extension (on home-made ethanol-fixed human neutrophils).

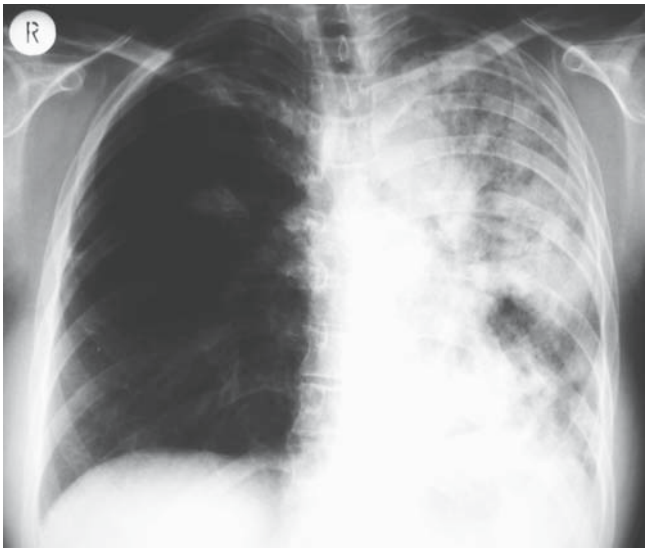


a

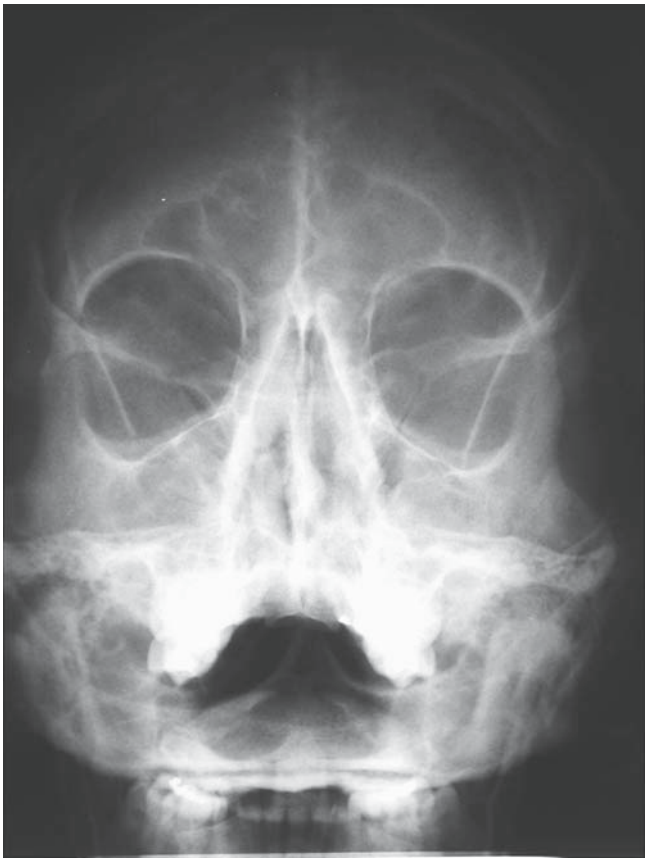

b

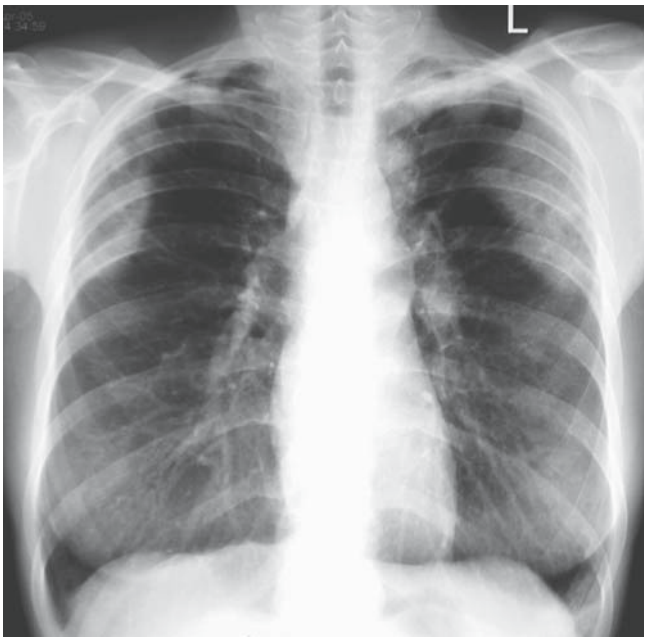


c

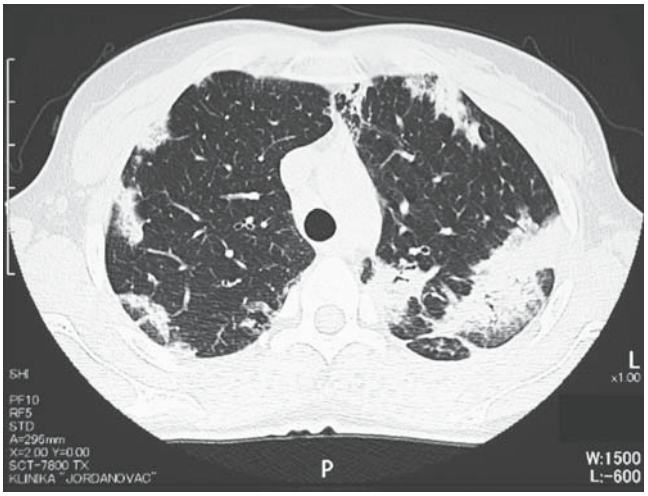


d

**Figure 26.3.** Plain radiograph of the chest at the time when the infiltrate of the lungs appeared for the first time in a patient with asthma and pansinusitis showed unilateral alveolar infiltrate with air bronchogram, with consecutive reduction of ipsilateral lung volume and mediastinal traction, and minor pleural effusion (a), and plain radiograph showed shaded sinuses, especially left maxillar sinus (b). One year later, plain chest x-rays showed multiple, bilateral, peripheral, alveolar infiltrates in the upper lobes, which reappeared following the cessation of corticosteroids (c). HRCT scan of the same patient showing minor ground-glass pattern and consolidations (d). The significance of the infiltrate is not univocal hence it may be due to eosinophilic infiltration or diffuse alveolar hemorrhage. In this particular patient, eosinophilic infiltrates were proven by bronchoalveolar lavage and transbronchial lung biopsy.

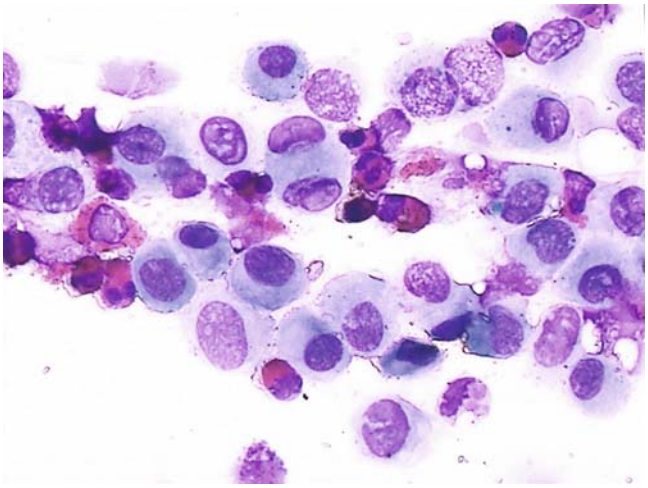

**Figure 26.4.** Lung lavage analysis shows the eosinophilic alveolitis, that is, more than 25% of the lavage cells are eosinophils. Numerous eosinophils and macrophages are seen. BAL fluid cytology, original magnification ×400, MGG stain (May-Grünwald-Giemsa).

## Bibliography

1. Masi AT, Hunder GG, Lie JT, Michel BA, Bloch DA, Arend WP, Calabrese LH, Edworthy SM, Fauci AS, Leavitt RY. The America College of Rheumatology 1990 criteria for the classification of Churg Strauss-syndrome (allergic granulomatosis and angiitis). Arthritis Rheum 1990;33:1094–1100.
2. Guillevin L, Cohen P, Gayraud M, Lhote F, Jarrousse B, Casassus P. Churg Strauss syndrome. Clinical study and long-term follow-up of 96 patients. Medicine (Baltimore) 1999;78:26–37.
3. Guillevin L, Pagnoux C, Mouthon L. Churg-Strauss syndrome. Sem Resp Crit Care Med 2004;25:535–545.
4. Cottin V, Cordier JF. Eosinophilic pneumonias. Allergy 2005;60:841–857.

# 27

# Goodpasture Disease

Goodpasture disease (Goodpasture syndrome, anti-GBM disease) is a term reserved for cases with pulmonary hemorrhage, rapid progressing glomerulonephritis, and circulating antibodies directed against glomerular basement membrane (anti-GBM) and pulmonary alveoli. It is not a classic systemic vasculitis because lungs and kidneys are the only organs involved.

Anti-GBM disease is an archetypal autoimmune disease, and an autoantibody against the noncollagenous domain of the alpha-3 chain of type 4 collagen (a3(IV) NC1) has been identified in virtually all patients. It seems that cigarette smoke and also volatile hydrocarbon exposure cause endothelial damage that facilitates the approach of autoantibodies to the basement membrane.

Viruses are also thought to play a role in the development of anti-GMB disease; small epidemic spread has been reported.

The typical patient is a young male smoker, but the disease can target at any age, both sexes, and all races, although the Europeans more frequently. Young male patients often suffer from lung forms of the disease with alveolar hemorrhage and older patients from isolated renal disease.

The *symptoms* are cough, dyspnea, and hemoptysis in the range from mild to fatal bleeding that usually precedes the renal symptomatology. The most frequent cause of abrupt, early death is abundant hemoptysis. Due to secondary anemia, malaise, dizziness, fatigue, and pallor develop. Fever, arthralgias, and other nonspecific symptoms are often present. Symptoms of glomerulonephritis represented first by small amounts of blood and protein in the urine, and other clinical symptoms with normal blood pressure, can be detected. Later in the course of the disease, renal failure progresses during weeks or month.

The *diagnosis* of Goodpasture disease rests upon the characteristic clinical feature, confirmation of the presence of serum anti-GBM antibodies (positive in 90% of patients) (Figure 27.1), and demonstration of linear deposits of IgG antibodies along the alveolar or glomerular basement membrane that is visible by direct immunofluorescence.

The chest radiograph finding depends on the frequency and intensity of hemorrhage. In the early stage of the disease diffuse alveolar opacities are found (Figure 27.2), sometimes they may be focal, predominantly involving perihilar and basilar regions. In advanced disease, linear and reticular pattern is revealed.

Kidney biopsy is usually performed. Focal proliferative and necrotizing glomerulonephritis and extracapillary crescent proliferates in the glomerulus are found. Linear deposits of IgG along the basement membranes are diagnostic (Figure 27.3a, b). Histopathological analysis of lung biopsy specimen is identical to the finding in idiopathic pulmonary hemosiderosis. Histopathological changes are caused by repetitive bleeding into the alveolar spaces, so in the acute phase there are erythrocytes (Figure 27.4), later siderophages, and in the chronic hyperplastic pneumocytes, dilated and tortuotic capillaries and interstitial fibrosis.

*Treatment* of Goodpasture disease requires corticosteroids, cyclophosphamide or azathioprine, and plasmapheresis. Such immunosuppressive regimen resembles that for

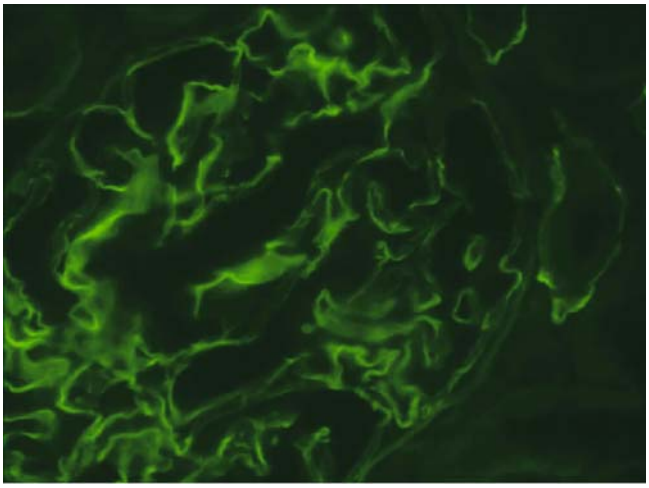

**Figure 27.1.** Antibodies against the glomerular basement membrane type IV collagen. Linear fluorescence of the glomerular basement membrane (monkey kidney; Eurroimmun, Lubeck, Germany).

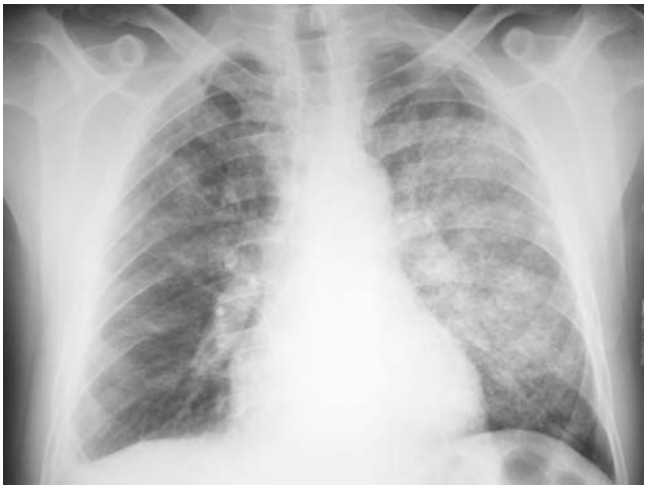

**Figure 27.2.** Chest radiograph shows typical finding of diffuse alveolar hemorrhage presenting in this case as symmetric, predominantly left-sided alveolar opacities.

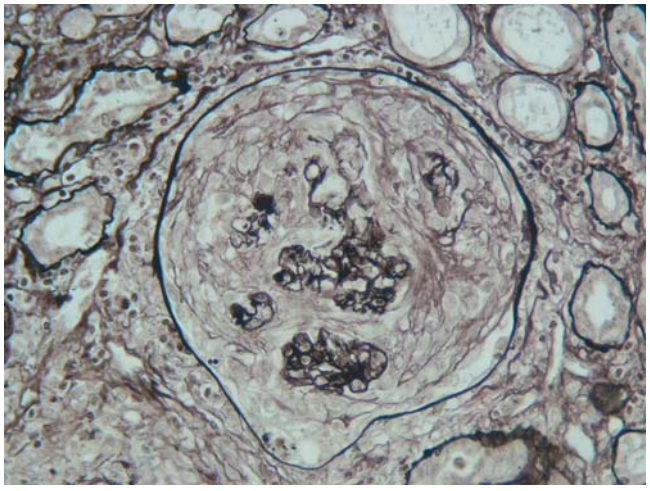

a

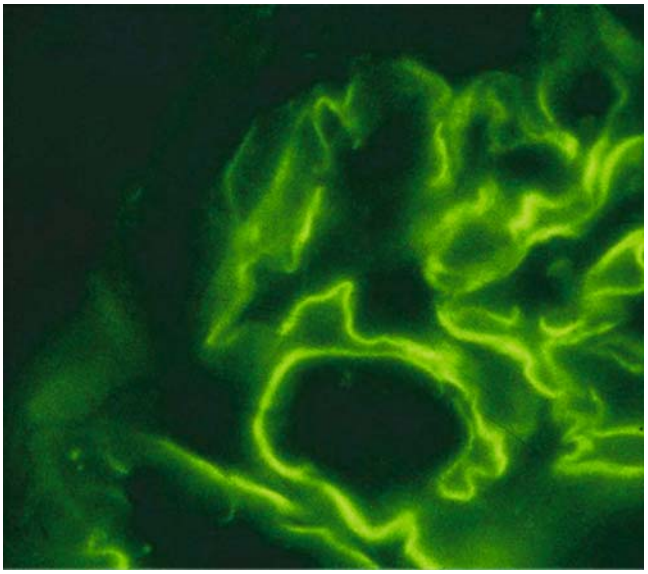

b

**Figure 27.3.** Kidney biopsy shows diffuse extracapillary necrotizing glomerulonephritis. The glomerulus with partially destroyed capillary ball and global fibrocellular crescent that fills the Bowman's space is seen (Jones's silver impregnation stain) (a). Linear deposits of IgG along the basement membranes have diagnostic value (b).

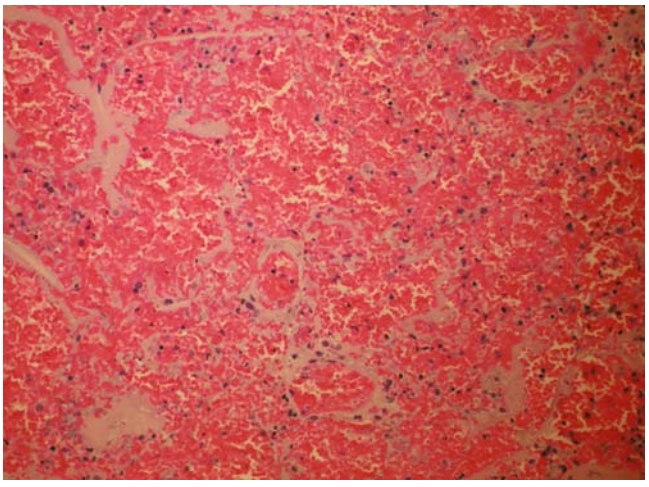

**Figure 27.4.** In the lungs, alveolar hemorrhage is the most frequent finding in Goodpasture syndrome, sometimes with necrosis.

ANCA-positive vasculitis. Untreated anti-GBM disease is usually rapidly fatal and renal function does not recover, but with aggressive therapy the recovery is substantial. Relapses are rare compared with ANCA-related vasculitis.

## Bibliography

1. Hluth DC, Rees AJ. Anti-glomerular basement membrane disease. J Am Soc Nephrol 1999;10:2446–2453.
2. Kalluri R, Sun MJ, Hudson BG, Neilson EG. The Goodpasture autoantigen: Structural delineation of two immunologically privileged epitopes on alpha 3 (IV) chain of type IV collagen. J Biol Chem 1996;271:9062–9068.
3. Donaghy M, Rees AJ. Cigarette smoking and lung haemorrhage in glomerulonephritis caused by autoantibodies to glomerular basement membrane. Lancet 1983;2:1390–1393.
4. Bombassei GJ, Kaplan AA. The association between hydrocarbon exposure and anti-glomerular basement membrane antibody-mediated disease (Goodpasture syndrome). Am J Ind Med 1992;21:141–153.
5. Little MA, Pusey CD. Rapidly progressive glomerulonephritis: Current and evolving treatment strategies. J Nephrol 2004;17:10–19.

# 28

# Two Vascular Multisystem Diseases with Pulmonary Involvement

## 28.1. Behçet Disease

Also known as the Silk Road disease, Behçet disease (BD) has a worldwide distribution but is seen most frequently in Turkey, Japan, China, and the Mediterranean littoral. Men and women are affected equally. The disease is a triad of oral ulcers (Figure 28.1a, b), genital ulcers, and uveitis (Figure 28.2a, b, c). In a study consisting of 2179 patients, pulmonary involvement occurred in about 1.1%. Pulmonary vascular lesions lead to the formation of pulmonary artery aneurysms, the most common pulmonary lesion in BD almost always associated with hemoptysis, thrombosis and occlusion of the vessels, pulmonary infarction, and hemorrhage (Figure 28.3). Symptoms include dyspnea, cough, hemoptysis, and pleural effusion. Pathological changes include arterial aneurysm, arterial and venous thrombosis, infarction, and vasculitis (Figures 28.4 and 28.5).

Current treatments of BD are topical, paraocular, and systemic corticosteroids, colchicine, dapsone, cyclosporine, azathioprine, methotrexate, cyclophosphamide, and chlorambucil. Patients with small nonspecific radiologic abnormalities should be followed up closely because early diagnosis of vascular lesions may be life-saving. Immunosuppression is the main therapy for the treatment of a vasculitis, and it is important that it is not mistaken for pulmonary thromboembolic disease because fatalities have occurred in BD shortly after initiation of anticoagulation/thrombolytic treatment.

## 28.2. Veno-Occlusive Lung Disease

Pulmonary veno-occlusive disease (PVOD) is a rare cause of pulmonary hypertension and interstitial disease that mainly affects children and young adults. PVOD is more common in men in contrast with primary pulmonary hypertension, which is more common in women. The predominant lesion is intimal fibrosis of small veins and venules (Figure 28.6). Changes in the arterial side cause muscular hypertrophy of the circulation and can result in pulmonary edema and alveolar hemorrhage. In about 50% of the patients, pulmonary arteries are affected.

Most cases of PVOD are idiopathic, and several theories have been proposed. Known causes of secondary PVOD include bleomycin, vincristine, cisplatin, carmustine, mitomycin, radiation, appetite-suppressant drugs, and herbal preparations. The most common symptom of PVOD is dyspnea, initially on exercise. Most of the patients have fatigue and sometimes sensation of fainting at the time of diagnosis; fewer have orthopnea and paroxysmal dyspnea. Progression of the disease leads to narrowing of the pulmonary veins, pulmonary hypertension, congestion, and pulmonary edema. Chest radiographs show enlarged pulmonary arteries and in some cases mild-to-moderate peripheral interstitial infiltrates or septal lines (Figure 28.7). Chest CT scan reveal the presence of ground-glass opacities (particularly with a centrilobular distribution), septal lines, and adenopathy (Figure 28.8).

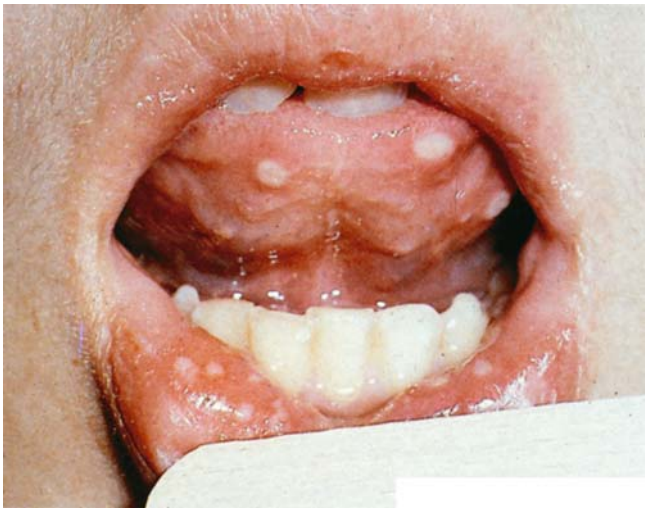

a

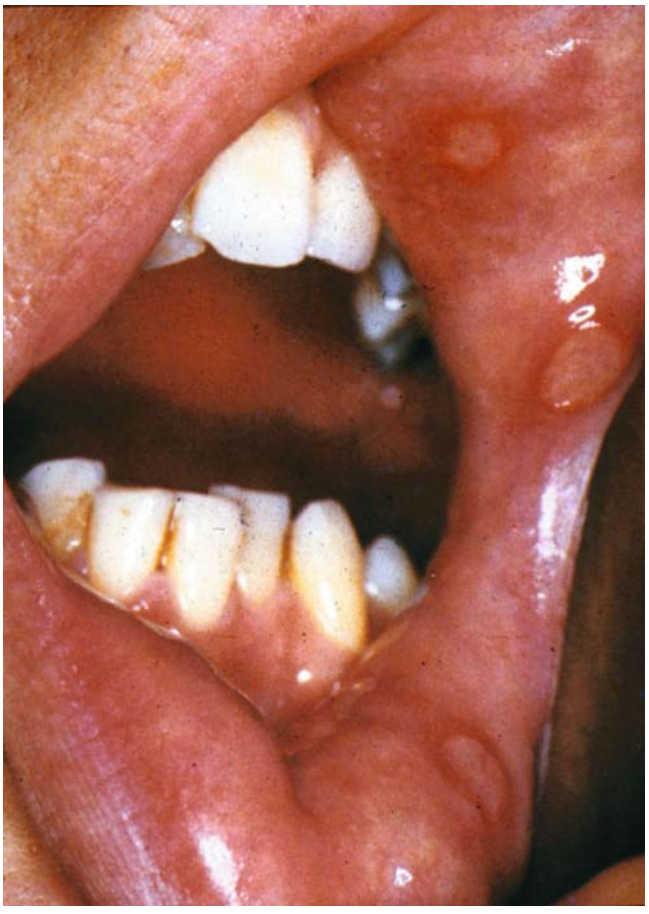

b

**Figure 28.1.** Behçet disease: Characteristic aphthous ulcers under the tongue (a). Aphthous ulcers inside the mouth (b).

a

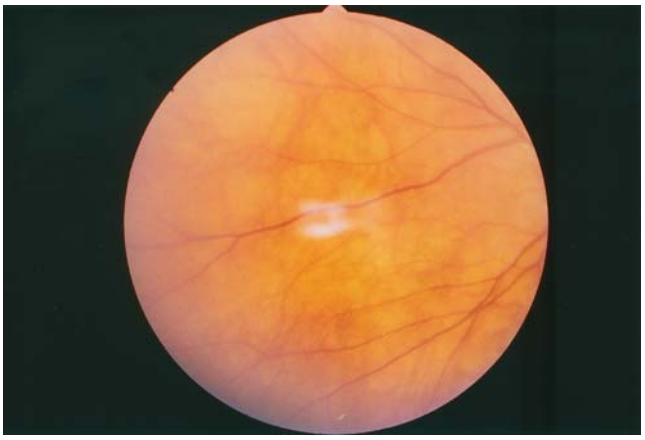

b

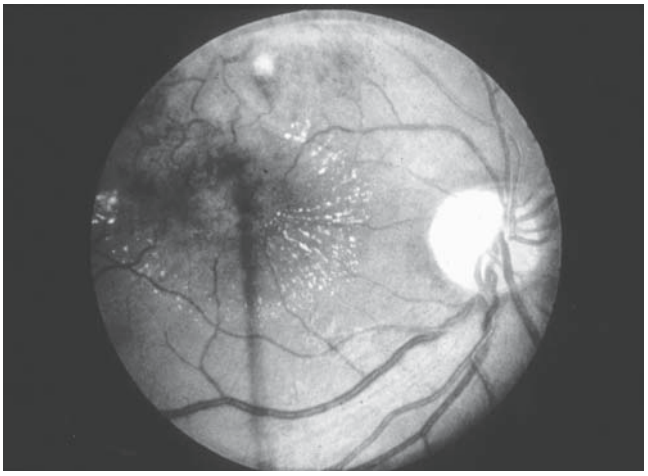

c

**Figure 28.2.** Ocular lesions occur in more than half of the cases of Behçet disease; frequently bilateral, they can eventually lead to blindness. The figure shows the posterior sinechiae; the obliteration of the lens and the iris obviating dilatation of the iris (a). Retinal vein occlusion. This occurred secondary to periphlebitis (b). The retina can also be involved in the form of vasculitis associated with lekage of inflamed retinal vessels (c).

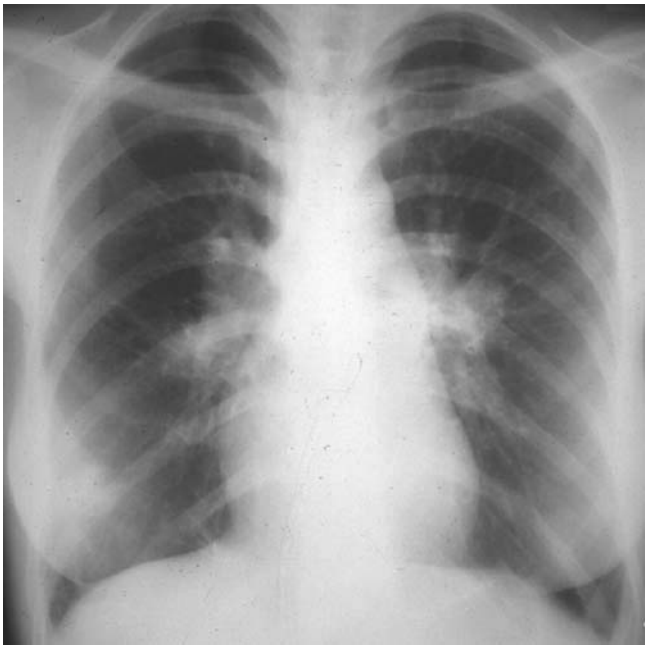

**Figure 28.3.** Chest x-ray film in a Japanese patient with Behçet disease showing pulmonary artery dilatation and aneurysm. (Courtesy Dr. Sonoko Nagai, Kyoto University, Japan.)

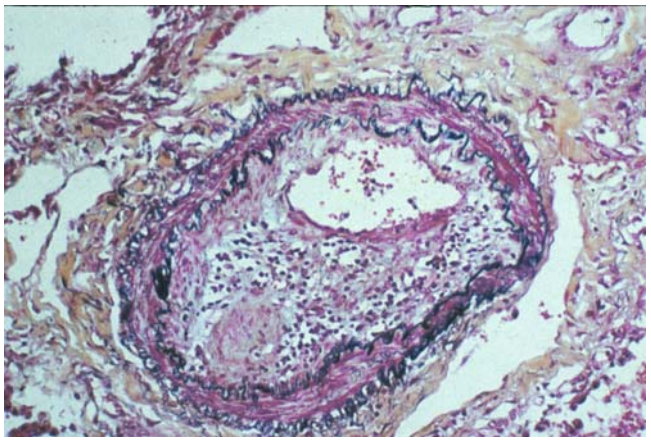

**Figure 28.4.** A lung biopsy specimen showing vasculitis with perivascular inflammation (small artery stained for elastic tissue) and lumen totally occupied with organized thrombus, which is partially recanalized, typical of Behçet disease.

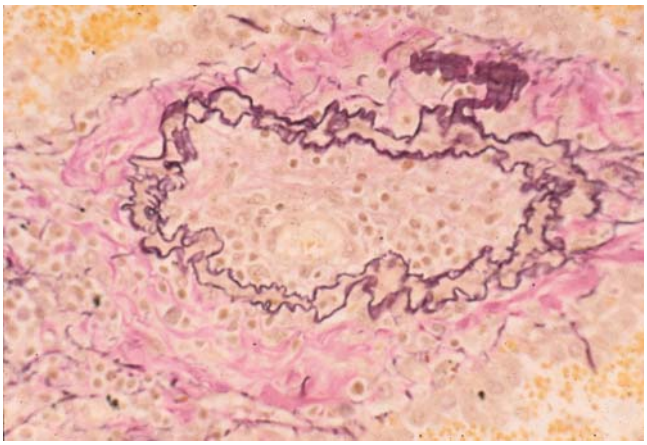

**Figure 28.5.** Elastica stain shows fragmentation of the vessel wall with degenerative changes in the elastic lamina. Small vessel is totaly filled with the clot (thrombus).

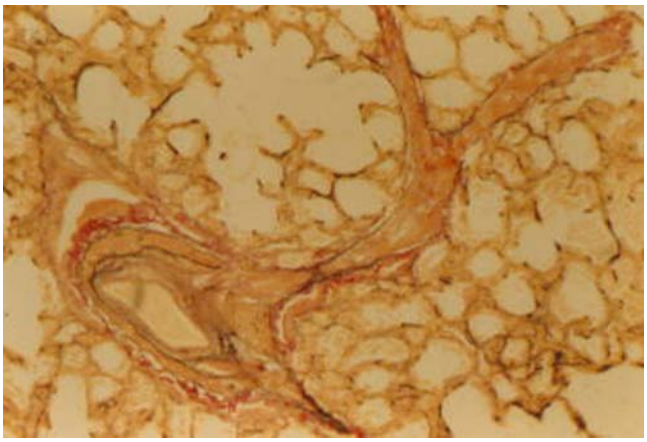

**Figure 28.6.** Y-shaped vein with partial duplication of elastica and thickening of intima.

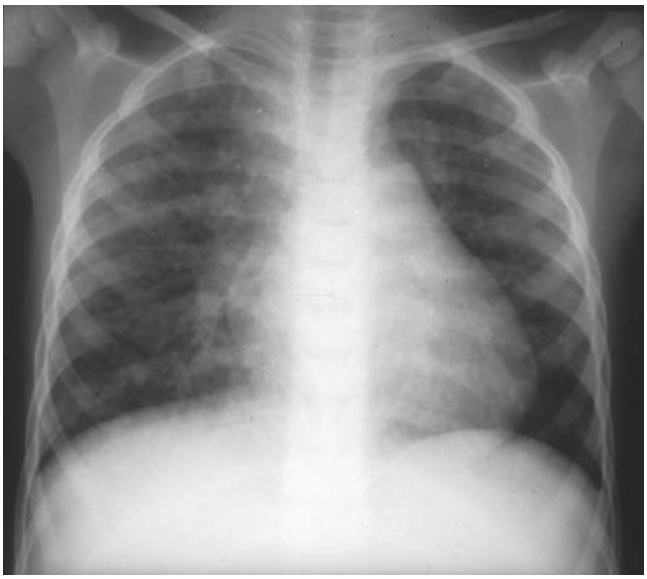

**Figure 28.7.** Chest x-ray film in a patient with veno-occlusive disease of the lung showing bilateral, soft patchy infiltrate.

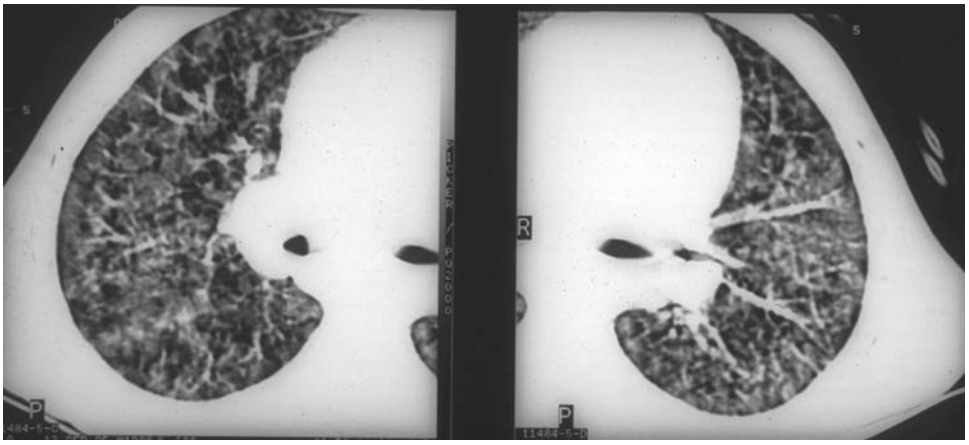

**Figure 28.8.** CT scan of the chest of the same patient as in Figure 28.7 showing diffuse nodular infiltrate.

**Table 28.1.** Differences between primary pulmonary hypertension and pulmonary veno-occlusive lung disease.

| Features | Primary Pulmonary Hypertension | Veno-occlusive Disease |
|---|---|---|
| Age | Adults | Children, young adults |
| Sex | Common in women | Common in men |
| Chest radiograph | Prominent pulmonary arteries | Large pulmonary arteries, Kerley-B lines, hilar adenopathy |
| Computed tomography | No centrilobular nodules or septal thickening | Centrilobular nodules, septal lines, adenopathy |
| Vasodilators | May be useful | May cause pulmonary edema |
| Prognosis | Median survival 30 months | Most patients die within 2 years of diagnosis |
| Lung transplantation | Effective | Effective |

The differential diagnosis of PVOD includes pulmonary parenchymal diseases, connective tissue disorders, HIV infection, recurrent pulmonary thromboembolism, and primary pulmonary hypertension (Table 28.1). PVOD is often difficult to distinguish from severe primary pulmonary hypertension. The treatment of primary pulmonary hypertension with prostacyclin can be fatal in patients with veno-occlusive disease, and an early pretreatment diagnosis is critical.

## Bibliography

1. Evereklioglu C. Current concepts in the etiology and treatment of Behcet disease. Surv Ophthalmol 2005;50:297–350.
2. Uzun O, Akpolat T, Erkan L. Pulmonary vasculitis in Behcet disease: A cumulative analysis. Chest 2005;127:2243–2253.
3. Veeraraghavan S, Koss M, Sharma, OP. Pulmonary veno-occlusive disease. Curr Opin Pulm Med 1999;5:310–313.
4. Resten A, Maitres S, Humbert M, Rabiller A, Sifbon O, Capron F, Simmoneau G, Musset D. Pulmonary hypertension: CT of the chest in pulmonary venooclusive disease. AJR Am J Roentgenol 2004;183:65–70.

# 29

# Idiopathic Pulmonary Hemosiderosis

The characteristic features of idiopathic pulmonary hemosiderosis (IPH) are recurrent intra-alveolar bleeding, accumulation of hemosiderin-laden macrophages (siderophages), and iron-deficiency anemia. The disease most commonly affects children and young adults. The diagnosis is established by excluding all other known causes of diffuse alveolar hemorrhage (DAH) (Table 29.1). The histopathological examination reveals bland alveolar hemorrhage (Figure 29.1a) (without capillaritis, or inflammation of other blood vessels), type II epithelial hyperplasia with capillary dilatation, and tortuosity. Hemosiderin-laden macrophages are seen in the alveolar spaces and interstitium. Breaks in the continuity of the capilllary basement membrane and focal ruptures are seen (Figure 29.1b).

*Major symptoms* in patients with IPH are dyspnea, cough, and hemoptysis. Hemoptyses may be absent if the bleeding is scanty, but sputum becomes brown-yellow (hemosiderin) even 14 days after the bleeding. The symptoms are episodic. Occasionally, the patient may present with malaise and fatigue due to anemia. Other nonspecific symptoms include fever, arthralgias, loss of appetite, and weight loss. The asynchronous sequential wheezing and squeaks are heard by stethoscope. Finger clubbing is uncommon. In adults, the disease is usually benign; spontaneous remissions occur. Sporadic cases of respiratory failure and death have been reported.

The *etiology* of IPH is poorly understood. Fifty percent of children with this disease have high serum IgA levels against cow's milk. IPH is also associated with celiac disease or jejunal villous atrophy. In an American study carried out between 1993 and 2000, 30 children were diagnosed with IPH; most of the cases were linked to exposure to fungus *Stachybotrys atra*. It raises the possibility of an external infectious or mycotoxic agent causing IPH.

*Diagnosis* of IPH should be suspected in a patient with hemoptysis, anemia, and presence of alveolar, perihilar, and bibasilar opacifications with an air bronchogram (Figure 29.2a). HRCT scan shows ground-glass pattern (Figure 29.2b). Recurrent bleeding induces fibrosis that on a plain radiograph and HRCT shows coarse linear and reticular infiltrate (Figure 29.3a, b, c, d, e).

Lung function tests after the episode of bleeding show restrictive ventilatory changes and characteristically increased $DL_{CO}$ due to enhanced binding of CO to hemoglobin in the sequestered erythrocytes in the lungs. In patients with lung fibrosis, the restrictive ventilatory changes are associated with decreased $DL_{CO}$ and hypoxemia.

Bronchoscopy and the analysis of bronchoalveolar lavage fluid are not useful in confirming the diagnosis of IPH. It only establishes the presence of blood. In acute alveolar hemorrhage each consecutive aspirated fraction of lavage fluid is more hemorrhagic (Figures 29.4 and 29.5). In chronic IPH, the color of lung lavage fluid is characteristically brown-yellow. If the patients do not cough up the blood, this finding is of extreme importance in establishing the diagnosis of DAH. In such cases, Prussian blue staining is necessary to demonstrate siderophages (Figure 29.6). Open lung biopsy may be necessary to exclude other causes of DAH, such as vasculitis or connective tissue disease.

Corticosteroid *therapy* is useful in acute bleeding, but its long-term benefit is unclear. If the corticosteroid therapy fails, azathioprine or other immunosuppressive agents should be administered. It has been reported that azathioprine and corticosteroids are effective in preventing relapses. Iron-deficiency anemia is treated with iron preparations.

**Table 29.1.** Causes of diffuse alveolar hemorrhage (DAH).

| | |
|---|---|
| Idiopathic | Idiopathic pulmonary hemosiderosis |
| Vasculitis | Wegener granulomatosis, microscopic polyangiitis, isolated pulmonary capillaritis, Behçet disease |
| Immunologic | Systemic lupus erythematosus, anti-GBM disease |
| Drugs | Acetylsalicylic acid, nitrofurantoin, amiodarone, retinoic acid, phenytoin, methotrexate, cocaine |
| Coagulation disorders | Thrombocytopenic purpura, anticoagulants, antiplatelet agents or thrombolytics |
| Other | Mitral stenosis, pulmonary veno-occlusive disease |

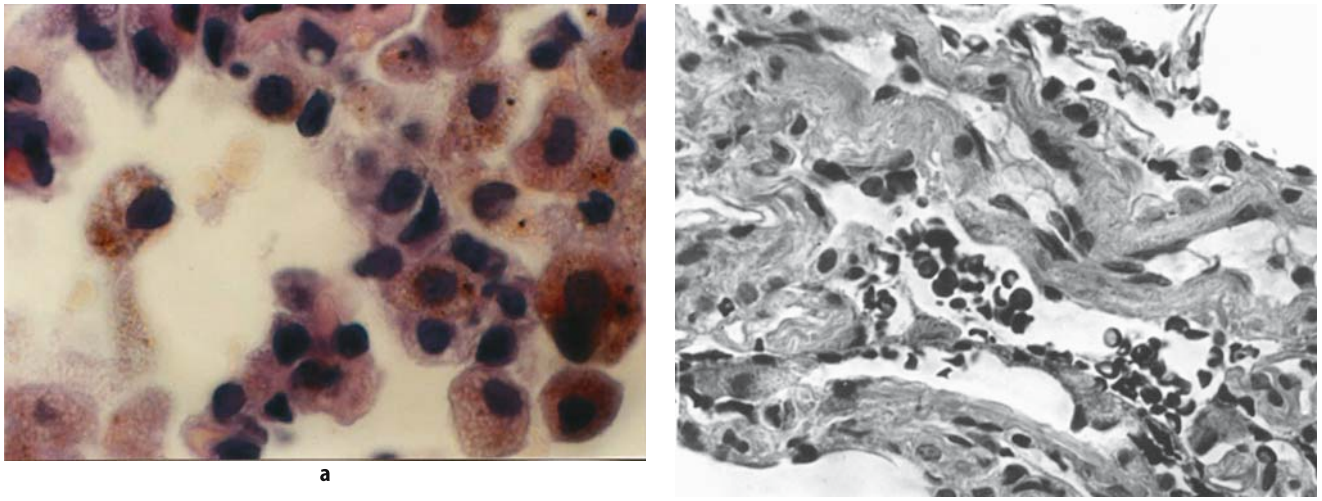

a b

**Figure 29.1.** Lung biopsy shows only "bland" hemorrhage without capillaritis (a); the erythrocyte passes the capillary layers (b).

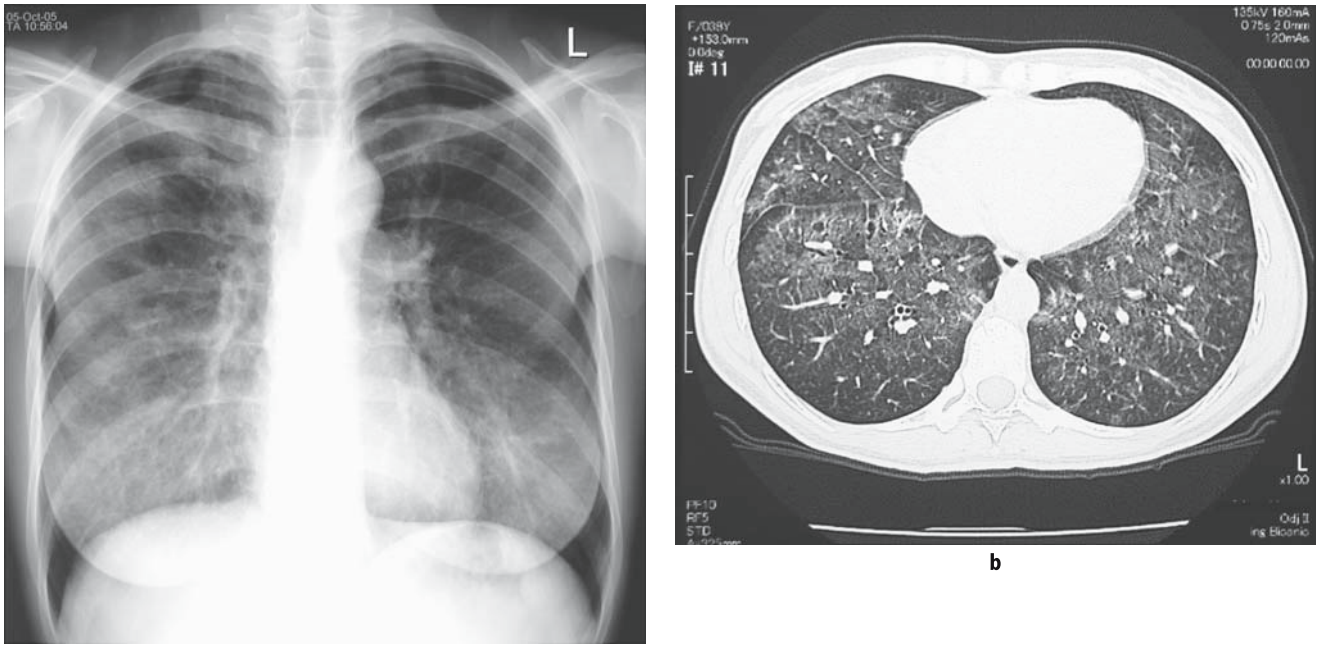


a b

**Figure 29.2.** Recent onset IPH. Plain chest radiograph in a patient with recent onset of the disease, which was revealed by hemoptysis, shows minimal interstitial infiltrates (a) but impressive, diffuse ground-glass opacities, and thickening of the interlobular septa by HRCT scanning (b).

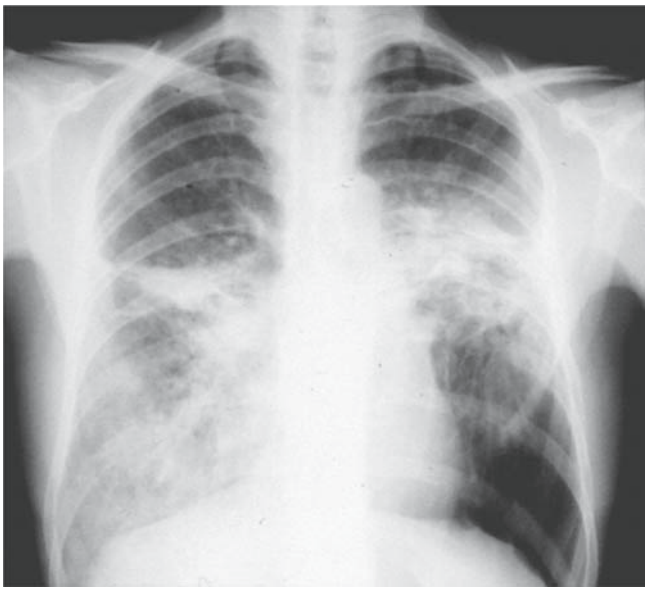

a

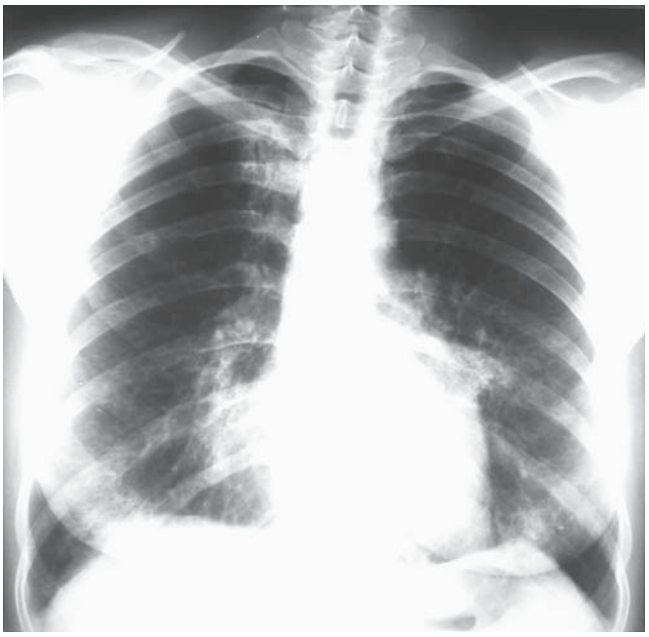

b

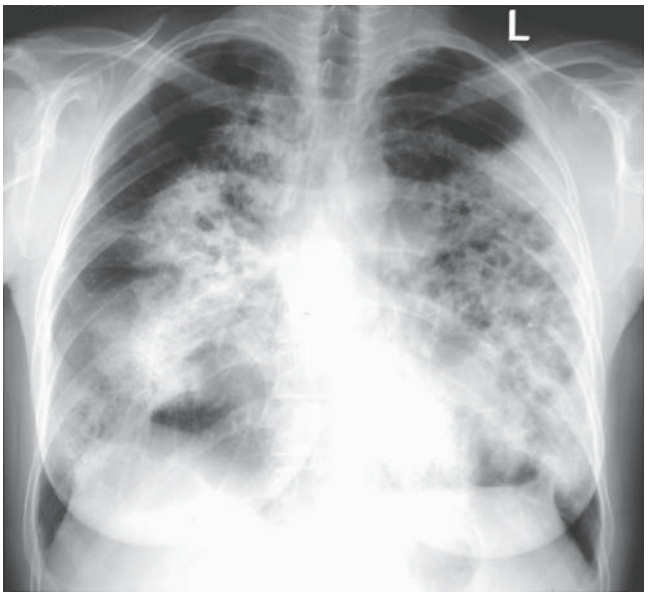


c

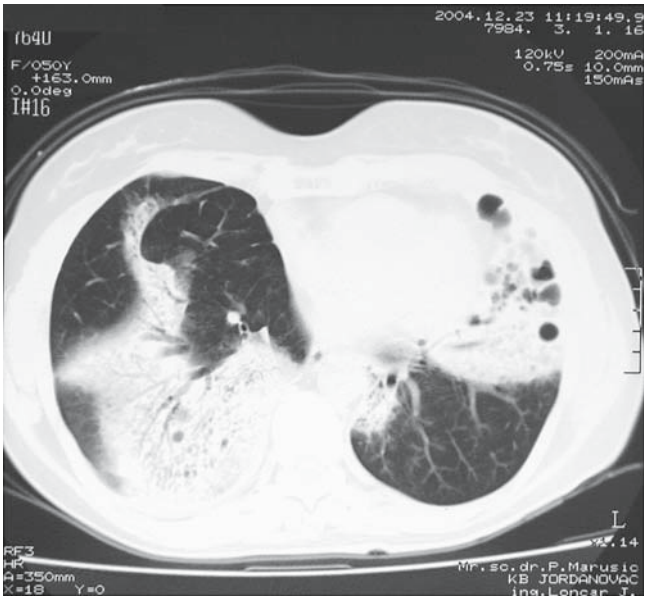


d

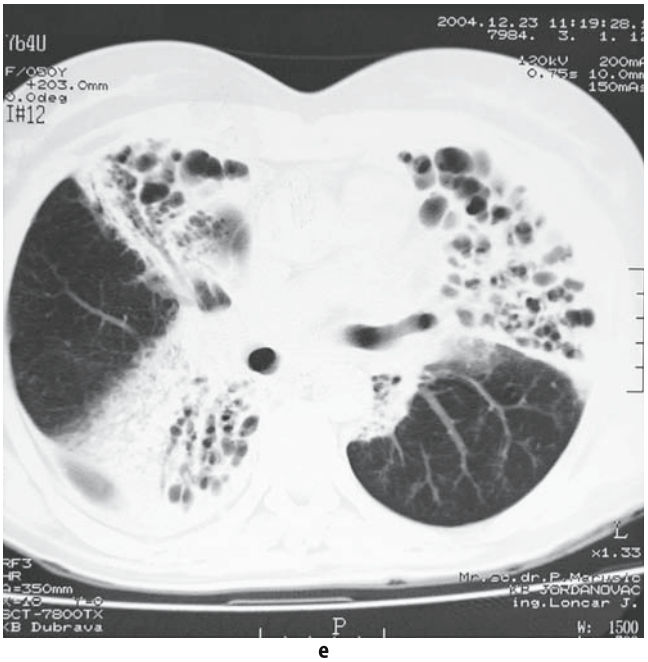


e

**Figure 29.3.** Chronic IPH. Plain chest radiograph in a patient 11 years after the time of initial diagnosis of IPH, with chronic disease showing parahilar coarse linear and reticular retractive pattern. The patient was admitted to the hospital due to the intercurrent right basal pneumonia (a) Another patient with long duration of IPH, plain radiograph 12 years ago (b) and in January 2005 showing dramatical clinical and radiological worsening with the development of middle and lower zone fibrosis with the distortion of parenchyma (c), seen also by CT scanning (d, e).

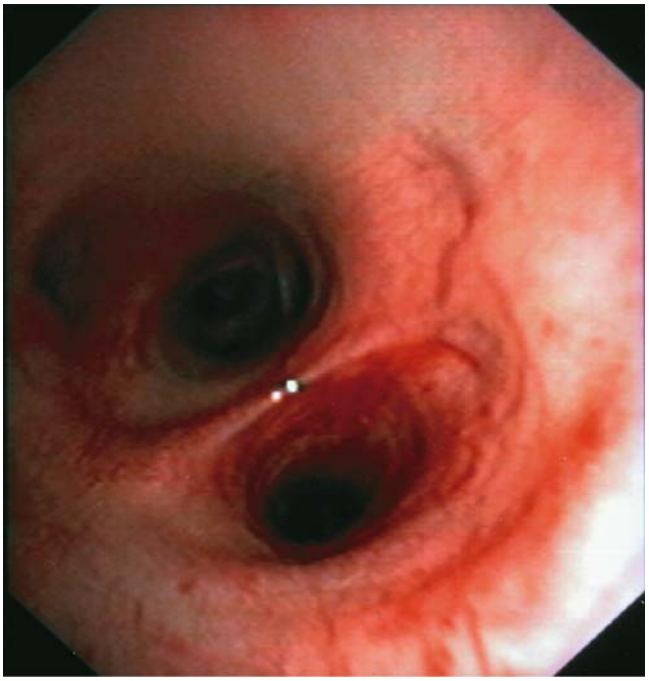

**Figure 29.4.** During bronchoscopy, the bleeding is visualized.

**Figure 29.5.** Lung lavage fluid in a patient with idiopathic pulmonary hemosiderosis is macroscopically hemorrhagic, and if the bleeding is minimal and chronic the lavage fluid becomes brownish.

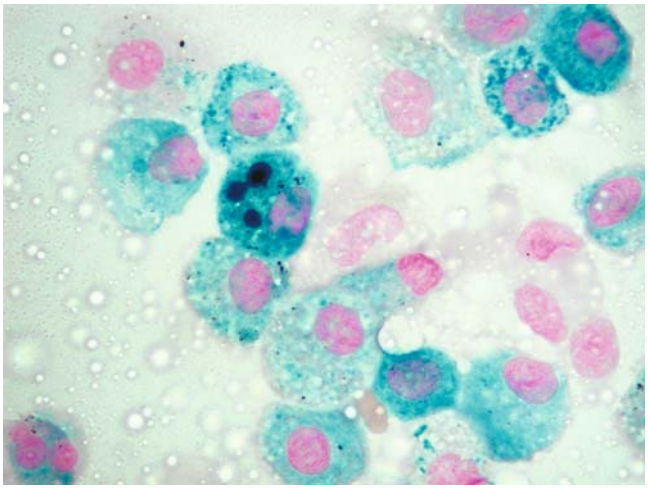

**Figure 29.6.** To confirm the diagnosis of DAH, more than 90% of the pigmentophages in the lung lavage fluid have to be siderophages. Prussian blue staining is necessary to demonstrate the siderophages. BAL fluid cytology, original magnification ×1000, Prussian blue.

## Bibliography

1. Demedts M, Thomeer M. Rare diffuse lung diseases and mimics of diffuse lung diseases. In: Olivieri D, du Bois RM, eds. Interstitial lung diseases. Eur.Respir.Monographs, Ed.ERS. 2000;5:267–288.
2. Dearborn DG, Smith PG, Dahms BB, Allan TM, Sorenson WG, Montana E, Etmel RA. Cinical profiles of 30 infants with acute pulmonary hemorrhage in Cleveland. Pediatrics 2002;110:623–637.
3. Collard HR, Schwartz MI. Diffuse alveolar hemorrhage. Clin Chest Med 2004;25:583–592.
4. Rossi GA, Balzano E, Battistini E. Long-term prednisone and azathioprine treatment of patient with idiopathic pulmonary hemosiderosis. Pediatr Pulmonol 1992;13:176–180.
5. Ioachimescu OC, Sieber S, Kotch A. Idiopathic pulmonary hemosiderosis revisited. Eur Respir J 2004;24:162–170.

# 30

# Pulmonary Alveolar Microlithiasis

Pulmonary alveolar microlithiasis (PAM) is a rare disease. The disease is described all over the world, although the highest incidence is found in Turkey and Italy.

Its cause is not known. It is characterized by intra-alveolar deposition of tiny, roundish corpuscles called *microliths*. These concretions slowly grow to diameters of 0.01–3 mm and fill up to 80% of the airspaces and they can come into contact with walls, which in the advanced stages are pressed, damaged, and replaced by fibrous tissue. The lungs become heavy, firm, and resemble stone (Figure 30.1).

PAM is usually diagnosed between 20 and 30 years of age, although it can occur at any age, even at the age of 80. The lack of symptoms is a typical clinical feature of the patients with PAM. The disease slowly develops and causes no health complaints; the diagnosis is usually accidental, when radiograph of the chest is performed for other purpose. The symptoms occur late and comprise dyspnea, cough, and chest pain. The discrepancy between the severity of chest radiograph finding and relatively mild symptoms is often striking. In advanced stage of PAM, bilateral crackles are present over the lung bases. Finger clubbing and respiratory failure appear late. Episodes of recurrent bronchitis and pneumonia are frequent. Chronic right heart failure develops late.

The family occurrence, in about 50% of the cases, with prevalent horizontal sibling incidence has been used to suggest an autosomal recessive mode of inheritance. The possibility of an environmental factor has been suggested. An inborn error of calcium metabolism involving serum calcium and phospohorus metabolism has been proposed.

Plain chest radiograph finding is characteristic for pulmonary microlithiasis PM. In the beginning, the lower lobes are involved, and then the middle and upper areas of the lungs, producing a "sandstorm-like" picture (Figure 30.2). In the advanced stage, "white" lung, representing extensive calcium deposits (Table 30.1), obscures the boundaries between the heart and lungs. HRCT reveals perilobular and bronchovascular distribution of microliths and preserved structure of the lobuli as well as the interlobular septa (Figure 30.3). The plain radiograph of the chest and HRCT findings are so characteristic that many authorities believe that these tests are diagnostic.

Lung functions are usually normal. In advanced stages, however, restrictive and obstructive changes supervene.

Microliths can be found in spontaneous or induced sputum, in bronchial wash, or in the bronchoalveolar lung lavage fluid. The diagnosis of PAM can be confirmed by histopathological analysis of the samples obtained by transbronchial or open lung biopsy.

The curative therapy of PAM does not exist; the microliths dwell lifelong in the lungs. The removal of the microliths by lavage procedure has been unsuccessful. The only effective therapy today is lung transplantation.

**Table 30.1.** Causes of diffuse pulmonary calcification and ossification.

| |
|---|
| Pulmonary Alveolar Microlithiasis |
| Interstitial ossification |
| Silicosis, idiopathic pulmonary fibrosis |
| Metastatic calcification |
| Idiopathic hypercalcemia, hyperparathyroidism, chronic renal failure, vitamin D intoxication, malignancies (multiple myeloma, T-cell leukemia) |
| Dystrophic calcification |
| Healed tuberculosis, histoplasmosis, varicella pneumonia |
| Intra-alveolar ossification |
| Chronic left heart failure, mitral stenosis |

**Figure 30.1.** Alveolar microlithiasis. Gross finding: cut surface is finely granular and very hard on section resembling stone.

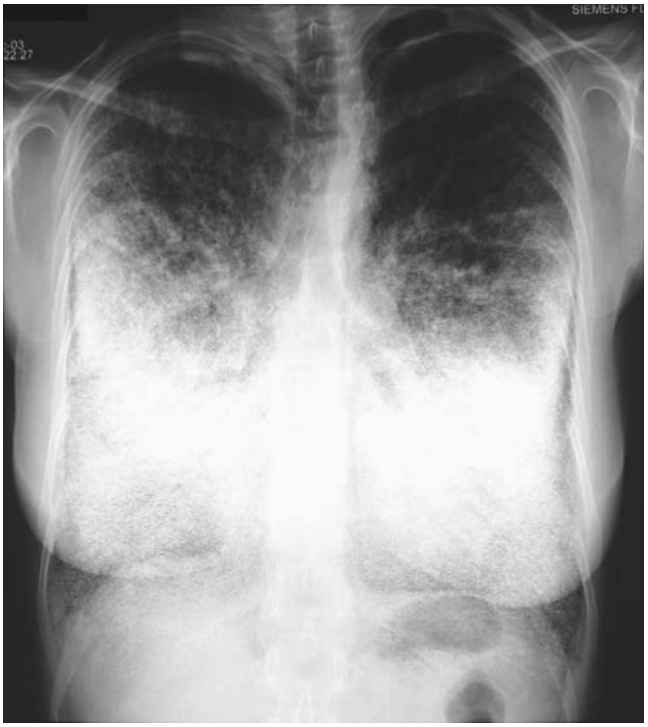

**Figure 30.2.** Plain chest radiograph of a patient who suffers from pulmonary alveolar microlithiasis for over 20 years shows a typical "snowstorm-like" image due to calcified microlith.

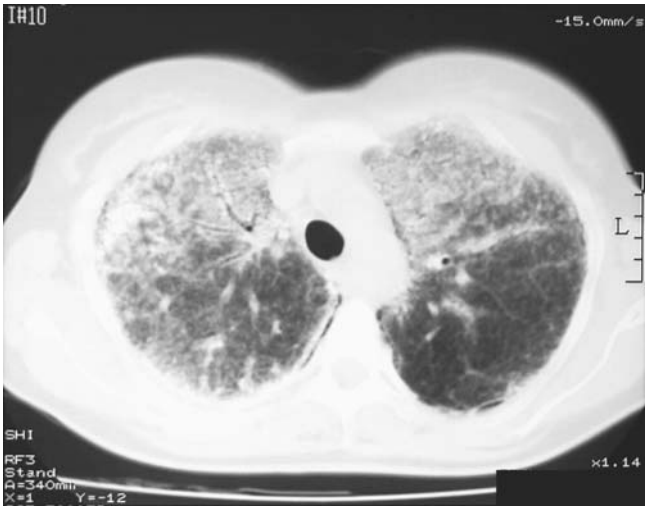


**Figure 30.3.** The HRCT scan of the same patient reveals perilobular and bronchovascular distribution of microliths and subpleural consolidation with calcifications in the right lung. The patient is respiratory insufficient and in need of permanent oxygenotherapy

## Bibliography

1. Mariotta S, Ricci A, Papale M, et al. Pulmonary alveolar microlithiasis: Report on 576 cases published in the literature. Sarcoidosis Vasc Diffuse Lung Dis 2004;21:173–181.
2. Castellano G, Gentile M, Castellana R, Fiorente P, Lamorgese V. Pulmonary alveolar microlithiasis: Clinical features, evolution of the phenotype and review of the literature. Am J Med Gen 2002;111:220–224.
3. Schmidt H, Lorcher U, Kitz R, Zielan S, Ahrems P, Konig R. Pulmonary alveolar microlithiasis in children. Pediatr Radiol 1996;26:33–36.
4. Cluzel P, Grenier P, Bernadac P, Laurent F, Picard JD. Pulmonary alveolar microlithiasis: CT findings. J Comput Assist Tomogr 1991;15:938–942.
5. Castellana G, Lamorgese V. Pulmonary alveolar microlithiasis. World cases and review of the literature. Respiration 2003;70:549–555.

# 31

# Pulmonary Alveolar Proteinosis

A rare disease, pulmonary alveolar proteinosis (PAP) is characterized by accumulation of surfactant-derived phospholipoproteinaceous material in alveoli and distal airways. The clinical course is diverse. Spontaneous recovery can occur. Less frequently, the disease progresses to fatal respiratory failure. The inherent feature of PAP is susceptibility to opportunistic organisms. There are three clinically distinct forms of PAP: congenital, secondary, and acquired.

The prevalence of PAP is 0.4 per 100,000 population; 90% of the cases have the acquired form of the disease. Men are 2–3 times more frequently affected than women. One third of all the patients are asymptomatic. Symptoms include dyspnea, cough with mucoid expectoration, hemoptysis, chest pain, fatigue, and loss of appetite. In some patients, the diagnosis is first made after an episode of pneumonia. In advanced stage of PAP, fine and course crackles can be heard over the lung fields. Fever is the ominous sign as it may reflect the presence of an infection with various microorganisms, including opportunistic organisms (*Aspergillus* spp., *Nocardia* spp., *Candida* spp., mycobacteria, viruses). The cyanosis and finger clubbing appear in advanced cases.

The *congenital form* of the disease arises due to the mutations of genes that control the production of surfactant B and C proteins or $\beta_c$ chain receptor of granulocyte-macrophage colony-stimulating factor (GM-CSF). The *secondary form* appears in clinical conditions with diminished number or functionally impaired alveolar macrophages. Such conditions include hematologic malignancies, pharmacologic immunosupression, inhalation of inorganic dusts (silica, aluminum, titan) and toxic fumes, and infections (mycoses, mycobacterioses, cytomegalovirus, *Pneumocystis jiroveci*).

The *acquired (idiopathic) form* of PAP is most probably an autoimmune disease. There is growing evidence that anti–GM-CSF autoantibodies are involved in the pathogenesis of idiopathic PAP. Neutralizing anti–GM-CSF autoantibodies develop specifically in patients with PAP, reducing GM-CSF activity, and the result is the inhibition of alveolar macrophage differentiation and function with consecutive surfactant accumulation.

Laboratory tests are usually within normal ranges except for lactate dehydrogenases, which are increased. Latex agglutination test is a reliable method for detection of anti GM-CSF autoantibodies, but the test is not yet readily available.

Plain radiograph of the chest shows diffuse alveolar, mainly perihilar opacities, mimicking pulmonary edema (Figure 31.1). HRCT scan is highly specific as it often reveals the "crazy paving" pattern (Figure 31.2). Lung function tests show restrictive ventilatory changes and reduced DLco. Hypoxemia is more pronounced during exercise.

In most cases, the diagnosis is confirmed by bronchoalveolar lung lavage fluid cytological analysis, thus avoiding the need of lung biopsy. Macroscopically, the recovered lung lavage fluid shows milky appearance (Figure 31.3) and microscopically characteristic acellular globules, foamy macrophages, and a dirty background of cell debris (Figure 31.4a, b). Lung biopsy histopathological finding shows PAS-positive material within the alveoli (Figure 31.5).

In about 30% of patients with idiopathic PAP, spontaneous remission may be expected. If the symptoms are grave and impact daily life activities, whole lung lavage is the treatment of choice. Treatment with GM-CSF is still under investigation, and the initial results are encouraging.

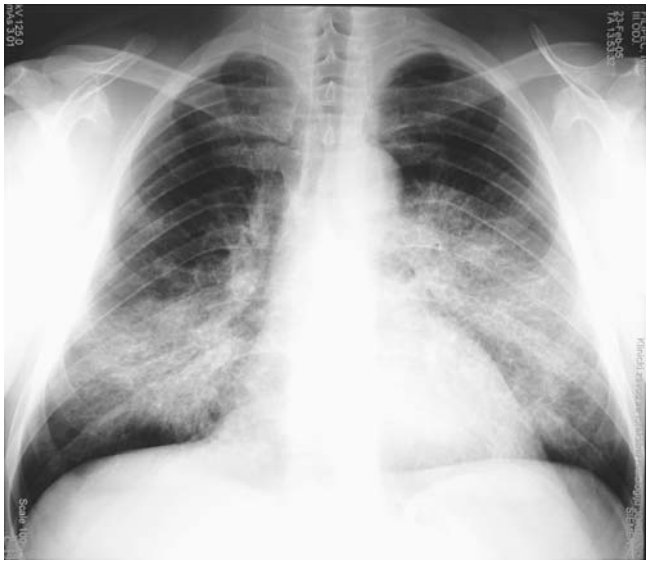

**Figure 31.1.** Plain radiograph of the patient with idiopathic pulmonary alveolar proteinosis shows diffuse reticulo-alveolar infiltrates, mimicking chronic pulmonary edema ("butterfly" or "bat wing" like). The patient was first diagnosed during an episode of pneumonia.

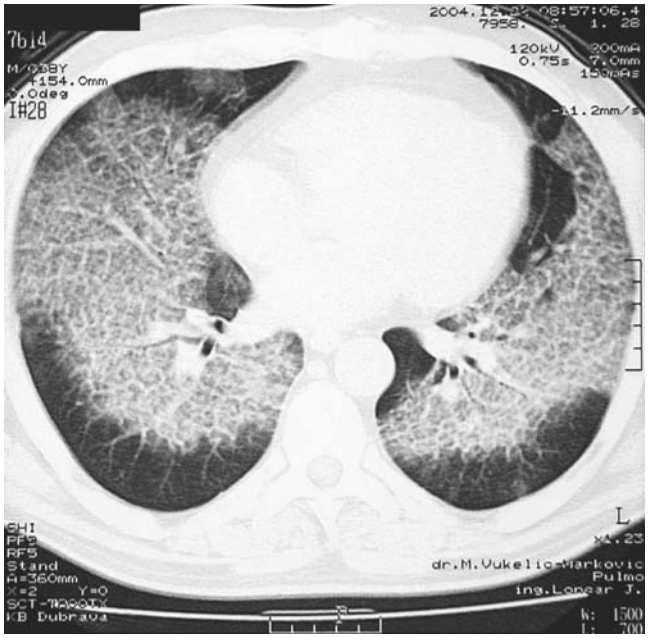


**Figure 31.2.** HRCT scan of the same patient reveals the thickened interlobular septa and ground-glass opacities in a "crazy paving" fashion, sharply demarked from normal lung creating a "geographic" pattern. As the patient is stable, physiological testing showed minimal restrictive ventilatory changes and reduction of $DL_{CO}$ with normal blood oxygenation; his quality of life satisfactory, the therapeutic whole-lung lavage procedure has not yet been advised.

**Figure 31.3.** Lung lavage macroscopically shows milky appearance of recovered fluid.

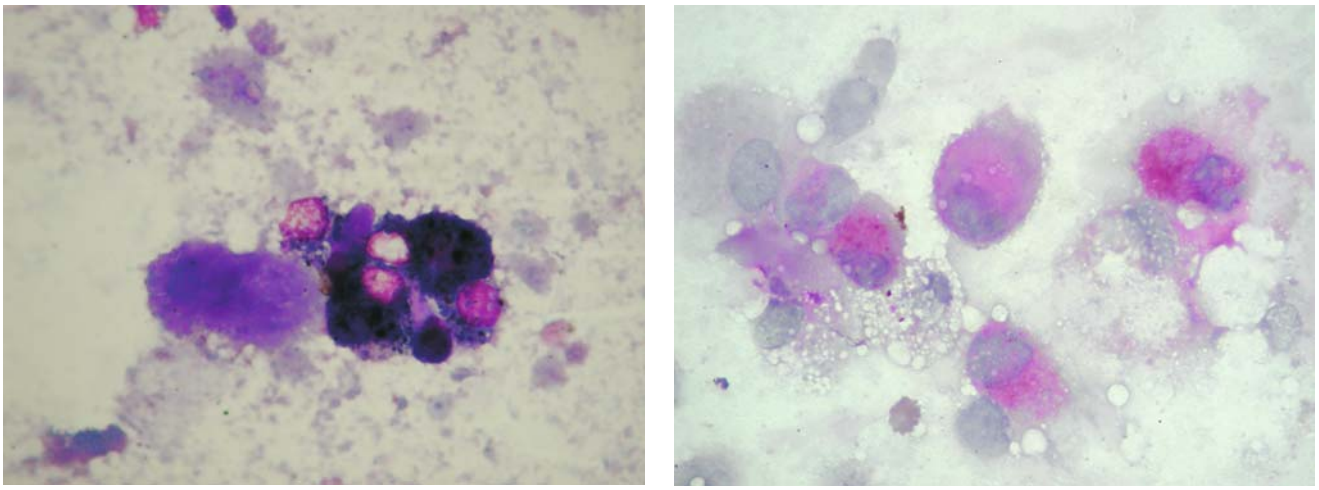

a b

**Figure 31.4.** Lung lavage microscopically shows characteristic acellular globules, some foamy macrophages, and a dirty background of cell debris. (Dirty background: cell debris, few macrophages.) BAL fluid cytology, original magnification ×1000, MGG stain (May-Grünwald-Giemsa) (a). PAS-positive macrophage. BAL fluid cytology, original magnification ×1000, PAS staining (b).

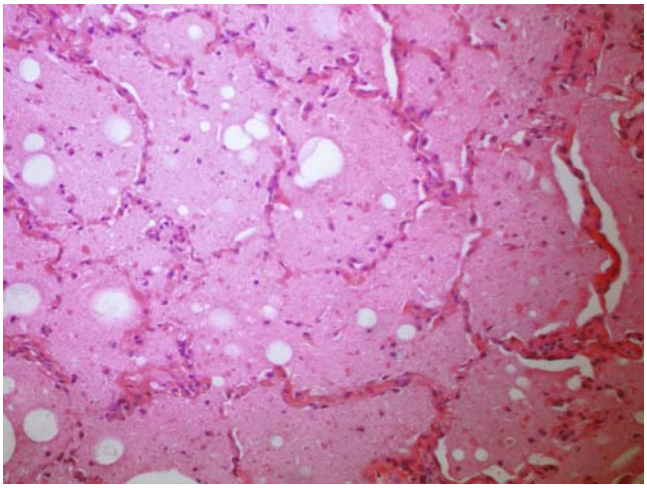

**Figure 31.5.** The alveolar spaces are filled with proteinaceous granular material. Alveolar septa are unremarkable.

## Bibliography


1. Trapnelli BC, Whitsett JA, Nakata K. Mechanisms of disease. Pulmonary alveolar proteinosis. N Engl J Med 2003;349:2527–2539.
2. Kitamura T, Uchida K, Tanaka N, Tsuchiya T, Watanabe J, Yamada Y, Hanaoka K, Seymour JF, Schoch OD, Doyle I, Inoue Y, Sakatani M, Kudoh S, Azuma A, Nukiwa T, Tomita T, Katagiri M, Fujita A, Kurashima A, Kanegasaki S, Nakata K. Serological diagnosis of idiopathic pulmonary alveolar proteinosis. Am J Respir Crit Care Med 2000;162:658–662.
3. Uchida K, Nakata K, Trapnell BC, Terakawa T, Hamano E, Mikami A, Matsushita I, Seymour JF, Oh-Eda M, Ishige I, Eishi Y, Kitamura T, Yamada Y, Hanaoka K, Keicho N. High-affinity autoantibodies specifically eliminate granulocyte-macrophage colony stimulating factor activity in the lungs of patients with idiopathic pulmonary alveolar proteinosis. Blood 2004;103:1089–1098.
4. Johkoh T, Itoh H, Muller NL, Ichikado K, Nakamura H, Ikezoe J, Akira M, Nagareda T. Crazy-paving appearance at thin section CT: Spectrum of disease and pathologic findings. Radiology 1999;211:155–160.

# 32

# Lymphangioleiomyomatosis

Pulmonary lymphangioleiomyomatosis (LAM) is rare. Its cause is not known, and it principally affects women during the childbearing years. LAM occurs sporadically (not as an inherited disease) or it can be one manifestation of tuberous sclerosis (one third of patients have LAM), which is an inheritable multiorgan hamartomatosis.

The underlying lesion that characterizes the disease is the diffuse proliferation of peribronchial, perivascular, and perilymphatic smooth muscle cells resulting in vascular and airway obstruction, cyst formation, and recurrent pneumothoraces (Figure 32.1a, b, c). Extrapulmonary manifestations include lymphadenopathy, angiomyolipomas, and benign tumors, most frequently of the kidney (one third of patients).

*Characteristic symptoms* are progressive dyspnea, cough, and recurrent pneumothoraces; less frequent are hemoptysis and chyloptysis. In the course of the disease, chylous pleural effusion can be found, unilateral or bilateral, but not as often as previously thought occurring, in only 10% of the patients.

The cellular and proliferating LAM cells are associated with increased expression of TGF-β1 and related extracellular matrix proteins. TGF-β is a potent cytokine that promotes mesenchymal cell proliferation and regulates the synthesis of extracellular matrix components, particularly fibronectin. The smooth muscle cells in the disease also have an affinity to HMB45, a monoclonal antibody with specific immunoreactivity for malignant melanoma (Figure 32.1d).

*What causes LAM* remains a mystery. The female preponderance indicates that the disease may be modulated by sex steroids. Oral contraceptives often contribute to the progression of the disease. Tissue from patients with LAM often, but not always, expresses estrogen and progesterone. Cells from involved tissue grown in culture show mitogenic response to estradiol.

*Diagnostic procedure* includes chest radiographic analysis, lung function testing, and open lung biopsy. In the early phase of the disease, chest radiographs show hyperinflation, reticular or linear interstitial bibasilar pattern, including Kerley-B lines due to expansion of lymphathic vessels, small nodules that probably represent hyperplastic aggregates of LAM cells (Figure 32.2a), and sometimes pleural effusion. HRCT scans are typical, cysts and nodes in the early phase (Figure 32.2b), and in the advanced phase the cysts increase in number and size (2–10 mm) (Figure 32.3a, b, c). There are other diffuse cystic diseases that can be confused with LAM (Table 32.1).

Pulmonary function tests reveal the combination of obstructive and restrictive changes, increased total lung capacity, residual volume, and reduced forced expiratory volume in the first second. DLco is reduced, with hypoxemia but rarely hypercapnia.

Recurrent pneumothoraces, chylothorax, and irreversible obstructive ventilatory changes in a never-smoking woman are of ultimate importance in differentiating LAM from other diseases with similar symptomatology. Lung biopsy shows characteristic histopathological pattern.

*Pulmonary LAM responds*, in selected cases, to oophorectomy, radioablation of the ovaries, or administration of progesterone, anti-estrogens, or androgens (Figure 32.4). Recurrence of the disease in the allograft after lung transplantation has been reported. The progression of the disease is common and the median survival is 8 to 10 years.

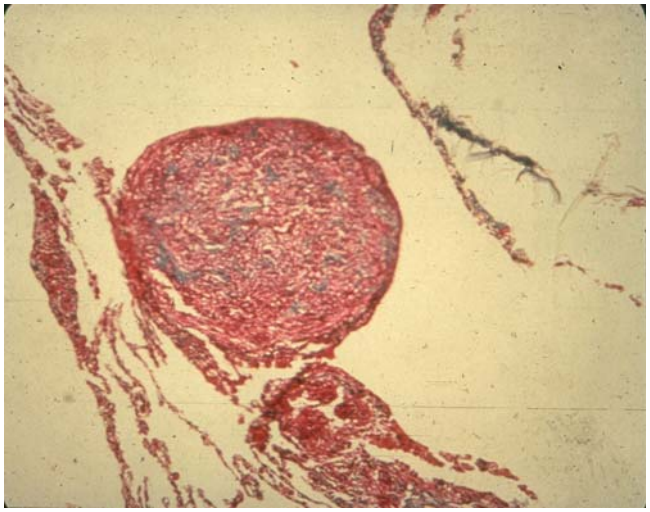

a

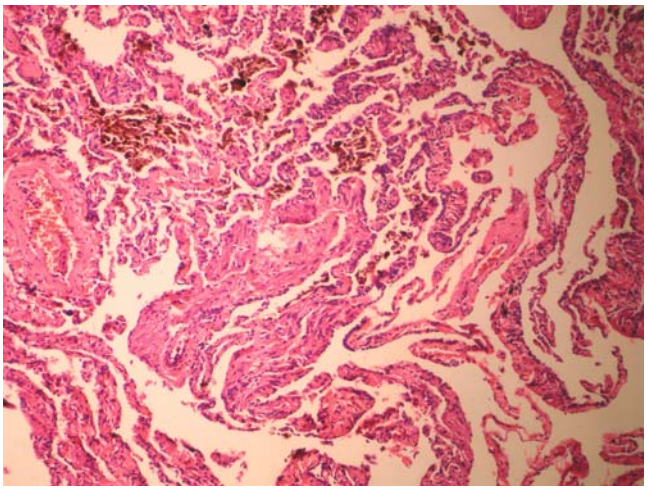

b

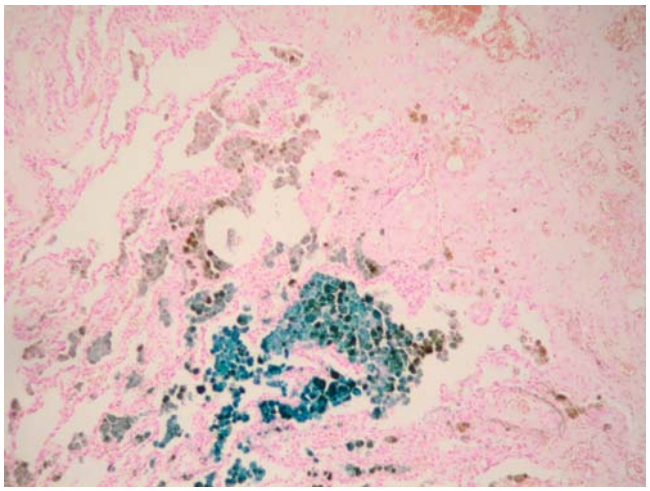

c

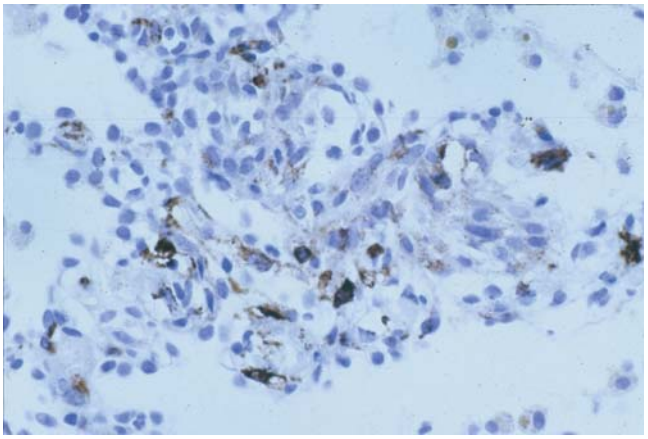

d

**Figure 32.1.** A lung biopsy specimen showing a typical LAM nodule. Nodule is composed of fusiform cells resembling smooth muscle cells (a). LAM cells infiltrating the walls of vessels causing hemorrhage (b). Alveolar spaces adjacent to LAM lesion contain hemosiderin-laden macrophages (Prussian blue stain) (c). A lung biopsy specimen shows a positive reaction with the monoclonal antibody HMB 45. LAM cells differ from normal smooth cells by the presence of a glycoprotein found in melanoma that reacts with a monoclonal antibody, HMB45 (d).

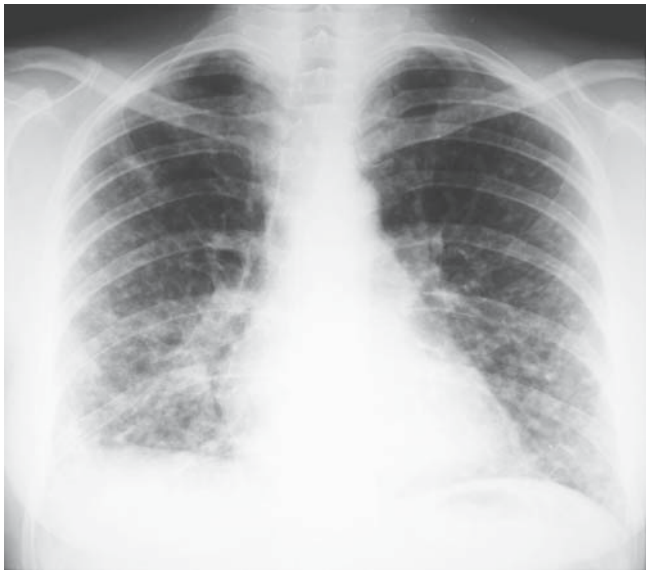

a

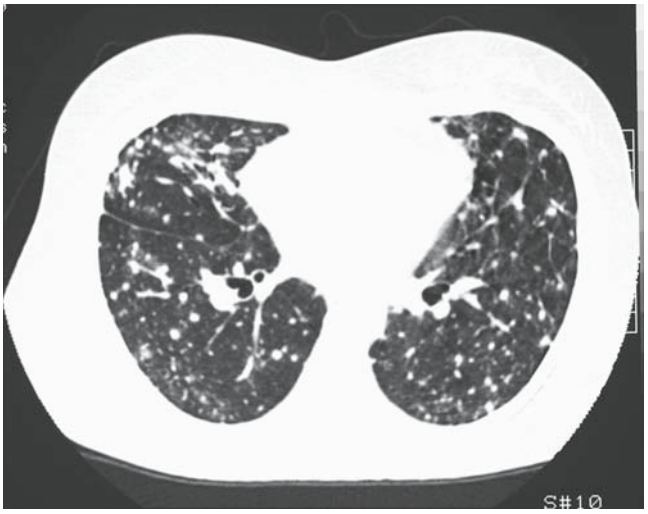


b

**Figure 32.2.** Recent onset LAM. Plain chest radiograph shows bilateral reticulonodular pattern, with majority nodules in the lung bases in a patient with recent onset of LAM (a) and multiple nodules with few thickened interlobular septa by HRCT scanning (b). The patient had few symptoms and at that moment did not require any therapy.

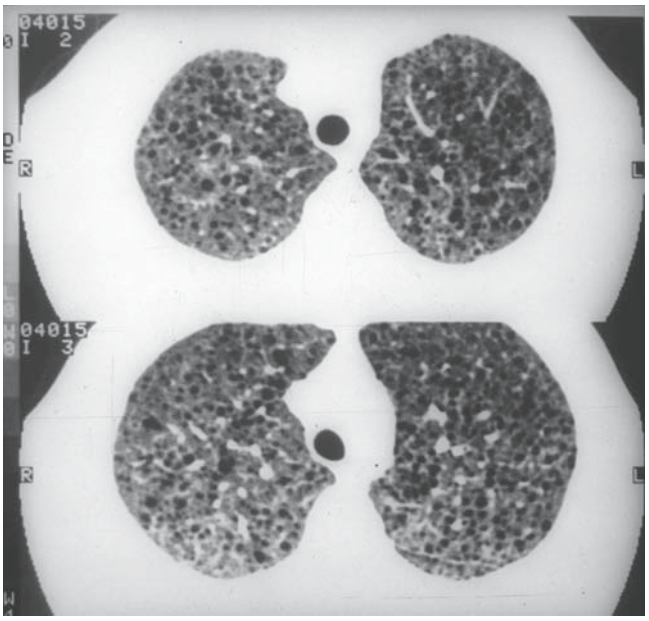


a

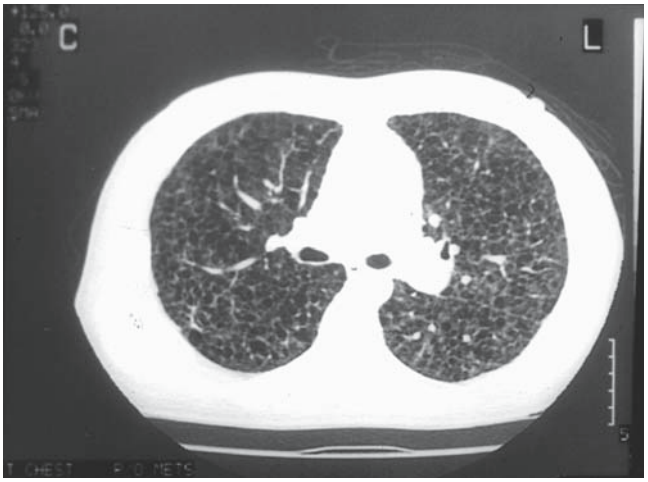


b

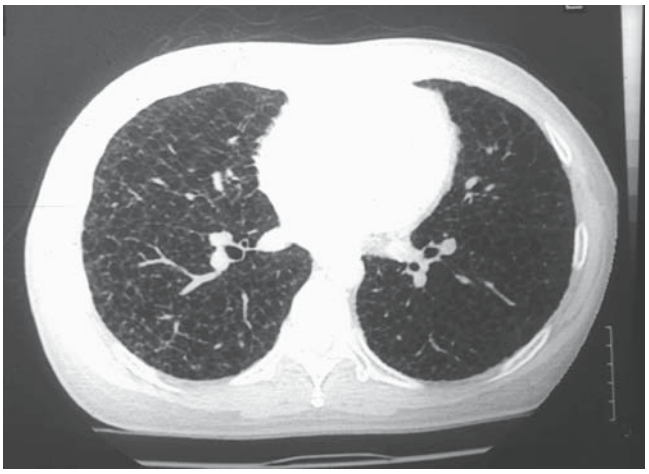

c

**Figure 32.3.** Advanced LA. CT scan of the lungs showing characteristic uniform cystic appearance of advanced case of LAM: (a) upper lobes; (b) middle lung fields; and (c) lower lung fields with discrete ground-glass opacifications in between the cysts. The number and the size of the cysts increase in craniocaudal direction.

**Table 32.1.** Causes of diffuse cystic and cavitary lung disease.

| |
|---|
| Pulmonary lymphangioleiomyomatosis |
| Pulmonary Langerhans cell histiocytosis |
| Honeycomb lung |
| Idiopathic pulmonary fibrosis |
| Connective tissue disease–related pulmonary fibrosis |
| Asbestosis |
| Chronic hypersensitivity pneumonitis |
| Advanced sarcoidosis |
| Bronchiectasis, diffuse |
| Metastatic disease (rare) |

From Ryu JH, Swensen SJ. Cystic and cavitary lung diseases: Focal and diffuse. Mayo Clin Proc 2003;78:744–752. Reprinted with permission from The Mayo Clinic College of Medicine, Rochester, MN, USA.

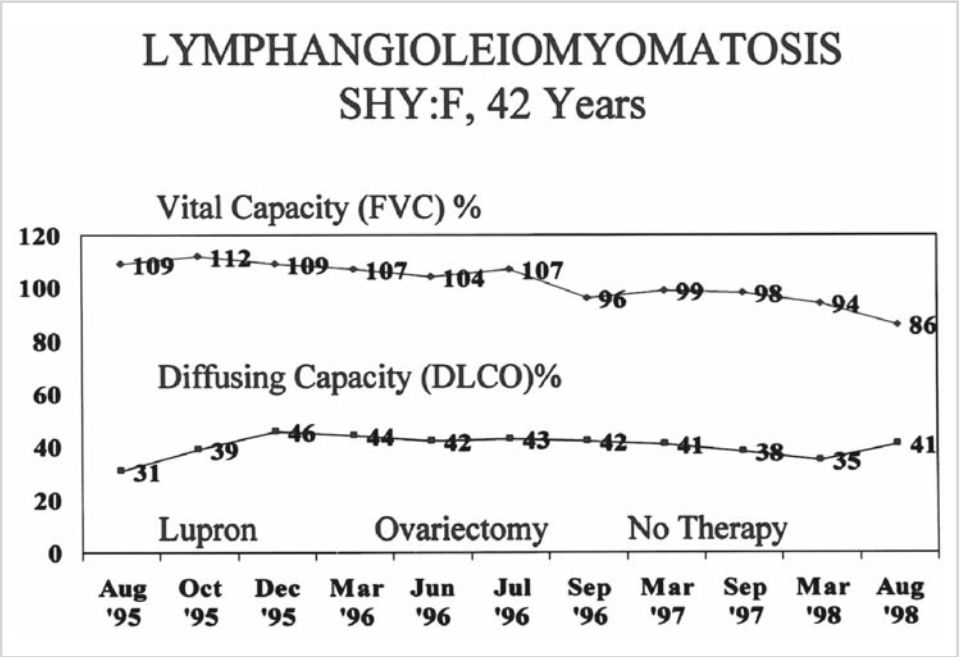


**Figure 32.4.** Clinical course of a 42-year-old Korean woman with biopsy-proved lymphangioleiomyomatosis. The patient was treated aggressively. Her disease has stabilized. Last seen in 2005, she was alive, had dyspnea, and was on supplemental oxygen.

## Bibliography

1. Glassberg M. Lymphangioleiomyomatosis. Clin Chest Med 2004;25:573–582.
2. Evans S, Colby T, Ryu T, Limper A. Transforming growth factor-beta 1 and extracellular matrix-associated fibronectin expression in pulmonary lymphangioleiomyomatosis. Chest 2004;125:1063–1070.
3. O'Brien J, Lium J, Parosa J, Deyoung B, Wick W, Trulock E. Lymphangioleiomyomatosis recurrence in the allograft after single-lung transplantation. Am J Respir Crit Care Med 1995;151:2033–2036.
4. Tanaka H, Imada A, Morikawa T, Shibusa T, Satoh M, Sekine K, Abe S. Diagnosis of pulmonary lymphangioleiomyomatosis by HMB45 in surgically treated pneumothorax. Eur Respir J 1995;8:1879–1882.
5. Kitaichi M, Izumi T. Lymphangioleiomyomatosis. Curr Opin Pulm Med 1995;1:417–424.
6. Ryu JH, Swensen SJ. Cystic and cavitary lung diseases: Focal and diffuse. Mayo Clin Proc 2003;78:744–752.

# 33

# Pulmonary Langerhans Cell Histiocytosis

Pulmonary Langerhans cell histiocytosis (LCH; histiocytosis X, eosinophilic granuloma) belongs to the spectrum of the diseases that are characterized by uncontrolled proliferation and infiltration of various organs by Langerhans cells (LCs). It is a rare disease most commonly affecting adult cigarette smokers. Men and women are almost equally affected, although a slightly higher proportion of women has recently been reported, most frequently between the ages of 20 to 40 years. Pulmonary LCH may present as an isolated form of LCH or it can present simultaneously with other organ involvement.

Usually, the *symptoms* are mild at the onset of the disease, cough and chest pain occur and are followed by hemoptysis and dyspnea. Some 20% of patients are symptomless at the time of diagnosis. Symptoms of pneumothorax occur in 10% of patients. Apart from respiratory symptoms, there can be signs of bone affection (4–20% of all LCH patients; Figure 33.1), joints, skin, mediastinal lymph nodes, pituitary gland (cause of diabetes insipidus), central nervous system, spleen, and liver. Constitutional symptoms also occur. About one quarter of patients recover spontaneously, another one quarter have slowly progressive course, and the rest of about 50% persist in a stable state of the disease.

The *etiology* of pulmonary LCH is not known although 90% of patients are heavy smokers. Langerhans cells are a specific population of dendritic cells that after the exposure to inhaled antigens migrate from beneath the epithelium of the tracheobronchial tree to regional lymph nodes where they stimulate lymphocyte proliferation response. The effect of cigarette smoke on LC function is poorly understood. It is possible that smoke may induce the production of various cytokines that facilitate the local expansion of LCs. These pathologic LCs persist in peribronchial regions and may locally induce T-cell proliferation and inflammatory granulomatous lesions in pulmonary form of LCH.

*Diagnostic procedures* include chest radiographic examinations, lung function testing, and cytological and/or histopathological analysis. Mild anemia is sometimes detected, and peripheral eosinophilia is rare. Physiological abnormalities depend on the time of examination. At the onset of the disease, most often reduced DLco and restrictive ventilatory changes are found. Later in the course of the disease, residual volume (RV) increases because the air is trapped in the cysts, and obstructive or mixed ventilatory changes are observed. Impaired exercise performance is common.

Chest plain radiograph shows bilateral, symmetrical reticular, and micronodular opacities in upper and middle lung zones, with relative sparing of costophrenic angles (Figure 33.2a). Sometimes mediastinal lymphadenopathy and pneumothorax (Figure 33.3a, b) are demonstrated. HRCT scan is of utmost importance in the diagnosis of pulmonary LCH. The most characteristic finding is nodules and cysts in the upper lung zones with sparing of the lung bases. Cysts are of varying size, sometimes of bizarre shape (Figure 33.2c). In the advanced stage, the distortion of the parenchyma is seen, and cysts can fuse and give radiological appearance almost indistinguishable from emphysema (Figure 33.2b). The HRCT finding of nodules and bizarre cysts is pathognomonic for pulmonary LCH.

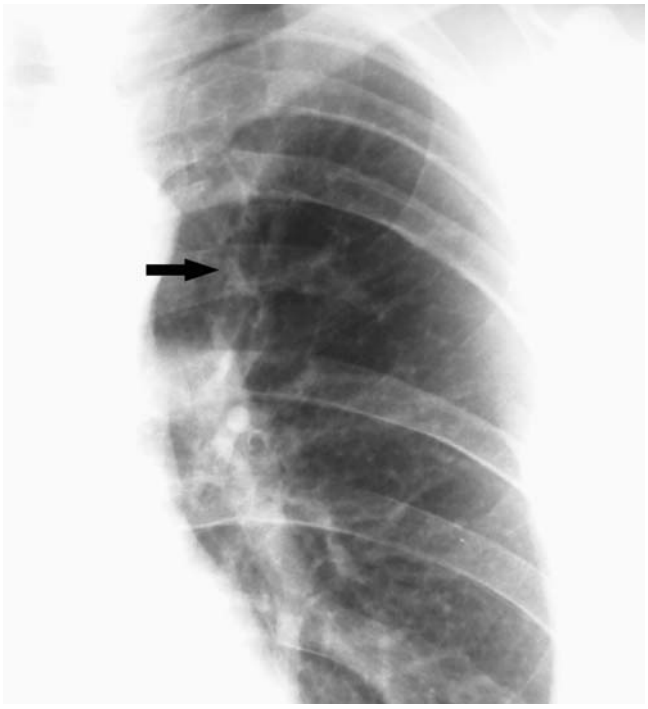

**Figure 33.1.** Plain radiograph showing absence of the part of the sixth rib on the left side; LCH was proven by the biopsy of the rib and that was the first sign of the disease.

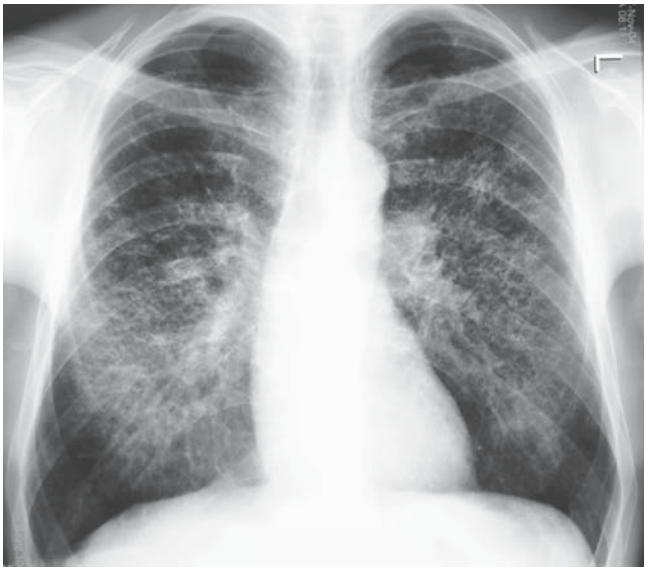

a

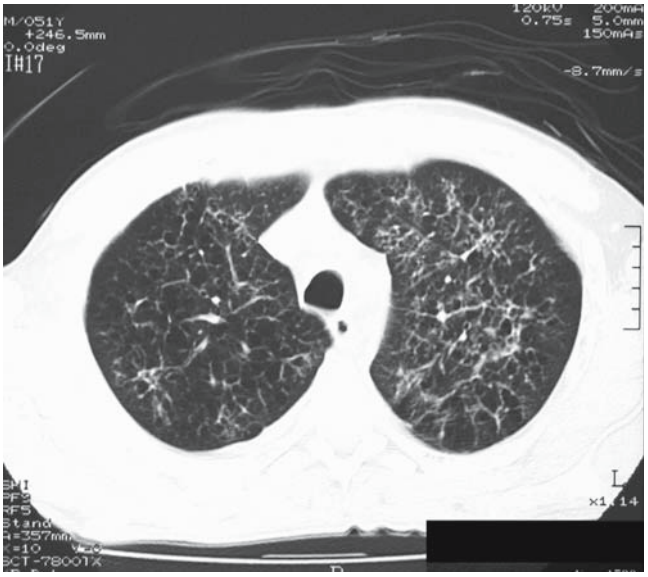


b

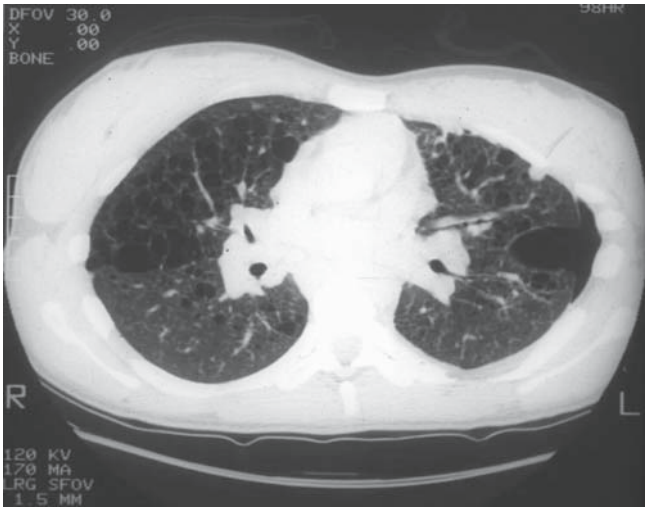


c

**Figure 33.2.** Plain chest radiograph shows predominantly reticular and minimal presence of micronodular pattern, with relative sparing of the bases and costophrenic angles. The mild increase of the lung volumes (hyperinflation) is noted, which is an unusual radiographic finding for most other fibrotic ILD (a). HRCT scan of the same patient shows thin-walled cysts with fibrosis and parenchymal distortion (b). CT scan of other patient showing multiple thin-walled cysts, some of bizarre shape (c).

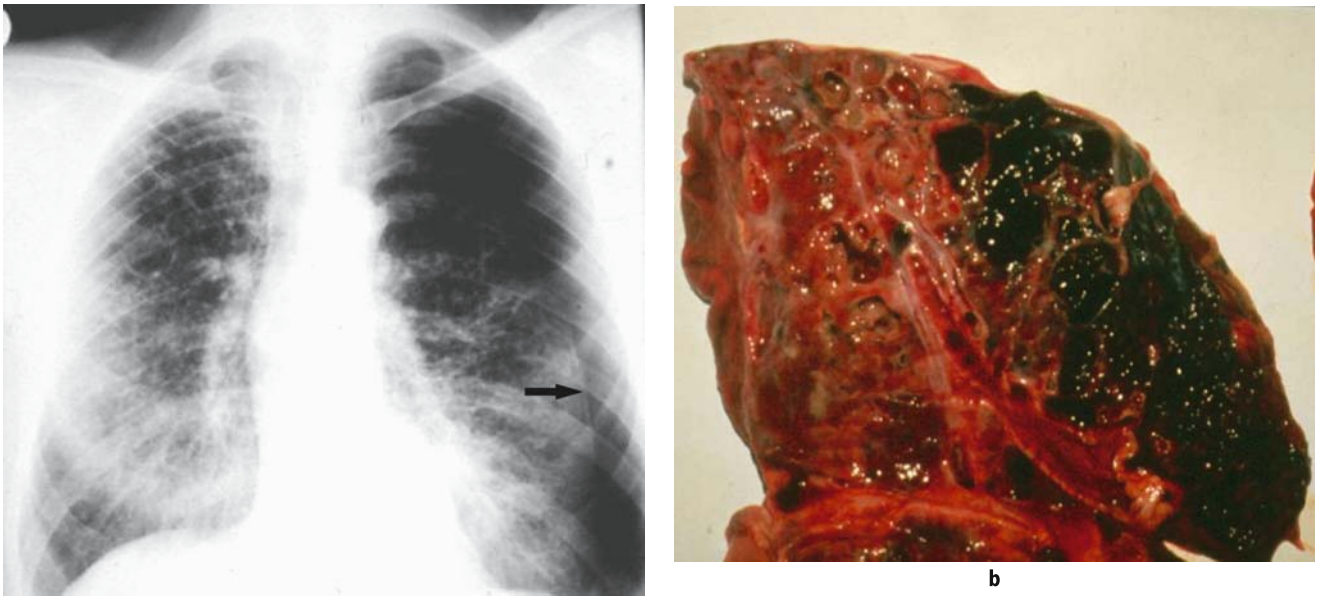

a b

**Figure 33.3.** Fatal LCH. Plain chest radiograph of a LCH patient who complained of severe abrupt dyspnea; the development of left-sided pneumothorax was confirmed. Cysts are seen in the upper lung lobes, predominantly in the right (a). The patient died and the postmortem appearance of the lungs is shown; the macrocysts and areas of hemorrhage are seen (b).

Bronchoscopy with transbronchial biopsy and bronchoalveolar lavage (BAL) is the usual procedure in most of the patients with suspected LCH, although the open lung biopsy is the gold standard procedure in most cases.

Transbronchial lung biopsy (TBB) is helpful in confirming the diagnosis in about 10–40% of cases. The lung lavage shows increased total cell count, alveolar macrophages, lymphocytes, neutrophils, and granulocytes. An increase of BAL $CD1a^{+}$ cells (Langerhans cells) of more than 5% is detected almost exclusively in pulmonary LCH; the specificity of the test is high, but the sensitivity is low (Figure 33.4). If the clinical features, HRCT finding, and histopathological analysis of TBB and BAL cytology are typical, pulmonary LCH can be diagnosed with these methods, which avoids open lung biopsy.

Characteristic histopathological findings early in the course of the disease are bronchiolocentric micronoduli, granulomas with preponderance of Langerhans cells, pig-

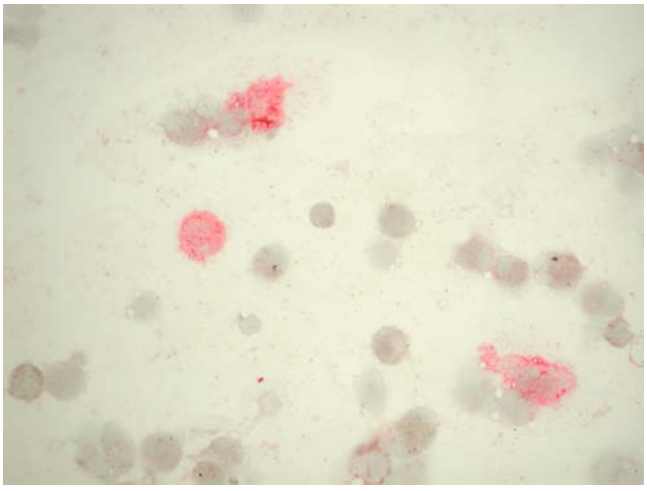

**Figure 33.4.** Lung lavage fluid is diagnostic for LCH if there is more than 5% of LCH cells; this patient had 6.6% of cells positively stained with CD1a monoclonal antibody. Positive LCH cells stained red (arrow). BAL fluid cytology, original magnification ×400, immunocytochemistry.

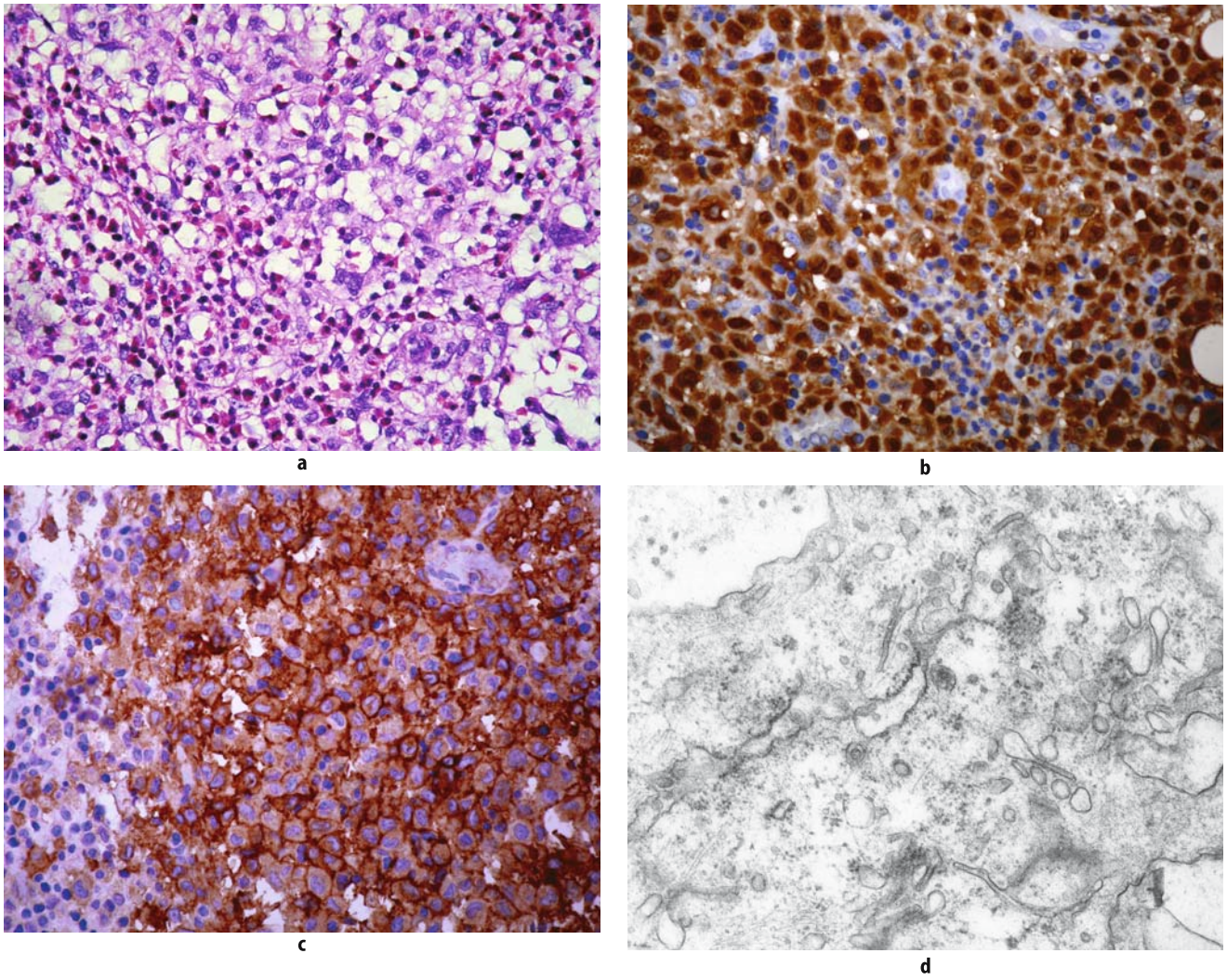


**Figure 33.5.** Pulmonary Langerhans cell histiocytosis: the admixture of eosinophils and Langerhans cells which have moderate cytoplasm and nuclear grooves (a); Langerhans cells are S-100+ (b). Langerhans cells are CD1a positive (c). Electron microscopy identifies Birbeck granules in LCH (d).

mented macrophages, eosinophils, neutrophils, plasma cells, and fibroblasts. Langerhans cells could be diagnosed by light microscope (Figure 33.5a), but it is much more accurate to identify them by staining for the S-100 protein (Figure 33.5b) and CD1a antigen (Figure 33.5c). Electron microscopy is also helpful in identification of LCs (Figure 33.5d) but is seldom utilized. Later in the course of the disease, active granulomas are rare; the excavated noduli and cysts are seen. The mechanism of cyst formation is thought to be from centrilobular nodular excavation followed by progressive bronchiolar dilatation and supervening fibrosis. The terminal pattern includes fibrosis, cysts, and emphysema, predominantly in upper lung lobes.

In mild cases, the only *therapy* is smoking discontinuation, so it should be strongly encouraged. In some cases, particularly if the disease is not in the fibrotic phase, spontaneous remissions or stabilization have been reported. If there are symptoms that influence the quality of life, corticosteroids should be given and may be effective especially in the cases with nodular changes. A rapidly progressive disease has been sporadically treated with aggressive immunosuppressive therapy. In severe systemic disease, allogenic bone marrow transplantation has been efficient. Lung transplantation has successfully been conducted.

## Bibliography

1. Vassalo R, Ryu JH, Colby TV, Hartman T, Limper AH. Pulmonary Langerhans'-cell histiocytosis. N Engl J Med 2000;342:1969–1978.
2. Tazi A, Moreau J, Begeron A, et al. Evidence that Langerhans cells in Langerhans cell histiocytosis are mature dendritic cells: Importance of the cytokine microenvironment J Immunol 1999;16:3511–3515.
3. Sundar KM, Gosselin MV, Chung HL, Cahill BC. Pulmonary Langerhans cell histiocytosis. Chest 2003;123:1673–1683.
4. Auerswald U, Barth J, Magnussen H. Value of CD1-positive cells in bronchoalveolar lavage fluid for diagnosis of pulmonary histiocytosis X. Lung 1991;169:305–309.
5. Vassalo R, Ryu JH. Pulmonary Langerhans' cell histiocytosis. Clin Chest Med 2004;25:561–571.

# 34

# Paraproteinemias

Paraproteinemias are a group of multisystem disorders characterized by neoplastic proliferation of a single clone of immunoglobulin-producing plasma cells. These disorders are

1. Amyloidosis
2. Multiple myeloma
3. Waldenstrom macrogammaglobulinemia
4. Heavy-chain diseases
5. Monoclonal gammopathy of uncertain significance (MGUS)

## 34.1 Amyloidosis

Amyloidosis is a multisystem disease of unknown etiology characterized by extracellular deposition of amyloid, a complex protein-polysaccharide, in various tissues. About 20 types of fibrils have been found in the amyloid deposits. The disease, depending on the type of amyloid fibril, is divided into two clinical groups. Primary amyloidosis occurs in patients who have no evidence of an underlying cause; the amyloid fibrils consist mainly of immunoglobulin light chains. The heart, tongue, gastrointestinal tract, nerves, and skin (Figure 34.1) are the frequently affected organs in the primary amyloidosis. The widespread organ dysfunction results in nephrotic syndrome and renal failure, cardiomyopathy and conduction disturbances, intestinal malabsorption, carpal-tunnel syndrome, macroglossia, neuropathy, end-organ insufficiency of endocrine glands, capillary damage, and echymosis. Pulmonary amyloidosis can be classified as follows.

### 34.1.1. Tracheobronchial

The amyloid deposits in the walls of the tracheobronchial tree produce submucosal plaques and endobronchial nodules. On bronchoscopic examination, the submucosal plaques appear as smooth, shiny ridges, often causing bronchial narrowing. The patients with submucosal plaques usually present with dyspnea, stridor, or hemoptysis. The endobronchial lesions are polypoid, usually solitary, and occur only in major bronchi (Figure 34.2a, b, c); localized tumors of the lower respiratory tract are uncommon. Males are more commonly affected than females. A variant of tracheobronchial amyloidosis, tracheobronchiopathica osteoplastica is characterized by diffuse airway calcification.

### 34.1.2. Parenchymal Nodules

Parenchymal nodules appear as discrete small opacities, usually in the peripheral lung fields, and may vary in size up to 15 cm in diameter. One third of all the nodules

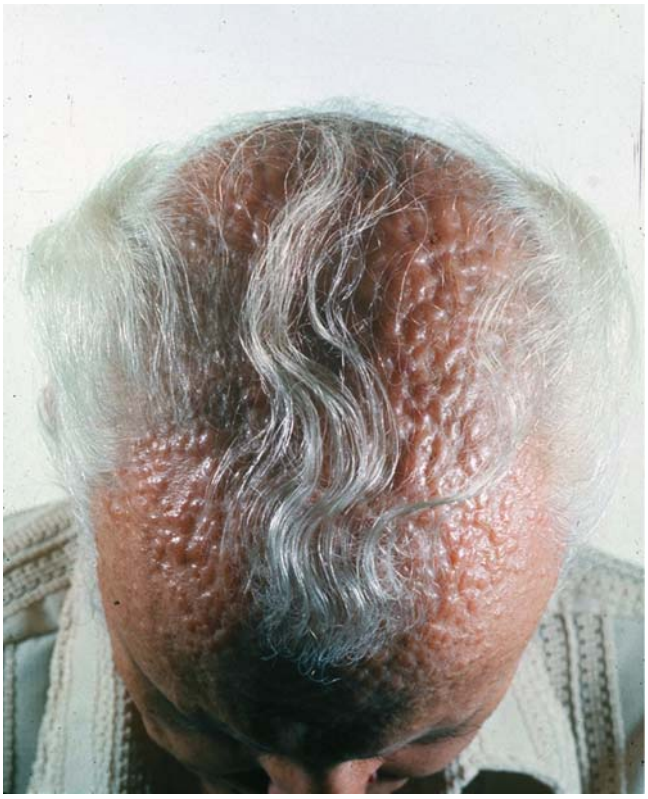

**Figure 34.1.** Multiple flat, translucent nodules on the scalp of the patient with amyloidosis. A skin biopsy showed amyloid material.

cavitate. Calcification when it occurs is described as stippled or cloud-like. Some of these nodules show increased activity on positron emission tomography (PET) using fluorodeoxyglucose (FDG).

### 34.1.3. Diffuse Alveolar Amyloidosis

Diffuse alveolar-interstitial pulmonary involvement is usually associated with systemic amyloidosis. In 1979, Kanada reviewed 12 patients with diffuse interstitial amyloidosis. All patients had dyspnea, and four had dry cough. The chest roentgenograms showed diffuse reticulo-nodular or interstitial pattern (Figure 34.3). Lung function abnormalities included a restrictive pattern with marked impairment of gas transfer. Diffuse interstitial involvement usually leads to death due to respiratory insufficiency within 6 weeks to 2 years (Figure 34.4). HRCT may reveal perilymphatic nodules mimicking sarcoidosis, military tuberculosis, disseminated histoplasmosis, and coccidioidomycosis.

### 34.1.4. Hilar and Mediastinal

Amyloidosis may cause unilateral or bilateral hilar adenopathy and may mimic sarcoidosis, lymphoma, primary tuberculosis, and coccidioidomycosis (Figure 34.5).

### 34.1.5. Pleural Involvement

Involvement of pleura is rare in amyloidosis, and when it occurs, it is usually associated with diffuse interstitial lung disease (Figure 34.6a, b).

The diagnosis of primary amyloidosis should be entertained in patients with unexplained proteinuria, congestive heart failure, peripheral neuropathy, macroglossia, tra-

cheobronchial nodules, interstitial lung diseases, pulmonary or pleural nodules, and hepato-splenomegaly. The diagnosis can be established by demonstrating amyloid fibrils in tissues. Lung biopsy specimens are highly specific and sensitive (Figure 34.7a, b). Biopsy of the gingival tissue, subcutaneous fat-pad, and testis (Figure 34.7c) are also utilized.

Primary amyloidosis is incurable. Combination therapy with melphalan and prednisone can cause symptomatic improvement in a small number of cases. Colchicine is useful, but the effectiveness of dimethyl sulfoxide has not been established. Endobronchial lesions can be removed at bronchoscopy. Laser therapy is indicated for lesions causing airway obstruction. Local parenchymal lesions can be excised.

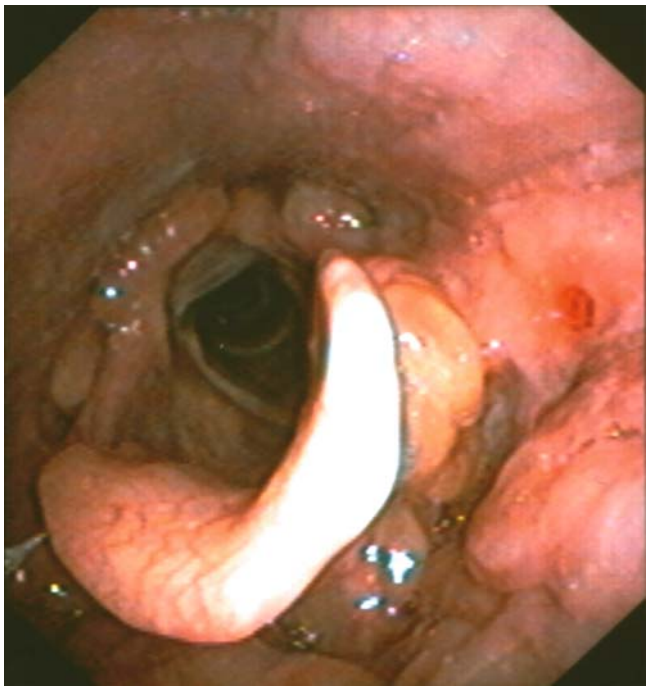

a

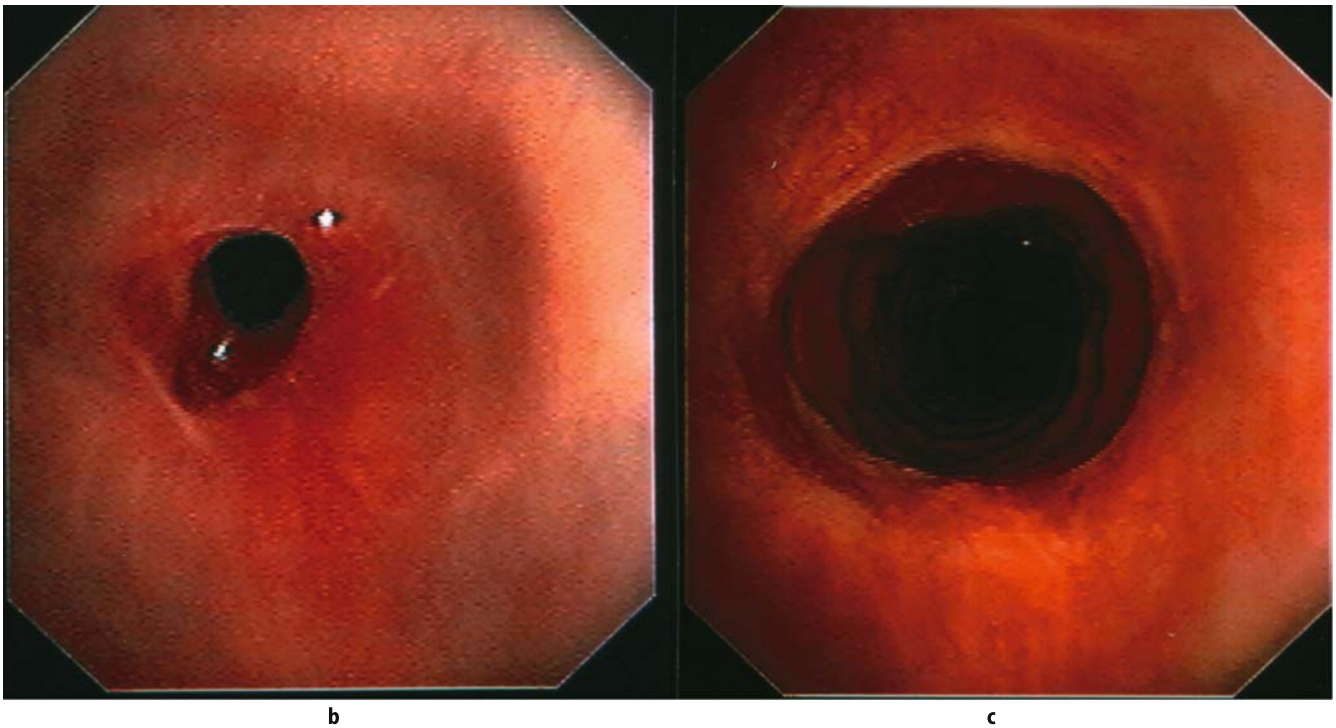

b c

**Figure 34.2.** Bronchoscopic finding of amyloid lesions of the upper respiratory tract (a) and trachea prior to (a) and following the surgical recanalization (c).

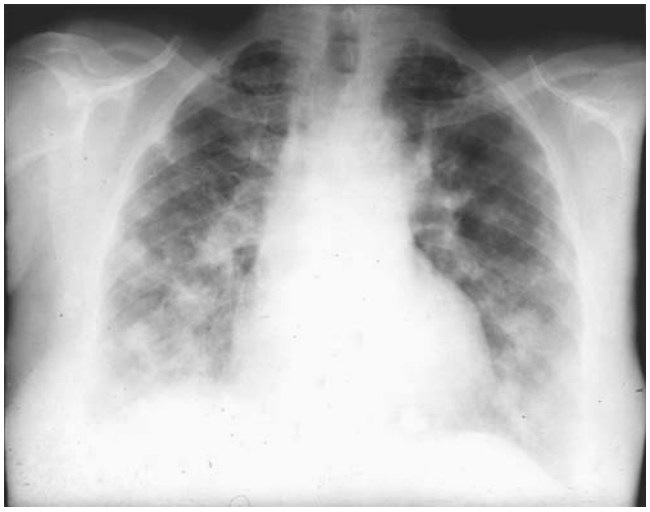

**Figure 34.3.** Diffuse mixed alveolar interstitial pattern on plain radiogram in a patient with amyloidosis. This relatively rare occurrence has a poor prognosis.

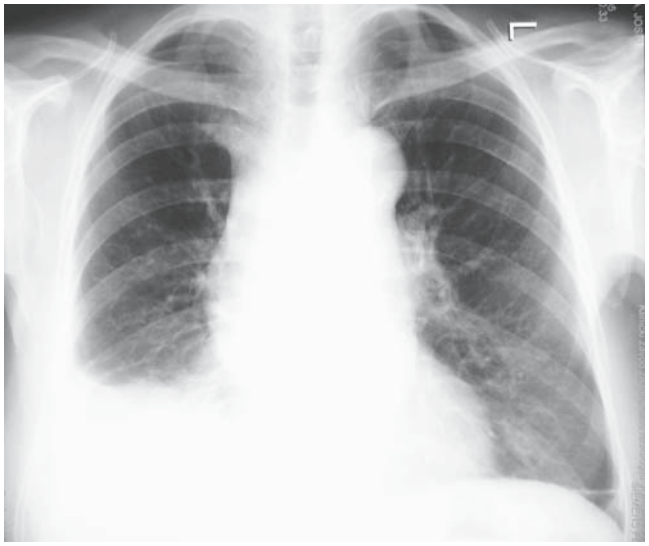

a

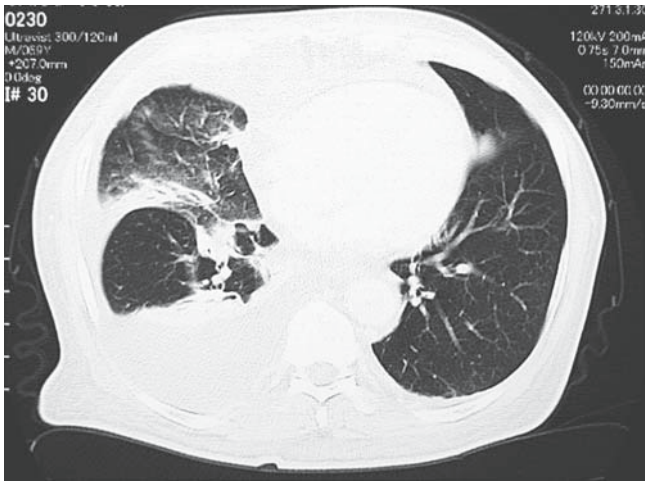


b

**Figure 34.6.** Plain radiograph in a patient with pulmonary amyloidosis with gross endoluminal affection of upper and lower respiratory tract and pleural effusion (a). HRCT scan of the same patient; the pleural effusion is seen on the right side with peribronchovascular fibrosis with retraction and consolidation (b).

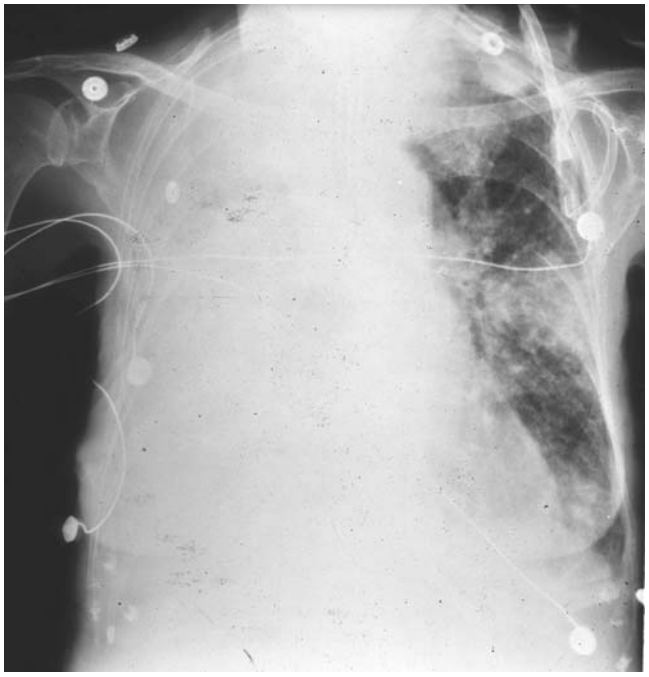

**Figure 34.4.** Total replacement of the right lung by amyloid tissue in an elderly man. Discrete reticular interstitial pattern and macronodular infiltrates on the left side. The diagnosis was made by transbronchial biopsy.

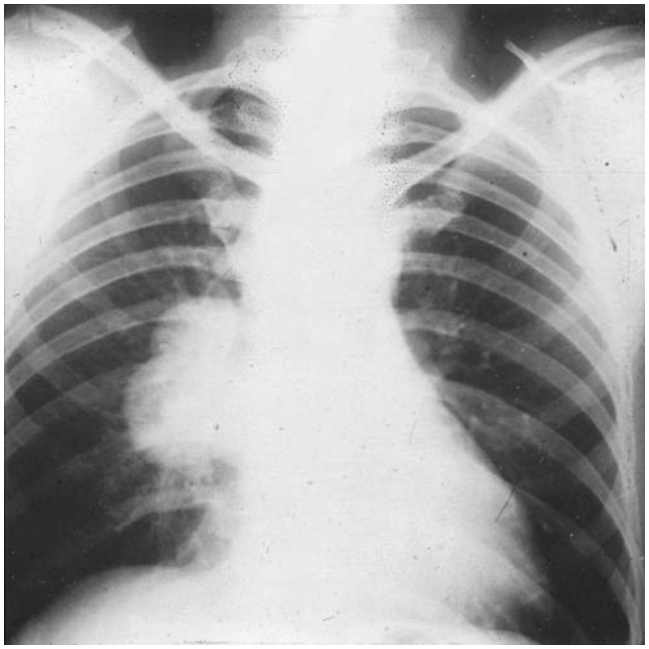

**Figure 34.5.** Unilateral hilar adenopathy in a patient with amyloidosis.

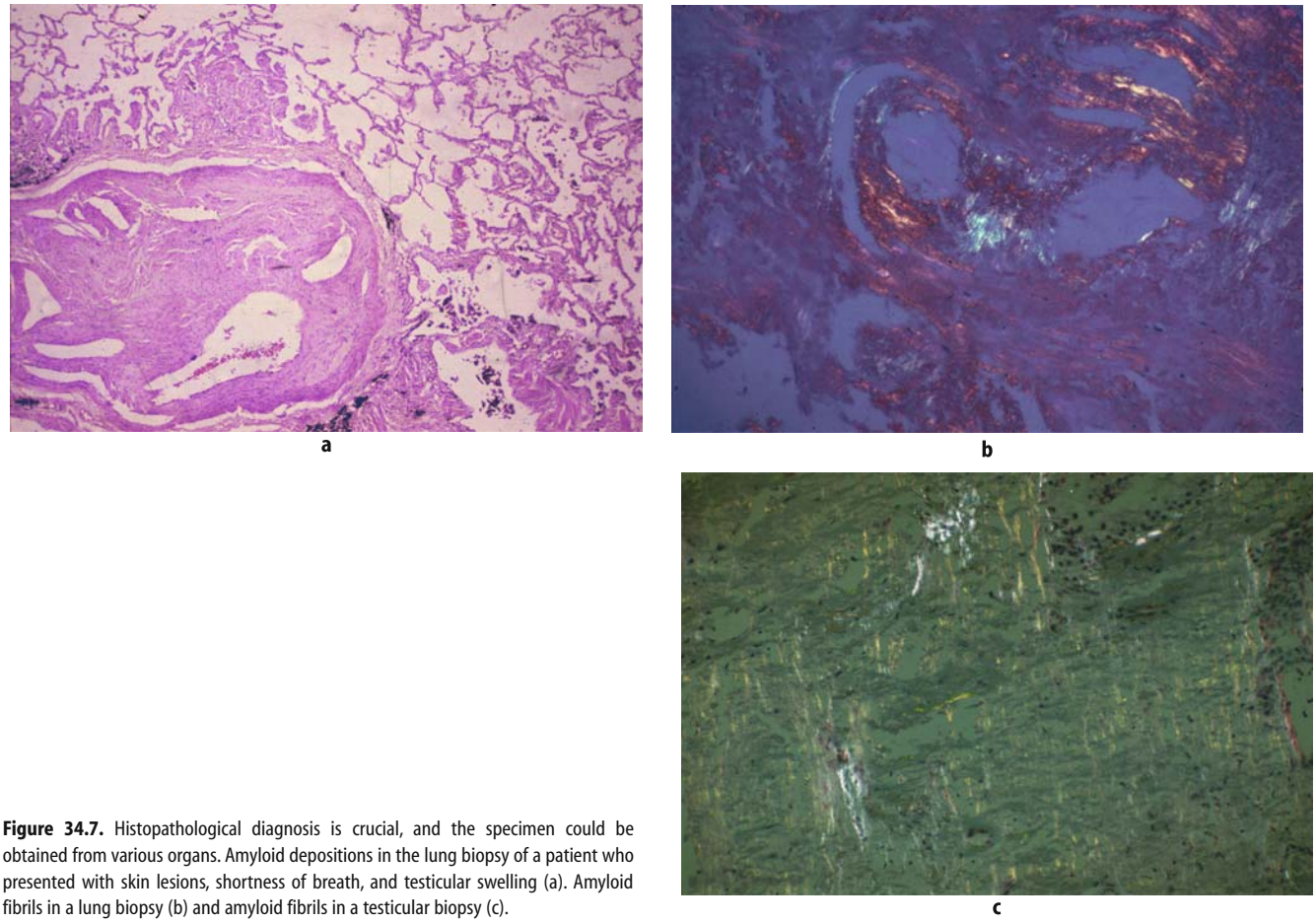

**Figure 34.7.** Histopathological diagnosis is crucial, and the specimen could be obtained from various organs. Amyloid depositions in the lung biopsy of a patient who presented with skin lesions, shortness of breath, and testicular swelling (a). Amyloid fibrils in a lung biopsy (b) and amyloid fibrils in a testicular biopsy (c).

## 34.2. Multiple Myeloma

Multiple myeloma is a neoplastic proliferation of plasma cells in the bone marrow and occasionally in other organs, such as the liver, spleen, and lymph nodes. The incidence of multiple myeloma is 3.6 per 100,000 population. It is slightly more common in men than in women, occurring mainly in the late middle age. Less than 2% of the cases have been reported in younger patients.

Thoracic myelomatosis is common and can manifest in the following ways.

### 34.2.1. Involvement of the Thoracic Cage

Multiple myeloma is the most common tumor to involve the vertebrae, ribs, clavicles, sternum, and scapula. Of the thoracic wall structures, ribs are the most frequently involved. In a study of 958 patients with multiple myeloma, 28% were found to have involvement of the thoracic cage, and 25% of the lesions were present on the initial chest roentgenogram. Osteolytic rib lesions may be single or multiple.

### 34.2.2. Plasmacytoma

Primary pulmonary plasmacytomas are rare. When they occur, they may cause airway obstruction. The treatment of choice remains surgical resection. Pleural involvement is rare.

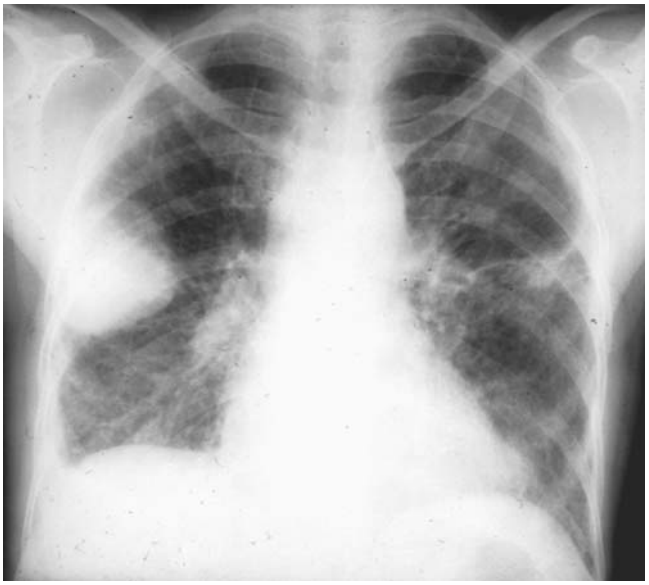

**Figure 34.8.** A posterio-anterior view of the chest showing a plasmocytoma against pleura in the right lung. The peripheral polycyclic macronodular lesion is seen in the middle lung field on the right side with the minimal pleural effusion.

### 34.2.3. Lung Parenchymal Involvement

A solitary homogenous mass (Figure 34.8), multiple nodules, and diffuse infiltration are some of the manifestations of the myeloma lung. These lesions cause wheezing, dyspnea, and cough. Parenchymal lesions may remain asymptomatic or produce cough, chest pain and dyspnea. Most patients when first seen are asymptomatic. Cough may be the earliest symptom. Pulmonary infiltrates may be segmental, lobar, or diffuse resembling bronchopneumonia. A rare parenchymal manifestation is calcinosis. It occurs in the presence of hypercalcemia and hyperphosphatemia

### 34.2.4. Pulmonary Infections

*Streptococcus pneumoniae* and Gram-negative organisms are the most common cause of pneumonia in patients with multiple myeloma. In these patients, ability to form humoral antibodies is impaired, whereas cell-mediated immunity remains intact.

Most of the patients die of renal failure or pulmonary infection. The patients with 1 or 2 plasmacytomas have the best prognosis. In general, the median survival is 2 to 3 years with treatment. Pulmonary embolism is the cause of death in 3% of the patients.

## 34.3. Waldenstrom Macrogammaglobulinemia

Waldenstrom macrogammaglobulinemia is characterized by monoclonal immunoglobulin M (IgM) gammopathy and plasmacytoid infiltration of the bone marrow. The disease has a slight familial preponderance, particularly if it occurs in elderly men. The clinical features include anemia, bleeding, lymphadenopathy, and hyperviscosity syndrome due to high IgM levels. The features of hyperviscosity syndrome are bleeding, purpuric spots, and retinopathy. Pulmonary involvement occurs in as many as 20% of the patients with Waldenstrom macrogammaglobulinemia. Dyspnea and cough are the common presenting symptoms; however, half of the patients remain asymptomatic. Characteristically, the chest roentgenogram shows a diffuse reticulo-nodular pattern, which is usually present at the time of initial diagnosis. Other radiographic abnormali-

ties include single or multiple masses and patchy consolidation. As many as 50% of the patients with Waldenstrom macrogammaglobulinemia have pleural effusions.

The lung biopsy specimens show lymphocytic and plasmacytoid infiltration. Pleural fluid generally contains the same monoclonal protein as found in the serum.

Pulmonary manifestations of Waldenstrom macrogammaglobulinemia respond to alkylating agents or radiotherapy.

## 34.4. Heavy-Chain Diseases

Heavy-chain diseases are malignant plasma cell disorders that produce excessive amounts of defective immunoglobulin consisting of abnormal heavy chains without light chains. Four types of heavy-chain diseases are described: alpha (IgA), gamma (IgG), mu (IgM), and delta (IgD). The diagnosis is established by demonstrating the presence, in urine or serum, of a protein component that reacts to antisera to heavy chain but not to light or Fab fragments.

Alpha heavy-chain disease is the most common and occurs in two forms. The first one, also known as Mediterranean lymphoma, presents with chronic diarrhea, malabsorption, and abdominal masses. The pulmonary form is less common and is characterized by the presence of pulmonary parenchymal infiltrates and enlarged mediastinal nodes. Dyspnea or recurrent infections is the presenting symptom.

In IgG heavy-chain disorder, enlargement of mediastinal lymph nodes is common. These patients are elderly. Splenomegaly is frequent. Anemia, thrombocytopenia, and eosinophilia are often present. Pulmonary infections are common and the cause of death in most patients within 1 year of diagnosis.

## 34.5. Monoclonal Gammopathy of Uncertain Significance

The diagnosis of MGUS is based on finding a monoclonal spike on a serum protein electrophoresis consisting of kappa or lambda chain. The incidence of MGUS increases with age and may approach 3% in persons 70 years of age or older. About one third of the patients with apparently benign monoclonal gammopathy develop lymphoid malignancies. Hilar and mediastinal adenopathy may occur; pulmonary infiltration is rare. Prognosis is favorable if the concentration of homogenous hemoglobulin is less than 2 g/dl, if there is no increase in immunoglobulin concentration from time of diagnosis, if there is no decrease in concentration of normal immunoglobulin, if the light chains are absent in the urine, and if serum albumin and serum hematocrit are normal.

## Bibliography


1. Howard M, Ireton J, Daniels F, Langton D, Manolitas N, Fogarty P, McDonald CF. Pulmonary presentations of amyloidosis. Radiology 2001;6:61–64.
2. Ollenberger G, Simon K, Andrews T. False-positive FDG positron emission tomography in pulmonary amyloidosis. Clin Nucl Med 2004;29:657–658.
3. Kanada D, Sharma O. Long-term survival with diffuse interstitial pulmonary amyloidosis. Am J Med 1979;67:879–882.
4. Kintzer J, Rosenow E, Kyle R. Thoracic and pulmonary abnormalities in multiple myeloma: A review of 958 cases. Arch Intern Med 1978;138:727–730.
5. Yokote T, Akioka T, Miyamoto H, Oka S, Hara S, Yamano T, Takasu T, Tsuji M, Hanafusa T. Pulmonary parenchymal infiltrates in a patient with CD20-positive multiple myeloma. Eur J Haematol 2005;74:61–65.
6. Reichenberger F, Heberlein J, Muller A, Wirtz H, Schauer J. Pulmonary Infiltrate, pleural Effusion and IgM macrogammaglobulinemia. Pneumologie 2004;58:33–35.
7. Okuda M, Okuda Y, Ogura T, Kashio M, Masuno T, Oji Y, Miyahaki M. Primary lung involvement with amyloid deposition in Waldenstrom's macrogammaglobilinemia: Observations from over 20 years. Respirology 2004;9:4–8.

8. Wahner-Roedler D, Witzig T, Loehrer L, Kyle R. [gamma]-Heavy Chain Disease: Review of 23 cases. Medicine 2003;82:236–250.
9. Kyle R, Therneau T, Rajkumar V, Larson D, Plevak M, Melton J. Long-term follow-up of 241 patients with monoclonal gammopathy of undetermined significance: The original Mayo Clinic series of 25 years later. Mayo Clinic Proceedings 2004;79:859–866.
10. Sharma A, Fried J, Sharma O. Monoclonal gammopathy of undetermined significance in sarcoidosis. Sarcoidosis 1992;9:70–72.

# 35

# Liver-Lung Relationship

The lungs and liver can be simultaneously involved in many infections, for instance, tuberculosis, brucellosis, Q fever, and histoplasmosis; granulomatous disease, such as sarcoidosis; and genetic anomaly, such as alpha-1 antitrypsin deficiency. Autoimmune diseases may involve both organs. A disease may start in the lung but be diagnosed because of hepatic involvement (e.g., cancer from the lung) or the illness may start in the liver but be recognized because of the pleuro-pulmonary expression (e.g., amebiasis). Some of the common liver-lung relationships are described below (Table 35.1).

## 35.1. Hyperventilation and Cirrhosis

Hyperventilation is a common respiratory manifestation of cirrhosis. Arterial hypoxemia may be the cause in some patients, but often the degree of hyperventilation is greater than one could expect based on the degree of arterial hypoxemia. Elevated ammonia levels and chronic interstitial lung edema related to decreased intravascular oncotic pressure play a role.

## 35.2. Hepato-pulmonary Syndrome

Hepato-pulmonary syndrome is a clinical triad of advanced liver disease, intrapulmonary vascular dilatations in the absence of a primary cardiopulmonary disease, and hypoxemia. The hypoxemia results from low ventilation-perfusion ratios in areas of precapillary/capillary dilatations and anatomic shunting through microvascular arteriovenous communications. A reduction in transfer factor is related to the thickening of the small veins and capillaries by a layer of collagen. The vasoactive substances that induce pulmonary vasodilatation are not precisely known, but the list includes nitric oxide (NO), endothelin-1, and arachidonic acid and its metabolites.

## 35.3. Porto-pulmonary Hypertension

As many as 20% of patients with advanced liver disease have mean pulmonary artery pressure of more than 25 mm Hg. The causes include hyperdynamic circulation, increased blood volume, and nonembolic pulmonary vasoconstriction/obliteration. The latter process is termed *porto-pulmonary hypertension*. The histological findings include medial and intimal hypertrophy, endothelial proliferation, and plexogenic/fibrotic changes.

**Table 35.1.** Pulmonary complications of liver diseases.

| Structure | Illness |
|---|---|
| Pulmonary circulation | Hyperventilation |
| | Hepato-pulmonary syndrome |
| | Porto-pulmonary hypertension |
| Lung parenchyma | bronchitis, bronchiectasis |
| | BOOP; LIP; NSIP; UIP |
| | Basal atelectasis |
| | Chest x-ray infiltrate |
| | Raised diaphragms |
| Pleura | Hydrothorax |
| | Chylothorax |
| | Thoracobiliary fistula |

## 35.4. Pleural Effusions

Pleural effusions, unilateral or bilateral, occur in about 10% of the patients with advanced liver disease. These transudative effusions are frequently right-sided in location and rarely occur in the absence of ascites. Nevertheless, pleural effusion may develop in the patient without clinically evident ascites. Negative pleural space pressure generated with inspiration draws in the ascitic fluid through small diaphragmatic defects called Lieberman pores.

## 35.5. Alpha-1 Antitrypsin Deficiency

Alpha-1 antitrypsin is synthesized in the rough endoplasmic reticulum of the liver. It comprises 80–90% of the serum alpha-1 globulin and is an inhibitor of trypsin and other proteases. The spectrum of alpha-1 antitrypsin deficient liver disease extends from asymptomatic liver involvement to severe liver disease requiring liver transplantation. Emphysema, the most common pulmonary manifestation of alpha-1 antitrypsin deficiency, affects predominantly the lung bases (Figure 35.1).

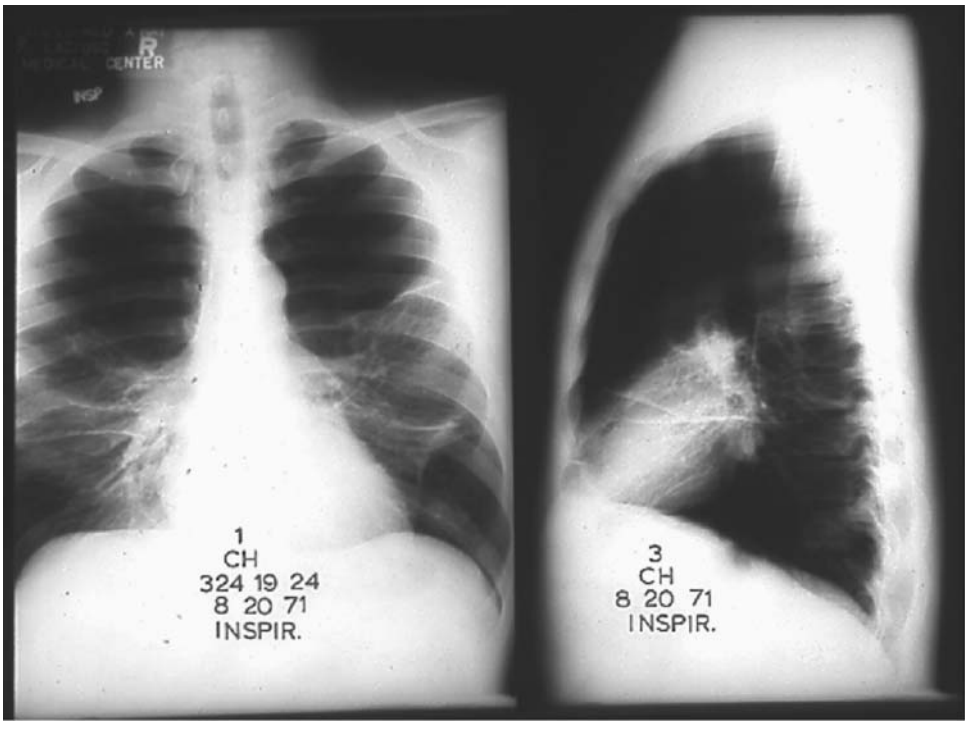


**Figure 35.1.** Posterior-anterior and lateral views of the chest of a 29-year-old man with a 17-year history of smoking. His alpha-1 antitrypsin level in the blood was 8 mg/dl (normal 180–240 mg/dl). Giant bullous emphysema is seen in the cranial half of the lung with the compression of the residual lung.

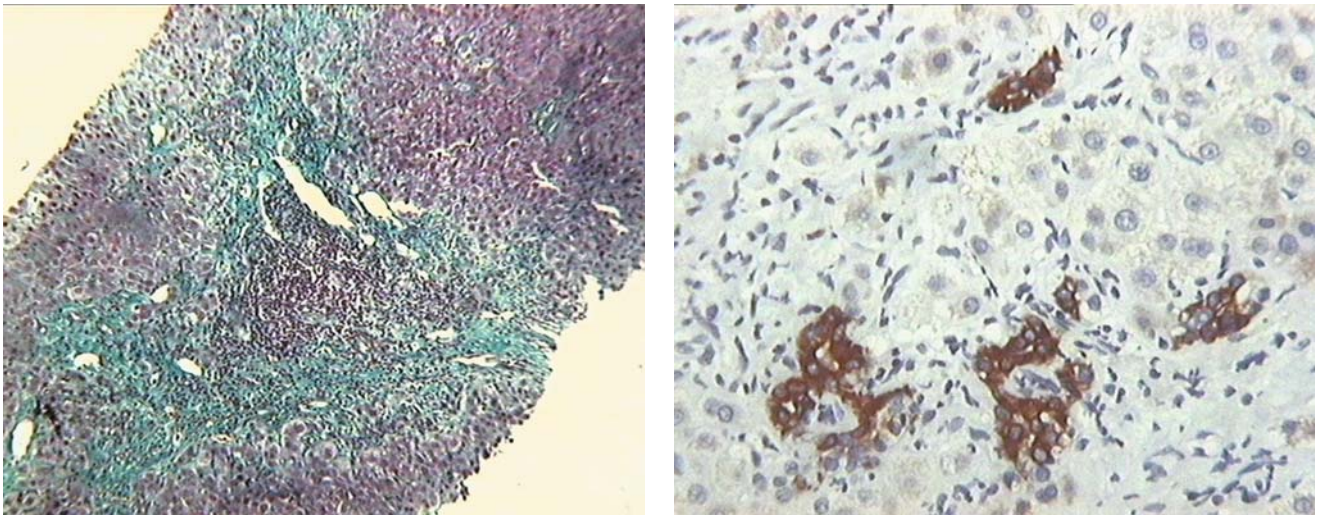

**Figure 35.2.** Biliary cirrhosis. Abundant connective tissue that surrounds the regenerative nodules (the pattern of cirrhosis). In a portal tract, an intense chronic infiltrate with mononuclear cells is seen, accompanied by the formation of aggregates. Abundant bile ductular proliferation is seen. Mallory stain (×6). Immunocytochemistry (a), cytokeratin 19 (b).

## 35.6. Primary Biliary Cirrhosis and Interstitial Lung Disease

Primary biliary cirrhosis (PBC) is a disease of unknown cause in which intrahepatic bile ducts are progressively destroyed (Figure 35.2a, b). T-helper cells and cytotoxic T cells play an important role in the pathogenesis. The true incidence of lung disease in PBC is very low. There are, however, many observations that point to the existence of subclinical or asympotmatic lung inflammation in these patients. In early stages of PBC, bronchoalveolar lavage may reveal lymphocytic alveolitis similar to that seen in the patients with sarcoidosis and Crohn disease. Gas transfer studies are abnormal particularly in those patients who have Sjögren or CREST syndrome in association with PBC. Chest radiograph abnormalities have included hilar adenopathy nodules and interstitial fibrosis. Lung biopsy specimens in the patients with associated Sjögren syndrome have shown giant cells. Occasionally, noncaseating granulomas resembling sarcoidosis has been described (Table 35.2).

**Table 35.2.** Sarcoidosis and primary biliary cirrhosis: A comparison.

| Features | Sarcoidosis | Primary Biliary Cirrhosis |
|---|---|---|
| Sex | Almost equal | 80% women |
| Age (years) | 20–45 | Middle age |
| Pulmonary symptoms | Yes | No |
| Chest x-ray | Abnormal | Normal |
| Pruritus | No | Yes |
| Jaundice | No | Yes |
| Serum alkaline phosphatase | Raised | Raised |
| Serum angiotensin converting enzyme | Raised | Raised |
| Mitochondrial antibody | Normal | Raised (98%) |
| Kveim-Siltzbach test | Positive | Negative |
| Bronchoalveolar lavage | Lymphocytosis | Lymphocytosis |
| Liver biopsy | Solid, discrete granulomas | Poorly formed granulomas |
| Lung biopsy | Noncaseating granulomas | No granulomas, lymphocytes |
| Prognosis | Generally good | Generally poor |

## Bibliography

1. Murray J. Pulmonary Complications of Systemic Disease. Lung Biology in Health Disease, Vol. 59. New York: Marcel Dekker Inc.; 1992.
2. Sharma O., Editor. Pulmonary manifestations of systemic disease. Sem Resp Med 1988;9(3).
3. Naeije R. Hepatopulmonary syndrome and portopulmonary hypertension. Swiss Med Wkly 2003;133:163–169.
4. Krowka MJ. Recent pulmonary observations in $\alpha_1$-antitrypsin deficiency, primary biliary cirrhosis, chronic hepatitis C, and other hepatic problems. Clin Chest Med 1996;17:67–82.

# 36

# Lungs and Gastrointestinal System

## 36.1. Gastroesophageal Reflux Disease (GERD)

Cough can be the sole presenting symptom of gastroesophageal reflux. It is caused by one of three mechanisms. Reflux of stomach contents may irritate the esophageal mucosa and initiate the cough reflex through vagal sensory pathways. Aspirated gastric material may irritate sensory receptors of the tracheobronchial tree. Lastly, stomach contents may reach the hypopharynx and larynx, irritating the afferent limb of the cough reflex without aspiration. Diagnosis is certain only when the cough goes away in response to antireflux therapy.

It has been suggested that gastroesophageal reflux may be involved in the pathogenesis of idiopathic pulmonary fibrosis, but aggressive, long-term antireflux therapy is needed to evaluate its influence on IPF. In patients with systemic sclerosis (SSc), some of the respiratory symptoms are due to the presence of severe gastroesophageal reflux, and there are suggestions that GER may be one of the contributing factors in development of ILD in SSc (Figure 36.1).

## 36.2. Pulmonary Complications of Esophageal Sclerotherapy

Esophageal varices are injected acutely at the time of bleeding; the remaining are obliterated later in the course of the illness. Fever, chest pain (usually retrosternal and nonpleuritic) and dysphagia are frequent complications. Pleural effusions (right, left, or bilateral) are frequent in those patients who have chest pain and have a large volume of sclerosant injected. The fluid is usually an exudate. Aspiration pneumonia is another complication. Rarely, acute respiratory distress syndrome may complicate esophageal sclerotherapy with sodium morrhuate. Broncho-esophageal fistula formation has been described after endoscopic sclerotherapy.

## 36.3. Pancreatitis

The lungs may be involved in 50–70% of patients with acute pancreatitis. The abnormalities include asymptomatic reduction in arterial oxygenation, significant hypoxemia with a normal chest radiograph, nonspecific infiltrates, pleural effusion, and ARDS (Figure 36.2). The latter occurs in about 15% of the patients with acute pancreatitis and carries a poor prognosis. The onset of pulmonary symptoms in the patient with acute pancreatitis portends a poor prognosis. Sixty percent of deaths from acute pancreatitis that occur during the first week are associated with respiratory failure. Only 25% of those who require mechanical ventilation survive. During and after the second week, pulmonary complications are usually the result of pancreatic infection or pseudocyst formation. Pleural effusions and ascites reflect the severity of the illness.

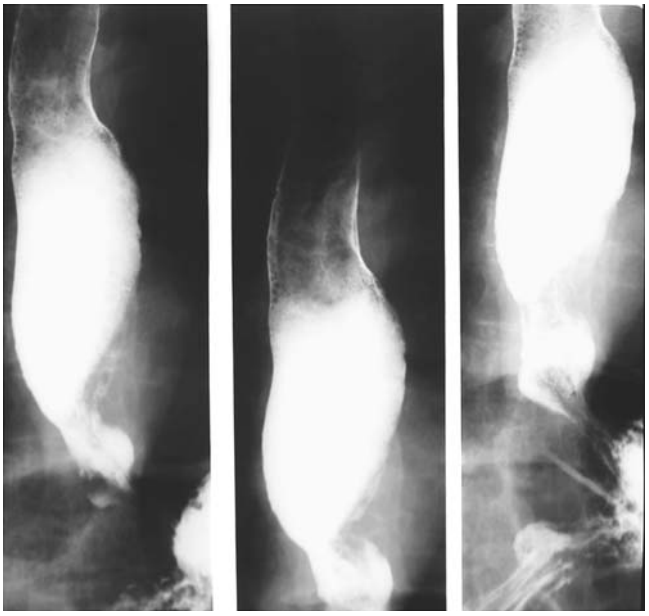

**Figure 36.1.** Esophagus disease in SSc is characterized by poorly functioning muscles that can lead to an abnormally wide esophagus that allows stomach acid to backflow into the esophagus. Double-contrast esophagography following a barium swallow reveals dilated esophagus with reduced mucosal folds and atony.

## 36.4. Inflammatory Bowel Disease

The pulmonary manifestations of inflammatory bowel (IBD) disease may be categorized by disease mechanism into drug-induced disease, anatomic disease, overlap syndromes, autoimmune disease, physiologic consequences of IBD, pulmonary function test abnormalities, and nonspecific lung disease (Table 36.1). There are other extrapulmonary manifestations of IBD, like arthritis and skin and eye disease, especially scleritis (Figure 36.3).

*Chronic airway inflammation*, both bronchiectasis and purulent bronchitis, is common in inflammatory bowel disease, particularly in *ulcerative colitis* (Figure 36.4a, b). Involvement of the small airways is unusual. Organizing pneumonia or bronchiolitis obliterans organizing pneumonia with bilateral, patchy opacities containing air-bronchograms, nonspecific interstitial pneumonitis, and eosinophilic pneumonias have been described in ulcerative colitis (Figure 36.5a, b, c). The pulmonary manifestations

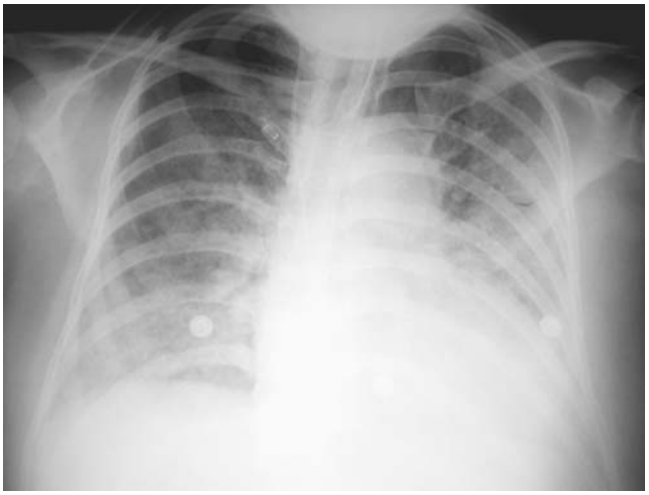

**Figure 36.2.** ARDS in a patient with pancreatitis. The patient died in ICU due to respiratory failure. The transparency of the lungs is reduced.

**Table 36.1.** Pulmonary manifestations of inflammatory bowel diseases.

| |
|---|
| Anatomic disease |
| Esophageal, colobronchial, and ileobronchial fistulas |
| Overlap syndromes |
| Lung granulomatosis |
| $\alpha_1$-antitrypsin deficiency |
| Pulmonary vasculitis |
| Wegener granulomatosis |
| Pulmonary capillaritis |
| Increased clotting tendency in IBD |
| Thromboembolism |
| Lung functions |
| Restrictive ventilatory changes |
| Hyperinflation |
| Reduced DLCO |
| Obstructive ventilatory changes |
| Bronchial hyperreactivity |
| Other pulmonary manifestations of IBD |
| Pleural effusion |
| Airway involvement: epiglotitis, tracheobronchitis, bronchiolitis, BOOP, bronchiectasis |
| Parenchymal: pulmonary eosinophilia, fibrosing alveolitis, cellular pneumonitis |
| Necrobiotic nodules |

Reprinted from Storch I, Sachar D, Katz S. Pulmonary manifestations of inflammatory bowel disease. Inflamm Bowel Dis 2003;9:104–115, with permission from Lippincott, Williams & Wilkins.

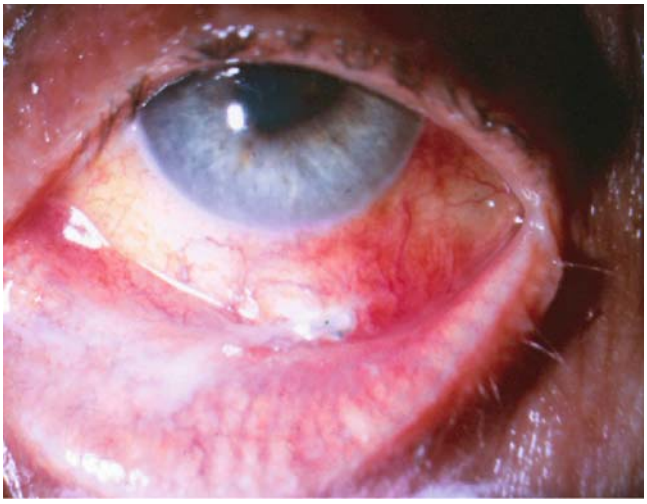

**Figure 36.3.** Scleritis in IBD. Red inflammation of the conjunctivae mimics "red eye"; the eye is red, burns, but vision is not affected.

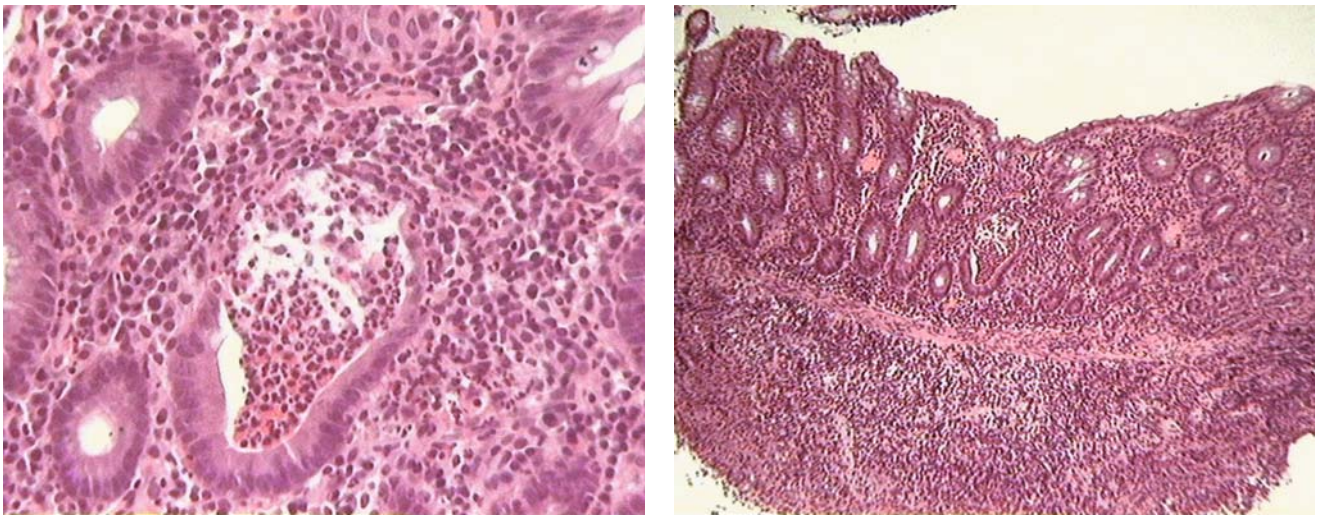

a b

**Figure 36.4.** Histopathological finding in ulcerous colitis. Ulcerative inflammation with shallow defects down to the muscular layer (a) is characterized by mixed inflammatory infiltrates and formation of kryptal abscesses (b). (H&E, ×6.)

may appear at any time during the course of the bowel disease but generally, they follow the clinical onset of the inflammatory bowel disease in 80% of the cases. The airway inflammation is unrelated to the activity of the bowel disease or therapy. Biopsies of the lung tissue usually show thickening of the epithelium and basement membrane with inflammatory cell infiltration of the underlying connective tissue.

*In Crohn disease* (Figures 36.6 and 36.7), on the other hand, subclinical inflammatory lung disease is frequent. Bronchoalveolar lavage fluid from patients with Crohn disease has shown lymphocytes predominate with increased T4 subset during active disease. Despite the presence of alveolar lymphocytosis, there have been only a few reported cases of otherwise unexplained lung disease in these patients. The mechanisms leading to alveolar lymphocytosis in Crohn disease and its relationship with sarcoidosis remains uncertain. Noninfectious pulmonary disease in patients with Crohn disease has variable histologic appearances, including granulomatous inflammation and airway-centered disease resembling that seen in patients with ulcerative colitis. Drugs may contribute to pulmonary disease in some patients.

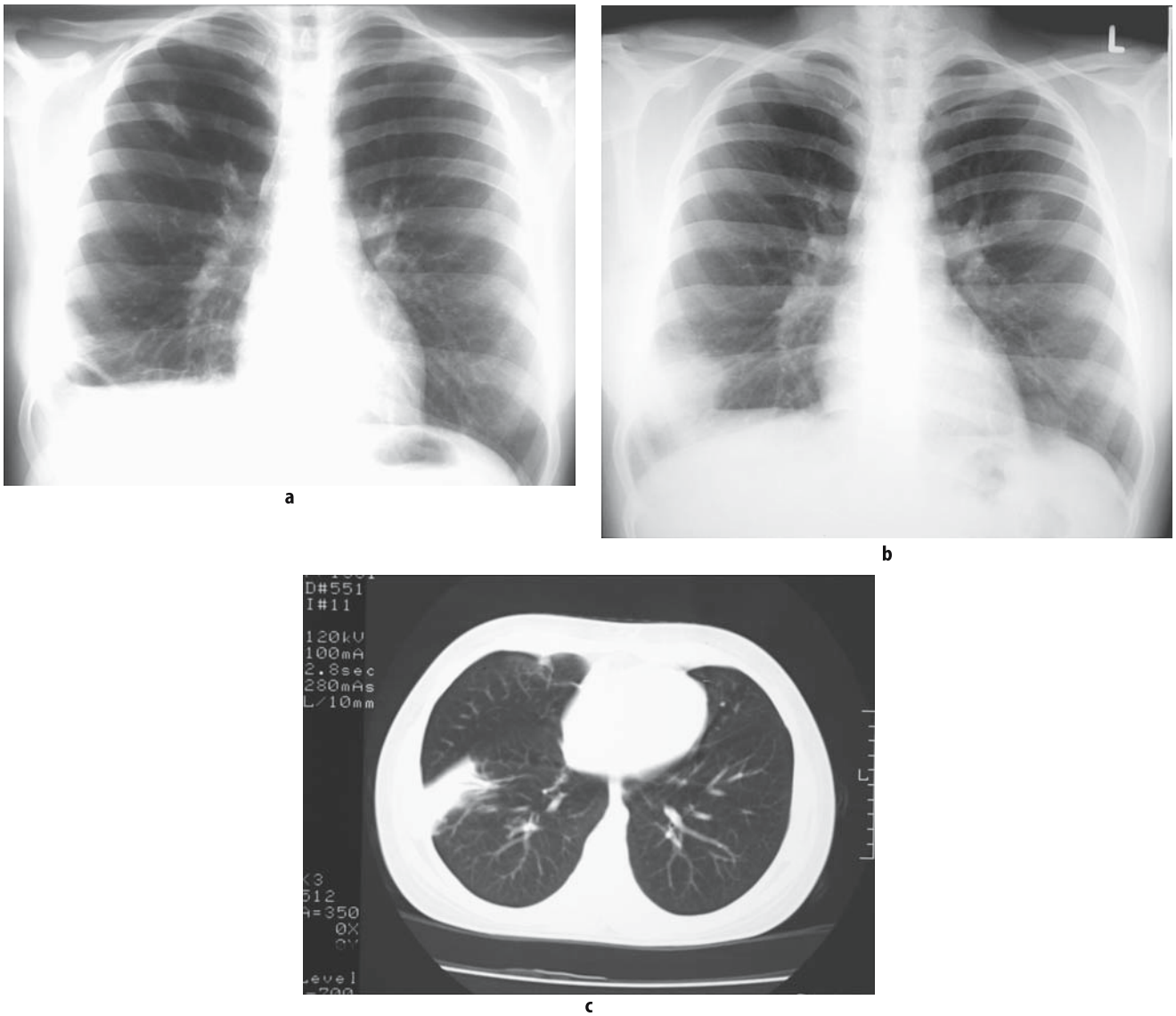


a b c

**Figure 36.5.** The initial inthrathoracic manifestation of the 19-year-old female patient with ulcerous colitis was pleural effusion and minor lower lobe infiltrate. At that time, the connection with the UC was not recognized (a). Plain radiograph of the chest 1 year later showed nodular lesion of apical segment of left lower lobe and infiltration of laterobasilar segment of right lower lobe, which was in contact with the pleura, but without the effusion. These changes represent the necrobiotic nodules; the transthoracal needle aspiration biopsy showed discrete sterile necrotic contents (b). The CT scan showed the air bronchogram and consolidation in the laterobasilar segment of the right lower lobe (c).

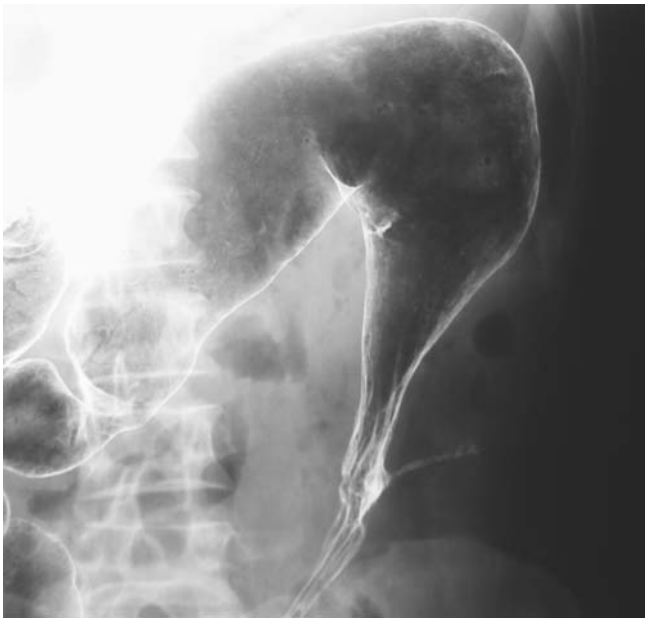

**Figure 36.6.** Fistulas are a feature of Crohn disease. Double-contrast barium meal shows dilated part of the small intestine with reduced mucosal folds and a stenosis visible distally. Fistulous track arising from the strictured part of the ileum can also be seen.

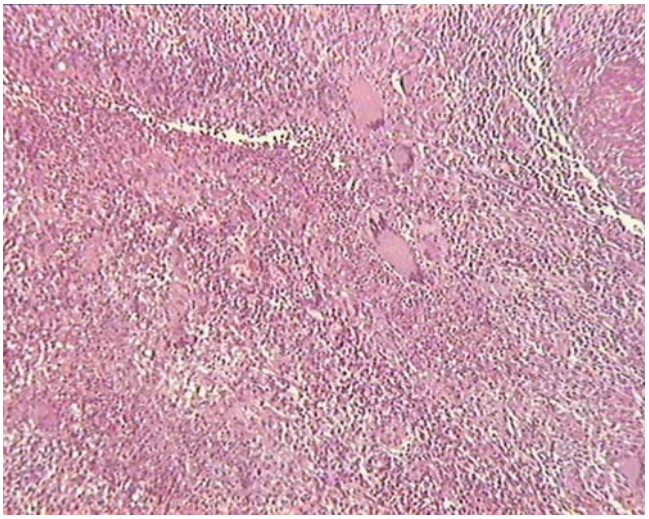

**Figure 36.7.** Histopathological finding in Crohn disease. Crohn disease is characterized by chronic, ulcerative inflammation causing defects through all the layers down to the muscle layer. The inflammatory infiltrates consist mainly of lymphocytes, with the formation of follicles and pseudofollicles and granulomas with giant cells. (H&E, ×25.)

## Bibliography


1. Raghu G. The role of gastroesophageal reflux in idiopathic pulmonary fibrosis. Am J Med 2003;115(Suppl 3A):60S–64S.
2. Marie I, Dominique S, Levesque H, Ducrotte P, Denis P, Hellot MF, Courtois H. Esophageal involvement and pulmonary manifestations in systemic sclerosis. Arthritis Rheum 2001;45(4):346–354.
3. Nassar A, Ghobrial G, Romero C. Culture of Mycobacterium avium subspecies paratuberculosis from the blood of patients with Crohn's disease. Lancet 2004;363:1039–1044.
4. Storch I, Sachar D, Katz S. Pulmonary manifestations of inflammatory bowel disease. Inflamm Bowel Dis 2003;9:104–115.

# 37

# Cancer in Interstitial Lung Disease

Cancer may complicate the course of any interstitial lung disease, including idiopathic pulmonary fibrosis, sarcoidosis, progressive systemic sclerosis (scleroderma), Langerhans cell granulomatosis, asbestosis, and tuberculosis. Nevertheless, how the previous injury in interstitial lung disease predisposes to lung cancer remains a mystery. Bronchiolar and epithelial hyperplasia, undifferentiated scar, and cuboidal transformation of the alveolar epithelium may predispose to malignant transformation. Inflammation, injury, repair, and fibrosis in interstitial diseases may cause genetic damage leading to cancer.

Alveolar cell hyperplasia, related to chronic pulmonary damage, is found in both animals and men, being frequently seen in scleroderma and idiopathic pulmonary fibrosis. When malignant it is called alveolar cell carcinoma. Certain patients with pulmonary fibrosis, particularly those with scleroderma, have an increased incidence of lung cancer (Figure 37.1). A third of the patients with idiopathic pulmonary fibrosis may develop lung cancer (Figure 37.2a, b). The incidence tends to be lower in nonsmokers because smoking is a risk factor for the development of lung cancer in patients with pulmonary fibrosis. In this group of patients, lung carcinomas tend to be peripheral and in the lower lobes. Squamous cell carcinoma occurs in male patients, whereas adenocarcinoma predominates in females. The distribution of the histologic type of lung cancer in interstitial lung disease is similar to that found in lung cancer patients without pulmonary fibrosis; however, it is dissimilar to the distribution observed in scar carcinoma. Finger clubbing is more common in patients with idiopathic pulmonary fibrosis and lung cancer than in those with IPF but no lung cancer.

The pathogenetic mechanisms responsible for the development of lung cancer in patients with interstitial pulmonary fibrosis are not known. A chronic scar may cause localized lymphatic obstruction resulting in an increase of potential carcinogens. The local accumulation of cancerous substances may then induce hyperplasia of alveolar lining that, in turn, under the influence of genes, cytokines, and chemokines, may become the site of inflammation, destruction, fibrosis, disorganization, and malignant transformation of the alveolar lining. Genes p53 and p21 are overexpressed in the hyperplastic bronchial and alveolar epithelial cells in patients with IPF and play a role in inhibiting cellular proliferation and promoting the repair of tissue injury. The chronic course of IPF may result in DNA damage that might lead to p53 mutations. The p53 mutation may be one of the reasons behind the high incidence of lung cancer in idiopathic pulmonary fibrosis patients.

Is there an increase in the incidence of lung cancer in patients with sarcoidosis? In a 10-year study of 2544 patients with pulmonary sarcoidosis, 48 developed malignant tumor, whereas only 33.8 cases were expected if sarcoidosis had the same rate as the general population. Romer et al. failed to demonstrate a high risk of malignancy and lymphoma in patients with sarcoidosis. Sarcoidosis patients develop breast cancer at the expected frequency. Because physical examination and mammograms are unable to distinguish between sarcoidosis and malignancy, biopsy of all suspicious lesions in patients with sarcoidosis is recommended.

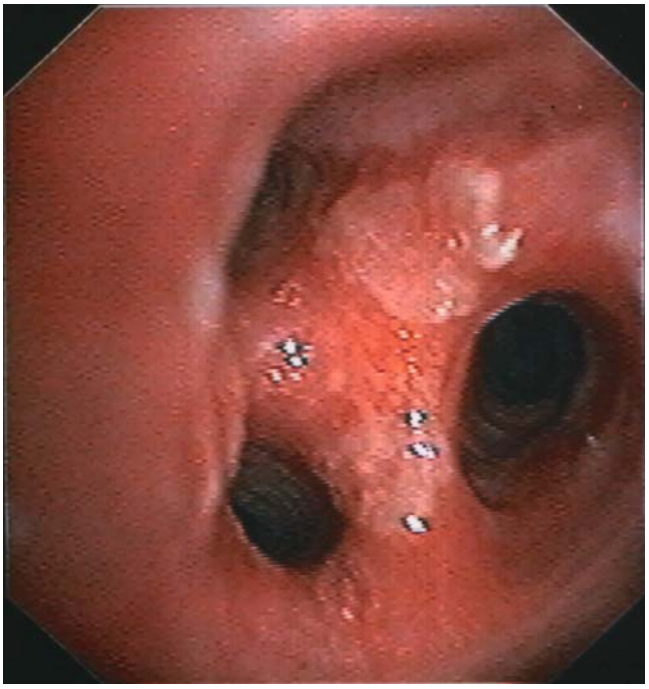

**Figure 37.1.** The increased incidence of cancer in ILD is not limited only to IPF but also occurs in patients with systemic sclerosis (SSc). How previous injury in interstitial fibrosis predisposes to lung cancer remains a mystery. The bronchoscopy reveals precancerous mucosal lesions in a patient with SSc.

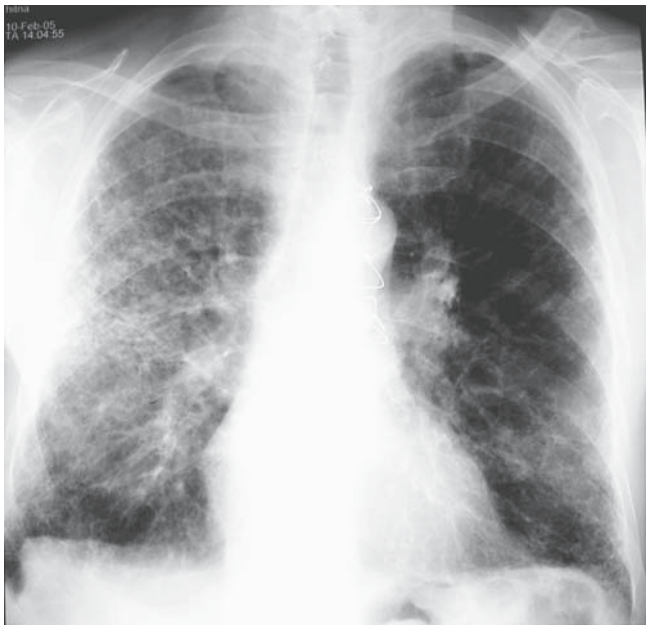

a

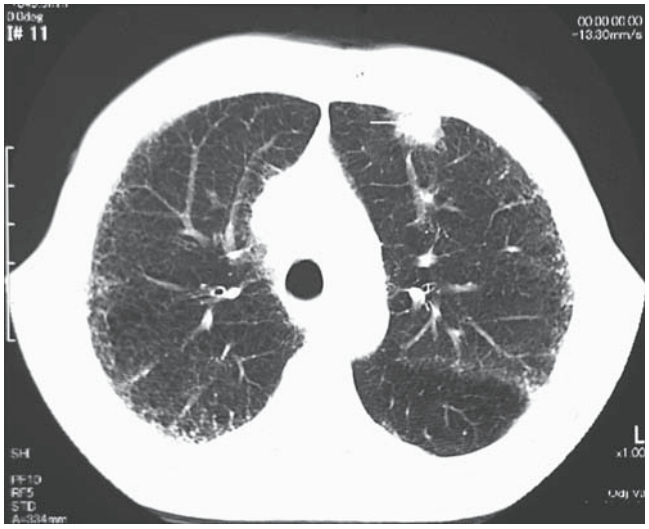

b

**Figure 37.2.** Lung cancer in a patient with idiopathic pulmonary fibrosis (IPF). Radiograph of the chest shows typical parenchymal lower lung changes of IPF with overall volume loss and no visible mass (a). CT of the chest shows a left lower lobe lung mass located peripherally and surrounded by subpleural parenchymal fibrosis, honeycomb change, and traction bronchiectasis. The cytoanalysis revealed squamous cell carcinoma (b).

**Table 37.1.** Differences between a nonspecific local sarcoid reaction and multisystem sarcoidosis.

| Features | Local Sarcoid Reaction | Multisystem Sarcoidosis |
|---|---|---|
| Organ involved | One | More than one |
| Age (years) | Any | 20–50 |
| Chest x-ray | Normal | Abnormal in 90% |
| Delayed hypersensitivity | Normal | Depressed |
| Elevated serum ACE | Less than 5% | More than 60% |
| Kveim-Siltzbach test | Negative | Positive |
| BAL lymphocytosis | Absent | Present |
| Slit-lamp examination | Normal | Positive 15–20% |
| Hypercalcemia | Absent | Present in 13% |
| Gallium body scan | Localized uptake | Multisystem uptake |

ACE, angiotensin converting enzyme; BAL, bronchoalveolar lavage.

Malignant disease may produce a local sarcoid reaction or mimic manifestations of systemic sarcoidosis. Testicular and renal cell carcinomas can cause hilar and mediastinal adenopathy. These sarcoid reaction or sarcoid-like granulomas may be found in regional lymph nodes draining a carcinoma or a lymphoma. Granulomas have also been found among the tumor cells at the site of the primary neoplasm; rarely, epithelioid cell granuloma may occur intermingled with the primary lung tumor. This occurs mostly in patients with adenocarcinoma. Sarcoid reactions may also occur in spleen in patients with gastric cancers. These local nonspecific "sarcoid" reactions should be distinguished from systemic sarcoidosis (Table 37.1).

Thus, we know neither the exact incidence of carcinoma complicating interstitial lung disease and sarcoidosis nor the reasons of such an association when present. The physician, however, should remain alert to the possibility of carcinoma occurring in patients with diffuse interstitial lung disease. Once the diagnosis is entertained, it should be confirmed by obtaining a biopsy. An early diagnosis assures therapeutic success.

Various other malignancies have higher incidence in certain ILDs. For instance, malignant pleural mesothelioma is much more frequent in patients with asbestosis (Figure 37.3). When we contemplate the problem of ILD and malignancies, we have to mention that lymphangitic carcinomatosis has to be considered in differential diagnosis of ILDs (Figure 37.4a, b, c).

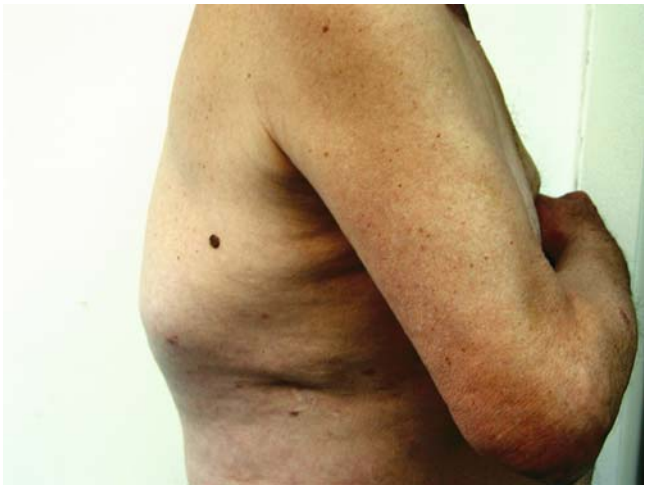

**Figure 37.3.** Malignant mesothelioma in a patient with asbestosis. The tumor spreads locally and grows along needle tracks. The scar due to diagnostic video-assisted thoracoscopy is seen. The thoracoscopic talc pleurodesis has also been performed.

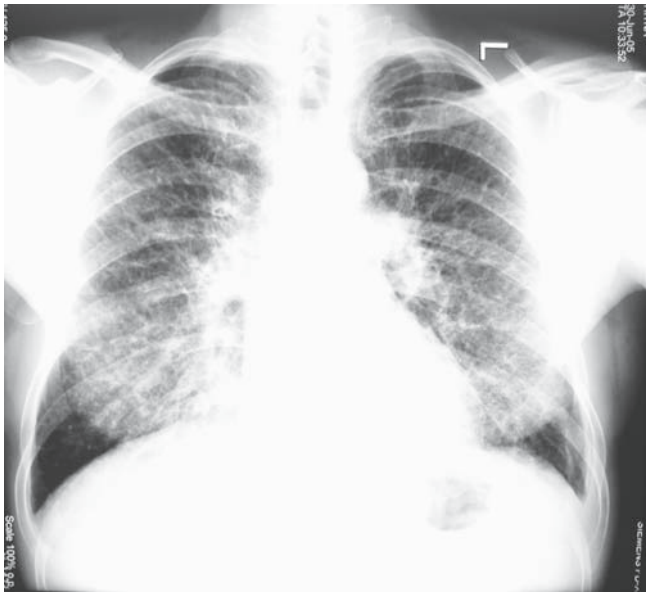

a

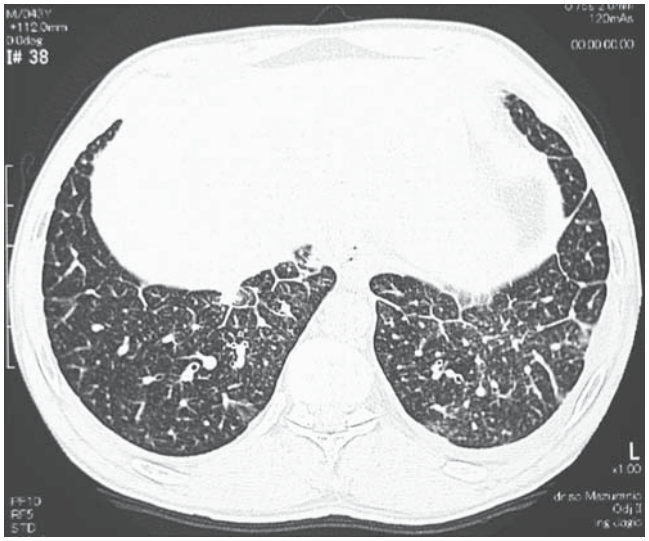

b

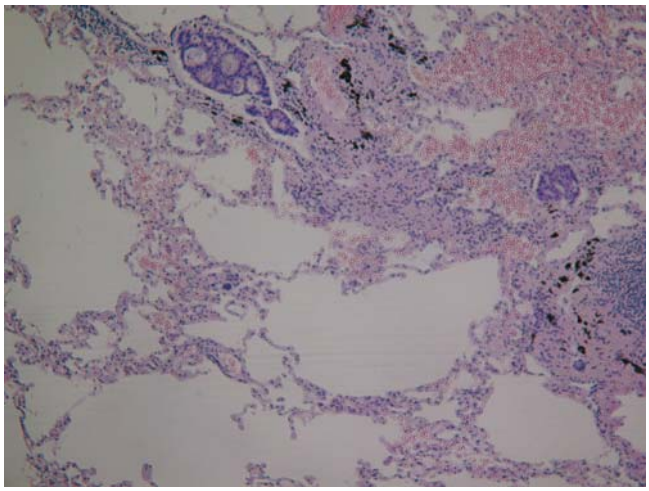

c

**Figure 37.4.** Lymphangitic carcinomatosis by plain radiograph showing reticular pattern (Kerley B-lines) (a) and HRCT scanning showing the interlobular, septal thickening (b) in a patient with breast carcinoma. Nests of neoplastic cells fill perivascular lymphatics (c).

## Bibliography


1. Bouros D, Hatzakis K, Labrakis H, Zeibecoglou K. Association of malignancy with diseases causing interstitial pulmonary changes. Chest 2002;121:1278–1289.
2. Aubry M, Myers J, Tazelaar H, Washington T, Hartman T, Deschamps C, Pankrantz VS. Primary pulmonary carcinoma in patients with idiopathic pulmonary fibrosis. Mayo Clin Proc 2002:77:763–770.
3. Seneviratne M, Koss M. Idiopathic pulmonary fibrosis and malignancy. Curr Opin Pulm Med 2001;7(5):278–282.
4. Turner-Warwick M, Lebowitz M, Burrows B, Johnson A. Cryptogenic fibrosing alveolitis and lung cancer. Thorax 1980;35:496–499.
5. Askling J, Gruenwald J, Eklund A, Hillerdae G, Ekbom A. Increased risk of cancer following sarcoidosis. Am J Respir Crit Care Med 1999;160:1668–1672.
6. Seersholm N, Vestbo J, Viskum K. Risks of malignant neoplasm in patients with pulmonary sarcoidosis. Thorax 1997; 52:892–894.
7. Romer F, Hommelgaard P, Schou G. S revisited: A long term follow up of 555 Danish sarcoidosis patients Eur Resp J 1998;12:906–912.
8. Suzuki M. Breast sarcoidosis. Jpn J Clini Med 2002;60:1818–1821.

# Index